

IMAGE-GUIDED RADIOTHERAPY FOR EFFECTIVE RADIOTHERAPY DELIVERY

EDITED BY: Nam Phong Nguyen and Ulf Lennart Karlsson

PUBLISHED IN: Frontiers in Oncology



Frontiers Copyright Statement

© Copyright 2007-2016 Frontiers Media SA. All rights reserved.

All content included on this site, such as text, graphics, logos, button icons, images, video/audio clips, downloads, data compilations and software, is the property of or is licensed to Frontiers Media SA ("Frontiers") or its licensees and/or subcontractors. The copyright in the text of individual articles is the property of their respective authors, subject to a license granted to Frontiers.

The compilation of articles constituting this e-book, wherever published, as well as the compilation of all other content on this site, is the exclusive property of Frontiers. For the conditions for downloading and copying of e-books from Frontiers' website, please see the Terms for Website Use. If purchasing Frontiers e-books from other websites or sources, the conditions of the website concerned apply.

Images and graphics not forming part of user-contributed materials may not be downloaded or copied without permission.

Individual articles may be downloaded and reproduced in accordance with the principles of the CC-BY licence subject to any copyright or other notices. They may not be re-sold as an e-book.

As author or other contributor you grant a CC-BY licence to others to reproduce your articles, including any graphics and third-party materials supplied by you, in accordance with the Conditions for Website Use and subject to any copyright notices which you include in connection with your articles and materials.

All copyright, and all rights therein, are protected by national and international copyright laws.

The above represents a summary only. For the full conditions see the Conditions for Authors and the Conditions for Website Use.

ISSN 1664-8714

ISBN 978-2-88919-849-8

DOI 10.3389/978-2-88919-849-8

About Frontiers

Frontiers is more than just an open-access publisher of scholarly articles: it is a pioneering approach to the world of academia, radically improving the way scholarly research is managed. The grand vision of Frontiers is a world where all people have an equal opportunity to seek, share and generate knowledge. Frontiers provides immediate and permanent online open access to all its publications, but this alone is not enough to realize our grand goals.

Frontiers Journal Series

The Frontiers Journal Series is a multi-tier and interdisciplinary set of open-access, online journals, promising a paradigm shift from the current review, selection and dissemination processes in academic publishing. All Frontiers journals are driven by researchers for researchers; therefore, they constitute a service to the scholarly community. At the same time, the Frontiers Journal Series operates on a revolutionary invention, the tiered publishing system, initially addressing specific communities of scholars, and gradually climbing up to broader public understanding, thus serving the interests of the lay society, too.

Dedication to quality

Each Frontiers article is a landmark of the highest quality, thanks to genuinely collaborative interactions between authors and review editors, who include some of the world's best academicians. Research must be certified by peers before entering a stream of knowledge that may eventually reach the public - and shape society; therefore, Frontiers only applies the most rigorous and unbiased reviews.

Frontiers revolutionizes research publishing by freely delivering the most outstanding research, evaluated with no bias from both the academic and social point of view.

By applying the most advanced information technologies, Frontiers is catapulting scholarly publishing into a new generation.

What are Frontiers Research Topics?

Frontiers Research Topics are very popular trademarks of the Frontiers Journals Series: they are collections of at least ten articles, all centered on a particular subject. With their unique mix of varied contributions from Original Research to Review Articles, Frontiers Research Topics unify the most influential researchers, the latest key findings and historical advances in a hot research area! Find out more on how to host your own Frontiers Research Topic or contribute to one as an author by contacting the Frontiers Editorial Office: researchtopics@frontiersin.org

IMAGE-GUIDED RADIOTHERAPY FOR EFFECTIVE RADIOTHERAPY DELIVERY

Topic Editors:

Nam Phong Nguyen, International Geriatric Radiotherapy Group, USA

Ulf Lennart Karlsson, Marshfield Clinic, USA

Image-guided radiotherapy (IGRT) is a new radiotherapy technology that combines the rapid dose fall off associated with intensity-modulated radiotherapy (IMRT) and daily tumor imaging allowing for high precision tumor dose delivery and effective sparing of surrounding normal organs. The new radiation technology requires close collaboration between radiologists, nuclear medicine specialists, and radiation oncologists to avoid marginal miss. Modern diagnostic imaging such as positron emission tomography (PET) scans, positron emission tomography with Computed Tomography (PET-CT), and magnetic resonance imaging (MRI) allows the radiation oncologist to target the positive tumor with high accuracy. As the tumor is well visualized during radiation treatment, the margins required to avoid geographic miss can be safely reduced, thus sparing the normal organs from excessive radiation. When the tumor is located close to critical radiosensitive structures such as the spinal cord, IGRT can deliver a high dose of radiation to the tumor and simultaneously decreasing treatment toxicity, thus potentially improving cure rates and patient quality of life.

During radiotherapy, tumor shrinkage and changes of normal tissues/volumes can be detected daily with IGRT. The volume changes in the target volumes and organs at risk often lead to increased radiation dose to the normal tissues and if left uncorrected may result in late complications. Adaptive radiotherapy with re-planning during the course of radiotherapy is therefore another advantage of IGRT over the conventional radiotherapy techniques. This new technology of radiotherapy delivery provides the radiation oncologist an effective tool to improve patient quality of life. In the future, radiation dose-escalation to the residual tumor may potentially improve survival rates. Because the treatment complexity, a great deal of work is required from the dosimetry staff and physicists to ensure quality of care. Preliminary clinical results with IGRT are encouraging but more prospective studies should be performed in the future to assess the effectiveness of IGRT in improving patient quality of life and local control. In this Frontiers Research Topic, we encourage submission of original papers and reviews dealing with imaging for radiotherapy planning, the physics and dosimetry associated with IGRT, as well as the clinical outcomes for cancer treatment with IGRT for all tumor sites.

Citation: Nguyen, N. P., Karlsson, U. L., eds. (2016). Image-Guided Radiotherapy for Effective Radiotherapy Delivery. Lausanne: Frontiers Media. doi: 10.3389/978-2-88919-849-8

Table of Contents

- 05 Editorial: Image-Guided Radiotherapy for Effective Radiotherapy Delivery**
Nam P. Nguyen and Ulf Lennart Karlsson
- 07 Would screening for lung cancer benefit 75- to 84-year-old residents of the United States?**
John M. Varlotto, Malcolm M. DeCamp, John C. Flickinger, Jessica Lake, Abram Recht, Chandra P. Belani, Michael F. Reed, Jennifer W. Toth, Heath B. Mackley, Christopher N. Sciamanna, Alan Lipton, Suhail M. Ali, Richkesvar P. M. Mahraj, Christopher R. Gilbert and Nengliang Yao
- 16 The utility of positron emission tomography in the treatment planning of image-guided radiotherapy for non-small cell lung cancer**
Alexander Chi and Nam Phong Nguyen
- 23 4D PET/CT as a strategy to reduce respiratory motion artifacts in FDG-PET/CT**
Alexander Chi and Nam P. Nguyen
- 27 The potential role of respiratory motion management and image guidance in the reduction of severe toxicities following stereotactic ablative radiation therapy for patients with centrally located early stage non-small cell lung cancer or lung metastases**
Alexander Chi, Nam Phong Nguyen and Ritsuko Komaki
- 39 Strategies of dose escalation in the treatment of locally advanced non-small cell lung cancer: image guidance and beyond**
Alexander Chi, Nam Phong Nguyen, James S. Welsh, William Tse, Manish Monga, Olusola Oduntan, Mohammed Almubarak, John Rogers, Scot C. Remick and David Gius
- 49 Moderately escalated hypofractionated (chemo) radiotherapy delivered with helical intensity-modulated technique in stage III unresectable non-small cell lung cancer**
Vittorio Donato, Stefano Arcangeli, Alessia Monaco, Cristina Caruso, Michele Cianciulli, Genoveva Boboc, Cinzia Chiostriini, Roberta Rauco and Maria Cristina Pressello
- 55 Feasibility of tomotherapy-based image-guided radiotherapy for small cell lung cancer**
Nam P. Nguyen, Wei Shen, Sarah Kratz, Jacqueline Vock, Paul Vos, Vinh-Hung Vincent, Gabor Altdorfer, Lars Ewell, Siyoung Jang, Ulf Karlsson, Juan Godinez, Melissa Mills, Thomas Sroka, Suresh Dutta, Alexander Chi and The International Geriatric Radiotherapy Group

- 59 *The potential role of magnetic resonance spectroscopy in image-guided radiotherapy***
Mai Lin Nguyen, Brooke Willows, Rihan Khan, Alexander Chi, Lyndon Kim, Sherif G. Nour, Thomas Sroka, Christine Kerr, Juan Godinez, Melissa Mills, Ulf Karlsson, Gabor Altdorfer, Nam Phong Nguyen, Gordon Jendrasiak and The International Geriatric Radiotherapy Group
- 65 *Potential applications of imaging and image-guided radiotherapy for brain metastases and glioblastoma to improve patient quality of life***
Nam P. Nguyen, Mai L. Nguyen, Jacqueline Vock, Claire Lemanski, Christine Kerr, Vincent Vinh-Hung, Alexander Chi, Rihan Khan, William Woods, Gabor Altdorfer, Mark D'Andrea, Ulf Karlsson, Russ Hamilton and Fred Ampil
- 72 *Five fraction image-guided radiosurgery for primary and recurrent meningiomas***
Eric Karl Oermann, Rahul Bhandari, Viola J. Chen, Gabriel Lebec, Marie Gurka, Siyuan Lei, Leonard Chen, Simeng Suy, Norio Azumi, Frank Berkowitz, Christopher Kalhorn, Kevin McGrail, Brian Timothy Collins, Walter C. Jean and Sean P. Collins
- 79 *A multicenter retrospective study of frameless robotic radiosurgery for intracranial arteriovenous malformation***
Eric K. Oermann, Nikhil Murthy, Viola Chen, Advaith Baimeedi, Deanna Sasaki-Adams, Kevin McGrail, Sean P. Collins, Matthew G. Ewend and Brian T. Collins
- 84 *Potential applications of image-guided radiotherapy for radiation dose escalation in patients with early stage high-risk prostate cancer***
Nam P. Nguyen, Rick Davis, Satya R. Bose, Suresh Dutta, Vincent Vinh-Hung, Alexander Chi, Juan Godinez, Anand Desai, William Woods, Gabor Altdorfer, Mark D'Andrea, Ulf Karlsson, Richard A. Vo, Thomas Sroka and the International Geriatric Radiotherapy Group
- 91 *Rationale for stereotactic body radiation therapy in treating patients with oligometastatic hormone-naïve prostate cancer***
Onita Bhattasali, Leonard N. Chen, Michael Tong, Siyuan Lei, Brian T. Collins, Pranay Krishnan, Christopher Kalhorn, John H. Lynch, Simeng Suy, Anatoly Dritschilo, Nancy A. Dawson and Sean P. Collins
- 98 *Image-guided radiotherapy and -brachytherapy for cervical cancer***
Suresh Dutta, Nam Phong Nguyen, Jacqueline Vock, Christine Kerr, Juan Godinez, Satya Bose, Siyoung Jang, Alexander Chi, Fabio Almeida, William Woods, Anand Desai, Rick David, Ulf Lennart Karlsson, Gabor Altdorfer and The International Geriatric Radiotherapy Group
- 104 *Image-guided radiotherapy for cardiac sparing in patients with left-sided breast cancer***
Claire Lemanski, Juliette Thariat, Federico L. Ampil, Satya Bose, Jacqueline Vock, Rick Davis, Alexander Chi, Suresh Dutta, William Woods, Anand Desai, Juan Godinez, Ulf Karlsson, Melissa Mills, Nam Phong Nguyen, Vincent Vinh-Hung and The International Geriatric Radiotherapy Group
- 108 *Image-guided radiotherapy for locally advanced head and neck cancer***
Nam P. Nguyen, Sarah Kratz, Claire Lemanski, Jacqueline Vock, Vincent Vinh-Hung, Olena Gorobets, Alexander Chi, Fabio Almeida, Michael Betz, Rihan Khan, Juan Godinez, Ulf Karlsson and Fred Ampil



Editorial: Image-Guided Radiotherapy for Effective Radiotherapy Delivery

Nam P. Nguyen^{1*} and Ulf Lennart Karlsson²

¹ Department of Radiation Oncology, Howard University, Washington, DC, USA, ² Department of Radiation Oncology, Marshfield Clinic, Marshfield, WI, USA

Keywords: cancer, computerized axial tomography, image-guided radiotherapy, comorbidity, disease-specific survival

During most of the last century, verification of patient position on the radiotherapy treatment table was considered adequate if exposed on a photographic film by a megavoltage beam. It was a general standard to expose such a film once a week, to be approved by a radiation oncologist. The latter approved it after comparison to a kilovoltage simulation film exposed at the time of initial setup of the patient before the treatment regimen started.

A common rule was to allow a $\pm <5$ mm variation from the simulation to the treatment portal film. This often resulted in either an approval for the next week's treatment fractions or a rejection and retake of that or the next day's portal film. There was no film record of the next four fractions. The problems included megavoltage film resolution judged from kilovoltage simulation films as well as unrecorded possible errors for the next four fractions. Another error source was soft tissue contrast in both of these films.

The evolution of computerized axial tomography (CAT) scan from the mid-twentieth century has allowed for 3D reconstruction of the patient's soft tissue structures by improved resolution in millimeter scan slices.

Development of the digital image visualization on computer screens now allows for fusing the reconstructed simulation image (DRR) from the CAT scanner with the mega- or kilovoltage rendering of the patient's treatment beams. This has allowed the skilled radiotherapist to adjust the beam within a preset millimeter 3D frame to the patient's anatomy. With this precision, a daily treatment fraction is given. The radiation oncologist can then check that body position errors have been corrected before each treatment.

Further improvement include the cone beam image obtained from the treatment accelerator and fused over the DRR, introduction of gold markers in the target volume and triangulating their positions into the simulation scan, as well as utilizing kilovoltage and or megavoltage images to attain precise beam geometry for each daily radiotherapy fraction. Another method is to use a diagnostic CAT scanner that is mechanically attached to the accelerator.

These imaging techniques are used to assure that the planned dose only covers the intended target and encompasses the IGRT concept in radiotherapy. If used properly, the precision of treatment is improved from centimeter to millimeter realms (1) and is expected to be used globally in cancer radiotherapy. Our experience is that few treatment portals need to be rejected as long as there is a requirement of immediate report to the oncologist that a specified position error has been discovered and corrected.

We consider it a necessary ingredient for clinical studies in order to measure and compare IGRT outcome data. It has the potential of not only providing better toxicity results but also to give better outcome data for patient groups who are thought to be at higher risk for toxicity, e.g., frail elderly and patients with abnormal radiosensitivity. It may also offer an avenue for dose escalation because of better organ sparing.

OPEN ACCESS

Edited and reviewed by:

Timothy James Kinsella,
Warren Alpert Medical School of
Brown University, USA

***Correspondence:**

Nam P. Nguyen
namphong.nguyen@yahoo.com

Specialty section:

This article was submitted to
Radiation Oncology, a section of the
journal Frontiers in Oncology

Received: 28 October 2015

Accepted: 02 November 2015

Published: 18 November 2015

Citation:

Nguyen NP and Karlsson UL (2015)
Editorial: Image-Guided Radiotherapy
for Effective Radiotherapy Delivery.
Front. Oncol. 5:253.

doi: 10.3389/fonc.2015.00253

Our preliminary evidence is encouraging for the use of IGRT.

Elderly (>70 years of age) and younger head and neck cancer groups both tolerated definitive chemo-IGRT, without difference in grade 3–4 toxicity, treatment breaks, and with less weight loss in the elderly group (2). Another study resulted in disease-specific survival of 75% at 4 years and acceptable toxicity (3).

Elderly patients with multiple comorbidities and locally advanced rectal cancer tolerated preoperative chemo-IGRT when compared to younger patients (4). These preliminary studies suggest that IGRT may become the treatment of choice for elderly cancer patients.

Another subset of patients who may benefit from IGRT is patients with human immunodeficiency virus (HIV) infection and anal cancer. They may have an increased sensitivity to radiation because of thiol deficiency (5). Grade 3–4 skin, hematologic and gastrointestinal toxicity were frequent among HIV positive patients undergoing standard chemoradiotherapy and may result in death (6, 7). Chemo-IGRT may therefore

provide HIV patients the opportunity to be treated with less toxicity (8, 9).

Finally, IGRT may allow for radiation dose escalation in cancers with high-risk for loco-regional recurrences. A recent randomized study reported a 2-year survival of 57 and 44% and local failure of 30 and 38% for locally advanced NSCLC treated to 60 and 74 Gy, respectively. The poor survival in the 74 Gy group may be associated with cardiac toxicity (10).

A 3-year survival of 45% and local failure of 15% was reported for patients with locally advanced NSCLC treated to 70–75 Gy with chemo-IGRT, with minimal toxicity (11). Dose escalation was also feasible in patients with locally advanced esophageal cancer because of lung and cardiac sparing (12).

These preliminary results are intriguing but need to be corroborated in future prospective studies.

AUTHOR CONTRIBUTIONS

UK and NN wrote and approved the manuscript.

REFERENCES

- Oehler C, Lang S, Dimmerling P, Bolesch C, Kloeck S, Tini A, et al. PTV margin definition in hypofractionated IGRT of localized prostate cancer using cone beam CT and orthogonal image pairs with fiducial markers. *Radiat Oncol* (2014) **9**:229. doi:10.1186/s13014-014-0229-z
- Nguyen NP, Vock J, Chi A, Vinh-Hung V, Dutta S, Ewell L, et al. Impact of intensity-modulated and image-guided radiotherapy on elderly patients undergoing chemoradiation for locally advanced head and neck cancer. *Strahlenther Onkol* (2012) **188**:677–83. doi:10.1007/s00660-012-0125-0
- Bahig H, Fortin B, Alizadeth M, Lambert L, Filion E, Guertin L, et al. Predictive factors of survival and treatment tolerance in older patients treated with chemotherapy and radiotherapy for locally advanced head and neck cancer. *Oral Oncol* (2015) **51**(5):521–8. doi:10.1016/j.oraloncology.2015.02.097
- Nguyen NP, Ceizyk M, Vock J, Vos P, Chi A, Vinh-Hung V, et al. Feasibility of image-guided radiotherapy for elderly patients with locally advanced rectal cancer. *PLoS One* (2013) **8**:e71250. doi:10.1371/journal.pone.0071250
- Vallis KA. Glutathione deficiency and radiosensitivity in AIDS patients. *Lancet* (1991) **337**:918–9. doi:10.1016/0140-6736(91)90250-S
- Alfa-Wali M, Allen-Mersh T, Antoniou A, Tait D, Newsom-Davis T, Gazzard B, et al. Chemoradiotherapy for anal cancer in HIV patients causes prolonged CD4 cell count suppression. *Ann Oncol* (2012) **23**:141–7. doi:10.1093/annonc/mdr050
- Cleator S, Fife K, Nelson M, Gazzard B, Phillips R, Bower M. Treatment of HIV-associated invasive anal cancer with combined chemoradiation. *Eur J Cancer* (2000) **36**:754–8. doi:10.1016/S0959-8049(00)00009-5
- Nguyen NP, Vock J, Sroka T, Khan R, Jang S, Chi A, et al. Feasibility of image-guided radiotherapy based on tomotherapy for the treatment of locally advanced anal cancer. *Anticancer Res* (2011) **31**:4393–6.
- Nguyen NP, Ceizyk M, Almeida F, Chi A, Betz M, Moderrassifar H, et al. Effectiveness of image-guided radiotherapy for locally advanced rectal cancer. *Ann Surg Oncol* (2011) **18**:380–5. doi:10.1245/s10434-010-1329-0
- Bradley J, Paulus R, Komaki R, Masters G, Blumenschen G, Schild S, et al. Standard dose versus high dose conformal radiotherapy with concurrent and consolidation carboplatin plus paclitaxel with and without cetuximab for patients with stage IIIA and IIIB non-small cell lung cancer (RTOG 0617): a randomized, two-by-two factorial phase II study. *Lancet Oncol* (2015) **16**: 187–99. doi:10.1016/S1470-2045(14)71207-0
- Nguyen NP, Kratz S, Chi A, Vock J, Vos P, Shen W, et al. Feasibility of image-guided radiotherapy and concurrent chemotherapy for locally advanced non-small cell lung cancer. *Cancer Invest* (2015) **33**:53–60. doi:10.3109/07357907.2014.1001896
- Nguyen NP, Jang S, Vock J, Vinh-Hung V, Chi A, Vos P, et al. Feasibility of intensity-modulated and image-guided radiotherapy for locally advanced esophageal cancer. *BMC Cancer* (2014) **14**:265. doi:10.1186/1471-2407-14-265

Conflict of Interest Statement: The authors declare that the research was conducted in the absence of any commercial or financial relationships that could be construed as a potential conflict of interest.

Copyright © 2015 Nguyen and Karlsson. This is an open-access article distributed under the terms of the Creative Commons Attribution License (CC BY). The use, distribution or reproduction in other forums is permitted, provided the original author(s) or licensor are credited and that the original publication in this journal is cited, in accordance with accepted academic practice. No use, distribution or reproduction is permitted which does not comply with these terms.



Would screening for lung cancer benefit 75- to 84-year-old residents of the United States?

John M. Varlotto^{1*}, Malcolm M. DeCamp², John C. Flickinger³, Jessica Lake⁴, Abram Recht⁵, Chandra P. Belani^{4,6}, Michael F. Reed^{4,7}, Jennifer W. Toth^{4,8}, Heath B. Mackley^{4,6}, Christopher N. Sciamanna⁹, Alan Lipton^{4,6}, Suhail M. Ali^{4,6}, Richkesvar P. M. Mahraj¹⁰, Christopher R. Gilbert^{4,8} and Nengliang Yao¹¹

¹ Department of Radiation Oncology, University of Massachusetts Medical Center, Worcester, MA, USA

² Division of Thoracic Surgery, Department of Surgery, Northwestern Memorial Hospital, Chicago, IL, USA

³ Department of Radiation Oncology, Pittsburgh Cancer Institute, Pittsburgh, PA, USA

⁴ Pennsylvania State University College of Medicine, Hershey, PA, USA

⁵ Department of Radiation Oncology, Beth Israel Deaconess Medical Center, Boston, MA, USA

⁶ Penn State Hershey Cancer Institute, Hershey, PA, USA

⁷ Heart and Vascular Institute, Penn State Hershey Medical Center, Hershey, PA, USA

⁸ Division of Pulmonary, Allergy, and Critical Care Medicine, Department of Medicine, Penn State Hershey Medical Center, Hershey, PA, USA

⁹ Department of Medicine, Penn State College of Medicine, Hershey, PA, USA

¹⁰ Department of Radiology, Penn State College of Medicine, Hershey, PA, USA

¹¹ Department of Healthcare Policy and Research, Virginia Commonwealth University College of Medicine, Richmond, VA, USA

Edited by:

Ulf Lennart Karlsson, Marshfield Clinic, USA

Reviewed by:

Daniel Grant Peteriet, Rapid City Regional Hospital, USA

Nam Phong Nguyen, International Geriatric Radiotherapy Group, USA

*Correspondence:

John M. Varlotto, Department of Radiation Oncology, University of Massachusetts Medical Center, 55 Lake Avenue North, Worcester, MA 01655, USA
e-mail: john.varlotto@umassmemorial.org

Background: The National Lung Screening Trial demonstrated that screening for lung cancer improved overall survival (OS) and reduced lung cancer mortality in the 55- to 74-year-old age group by increasing the proportion of cancers detected at an early stage. Because of the increasing life expectancy of the American population, we investigated whether screening for lung cancer might benefit men and women aged 75–84 years.

Materials/Methods: Rates of non-small cell lung cancer (NSCLC) from 2000 to 2009 were calculated in both younger and older age groups using the surveillance epidemiology and end reporting database. OS and lung cancer-specific survival (LCSS) in patients with Stage I NSCLC diagnosed from 2004 to 2009 were analyzed to determine the effects of age and treatment.

Results: The per capita incidence of NSCLC decreased in the 55–74 cohort, but increased in the 75–84 cohort over the study period. Crude lung cancer death rates in the two age groups who had no specific treatment were 39.5 and 44.9%, respectively. These rates fell in both age groups when increasingly aggressive treatment was used. Rates of OS and LCSS improved significantly with increasingly aggressive treatment in the 75–84 age group. The survival benefits of increasingly aggressive treatment in 75- to 84-year-old females did not differ from their counterparts in the younger cohort.

Conclusion: Screening for lung cancer might be of benefit to individuals at increased risk of lung cancer in the 75–84 age group. The survival benefits of aggressive therapy are similar in females between 55–74 and 75–84 years old.

Keywords: lung cancer, elderly, screening, radiotherapy, thoracic surgery

INTRODUCTION

The results of the National Lung Screening Trial (NLST) were reported in 2011 (1). This study randomized 53,454 patients who had at least a 30-pack-year history of smoking, did not have a previous history of lung cancer, and were between ages 55 and 74 years old to receive three annual low-dose computerized tomograms (CT) or a single posteroanterior chest X-ray. Patients in the CT arm had a 20% relative reduction in lung cancer-specific mortality and a 6.7% reduction in the risk of death from any cause. These reductions appear due to finding cancers at a much earlier, more curable stage than otherwise expected (1, 2). However, this trial did not include individuals aged 75 years or older (defined as “elderly”), yet more than half of all lung cancers in North Americans occur in patients aged over 70 years (3, 4). The

elderly population in the United States is increasing rapidly. Life expectancy has increased over time in all races, and the burden of lung cancer remains substantial in the elderly (5). Women aged 75 years have an average life expectancy of 12.9 years, and men have an average of 11.0 years (6).

We therefore chose to investigate whether screening might be beneficial in the elderly population (75–84 years old) by determining the outcome for patients with Stage I non-small cell lung cancer (NSCLC) in this age cohort and comparing it to that of patients 55–74 years old. Our findings suggest that individuals in both age cohorts have similar outcomes when treated in the same fashion, and therefore screening may be of benefit to elderly individuals at increased risk of lung cancer who are fit enough to undergo treatment.

DATA AND METHODS

DATA SOURCE

Data for this study were taken from the surveillance epidemiology and end results (SEER) program of the National Cancer Institute (NCI), which started to collect and publish cancer incidence and survival data from population-based cancer registries in 1973. The “SEER-9” registries are Atlanta, Connecticut, Detroit, Hawaii, Iowa, New Mexico, San Francisco-Oakland, Seattle-Puget Sound, and Utah. Data are available for cases diagnosed from 1973 and later for most of these registries. The “SEER-18” database used in this study includes the above registries and those in Los Angeles, San Jose-Monterey, Rural Georgia, Greater California, Kentucky, Louisiana, New Jersey, Greater Georgia, and the Alaska Native Tumor Registry (7). Data are available from all cases diagnosed from 2000 and later for these registries. The SEER-18 sites cover approximately 28% of the American population (8).

COHORT SELECTION

Since small cell lung cancer rarely presents at an early stage even when screening is employed (1–2.2%) (9), we excluded patients with this histology from our study. We included adults aged 55–84 years who were diagnosed with NSCLC in the SEER-18 data-base during 2004–2009. A total of 191,868 patients aged 55–74 years and 94,828 patients aged 75–84 years met the eligibility criteria. Since the data from the SEER registry are de-identified, no IRB approval was requested.

Outcome was examined for the 14,007 patients with NSCLC diagnosed during the years 2004–2009 for whom sufficient information was collected to assess the outcome of treatment in relation to patient and histopathologic variables. Patients included in this

investigation had NSCLC as their first primary cancer, tumor size 4 cm or smaller, clinical T1-2N0 disease, extension codes 100, 110, or 300, and only one type of local treatment (e.g., patients receiving both radiation and surgery were excluded).

OUTCOME VARIABLES AND OTHER COVARIATES

The outcome variables were overall survival (OS) and lung cancer-specific survival (LCSS). Deaths from other causes were treated as censoring events. The exploratory variable of main interest was the type of treatment that patients received. Treatments were categorized as: observation only; radiation only; subtotal resection (sub-lobar resection; segmental resection, including linguectomy; or wedge resection); and lobectomy or greater (lobectomy or bi-lobectomy, with or without extension to include the chest wall; lobectomy with mediastinal node dissection; extended lobectomy or bi-lobectomy, not otherwise specified; pneumonectomy with mediastinal node dissection; or pneumonectomy, not otherwise specified).

Other variables (in addition to age cohort) examined for their potential effect on outcome were: gender; year of diagnosis; marital status; race; Hispanic origin; tumor size; histology; grade; location; and extension. Median follow-up time was 26 and 21 months in the 55- to 74- and 75- to 84-year-old age groups, respectively.

STATISTICAL ANALYSIS

The incidence rates of NSCLC per 100,000 individuals in the SEER-18 population were calculated via SEERSTAT. *T*-tests were performed to analyze if there was significant difference in incidence rates by age group. Trend analyses were used to determine if incidence rates exhibit an increasing or decreasing trend over time.

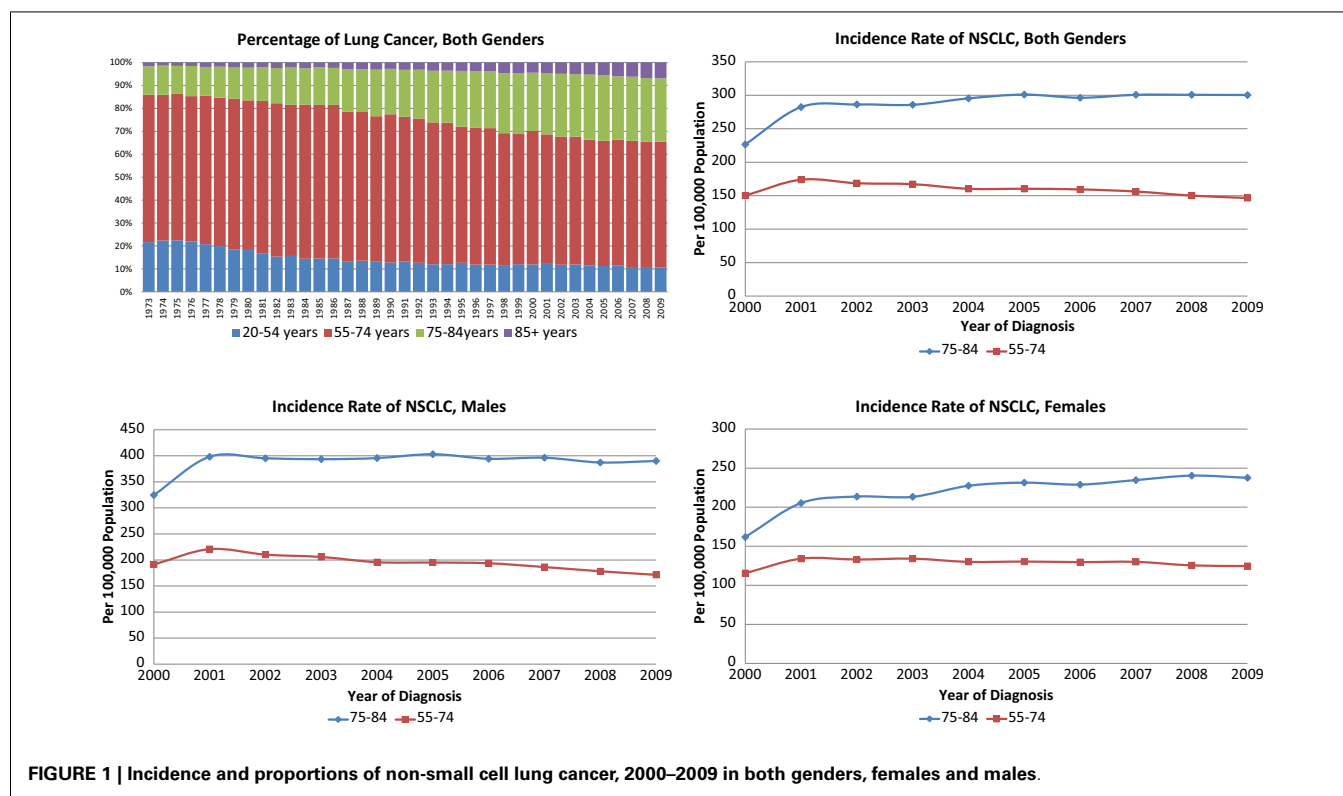


FIGURE 1 | Incidence and proportions of non-small cell lung cancer, 2000–2009 in both genders, females and males.

Table 1 | Patient characteristics by age groups (N = 14,007).

	55–74	75–84	p-Value		55–74	75–84	p-Value	
TREATMENT								
Observation	612 (6.4)	541 (12.2)	<0.0001	Left, NOS	64 (0.7)	42 (1.0)		
Radiation	903 (9.4)	829 (18.8)		Right, NOS	71 (0.7)	40 (0.9)		
Subtotal resection	1,621 (16.9)	818 (18.5)		NOS	51 (0.5)	17 (0.4)		
Lobectomy	6,452 (67.3)	2,231 (50.5)		Median tumor size, mm	19.1 (6.5)	20.5 (6.3)	<0.0001	
YEAR AT DIAGNOSIS								
2004	1,476 (15.4)	659 (14.9)	0.6155	<i>Values are N (%) or median (standard error).</i>				
2005	1,468 (15.3)	689 (15.6)		<i>Chi-square tests and t-tests.</i>				
2006	1,620 (16.9)	726 (16.4)		<i>Some values missing.</i>				
2007	1,661 (17.3)	735 (16.6)						
2008	1,664 (17.4)	788 (17.8)						
2009	1,699 (17.7)	822 (18.6)						
MARITAL STATUS								
Married	5,618 (58.6)	2,203 (49.9)	<0.0001					
Separated	91 (1.0)	16 (0.4)						
Single (never married)	989 (10.3)	245 (5.5)						
Widowed	1,315 (13.7)	1,482 (33.5)						
Unknown	281 (2.9)	135 (3.1)						
GENDER								
Female	5,189 (54.1)	2,504 (56.7)	0.0049					
Male	4,399 (45.9)	1,915 (43.3)						
RACE								
White	8,215 (85.7)	3,951 (89.4)	<0.0001					
American Indian/Alaska native	34 (0.4)	10 (0.2)						
Asian or Pacific Islander	459 (4.8)	221 (5.0)						
Black	848 (8.8)	227 (5.1)						
Other unspecified (1991+)	7 (0.1)	4 (0.1)						
Unknown	25 (0.3)	6 (0.1)						
HISPANIC ORIGIN								
Non-Spanish–Hispanic–Latino	9,209 (96.1)	4,241 (96.0)	0.8324					
Spanish–Hispanic–Latino	379 (4.0)	178 (4.0)						
HISTOLOGY								
Squamous	2,411 (28.8)	1,295 (33.1)	<0.0001					
Adenocarcinoma-BAC	780 (9.3)	282 (7.2)						
Large cell	310 (3.7)	139 (3.6)						
Adenocarcinoma	3,956 (47.3)	1,651 (42.1)						
Other NSCLC	177 (2.1)	78 (2.0)						
NSCLC NOS	727 (8.7)	473 (12.1)						
GRADE								
Well-differentiated	1,537 (16.0)	677 (15.3)	<0.0001					
Moderately differentiated	3,648 (38.1)	1,563 (35.4)						
Poorly differentiated	2,705 (28.2)	1,148 (26.0)						
Undifferentiated; anaplastic	165 (1.7)	76 (1.7)						
Unknown	1,532 (16.0)	955 (21.6)						
LOCATION (%)								
Left lower lobe	1,214 (12.7)	618 (14.0)	0.0545					
Right lower lobe	1,565 (16.3)	743 (16.8)						
Main bronchus	15 (0.2)	10 (0.2)						
Left upper lobe	2,637 (27.5)	1,241 (28.1)						
Middle Lobe	496 (5.2)	227 (5.1)						
Overlapping lesions	41 (0.5)	21 (0.5)						
Right upper lobe	3,434 (35.8)	1,460 (33.0)						

(Continued)

Chow tests were used to determine whether the slopes in two linear trend lines of incidence rates were equal by age group (10).

Chi-square and *t*-test were used to compare difference between the two age cohorts with respect to treatment, patient characteristics, and tumor characteristics. OS and LCSS were calculated using Kaplan–Meier estimation (11). The statistical significance of differences between these rates was calculated using the log-rank test. Cox proportional hazards model estimates (12) were used to show how treatment and other covariates were related to outcome. The older cohort was divided into two age groups in the multivariate analyses (aged 75–79 and 80–84 years). The hazards ratio (HR) for treatments and their corresponding *p*-values were estimated from the regression coefficient, and the standard error from the proportional hazards models.

To better understand the relationship of treatment and survival between the age cohorts, we included an interaction effect between treatment and age group in proportional hazards models. All multivariate analyses were conducted using SAS software version 9.2, and all statistical tests assumed a two-tailed $\alpha = 0.05$.

RESULTS

The annual incidence rates per 100,000 persons for NSCLC were significantly higher in the 75–84-year-old age group than in the younger age group (Figure 1). Of note, the annual incidence rates increased over time for the older female age cohort ($p = 0.0017$) while staying stable for older males and younger females and decreasing for younger males ($p = 0.0065$). The Chow tests revealed significant difference in the slopes of trend lines ($p = 0.0017$), especially for women ($p = 0.0011$). The proportion of NSCLC cases fell in the 55–74 group and increased in the 75–84 group during the study period for all stages as well as Stage I tumors ≤ 4 cm (data not shown).

Characteristics of the 14,007 patients who met our study's eligibility criteria for outcome analysis (9,588 in the younger and 4,419 in the older cohorts) are listed in Table 1. The study cohort was evenly distributed during 2004–2009, and the yearly distributions were not significantly different in the two age groups. The proportion of widowed patients in the younger group was substantially lower than in the older group (13.7 vs. 33.5%; $p < 0.0001$); 54.1% of patients in the younger group were female, which was lower than the older group (56.7%, $p = 0.0049$); and 85.7% of patients in the younger group were white, lower than in the older group (89.4%, $p < 0.0001$). Approximately 96% of

Table 2 | Top three causes of death and 5-year overall survival rates in patients with stage I non-small cell lung cancer, 2004–2009.

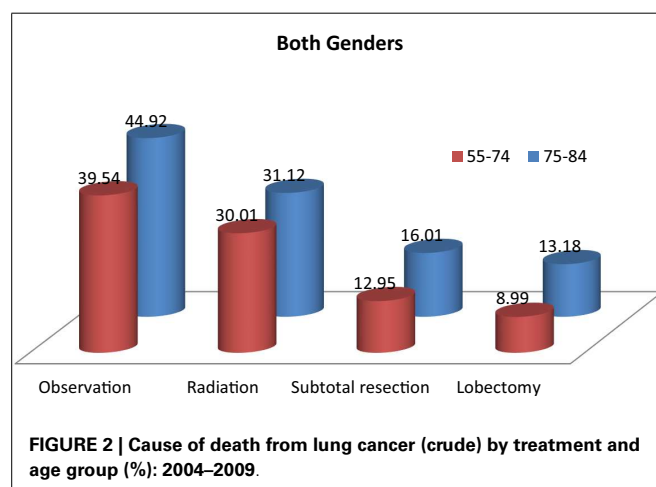
	55–74 Age group				75–84 Age group			
	Observation	Radiation	Subtotal resection	Lobectomy	Observation	Radiation	Subtotal resection	Lobectomy
Sample N	612	903	1,621	6,452	541	829	818	2,231
Alive %	40.0	54.3	77.9	84.1	33.8	53.4	68.3	74.7
Death from lung cancer %	39.5	30.0	13.0	9.0	44.9	31.1	16.0	13.2
Diseases of heart %	4.7	2.8	1.4	1.7	5.2	4.3	5.1	2.8
Chronic obstructive pulmonary disease and allied cond %	5.1	5.2	2.2	1.1	3.7	4.0	3.2	1.8
SAMPLE N								
Male	299	421	748	2,931	234	342	359	980
Female	313	482	873	3,521	307	487	459	1,251
DIED OF LUNG CANCER								
Male %	43.5	32.8	13.8	10.5	43.2	30.7	19.5	16.0
Female %	35.8	27.6	12.3	7.7	46.3	31.4	13.3	11.0
5-YEAR OVERALL SURVIVAL								
Male %	10.5	22.4	59.2	69.6	8.8	13.0	34.2	50.8
Female %	25.0	28.7	61.7	75.7	10.9	19.8	57.9	64.2

patients were non-Hispanic, and the distributions of Hispanic ethnicity were not significantly different in the two age groups. There were fewer squamous cell carcinoma patients in the younger group than in the older group (28.8 vs. 33.1%, $p < 0.0001$); and 54.1% of the tumors in the younger group were well-differentiated or moderately differentiated, higher than among patients in the older group (50.7%, $p < 0.0001$). Approximately 28% of patients had cancer diagnosed in the left upper lobe, and the distributions of location were not significantly different in the two age groups. The average tumor size was 1.4 mm smaller in the younger group than the older group (19.1 vs. 20.5 mm, $p < 0.0001$). As expected, younger patients were more likely to be treated with lobectomy or pneumonectomy (67.3 vs. 50.5%, $p < 0.0001$).

Table 2 and Figure 2 show the proportion of NSCLC patients who died (crude death rates) from lung cancer by treatment and age group during 2004–2009. Lung cancer was the most common cause of death in all treatment groups in the younger age cohort. Lung cancer was also the most common cause of death in all treatment groups in the older cohort. Crude death rates from lung cancer decreased in both age cohorts as the aggressiveness of treatment increased.

Table 2 also shows that the 5-year OS rates improved significantly with increasingly aggressive treatment in both the 55–74 and 75–84-year age groups. The survival curves in Figure 3 again reveal that OS improved significantly with increasingly aggressive treatment in the 75–84 group among both genders. The survival curves in the older group for each treatment appear to be similar to those for the younger group.

Adjusted risks of death were determined using standard multivariate Cox proportional hazards models, including year of diagnosis, marital status, race, Hispanic ethnicity, tumor size, tumor grade, tumor location, histology, tumor extension, and treatment covariates. Table 3 displays the predictors of OS and LCSS from

**FIGURE 2 | Cause of death from lung cancer (crude) by treatment and age group (%): 2004–2009.**

the hazards models in males and females in three age groups (the elderly group was split into 75- to 79- and 80- to 84-year age groups). Similar to the younger cohort, the risk of death due to any cause in the 75–79 and 80–84-year age group was significantly higher in patients treated with subtotal resection, radiation, or observation than for patients treated with lobectomy or greater.

Multivariate analysis included an interaction effect between treatment and age group showed that there are gender differences in how aggressive treatment affects outcome for patients in different age cohorts (Table 4). For female patients, the survival benefits of aggressive therapy are similar between 55–74 and 75–84 year-old age groups. In contrast, the survival benefits of aggressive therapy are different between the 55–74 group and the 75–84 group in male patients.

Table 3 | Adjusted hazards ratios for survival among the elderly age group: comparison between treatments.

	Overall survival	Lung cancer-specific survival
55–74-YEAR AGE GROUPS		
Male	<i>N</i> = 3,951	<i>N</i> = 3,951
Observation	6.090 (<0.0001)	7.285 (<0.0001)
Radiation	3.781 (<0.0001)	4.652 (<0.0001)
Subtotal resection	1.387 (0.0003)	1.401 (0.0055)
Lobectomy (reference)	1.000	1.000
Female	<i>N</i> = 4,301	<i>N</i> = 4,301
Observation	5.497 (<0.0001)	6.170 (<0.0001)
Radiation	3.487 (<0.0001)	3.838 (<0.0001)
Subtotal resection	1.697 (0.0271)	1.789 (<0.0001)
Lobectomy (reference)	1.000	1.000
75–79-YEAR AGE GROUPS		
Male	<i>N</i> = 1,087	<i>N</i> = 1,087
Observation	3.940 (<0.0001)	5.302 (<0.0001)
Radiation	2.008 (<0.0001)	2.665 (<0.0001)
Subtotal resection	1.325 (0.0451)	1.340 (0.1405)
Lobectomy (reference)	1.000	1.000
Female	<i>N</i> = 1,324	<i>N</i> = 1,324
Observation	6.268 (<0.0001)	10.283 (<0.0001)
Radiation	2.862 (<0.0001)	3.962 (<0.0001)
Subtotal resection	1.420 (0.0221)	1.533 (0.0389)
Lobectomy (reference)	1.000	1.000
80–84-YEAR AGE GROUPS		
Male	<i>N</i> = 631	<i>N</i> = 631
Observation	3.862 (<0.0001)	3.955 (<0.0001)
Radiation	1.999 (0.0003)	2.261 (0.0011)
Subtotal resection	1.878 (0.0005)	1.672 (0.0424)
Lobectomy (reference)	1.000	1.000
Female	<i>N</i> = 827	<i>N</i> = 827
Observation	4.459 (<0.0001)	5.874 (<0.0001)
Radiation	3.276 (<0.0001)	4.653 (<0.0001)
Subtotal resection	1.137 (0.5387)	1.090 (0.7816)
Lobectomy (reference)	1.000	1.000

Adjusted for year of diagnosis, marital status, race, Hispanic ethnicity, tumor size, tumor grade, tumor location, histology, and tumor extension.

Causes of mortality and death rates within 90 days of treatment are listed in **Table 5**. The mortality rates within the observation arms exceeded those of the active treatment arms for both age group categories.

DISCUSSION

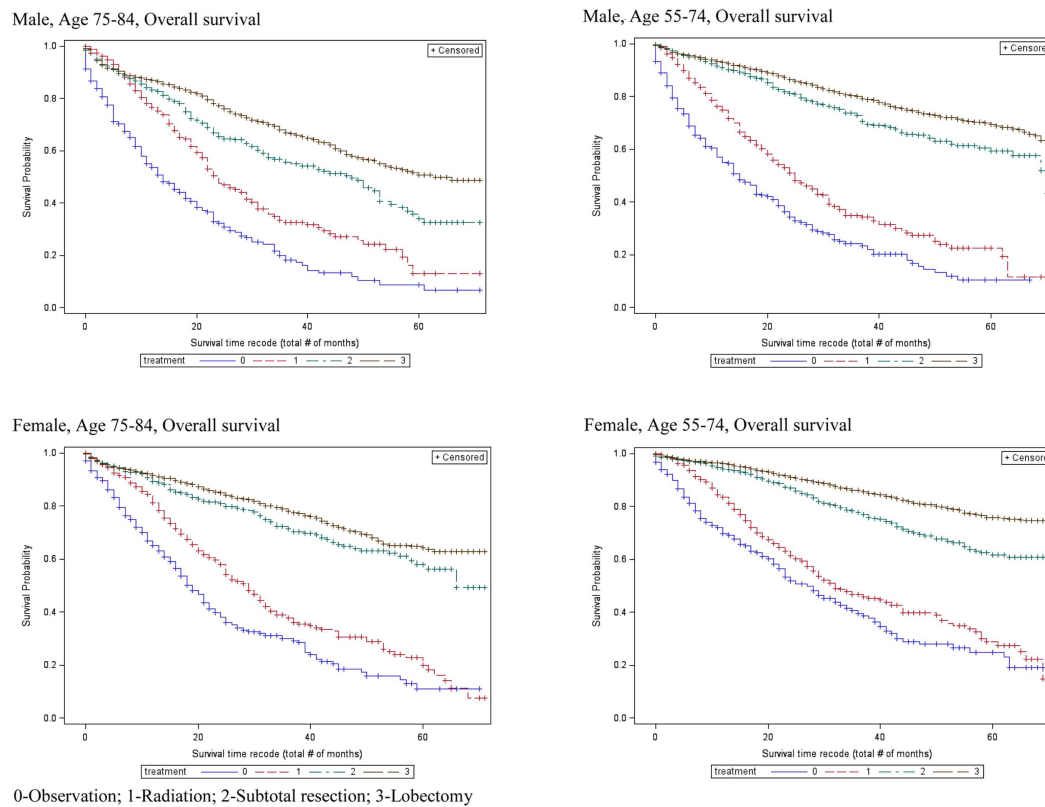
After the NLST trial report appeared, an expert panel composed of members of the National Comprehensive Cancer Network (NCCN), American College of Chest Physicians, American Society of Clinical Oncology, and American Cancer Society reviewed the literature and endorsed screening in patients aged 55–74 years who have a 30-pack-year history of smoking who continue to smoke or quit smoking within the past 15 years (13). However, the American Association for Thoracic Surgery recommended screening for smokers and former smokers with a 30-pack-year history

of smoking and long-term lung cancer survivors aged 55–79 years (4). The NCCN has recommended screening according to risk criteria starting at the age of 50, but did not recommend an upper age limit (14). Elderly patients were not included in four prospective, randomized trials investigating the role of low-dose CT screening (15–18). Although three trials included patients older than the NLST [maximum age 75, 76, and 80 years, respectively (19–21)], all are much smaller and have not reported an effect of CT screening on LCSS and OS. This is unfortunate, since the elderly make up a rapidly increasing part of the population of the United States and other industrialized countries, and their incidence rate of lung cancer is higher than for younger age groups.

The role of aggressive treatment for lung cancer in elderly patients has been controversial. Clearly some patients who might be eligible for a screening program based on smoking history will not receive either radiation or surgery because of refusal or co-morbidities. Additionally, smoking-related co-morbidities and quality of life worsen in the elderly smoking population as compared to younger patients (22). However, in our investigation, lung cancer remains the most common cause of death for patients in this age group who develop this diagnosis, and aggressive treatment seemed to benefit those who underwent it (particularly for women). Moreover, lung cancer deaths remain the most common cause of death despite the inclusion of only Stage I tumors and without the exclusion of patients with multiple co-morbidities. Additionally, despite the broad spectrum of treating physicians in SEER, the 90-day mortality remained low (<6%) in all active treatment arms, suggesting appropriate candidate selection. Because the majority of patients receive a definitive surgical procedure in the younger and older populations (84.2 and 69.0%, respectively), we assume that like past studies (23, 24), those patients not selected for surgery most likely were medically inoperable. It should be emphasized that even in this unselected population, the majority of the elderly population with Stage I NSCLC were able to receive surgery, the standard of care, with relatively low rates of mortality (30- and 31- to 90-day mortalities were 2.1 and 3.5% in the lobectomy group and 1.8 and 3.5% in the sub-lobar resection group) during the post-operative time period.

As a society, we must be concerned with the costs of screening as well as the radiation exposure in the patients undergoing screening. Nevertheless, low-dose CT screening could also be used to detect other smoking-related ailments such as coronary artery disease, chronic pulmonary disease, and osteoporosis (25) as well as other smoking-related cancers (26). Furthermore, because radiographic signs associated with COPD (pulmonary artery enlargement and percentage of lung with a density of ≤ -950 Hounsfield units) (27, 28) are associated with acute COPD and changes in FEV1, such changes could be used for evaluation and treatment.

There are many limitations to the SEER database. It does not include information concerning co-morbidities, past or present cigarette use, type of radiotherapeutic treatment [stereotactic body radiation therapy (SBRT) or conventional external beam], family history of cancer, medications, chemotherapeutic treatments, occupational exposures, symptoms of lung cancer, and recent weight loss. Additionally, our patient population is predominantly

**FIGURE 3 | Overall survival curves for patients by age groups.****Table 4 | Wald tests of the interaction effect between age group and treatment in Cox proportional hazards model.**

	N	Wald chi-square	Pr > Chi Sq
Overall survival, male, 55–74 vs. 75–79	5,038	17.3800	<0.0001
Lung cancer-specific survival, male, 55–74 vs. 75–79	5,038	6.6519	0.0839
Overall survival, male, 55–74 vs. 80–84	4,582	29.1234	<0.0001
Lung cancer-specific survival, male, 55–74 vs. 80–84	4,582	14.5713	0.0022
Overall survival, female, 55–74 vs. 75–79	5,625	6.4545	0.0915
Lung cancer-specific survival, female, 55–74 vs. 75–79	5,625	8.1917	0.0422
Overall survival, female, 55–74 vs. 80–84	5,128	7.6409	0.0540
Lung cancer-specific survival, female, 55–74 vs. 80–84	5,128	4.8190	0.1855

Adjusted for year of diagnosis, marital status, race, Hispanic ethnicity, tumor size, tumor grade, tumor location, histology, tumor extension, age group, and treatment.

Caucasian, therefore, our results may not pertain to other racial groups. Nonetheless, we feel that the findings from our study are provocative.

The success of any screening program depends upon the ability to find early-stage disease and whether treatment of early-stage disease is beneficial. Because lung cancer survival depends greatly upon initial tumor stage (29) and only small improvements in survival have been seen in the last several decades in advanced disease (30), we feel that our study may help identify a population who were not identified in the initial screening studies and who

may benefit from lung cancer screening. Although, screening may result in unnecessary treatment for breast and prostate cancers, our results show that even in Stage I tumors (4 cm or less in size) almost 40% of patients in both the younger and older groups will succumb to lung cancer if they do not receive radiation or surgery. Additionally, despite the expected increase in smoking-related comorbidities with age (22), the majority of the elderly population received surgical treatment and had an increase in survival as the treatment became increasingly aggressive similar to the younger patient group who would be eligible for screening. Furthermore,

Table 5 | Mortality rates and causes of mortality within 90 days of treatment.

	55–74 Group				75–84 Group			
	Observation	Radiation	Sub-lobar	Lobectomy	Observation	Radiation	Sub-lobar	Lobectomy
Initial patient #	612	903	1,621	6,452	541	829	818	2,231
% Mortality 30 days	8.5	0.8	1.3	1.0	9.6	1.7	1.8	2.1
% Mortality in 31–90 days	7.4	2.8	1.0	1.4	5.1	2.5	3.5	3.5
CAUSES OF MORTALITY IN FIRST 90 DAYS^a								
Lung cancer (%)	52	84	46	53	48	64	24	50
Heart disease (%)	14		11	12	17	12	26	10
COPD and related conditions (%)	9		6		7	6	17	9
Suicide and self-inflicted injury (%)		6						
Unknown (%)	7		11	13		12	7	14
Pneumonia and influenza (%)							7	6
Other infectious diseases (%)			6					
CVA (%)								5

^aOnly causes of death exceeding 5.0% were listed for each treatment and age group category.

lung cancer is the most frequent cause of cancer death in both genders (31).

It should be noted that our results demonstrate an increasing incidence of lung cancer, and beneficial effects from aggressive treatment in the 75- to 84-year-old age group, but they do not suggest a screening population *per se*. Like the NLST, we eliminated all patients with previous lung cancer and information concerning co-morbidities was not available. Additionally, co-morbidity data within large administrative databases depend upon the accuracy of coding which has been noted to be subject to much variability and underreporting in the past (32–34). However, differently than the NLST, smoking history was not known. Therefore we could not limit our analysis to patients with a 30-pack-year history of smoking. Nevertheless, because greater than 85% of lung cancers in the US are caused by cigarette smoking (35), the majority of patients in our study were most likely current or past cigarette smokers. Furthermore, even within the NLST, it appears the further refinement of eligible patients would result in a more optimal selection of candidates for screening. Sixty percent of patients at highest risk for lung cancer death in 5 years accounted for 88% of screening-prevented lung cancer deaths. These authors noted similar results when assessing the benefits of screening according to lung cancer incidence and that both the estimate of lung cancer death and incidence increased with age (36). Therefore, we feel that prospective studies are needed to assess the most beneficial populations to screen for lung cancer, but we do not feel that patients should be discriminated against screening based upon age alone.

We feel that the beneficial effects of treatment may have been underestimated in our patient population. SEER-18 represents approximately 28% of the US population regardless of physician expertise or hospital volume. Because lung cancer surgery depends greatly upon both hospital (37) and physician volume (38), the surgical outcomes may not be optimized. Additionally, SBRT has higher control rates than conventional radiotherapy and may offer an improvement in survival and control rates similar to surgical resection (24, 39). However, as of 2007, only 1.1% of

the patients with Stage I NSCLC in the Medicare-SEER population received SBRT as compared to 14.8% who received conventional radiotherapy (40). Therefore, the full beneficial effects of radiotherapy are probably under appreciated in our investigation. Moreover, SBRT can be easily administered to patients with multiple co-morbidities and may result in fewer patients being observed (39).

CONCLUSION

Because the rates of lung cancer are rising in the elderly and because increasingly aggressive treatment is beneficial in these patients, screening the 75- to 84-year-old age groups may be beneficial. Furthermore, it should be noted that most of this unselected, elderly population was able to undergo a definitive surgical resection. As recently shown in patients who were eligible for the NLST, even in the 55- to 74-year-old age group, further refinement of the at-risk patient populations is needed to find who would benefit most from screening (33). We feel that patients 75 and older should not be discriminated against lung cancer screening based upon age alone.

AUTHOR CONTRIBUTIONS

Data acquisition: Nengliang Yao, John M. Varlotto; Data analysis: John M. Varlotto, Jessica Lake, John C. Flickinger, Nengliang Yao; Manuscript writing: Abram Recht, John M. Varlotto, Nengliang Yao; Final approval: Abram Recht, John M. Varlotto, Nengliang Yao, Malcolm M. DeCamp, John C. Flickinger, Jessica Lake, Chandra P. Belani, Michael F. Reed, Jennifer W. Toth, Heath B. Mackley, Christopher N. Sciamanna, Alan Lipton, Suhail M. Ali, Christopher R. Gilbert, and Richkesvar P. M. Mahraj. Guarantor of the entire manuscript: John M. Varlotto.

REFERENCES

- National Lung Screening Trial Research Team, Aberle DR, Adams AM, Berg CD, et al. Reduced lung-cancer mortality with low-dose computed tomographic screening. *N Engl J Med* (2011) 365(5):395–409. doi:10.1056/NEJMoa1102873
- International Early Lung Cancer Action Program Investigators, Henschke CI, Yankelevitz DF, Libby DM, Pasmantier MW, Smith JP, et al. Survival of patients

- with stage I lung cancer detected on CT screening. *N Engl J Med* (2006) **355**(17):1763–71. doi:10.1056/NEJMoa060476
3. Canadian Partnership Against Cancer. *System Performance Report 2010*. Toronto: Canadian Partnership Against Cancer (2010).
 4. Jacobson FL, Austin JHM, Field JK, Jett JR, Keshavjee S, MacMahon H, et al. Development of the American Association for Thoracic Surgery guidelines for low-dose computed tomographic scans to screen for lung cancer in North America: recommendations of the American Association for Thoracic Surgery Task Force for lung cancer screening and surveillance. *J Thorac Cardiovasc Surg* (2012) **144**(1):25–32. doi:10.1016/j.jtcvs.2012.05.059
 5. Minimo AM, Murphy SL. Death in the United States, 2010. *NCHS Data Brief* (2012) **99**:1–7.
 6. National Center for Health Statistics. *Health, United States, 2011: With Special Feature on Socioeconomic Status and Health*. Hyattsville, MD: National Center for Health Statistics (2012).
 7. Surveillance, Epidemiology, and End Results (SEER) Program. *SEER Public-use Data (1973–2009)*. Bethesda, MD: National Cancer Institute, DCCPS, Surveillance Research Statistics Branch (2012). Available from: <http://seer.cancer.gov/registries/list.html>
 8. Surveillance, Epidemiology, and End Results (SEER) Program. *SEER Public-use Data (1973–2009)*. Bethesda, MD: National Cancer Institute, DCCPS, Surveillance Research Statistics Branch (2012). Available from: <http://www.seer.cancer.gov/>
 9. Varlotto JM, Recht A, Flickinger JC, Medford-Davis LN, Dyer AM, DeCamp MM. Lobectomy leads to optimal survival in early-stage small cell lung cancer: a retrospective analysis. *J Thorac Cardiovasc Surg* (2011) **142**(3):538–46. doi:10.1016/j.jtcvs.2010.11.062
 10. Chow GC. Tests of equality between sets of coefficients in two linear regressions. *Econometrica* (1960) **28**:591–605. doi:10.2307/1910133
 11. Kaplan ES, Meier P. Non-parametric estimation from incomplete observation. *J Am Stat Assoc* (1958) **53**:477–80. doi:10.1080/01621459.1958.10501452
 12. Cox DR. Regression models and life tables. *J R Stat Soc* (1972) **34**:187–220.
 13. Bach PB, Mirkin JN, Oliver TK, Azzoli CG, Berry DA, Brawley OW, et al. Benefits and harms of CT screening for lung cancer: a systematic review. *JAMA* (2012) **308**:1324–35. doi:10.1001/jama.2012.5521
 14. National Comprehensive Cancer Network. Fort Washington, PA (2012). Available from: http://www.nccn.org/patients/guidelines/lung_screening/index.html
 15. Saghir Z, Dirksen A, Ashraf H, Bach KS, Brodersen J, Clementsen PF, et al. CT screening for lung cancer brings forward early disease: the randomised Danish Lung Cancer Screening Trial: status after five annual screening rounds with low-dose CT. *Thorax* (2012) **67**(4):296–301. doi:10.1136/thoraxjnl-2011-200736
 16. Lopes Pegna A, Picozzi G, Mascalchi M, Maria Carozzi F, Carrozza L, Comin C, et al. Design, recruitment and baseline results of the ITALUNG trial for lung cancer screening with low-dose CT. *Lung Cancer* (2009) **64**(1):34–40. doi:10.1016/j.lungcan.2008.07.003
 17. Infante M, Cavuto S, Lutman FR, Brambilla G, Chiesa G, Ceresoli G, et al. A randomized study of lung cancer screening with spiral computed tomography: three-year results from the DANTE trial. *Am J Respir Crit Care Med* (2009) **180**(5):445–53. doi:10.1164/rccm.200901-0076OC
 18. Gohagan JK, Marcus PM, Fagerstrom RM, Pinsky PF, Kramer BS, Prorok PC, et al. Final results of the Lung Screening Study, a randomized feasibility study of spiral CT versus chest X-ray screening for lung cancer. *Lung Cancer* (2005) **47**(1):9–15. doi:10.1016/j.lungcan.2004.06.007
 19. van Klaveren RJ, Oudkerk M, Prokop M, Scholten ET, Nackaerts K, Vernhout R, et al. Management of lung nodules detected by volume CT scanning. *N Engl J Med* (2009) **361**(23):2221–9. doi:10.1056/NEJMoa0906085
 20. Blanchon T, Bréchet JM, Grenier PA, Ferretti GR, Lemarié E, Milleron B, et al. Baseline results of the Dépiscan study: a French randomized pilot trial of lung cancer screening comparing low dose CT scan (LDCT) and chest X-ray (CXR). *Lung Cancer* (2007) **58**(1):50–8. doi:10.1016/j.lungcan.2007.05.009
 21. Garg K, Keith RL, Byers T, Kelly K, Kerzner AL, Lynch DA, et al. Randomized controlled trial with low-dose spiral CT for lung cancer screening: feasibility study and preliminary results. *Radiology* (2002) **225**(2):506–10. doi:10.1148/radiol.2252011851
 22. Kalucka S. Social aspects of tobacco addiction and the quality of life of people smoking and non-smoking tobacco. *Przegl Lek* (2012) **69**(10):908–13.
 23. McGarry RC, Song G, des Rosiers P. Observation-only management of early stage, medically inoperable lung cancer: poor outcome. *Chest* (2002) **121**:1155–8. doi:10.1378/chest.121.4.1155
 24. Varlotto J, Fakiris A, Flickinger J, Medford-Davis L, Liss A, Shelkey J, et al. Matched-pair and propensity score comparisons of outcomes of patients with clinical stage I non-small cell lung cancer treated with resection or stereotactic radiosurgery. *Cancer* (2013) **119**(15):2683–91. doi:10.1002/cncr.28100
 25. Mets OM, de Jong PA, Prokop M. Computed tomographic screening for lung cancer: an opportunity to evaluate other diseases. *JAMA* (2012) **308**:1433–4. doi:10.1001/jama.2012.12656
 26. American Cancer Society. (2012). Available from: <http://www.cancer.org/cancer/cancercauses/tobaccocancer/tobacco-related-cancer-fact-sheet>.
 27. Wells JM, Washko GR, Han MK, Abbas N, Nath H, Mamary AJ, et al. Pulmonary arterial enlargement and acute exacerbations of COPD. *New Engl J Med* (2012) **367**:913–21. doi:10.1056/NEJMoa1203830
 28. Vestbo J, Edwards LD, Scanlon PD, Yates JC, Agusti A, Bakke P, et al. Changes in forced expiratory volume in 1 second over time in COPD. *N Engl J Med* (2011) **365**(13):1184–92. doi:10.1056/NEJMoa1105482
 29. Chansky K, Sculier JP, Crowley JJ. The International Association for the Study of Lung Cancer Staging Project: prognostic factors and pathologic TNM stage in surgically managed non-small cell lung cancer. *J Thorac Oncol* (2009) **4**(7):792–801. doi:10.1097/JTO.0b013e3181a7716e
 30. NSCLC Meta-Analyses Collaborative Group. Chemotherapy in addition to supportive care improves survival in advanced non-small-cell lung cancer: a systematic review and meta-analysis of individual patient data from 16 randomized controlled trials. *J Clin Oncol* (2008) **26**(28):4617–25. doi:10.1200/JCO.2008.17.7162
 31. Kohler BA, Ward E, McCarthy BJ, Schymura MJ, Ries LA, Eheman C, et al. Annual report to the nation on the status of cancer, 1975–2007, featuring tumors of the brain and other nervous system. *J Natl Cancer Inst* (2011) **103**:714–36. doi:10.1093/jnci/djr077
 32. Green J, Winfield N. How accurate are hospital discharge data for evaluating effectiveness of care? *Med Care* (1993) **31**(8):719–31. doi:10.1097/00005650-199308000-00005
 33. Glance LG, Osler TM, Mukamel DB, Dick AW. Impact of the present-on-admission indicator on hospital quality measurement: experience with the Agency for Healthcare Research and Quality (AHRQ) Inpatient Quality Indicators. *Med Care* (2008) **46**(2):112–9. doi:10.1097/MLR.0b013e318158aed6
 34. Romano PS, Roos LL, Luft HS, Jollis JG, Dolisny K. A comparison of administrative versus clinical data: coronary artery bypass surgery as an example. Ischemic Heart Disease Patient Outcomes Research Team. *J Clin Epidemiol* (1994) **47**:249–60. doi:10.1016/0895-4356(94)90006-X
 35. De Groot P, Munden RF. Lung cancer epidemiology, risk factors, and prevention. *Radiol Clin North Am* (2012) **50**(5):863–76. doi:10.1016/j.rcl.2012.06.006
 36. Kovalchik SA, Tammemagi M, Berg CD, Caporaso NE, Riley TL, Korch M, et al. Targeting of low-dose CT screening according to the risk of lung-cancer death. *N Engl J Med* (2013) **369**:245–54. doi:10.1056/NEJMoa1301851
 37. Hannan EL, Radzyner M, Rubin D, Dougherty J, Brennan MF. The influence of hospital and surgeon volume on in-hospital mortality for colectomy, gastrectomy, and lung lobectomy in patients with cancer. *Surgery* (2002) **131**(1):6–15. doi:10.1067/msy.2002.120238
 38. Bach PB, Cramer LD, Schrag D, Downey RJ, Gelfand SE, Begg CB. The influence of hospital volume on survival after resection for lung cancer. *N Engl J Med* (2001) **345**(3):181–8. doi:10.1056/NEJM200107193450306
 39. Palma D, Visser O, Lagerwaard FJ, Belderbos J, Slotman BJ, Senan S. Impact of introducing stereotactic lung radiotherapy for elderly patients with stage I non-small-cell lung cancer: a population-based time-trend analysis. *J Clin Oncol* (2010) **28**(35):5153–9. doi:10.1200/JCO.2010.30.0731
 40. Shirvani SM, Jiang J, Chang JY, Welsh JW, Gomez DR, Swisher S, et al. Comparative effectiveness of 5 treatment strategies for early-stage non-small cell lung cancer in the elderly. *Int J Radiat Oncol Biol Phys* (2012) **84**(5):1060–70. doi:10.1016/j.ijrobp.2012.07.2354

Conflict of Interest Statement: The authors declare that the research was conducted in the absence of any commercial or financial relationships that could be construed as a potential conflict of interest.

Received: 02 January 2014; accepted: 12 February 2014; published online: 07 March 2014.

Citation: Varlotto JM, DeCamp MM, Flickinger JC, Lake J, Recht A, Belani CP, Reed MF, Toth JW, Mackley HB, Sciamanna CN, Lipton A, Ali SM, Mahraj RPM, Gilbert

CR and Yao N (2014) Would screening for lung cancer benefit 75- to 84-year-old residents of the United States? *Front. Oncol.* **4**:37. doi: 10.3389/fonc.2014.00037
This article was submitted to Radiation Oncology, a section of the journal Frontiers in Oncology.
Copyright © 2014 Varlotto, DeCamp, Flickinger, Lake, Recht, Belani, Reed, Toth, Mackley, Sciamanna, Lipton, Ali, Mahraj, Gilbert and Yao. This is an open-access

article distributed under the terms of the Creative Commons Attribution License (CC BY). The use, distribution or reproduction in other forums is permitted, provided the original author(s) or licensor are credited and that the original publication in this journal is cited, in accordance with accepted academic practice. No use, distribution or reproduction is permitted which does not comply with these terms.



The utility of positron emission tomography in the treatment planning of image-guided radiotherapy for non-small cell lung cancer

Alexander Chi^{1*} and Nam P. Nguyen²

¹ Department of Radiation Oncology, Mary Babb Randolph Cancer Center, West Virginia University, Morgantown, WV, USA

² International Geriatric Radiotherapy Group, Tucson, AZ, USA

Edited by:

Ulf Lennart Karlsson, Marshfield Clinic, USA

Reviewed by:

Michael Chan, Wake Forest University, USA

Sunyoung Jang, Princeton Radiation Oncology, USA

***Correspondence:**

Alexander Chi, Department of Radiation Oncology, Mary Babb Randolph Cancer Center, West Virginia University, 1 Medical Center Dr. Morgantown, WV 26505, USA
e-mail: achia2010@gmail.com

In the thorax, the extent of tumor may be more accurately defined with the addition of ¹⁸F-fluorodeoxyglucose (FDG) positron emission tomography (PET) to computed tomography (CT). This led to the increased utility of FDG-PET or PET/CT in the treatment planning of radiotherapy for non-small cell lung cancer (NSCLC). The inclusion of FDG-PET information in target volume delineation not only improves tumor localization but also decreases the amount of normal tissue included in the planning target volume (PTV) in selected patients. Therefore, it has a critical role in image-guided radiotherapy (IGRT) for NSCLC. In this review, the impact of FDG-PET on target volume delineation in radiotherapy for NSCLC, which may increase the possibility of safe dose escalation with IGRT, the commonly used methods for tumor target volume delineation FDG-PET for NSCLC, and its impact on clinical outcome will be discussed.

Keywords: NSCLC, IGRT, PET, target volume delineation, treatment planning

INTRODUCTION

In recent years, ¹⁸F-fluorodeoxyglucose (FDG) positron emission tomography (PET) has emerged to be an essential tool in the staging of non-small cell lung cancer (NSCLC) (1). Tumor imaging through FDG-PET is achieved based on the difference in glucose metabolism between malignant and normal tissue, which leads to relatively increased FDG accumulation in tumor cells. FDG undergoes positron emission decay, which ultimately leads to the production of a pair of positron annihilation gamma (γ) rays (511 keV each) traveling in opposite directions (2). These two gamma rays are then detected by two opposing coincidence detectors in a PET scanner for imaging (2). Because of the ability of FDG-PET to detect malignancy prior to the development of any noticeable anatomical changes, it was consistently found to have superior sensitivity and specificity in the staging of lung cancer (3, 4). This is especially true for mediastinal staging. As shown in a meta-analysis by Gould et al., FDG-PET has superior median sensitivity and specificity over CT (85 vs. 61%, 90 vs. 79%, $p < 0.001$) in the identification of lymph node involvement by NSCLC (5). CT's median specificity improves to be superior to FDG-PET in the evaluation of enlarged lymph nodes in the same study (93 vs. 78%, $p = 0.002$). However, FDG-PET may provide additional information on the extent of tumor involvement at the primary site and in the regional lymph nodes during target volume delineation for radiotherapy planning in the treatment of NSCLC to avoid geometric tumor miss, and unnecessary inclusion of normal tissue. In the following sections, the impact of FDG-PET on radiotherapy target volume delineation for NSCLC, which may increase the likelihood of dose escalation with IGRT, the commonly used methods of defining gross tumor on FDG-PET, 4D-PET/CT imaging, and FDG-PET's impact on treatment outcome will be discussed.

IMPACT OF FDG-PET ON TARGET VOLUME DELINEATION

The incorporation of FDG-PET during target volume delineation has frequently led to changes in the shape and size of the target volumes; as well as the tumor stage when FDG-PET was not done as a part of the initially staging evaluation in patients with NSCLC. This fact has been well illustrated in multiple studies (6–14). As shown in Table 1, changes in the target volumes of over 20% and stage alteration of 20–50% have been consistently observed when FDG-PET was incorporated in target volume delineation and when FDG-PET was not a part of the initial staging studies. Most prominent changes are often associated with the presence of atelectasis in the treated areas (Figure 1), or the identification of additional nodal disease, which is difficult to visualize on CT (6–9, 11, 14) (Figure 2). This is well illustrated by Bradley et al., who demonstrated PTV and stage alteration of 58 and 31% in patients with stage I–III NSCLC when FDG-PET was incorporated in target volume delineation (9). Among 24 patients planned for definitive three-dimensional conformal radiotherapy (3D-CRT), PET led to a GTV reduction in 3 patients with atelectasis, and an increase in GTV due to the identification of additional regional nodal disease in 10 patients, and the identification of an additional parenchymal disease in 1 patient. GTV-reduction due to the utilization of PET resulted in dose reduction to the normal lungs and esophagus in patients with tumor-related atelectasis in this study, which suggests a potential advantage in the sparing of thoracic organs at risk (OAR) with the incorporation of FDG-PET in target volume delineation. This is corroborated in similar studies, which demonstrated similar PET-related target volume alterations, and the resulting decrease in the dose to the heart, esophagus, spinal cord, and the normal lungs (7, 8, 11, 12, 14). In one study, PET-related exclusion of metabolically inactive lymph

Table 1 | FDG-PET-related alteration of target volumes in NSCLC.

Reference	Stage	Volume changes due to FDG-PET	Dosimetric impact
Nestle et al. (6)	IIIB-IV	Change in size and shape of radiation fields: 35% Field size reduction: 26% (median 19.3%) More changes observed in the presence of atelectasis ($p = 0.03$)	
Erdi et al. (7)	Unknown	PTV increase (additional nodal disease): 19% ^a PTV reduction: 18% ^a	Mean heart dose decreased by 50% in the PET plan in one case
Mah et al. (8)	III (2/7)	Stage alteration: 23% PTV reduction and increase among three observers: 24–70 and 30–76%	Maximum spinal cord dose is decreased on average with PET/CT-based planning ($p \leq 0.01$)
Bradley et al. (9)	I–III (65% stage III)	Stage alteration: 31% PTV alteration: 58% GTV reduction (atelectasis): 12% GTV increase (additional primary and nodal disease): 46%	Alteration of the GTV led to corresponding changes in the dose to the esophagus and the normal lungs
van Der Wel et al. (10)	III	Nodal GTV decreased by 3.8 cm^3 on average ($p = 0.011$) Radiation field change: 66.7% (decreased in 52.4%, increased in 14.3%)	Alteration of the GTV led to corresponding changes in dose to the esophagus and the normal lungs PET enabled dose escalation from 56 Gy to 71 Gy on average ($p = 0.038$) & increased TCP by at least 6% on average ($p < 0.05$)
Ceresoli et al. (11)	66.7% III	Stage alteration: 48% $\geq 25\%$ change in GTV: 39% 5/7 with GTV increase (additional nodal disease) 2/7 with GTV reduction (PET negative enlarged LN and atelectasis)	Dose reduction to the spinal cord was observed in PET plans (median 41.7 Gy vs. 45.7 Gy, $p < 0.05$) Changes in GTV led to corresponding changes in dose to normal lung tissue
Faria et al. (13)		Stage alteration: 44% GTV alteration: 56% Decrease: 37.3% Increase: 18.7%	
Yin et al. (14)	IIIB ^b	GTV alteration: 100% (≥ 25 in 40% of patients) Decrease: 73.3% ($155.1\text{--}111.4 \text{ cm}^{3c}$) Increase: 26.7% ($125.8\text{--}144.7 \text{ cm}^{3c}$)	PET led to significant changes in V_{20} , V_{30} for the lungs and V_{50} , V_{55} of the esophagus

^aAverage; TCP, tumor control probability.^bAtelectasis present in all patients.^cMedian.

node and atelectasis resulted in GTV reduction of 39 and 84%, respectively, which led to the reduction of the mean lung dose (MLD) and volume of the normal lungs receiving 20 Gy (V_{20}) by 6.1 Gy and 12% on average (11). In the same study, the median dose to the spinal cord was reduced from 45.7 to 41.7 Gy with the incorporation of FDG-PET in target volume delineation ($p < 0.05$). In another study, GTV reduction was observed in 73.3% of patients with stage III NSCLC in the presence of atelectasis, which possibly led to statistically significant decrease in commonly used dosimetric parameters, such as V_{20} for the normal lungs, and V_{55} for the esophagus (14).

PET-related increase in the GTV has been mainly due to the identification of additional regional nodal disease (Table 1). This has been shown to result in an increase in the dose to the surrounding normal tissue (9, 11). However, this increase may not be clinically significant in all patients. As shown by Ceresoli et al., PET-related increase in GTV only resulted in an increase of the

MLD by 1.08 Gy, and the V_{20} by 2.4% on average (11). In addition, incorporation of FDG-PET in the delineation of regional nodal disease may lead to a decrease in the nodal GTV. This has been demonstrated in patients with N2-N3 disease by van Der Wel et al., who showed a PET-related decrease of the nodal GTV from 13.7 ± 3.8 to $9.9 \pm 4.0 \text{ cm}^3$ ($p = 0.011$) (10). It led to significant decrease in radiation dose to the esophagus (V_{55} decreased from 30.6 ± 3.2 to $21.9 \pm 3.8\%$, $p = 0.004$); and the normal lungs (V_{20} decreased from 24.9 ± 2.3 to $22.3 \pm 2.2\%$, $p = 0.012$). As a result, dose escalation from 56.0 ± 5.4 to 71.0 ± 13.7 Gy ($p = 0.038$) became feasible, which led to improved TCP from 14.2 ± 5.6 to $22.8 \pm 7.1\%$ ($p = 0.026$) without accounting for geometric misses, and improved TCP from 12.5 to 18.3% when that is accounted for ($p = 0.009$). These findings further demonstrate the advantage of incorporating FDG-PET information in target volume delineation especially for stage III NSCLC, which makes dose escalation possible.

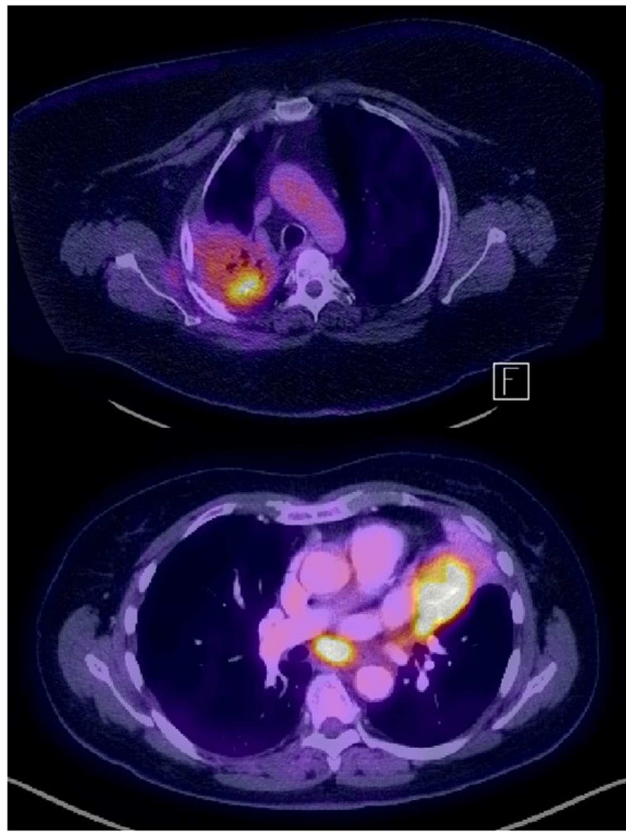


FIGURE 1 | Examples of PET-avid NSCLC in the presence of fibrosis (recurrence after chemo-radiation, top) and atelectasis (bottom).

To further investigate the accuracy of FDG-PET in identifying nodal disease, 73 NSCLC patients with known positive lymph nodes by CT, or PET and pathology data for all suspected lymph nodes were further assessed by Vanuytsel et al. (12). Using PET-CT data, inclusion of pathological nodes in the nodal GTV was found to increase from 75% with CT alone to 89% ($p = 0.005$). In their study, PET-related GTV alteration was observed in 62% of the patients. Among them, PET-related GTV increase was observed in 16/45 patients. While 11 of these 16 patients' GTV increase was supported by pathologic findings, it was unnecessary in five patients. PET incorporation resulted in GTV reduction in 29/45 patients. Twenty-five of them were correlated with pathological findings. Overall, 80% of all the PET-related GTV alterations were correct and inappropriate changes often were due to low tumor burden that is beyond the resolution of FDG-PET, or misinterpretation of the location of nodal disease. Pathology correlation in this study supports the utilization of FDG-PET in the delineation of nodal disease for NSCLC, which is shown to be more accurate than CT alone. The improved accuracy in identifying nodal disease with FDG-PET was shown by Faria et al. as well (13). However, how to improve the accuracy of PET-based identification of nodal disease from NSCLC remains to be investigated in the future. PTV reduction due to PET-related GTV reduction was again demonstrated in the study by Vanuytsel et al. in 10

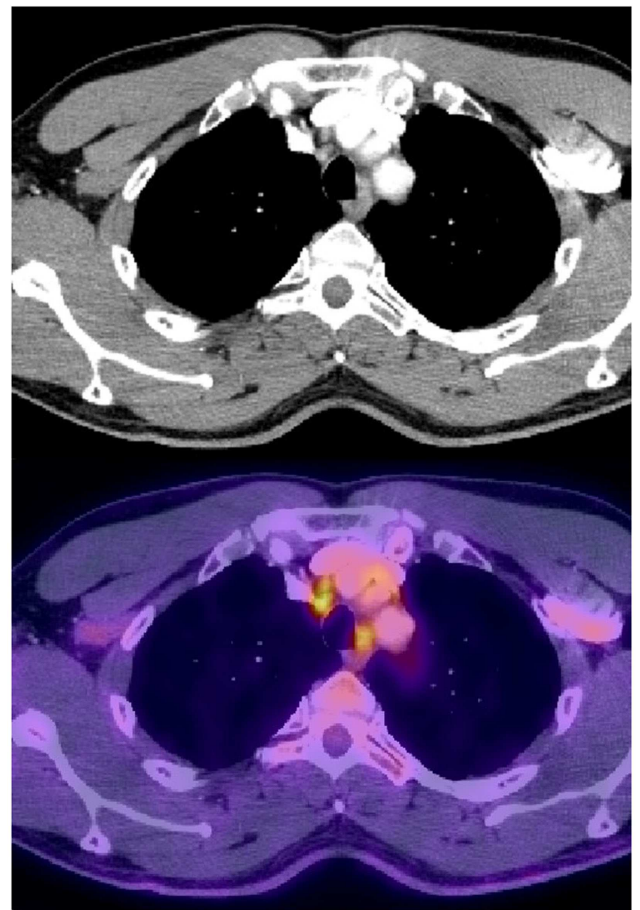


FIGURE 2 | Normal sized mediastinal lymph nodes (2R) that were PET avid and were biopsied positive in a patient with stage IIIB adenocarcinoma of the right lower lobe.

selected stage III NSCLC patients, which led to a decrease of V₂₀ of the normal lungs by $27 \pm 18\%$ ($p = 0.001$) (12). Thus, further demonstrates an advantage in OAR sparing with incorporation of PET information in target volume delineation for NSCLC, which may increase the likelihood of dose escalation in the treatment of loco-regionally confined NSCLC with definitive radiotherapy.

METHODS OF TARGET VOLUME DELINEATION ON FDG-PET

Given the multiple variables that exist in PET imaging for NSCLC (2, 3), there is no consensus on how to best delineate gross tumor on FDG-PET at the current time. Visual interpretation of the PET or PET/CT images with an expert nuclear medicine physician remains to be a frequently used approach when delineating the GTV. The maximum standardized uptake value (SUV_{max}) was quantitatively used to determine FDG-PET activity because it is the most consistent and reliable parameter used to assess tumor activity in clinical practice. It is defined as the maximum tumor concentration of FDG divided by the injected dose of FDG, corrected for the body weight of the patient [SUV_{max} = maximum activity concentration/(injected dose/body weight)]. In 87 patients with malignant and benign focal pulmonary lesions who had a

firm pathological diagnosis and at least 2 years of follow up, the sensitivity, specificity, and accuracy of 97, 82, and 92% were found when a SUV threshold of 2.5 was used for the diagnosis of lung cancer (15). This SUV threshold of 2.5 was proposed to be used as a cut-off for GTV delineation in radiotherapy planning (16). Slightly lower SUV threshold of 2 ± 0.4 has been proposed based on the PET/CT of 19 patients with stage II-III NSCLC, which could be distinctively visualized (17). Alternatively, fixed threshold from 36 to 44% of the SUV_{max} based on the source-to-background ratio for volumes larger than 4 mL has been shown to accurately identify the tumor volume in phantoms (18).

Various approaches of PET-GTV delineation of the primary tumor were compared in a study by Nestle et al. (19). The fixed 40% thresholding method was found to be inadequate especially in the setting of inhomogeneous FDG-uptake within the tumor. However, PET-GTV contoured based on direct visualization, the $SUV \geq 2.5$, and an algorithm accounting for the source-to-background

FDG-uptake ratio all correlated well with GTV of the primary tumor contoured on CT. The poor correlation between CT-based GTV and PET-GTV generated with percent thresholding was also demonstrated in a study by Devic et al. (20). Upon further analysis of 20 peripheral NSCLC, the optimal threshold was found to be dependent on tumor size: $15 \pm 6\%$ for tumors > 5 cm, $24 \pm 9\%$ for tumors $3-5$ cm, $42 \pm 2\%$ for tumors < 3 cm (21). Larger SUV_{max} was found in larger tumors in this study. Thus, a single fixed percent-threshold method of GTV delineation appears to be inadequate and this may be due to multiple factors, such as the background FDG-uptake, heterogeneous FDG-uptake in the tumor, as well as respiratory motion and tumor size.

Multiple studies have attempted to investigate how well different GTV delineation strategies correlate with the true tumor volume in surgical specimens for NSCLC (**Table 2**). In correlation with surgical pathology findings, PET/CT has been shown to be more accurate than CT or FDG-PET alone in the estimation of

Table 2 | Methods of GTV delineation on PET in correlation with surgical specimens.

	Patient no.	Method of GTV delineation on PET	Correlation between CT, PET, PET/CT, and pathological tumor size
Lin et al. (22)	37	Halo for tumor observed in fused PET-CT images	Stronger correlation between GTV and pathological tumor dimensions were observed with PET/CT Mean SUV of the external margin of halo was 2.41 ± 0.73 T stage and histology significantly influenced SUV at the edge of the halo
Yu et al. (23)	52	SUV of 2.5	FDG-PET/CT has significantly better correlation with surgical specimens than CT or PET alone, especially in the presence of atelectasis
Yu et al. (24)	15		Best correlation between PET GTV and the actual tumor was found at the SUV threshold of $31 \pm 11\%$, and absolute SUV cut-off of 3.0 ± 1.6
Wu et al. (25)	31	Thresholding with 20–55% of SUV_{max}	Maximal primary tumor dimension was more accurately predicted by CT at the window-level of 1,600 and –300 HU than PET GTVs (best correlation with pathological tumor volume at 50% SUV_{max})
Schaefer et al. (27)	15	Tumor threshold = A * mean $SUV_{70\%}$ + B * background	Pathological tumor volume: 39 ± 51 mL PET tumor volume: 48 ± 62 mL CT tumor volume: 60.6 ± 86.3 mL Both CT and PET volumes are highly correlated with pathological volumes ($p < 0.001$). Increased variation between PET and pathological tumor volumes were observed in lower lobes
van Baardwijk et al. (28)	33	Source-to-background ratio auto-segmentation	Maximal tumor diameter of the PET GTV is highly correlated with that in surgical specimens ($CC = 0.90$). Auto-segmented GTVs are smaller than manually contoured GTVs on PET/CT
Wanet et al. (31)	10	Gradient-based method Fixed threshold at 40 and 50% of the SUV_{max} . Adaptive thresholding based on the source-to-background ratio	Comparison of both CT and PET GTV Gradient-based method led to the best estimation of the GTV PET GTVs were smaller than CT GTVs in general
Cheebsumon et al. (32)	19	Absolute SUV cut-off (2.5) Fixed threshold at 50% and 70% SUV_{max} Adaptive thresholding 41–70% SUV_{max} Contrast-oriented algorithm Source-to-background ratio Gradient-based method	Adaptive 50% and gradient-based methods generated the most consistent maximal tumor dimension, which had a fair correlation with the pathological tumor size

tumor size for NSCLC (22, 23). In a study of 37 patients, the mean SUV at the edge of the PET tumor halo which corresponded to the edge of the tumor on pathology was 2.41 ± 0.73 (22). In a different study, GTV delineated on PET/CT using a SUV cut-off value of 2.5 resulted in the best correlation with the pathological tumor volume (23). In an analysis of 15 lobectomy specimens after PET/CT imaging, the most optimal percent threshold, and absolute SUV cut-off that correlated with the pathologic tumor volume (GTV_{path}) were found to be $31 \pm 11\%$, and 3.0 ± 1.6 , respectively (24). Only the SUV percent threshold was correlated with the GTV_{path} and the tumor diameter in this study ($p < 0.05$). However, limitations have been observed with both approaches of GTV delineation based on pathological correlation. The SUV cut-off at the edge of the tumor on PET has been shown to be dependent on tumor size and histology by Lin et al. (22). In their study, higher mean SUV is observed with tumors over 3 cm and of squamous histology. In contrary to the studies described above, thresholding has been shown to be less accurate than CT in predicting the maximal tumor dimension in pathological tumor specimens in 31 patients who underwent lobectomy shortly after PET/CT (25). The uncertainties associated with percent thresholding or the use of an absolute SUV cut-off for GTV delineation appear to be influenced by the background FDG concentration and the tumor size, which are reflected by the mean SUV. To minimize the impact of these factors, it was proposed to adjust percent thresholding based on the mean target SUV in order to accurately define the gross tumor (26).

To account for the effects of tumor volume and background FDG concentration, a contrast-oriented thresholding algorithm (COA) was proposed for the delineation of PET GTV for NSCLC (27). This approach was shown to reduce the GTV volume when compared to CT alone. Also, it was shown to be highly correlated to the pathological tumor volume. Similar findings were obtained in a study of 33 patients with NSCLC when a source-to-background ratio based auto-segmentation approach was used (28). These studies demonstrate the feasibility of an adaptive thresholding approach for GTV delineation on PET. However, higher variation between pathological and PET tumor volumes were observed in the lower lobes with the COA, suggesting respiratory motion to be a source of inaccuracy in GTV delineation on PET (27).

A gradient-based approach for PET-GTV delineation has been proposed to minimize the statistical noise, and resolution blur (more pronounced in the setting of large respiration induced tumor motion) (29). When compared to other methods of GTV delineation on PET, this method was found to be the most accurate in a phantom study by Werner-Wasik et al. (30). This approach was also compared with other methods of GTV delineation in surgical specimen correlations studies (31, 32). It was found to be superior to manual, fixed thresholding at 40 and 50%, and the source-to-background ratio methods of PET-GTV delineation, and manual CT GTV delineation on 4D-PET/CT in 10 patients with stage I-II NSCLC who underwent lobectomy (31). In another study of 19 patients who underwent free-breathing PET/CT prior to surgery, the gradient method was found to be highly correlated with the maximal tumor size in surgical specimens as well (32). Thus, the gradient-based method is highly promising, which warrants further investigation in future trials. While the various methods discussed are shown to be feasible, they are often confounded by

factors, such as statistical noise, blurring effect due to respiratory motion, and uncertainties in the estimation of pathological tumor size in surgical correlative studies. Thus, further studies need to be conducted to explore what would be the best method for the most accurate GTV delineation on PET.

IMPROVING PET-GTV DELINEATION WITH 4D-PET/CT

Respiratory motion often causes blurring and alteration of the FDG-uptake within the tumor, which lead to uncertainties in the delineation of the gross tumor volume on PET (33). These uncertainties may potentially be minimized with 4D-PET/CT imaging for more accurate identification of the true extent of the tumor in various portions of the respiratory cycle, and low volume disease, which may be missed on free-breathing PET/CT (34, 35). As shown by Lamb et al., tumor volumes delineated on 4D-PET not only correlates better with that delineated on 4D CT, but also enhances the estimation of the true extent of tumor in the vicinity of similar density soft tissues, such as the diaphragm, chest wall, and the heart (36). Thus, the GTV delineation on PET can be improved with 4D-PET/CT imaging. This is, especially, helpful in image-guided radiotherapy (IGRT) due to the very small PTV margins used, which allows for dose escalation to the gross disease without significantly increase the risk of severe toxicities to normal thoracic structures. Therefore, 4D-PET-based tumor target delineation should be used as often as possible when a high dose of radiation is delivered in the thorax.

DELINEATION OF NODAL DISEASE ON PET

The delineation of regional nodal disease on PET has been conducted in similar ways as that for the primary tumor. Various methods were compared by Nestle et al., who again demonstrated that an algorithm accounting for the source-to-background FDG-uptake ratio was superior to direct visualization, 40% thresholding, or the $\text{SUV} \geq 2.5$ cut-off methods (37). Furthermore, the nodal volume delineated on PET tends to be larger than that delineated on CT, which was felt to be possibly caused by respiratory motion. This was corroborated in a study on 4D-PET-based nodal disease delineation (38). As shown in this study, a 3D nodal internal target volume (ITV) expansion of over 1 cm is required to cover 91% of the lymph nodes while accounting for respiratory motion. While it is still inadequate in situations of highly mobile lymph nodes. On the contrary, 4D-PET-based ITV was able to not only adequately encompass nodal disease in the setting of respiratory motion, but also sparing additional normal tissue ($45 \pm 34 \text{ cm}^3$) when compared with 3D nodal ITV generated with large margins that would be required to account for respiratory motion in the majority of the cases. Thus, 4D-PET imaging may improve precise and accurate localization of mediastinal disease over CT, which can potentially improve targeting in the mediastinum for the delivery of IGRT in the treatment of lung cancer.

CLINICAL OUTCOME FOLLOWING PET-BASED PLANNING

In recent years, two studies have reported the clinical outcome following concurrent chemo-radiation for stage II-III NSCLC when the target volumes were delineated based on FDG-PET findings (39, 40). In a pilot study of 32 patients, only one regional failure and one local progression were observed shortly after concurrent chemo-radiation when only PET-avid disease was included

in the target volume (39). The nodal failure was later identified to be a missed PET-avid lymph node that was not included in the target volume. In another study of 137 patients with stage III NSCLC, local-regional recurrence alone as the first event was only 14.6%, while that combined with distant metastasis as the first event was 16.8% following concurrent chemo-radiation to a median dose of 65 ± 6 Gy when only PET-avid disease was treated (40). These findings suggest that PET-based planning may lead to at least equivalent clinical outcomes when compared with CT-based planning (41). However, additional normal tissue sparing may be achieved with PET-based GTV delineation, which may aid dose escalation to the primary tumor to improve the local control of locally advanced NSCLC. As suggested in a meta-analysis, this may potentially improve patient survival (42).

NOVEL PET TRACERS FOR DOSE PAINTING

Residual disease at the primary tumor site can often be identified on the pre-radiotherapy PET, which may be treated with a higher dose with dose painting through IMRT to enhance local control of the primary tumor (43). To better identify radio-resistant tumor cells within the primary tumor, hypoxia imaging with PET has been explored in recent years. PET with hypoxia tracers, such as F-MISO, 18F-FAZA, or 18F-HX4, have been shown to be able to identify areas of hypoxia in multiple cancers, including lung cancer (44–46). This may help identify areas at a higher risk for tumor recurrence, which may need to be treated with a higher daily dose than the remaining portions of the gross tumor with dose painting (47, 48). As of current, dose painting to deliver a higher dose to areas of higher radio-resistance remains to be further investigated.

REFERENCES

- Truong MT, Viswanathan C, Erasmus JJ. Positron emission tomography/computed tomography in lung cancer staging, prognosis, and assessment of therapeutic response. *J Thorac Imaging* (2011) **26**:132–46. doi:10.1097/RTI.0b013e3182128704
- Nestle U, Kremp S, Grosu AL. Practical integration of [18F]-FDG-PET and PET-CT in the planning of radiotherapy for non-small cell lung cancer (NSCLC): the technical basis, ICRU-target volumes, problems, perspectives. *Radiother Oncol* (2006) **81**:209–25. doi:10.1016/j.radonc.2006.09.011
- Coleman RE. PET in lung cancer. *J Nucl Med* (1999) **40**:814–20.
- Gambhir SS, Czernin J, Schwimmer J, Silverman DHS, Coleman E, Phelps ME. A tabulated summary of the FDG PET literature. *J Nucl Med* (2001) **42**:IS–93S.
- Gould MK, Kuschner WG, Rydzak CE, Maclean CC, Demas AN, Shigemitsu H, et al. Test performance of positron emission tomography and computed tomography for mediastinal staging in patients with non-small-cell lung cancer: a meta-analysis. *Ann Intern Med* (2003) **139**:879–92. doi:10.7326/0003-4819-139-11-200311180-00013
- Nestle U, Walter K, Schmidt S, Licht N, Nieder C, Motaref B, et al. ^{18}F -deoxyglucose positron emission tomography (FDG-PET) for the planning of radiotherapy in lung cancer: high impact in patients with atelectasis. *Int J Radiat Oncol Biol Phys* (1999) **44**:593–7. doi:10.1016/S0360-3016(99)00061-9
- Erdi YE, Rosenzweig K, Erdi AK, Macapinlac HA, Hu YC, Brabian LE, et al. Radiotherapy treatment planning for patients with non-small cell lung cancer using positron emission tomography (PET). *Radiother Oncol* (2002) **62**:51–60. doi:10.1016/S0167-8140(01)00470-4
- Mah K, Caldwell CB, Ung YC, Darjoux CE, Balogh JM, Ganguli SN, et al. The impact of 18FDG-PET on target and critical organs in CT-based treatment planning of patients with poorly defined non-small-cell lung carcinoma: a prospective study. *Int J Radiat Oncol Biol Phys* (2002) **52**:339–50. doi:10.1016/S0360-3016(01)01824-7
- Bradley J, Thorstad WL, Mutic S, Miller TR, Dehdashti F, Siegel BA, et al. Impact of FDG-PET on radiation therapy volume delineation in non-small-cell lung cancer. *Int J Radiat Oncol Biol Phys* (2004) **59**:78–86. doi:10.1016/j.ijrobp.2003.10.044
- van Der Wel A, Nijsten S, Hochstenbag M, Lamers R, Boersma L, Wanders R, et al. Increased therapeutic ratio by 18FDG-PET CT planning in patients with clinical CT stage N2-N3M0 non-small-cell lung cancer: a modeling study. *Int J Radiat Oncol Biol Phys* (2005) **61**:649–55. doi:10.1016/j.ijrobp.2004.06.205
- Ceresoli GL, Cattaneo GM, Castellone P, Rizzos G, Landoni C, Gregorc V, et al. Role of computed tomography and $[^{18}\text{F}]$ fluorodeoxyglucose positron emission tomography image fusion in conformal radiotherapy of non-small cell lung cancer: a comparison with standard techniques with and without elective nodal irradiation. *Tumori* (2007) **93**:88–96.
- Vanuytsel LJ, Vansteenkiste JF, Stroobants SG, De Leyn PR, De Wever W, Verbeke EK, et al. The impact of (18) F-fluoro-2-deoxy-D-glucose positron emission tomography (FDG-PET) lymph node staging on the radiation treatment volumes in patients with non-small cell lung cancer. *Radiother Oncol* (2000) **55**:317–24. doi:10.1016/S0167-8140(00)00138-9
- Faria SL, Menard S, Devic S, Sirois C, Souhami L, Lisbona R, et al. Impact of FDG-PET/CT on radiotherapy volume delineation in non-small-cell lung cancer and correlation of imaging stage with pathologic findings. *Int J Radiat Oncol Biol Phys* (2008) **70**:1035–8. doi:10.1016/j.ijrobp.2007.07.2379
- Yin LJ, Yu XB, Ren YG, Gu GH, Ding TG, Lu Z. Utilization of PET-CT in target volume delineation for three-dimensional conformal radiotherapy in patients with non-small cell lung cancer and atelectasis. *Multidiscip Respir Med* (2013) **8**:21. doi:10.1186/2049-6958-8-21
- Duhaylongsod FG, Lowe VJ, Patz EF Jr, Vaughn AL, Coleman RE, Wolfe WG. Detection of primary and recurrent lung cancer by means of F-18 fluorodeoxyglucose positron emission tomography (FDG PET). *J Thorac Cardiovasc Surg* (1995) **110**:130–9. doi:10.1016/S0022-5223(05)80018-2
- Paulino AC, Johnstone PA. FDG-PET in radiotherapy treatment planning: Pandora's box? *Int J Radiat Oncol Biol Phys* (2004) **59**:4–5. doi:10.1016/j.ijrobp.2003.10.045
- Ashamalla H, Rafla S, Parikh K, Mokhtar B, Goswami G, Kambam S, et al. The contribution of integrated PET/CT to the evolving definition of treatment volumes in radiation treatment planning in lung cancer. *Int J Radiat Oncol Biol Phys* (2005) **63**:1016–23. doi:10.1016/j.ijrobp.2005.04.021
- Erdi YE, Mawlawi O, Larson SM, Imbriaco M, Yeung H, Finn R, et al. Segmentation of lung lesion volume by adaptive positron emission tomography image thresholding. *Cancer* (1997) **80**:2505–9. doi:10.1002/(SICI)1097-0142(19971215)80:12<2505::AID-CNCR24>3.3.CO;2-B
- Nestle U, Kremp S, Schaefer-Schuler A, Sebastian-Welsch C, Hellwig D, Rübe C, et al. Comparison of different methods for delineation of ^{18}F -FDG PET-positive tissue for target volume definition in radiotherapy of patients with non-small cell lung cancer. *J Nucl Med* (2005) **46**:1342–8.
- Devic S, Tomic N, Faria S, Menard S, Lisbona R, Lehnert S. Defining radiotherapy target volumes using 18F-fluoro-deoxy-glucose positron emission tomography/computed tomography: still a pandora's box? *Int J Radiat Oncol Biol Phys* (2010) **78**:1555–62. doi:10.1016/j.ijrobp.2010.02.015
- Biehl KJ, Kong FM, Dehdashti F, Jin JY, Mutic S, El Naqa I, et al. 18F-FDG PET definition of gross tumor volume for radiotherapy of non-small cell lung cancer: is a single standardized uptake value threshold approach appropriate? *J Nucl Med* (2006) **47**:1808–12.
- Lin S, Han B, Yu L, Shan D, Wang R, Ning X. Comparison of PET-CT images with the histological picture of a resectable primary tumor for delineating GTV in nonsmall cell lung cancer. *Nucl Med Commun* (2011) **36**:479–85. doi:10.1097/MNM.0b013e32834508d2
- Yu HM, Liu YF, Hou M, Liu J, Li XN, Yu JM. Evaluation of gross tumor size using CT, ^{18}F -FDG PET, integrated ^{18}F -FDG PET/CT and pathological analysis in non-small cell lung cancer. *Eur J Radiol* (2009) **72**:104–13. doi:10.1016/j.ejrad.2008.06.015
- Yu J, Li X, Xing L, Mu D, Fu Z, Sun X, et al. Comparison of tumor volumes as determined by pathologic examination and FDG-PET/CT images of non-small-cell lung cancer: a pilot study. *Int J Radiat Oncol Biol Phys* (2009) **75**:1468–74. doi:10.1016/j.ijrobp.2009.01.019
- Wu K, Ung YC, Hornby J, Freeman M, Hwang D, Tsao MS, et al. PET CT thresholds for radiotherapy target definition in non-small-cell lung cancer: how close are we to the pathologic findings? *Int J Radiat Oncol Biol Phys* (2010) **77**:699–706. doi:10.1016/j.ijrobp.2009.05.028
- Black QC, Grills IS, Kestin LL, Wong CY, Wong JW, Martinez AA, et al. Defining a radiotherapy target with positron emission tomography. *Int J Radiat Oncol Biol Phys* (2004) **60**:1272–82. doi:10.1016/j.ijrobp.2004.06.254

27. Schaefer A, Kim YJ, Kremp S, Mai S, Fleckenstein J, Bohnenberger H, et al. PET-based delineation of tumour volumes in lung cancer: comparison with pathological findings. *Eur J Nucl Med Mol Imaging* (2013) **40**:1233–44. doi:10.1007/s00259-013-2407-x
28. van Baardwijk A, Bosmans G, Boersma L, Buijsen J, Wanders S, Hochstenbag M, et al. PET-CT-based auto-contouring in non-small-cell lung cancer correlates with pathology and reduces interobserver variability in the delineation of the primary tumor and involved nodal volumes. *Int J Radiat Oncol Biol Phys* (2007) **68**:771–8. doi:10.1016/j.ijrobp.2006.12.067
29. Geets X, Lee JA, Bol A, Lonneux M, Grégoire V. A gradient-based method for segmenting FDG-PET images: methodology and validation. *Eur J Nucl Med Mol Imaging* (2007) **34**:1427–38. doi:10.1007/s00259-006-0363-4
30. Werner-Wasik M, Nelson AD, Choi W, Arai Y, Faulhaber PF, Kang P, et al. What is the best way to contour lung tumors on PET scans? Multiobserver validation of a gradient-based method using a NSCLC digital PET phantom. *Int J Radiat Oncol Biol Phys* (2012) **82**:1164–71. doi:10.1016/j.ijrobp.2010.12.055
31. Wanet M, Lee JA, Weynand B, De Bast M, Poncelet A, Lacroix V, et al. Gradient-based delineation of the primary GTV on FDG-PET in non-small cell lung cancer: a comparison with threshold-based approaches, CT and surgical specimens. *Radiother Oncol* (2011) **98**:117–25. doi:10.1016/j.radonc.2010.10.006
32. Cheeseman P, Boellaard R, de Ruyscher D, van Elmpt W, van Baardwijk A, Yaqub M, et al. Assessment of tumour size in PET/CT lung cancer studies: PET- and CT-based methods compared to pathology. *EJNMMI Research* (2012) **2**:56. doi:10.1186/2191-219X-2-56
33. Nehmeh SA, Erdi YE, Ling CC. Effect of respiratory gating on reducing lung motion artifacts in PET imaging of lung cancer. *Med Phys* (2002) **29**:366–71. doi:10.1118/1.1448824
34. Aristophanous M, Yap JT, Killoran JH, Chen AB, Berbeco RI. Four-dimensional positron emission tomography: implications for dose painting of high-uptake regions. *Int J Radiat Oncol Biol Phys* (2011) **80**:900–8. doi:10.1016/j.ijrobp.2010.08.028
35. Aristophanous M, Berbeco RI, Killoran JH, Yap JT, Sher DJ, Allen AM, et al. Clinical utility of 4D FDG-PET/CT scans in radiation treatment planning. *Int J Radiat Oncol Biol Phys* (2012) **82**:e99–105. doi:10.1016/j.ijrobp.2010.12.060
36. Lamb JM. Generating lung tumor internal target volumes from 4D-PET maximum intensity projections. *Med Phys* (2011) **38**:5732–7. doi:10.1118/1.3633896
37. Nestle U, Schaefer-Schuler A, Kremp S, Groeschel A, Hellwig D, Rübe C, et al. Target volume definition for ¹⁸F-FDG PET-positive lymph nodes in radiotherapy of patients with non-small cell lung cancer. *Eur J Nucl Med Mol Imaging* (2007) **34**:453–62. doi:10.1007/s00259-006-0252-x
38. Lamb JM, Robinson CG, Bradley JD, Low DA. Motion-specific internal target volumes for FDG-avid mediastinal and hilar lymph nodes. *Radiother Oncol* (2013) **109**:112–6. doi:10.1016/j.radonc.2013.07.015
39. Fleckenstein J, Hellwig D, Kremp S, Grgic A, Gröschel A, Kirsch CM, et al. F-18-FDG-PET confined radiotherapy of locally advanced NSCLC with concomitant chemotherapy: results of the PET-PLAN pilot trial. *Int J Radiat Oncol Biol Phys* (2011) **81**:e283–9. doi:10.1016/j.ijrobp.2011.01.020
40. van Baardwijk A, Reymen B, Wanders S, Borger J, Ollers M, Dingemans AM, et al. Mature results of a phase II trial on individualised accelerated radiotherapy based on normal tissue constraints in concurrent chemo-radiation for stage III non-small cell lung cancer. *Eur J Cancer* (2012) **48**:2339–46. doi:10.1016/j.ejca.2012.04.014
41. Chi A, Nguyen NP, Welsh JS, Tse W, Monga M, Oduntan O, et al. Strategies of dose escalation in the treatment of locally advanced non-small cell lung cancer: image guidance and beyond. *Front Oncol* (2014) **4**:156. doi:10.3389/fonc.2014.00156
42. Aupérin A, Le Péchoux C, Rolland E, Curran WJ, Furuse K, Fournel P, et al. Meta-analysis of concomitant versus sequential radiochemotherapy in locally advanced non-small-cell lung cancer. *J Clin Oncol* (2010) **28**:2181–90. doi:10.1200/JCO.2009.26.2543
43. Aerts HJ, Bussink J, Oyen WJ, van Elmpt W, Folgering AM, Emans D, et al. Identification of residual metabolic-active areas within NSCLC tumours using a pre-radiotherapy FDG-PET-CT scan: a prospective validation. *Lung Cancer* (2012) **75**:73–6. doi:10.1016/j.lungcan.2011.06.003
44. Tachibana I, Nishimura Y, Shibata T, Kanamori S, Nakamatsu K, Koike R, et al. A prospective clinical trial of tumor hypoxia imaging with ¹⁸F-fluoromisonidazole positron emission tomography and computed tomography (F-MISO PET/CT) before and during radiation therapy. *J Radiat Res* (2013) **54**:1078–84. doi:10.1093/jrr/rrt033
45. Postema EJ, McEwan AJ, Riauka TA, Kumar P, Richmond DA, Abrams DN, et al. Initial results of hypoxia imaging using 1-alpha-D: -(5-deoxy-5-[¹⁸F]-fluoroarabinofuranosyl)-2-nitroimidazole (¹⁸F-FAZA). *Eur J Nucl Med Mol Imaging* (2009) **36**:1565–73. doi:10.1007/s00259-009-1154-5
46. Zegers CM, van Elmpt W, Wierts R, Reymen B, Sharifi H, Öllers MC, et al. Hypoxia imaging with [¹⁸F]HX4 PET in NSCLC patients: defining optimal imaging parameters. *Radiother Oncol* (2013) **109**:58–64. doi:10.1016/j.radonc.2013.08.031
47. Eschmann SM, Paulsen F, Reimold M, Dittmann H, Welz S, Reischl G, et al. Prognostic impact of hypoxia imaging with ¹⁸F-misonidazole PET in non-small cell lung cancer and head and neck cancer before radiotherapy. *J Nucl Med* (2005) **46**:253–60.
48. Gagel B, Reinartz P, Demirel C, Kaiser HJ, Zimmy M, Piroth M, et al. [¹⁸F] fluoromisonidazole and [¹⁸F] fluorodeoxyglucose positron emission tomography in response evaluation after chemo-/radiotherapy of non-small-cell lung cancer: a feasibility study. *BMC Cancer* (2006) **6**:51. doi:10.1186/1471-2407-6-51

Conflict of Interest Statement: The Guest Associate Editor Ulf Lennart Karlsson declares that, despite having collaborated with Nam P. Nguyen, the review process was handled objectively and no conflict of interest exists. The authors declare that the research was conducted in the absence of any commercial or financial relationships that could be construed as a potential conflict of interest.

Received: 31 March 2014; accepted: 20 September 2014; published online: 07 October 2014.

*Citation: Chi A and Nguyen NP (2014) The utility of positron emission tomography in the treatment planning of image-guided radiotherapy for non-small cell lung cancer. *Front. Oncol.* **4**:273. doi: 10.3389/fonc.2014.00273*

*This article was submitted to Radiation Oncology, a section of the journal *Frontiers in Oncology*.*

Copyright © 2014 Chi and Nguyen. This is an open-access article distributed under the terms of the Creative Commons Attribution License (CC BY). The use, distribution or reproduction in other forums is permitted, provided the original author(s) or licensor are credited and that the original publication in this journal is cited, in accordance with accepted academic practice. No use, distribution or reproduction is permitted which does not comply with these terms.



4D PET/CT as a strategy to reduce respiratory motion artifacts in FDG-PET/CT

Alexander Chi^{1*} and Nam P. Nguyen²

¹ Department of Radiation Oncology, Mary Babb Randolph Cancer Center, West Virginia University, Morgantown, WV, USA

² The International Geriatric Radiotherapy Group, Tucson, AZ, USA

Edited by:

Ulf Lennart Karlsson, Marshfield Clinic, USA

Reviewed by:

Kathryn Huber, Tufts Medical Center, USA

Alina Mihaela Mihai, UPMC Beacon Hospital, Ireland

Ulf Lennart Karlsson, Marshfield Clinic, USA

***Correspondence:**

Alexander Chi, Mary Babb Randolph Cancer Center, West Virginia University, P.O. Box 9234, 1 Medical Center Drive, Morgantown, WV 26505, USA
e-mail: achiaz2010@gmail.com

The improved accuracy in tumor identification with FDG-PET has led to its increased utilization in target volume delineation for radiotherapy treatment planning in the treatment of lung cancer. However, PET/CT has constantly been influenced by respiratory motion-related image degradation, which is especially prominent for small lung tumors in the peri-diaphragmatic regions of the thorax. Here, we describe the current findings on respiratory motion-related image degradation in PET/CT, which may bring uncertainties to target volume delineation for image guided radiotherapy (IGRT) for lung cancer. Furthermore, we describe the evidence suggesting 4D PET/CT to be one strategy to minimize the impact of respiratory motion-related image degradation on tumor target delineation for thoracic IGRT. This, in our opinion, warrants further investigation in future IGRT-based lung cancer trials.

Keywords: lung cancer, IGRT, PET, PET/CT, target volume delineation

INTRODUCTION

In recent years, ¹⁸F fluorodeoxyglucose positron emission tomography/computed tomography (FDG-PET/CT) is increasingly used in the delineation of gross tumor for thoracic radiotherapy planning purposes (1, 2). As of now, multiple methods of PET-based tumor volume delineation exist and are being used in clinical practice (3, 4). Although PET/CT may potentially improve tumor delineation, quality and FDG uptake quantification of the PET/CT image are often impaired by respiratory motion. This may lead to decreased accuracy in lung cancer target volume delineation, which decreases the efficacy of thoracic image guided radiotherapy (IGRT), as the utmost accuracy in tumor localization is desired in IGRT to achieve the most optimal tumor control and normal tissue sparing at the same time. The main cause of this limitation is the difference in the speed of imaging between PET and CT.

In the following sections, the respiratory motion artifacts in PET/CT imaging; and four-dimensional (4D, which accounts for changes in time) PET/CT as a potential strategy to reduce respiratory motion artifacts in the PET/CT imaging of lung cancer will be discussed as this may potentially improve the target volume delineation for thoracic IGRT.

RESPIRATION MOTION ARTIFACTS IN FDG-PET/CT

Computed tomography and positron emission tomography imaging are done at different speeds. While a CT scan can be completed in seconds, the PET is usually done through a sequence of fields of view (FOV) in a matter of several minutes per FOV. As a result, the CT image may capture the lung tumor in a segment of the respiratory cycle only, while the PET image tends to represent an average of the tumor position over several respiratory cycles. This

often leads to blurring and/or misrepresentation of the extent of the gross tumor in the registered PET/CT images of the thorax (Figure 1). At the same time, the pattern of FDG uptake intensity within the gross tumor can be changed by respiration, leading to a decrease in the max SUV of the tumor.

Respiratory motion artifacts on PET/CT have been well described in a series of studies (Table 1). In one study, different anatomical points between the apices and the diaphragmatic domes of the lungs on PET/CTs were identified and matched (5). For each patient, the PET was registered to CTs obtained during maximum inspiration, maximum expiration, free breathing, and normal expiration. Prominent mismatch between FDG-PET and CT was found during maximum inspiration and maximum expiration, and the best PET/CT co-registration occurred when the CT was obtained during normal expiration (5). Mismatch between PET and CT was most prominent at the diaphragmatic dome. On average, it was 0.4 mm with the CT taken during normal expiration, but 44.4 mm with the CT taken during maximum inspiration ($p = 0.001$). This has a direct influence on image registration for tumor in PET/CT.

In another study, the accuracy of PET and CT registration for non-small cell lung cancer was investigated with CT obtained during shallow breathing or normal expiration (6). The most prominent incongruence of gross tumor on CT and on PET was observed at the periphery and the base of the lungs (0.5–14.7, 2.9–11.3 mm, respectively). Much less incongruence was observed in the central and apical regions of the lungs (1.7–5.4, 0.7–5.9 mm, respectively) ($p < 0.0001$). In this study, normal expiration appears to be better than shallow breathing for PET/CT matching ($p = 0.024$).

Errors in spatial registration of lung lesions on PET/CT were also observed in free-breathing (FB) patients by Cohade et al. (7).

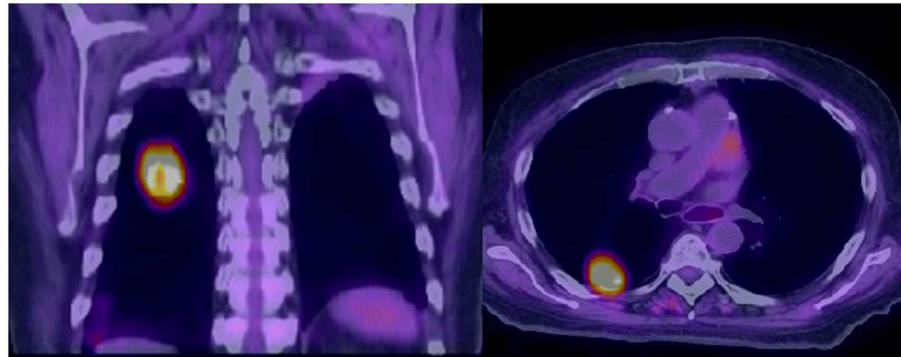


FIGURE 1 | Misalignment of a recurrent squamous cell carcinoma between free-breathing PET and CT is demonstrated. The superior portion of the PET avid tumor does not correspond to any anatomically visible tumor on CT.

Table 1 | Motion artifacts observed in FDG-PET/CT.

Artifacts observed	
Goerres et al. (5)	Mismatch of the diaphragmatic dome between PET and CT was 44.4 ± 25.5 mm between free-breathing PET and CT obtained during maximum inspiration. It ranged between 8.7 and 82.9 mm
Goerres et al. (6)	Mismatch of NSCLC lesions was most prominent at the lung periphery: Breathing: 6.5 ± 3.6 mm (3.4–14.7 mm) Breath hold: 6 ± 2.9 mm (0.5–11.4 mm) And the lung base: Breathing: 8.2 ± 1 mm (7.2–9.8 mm) Breath hold: 6.2 ± 2.6 mm (2.9–11.3 mm)
Cohade et al. (7)	Misregistration of free-breathing PET and CT was 7.55 ± 4.73 mm Lower lungs: 10.2 ± 6.55 mm Upper lungs: 6.67 ± 4.28 mm Left lung: 8.33 ± 5.05 mm Right lung: 6.25 ± 3.92 mm
Osman et al. (8)	Six patients with liver metastases at the liver dome mislocalized to the right lower lobe of the lung on free-breathing PET
Goerres et al. (9)	PET attenuation by CT taken during maximum inspiration led to a decrease in FDG concentration in lung tumors by $42 \pm 12\%$ when compared to that attenuated by CT taken during maximum expiration
Erdi et al. (10)	Tumor displacement of 6.4–24.7 mm, and tumor maximum SUV reduction of 6–24% were observed between maximum inspiration and expiration
Nehmeh et al. (11)	4D PET can lead to a 28% reduction in tumor volume and 56.5% increase in tumor maximum SUV in a patient when compared to free-breathing PET/CT
Liu et al. (12)	Diaphragmatic motion of 11 mm can cause maximum SUV underestimation of 28% and tumor volume overestimation of 130% on average for 1 cm lung lesions

In their study, the distance between the center of lung lesions defined on PET and CT was 7.55 mm on average, which tended to be more pronounced in lower lobe tumors. As shown in these studies, errors in PET/CT registration may become significant in the peri-diaphragmatic region, which can lead to mislocalization of a tumor into an adjacent organ in extreme cases (8).

In addition to image registration mismatch, respiratory motion can also lead to a decrease in measured FDG concentration in lung

tumors, which may be further confounded by other factors, such as the body size, blood glucose concentration, uptake time allowed, interscanner variability, and image reconstruction parameters (9, 13). This is well described by Erdi et al. when PET was registered with respiration-corrected CT over 10 phases (10). Between maximum inspiration and expiration, lesion displacement of 6.4–24.7 mm was observed on 4D CT, which correlated with decrease in tumor maximum SUV of 6–24% between end inspiration and

end expiration. The reduction of FDG uptake intensity observed is due to a redistribution of FDG activity concentration over the range of respiratory motion, which leads to a drop in maximum activity concentration within the tumor (11). As FDG uptake distribution within a tumor is altered, the shape of the gross tumor may also be altered, leading to an increase in tumor size on PET.

The respiratory motion induced change in FDG uptake intensity is further demonstrated in an analysis of routine PET/CT studies in correlation with over 1000 respiratory traces that is validated in a phantom study (12). In this study, a mean maximum SUV underestimation of 28% and mean lesion volume overestimation of 130% in PET/CT images of 1 cm lesions were observed when respiratory motion at the diaphragm is 11 mm. The underestimation of FDG intensity appears to be proportional to respiratory motion amplitude.

In the same study, PET/CT mismatch-related FDG intensity overestimation for lower lobe lung lesions located close to the dome of the liver was also reported. The fluctuation in activity concentration within the tumor may potentially decrease the quality and capability of tumor imaging, which may affect the appropriate delineation of the gross tumor volume (GTV) during radiotherapy treatment planning.

Various strategies have been proposed to reduce respiratory motion artifacts in PET/CT. Among them, PET registered with a respiratory motion averaged CT has been proposed by Chi et al. (14). Motion averaged CT is conducted following routine PET/CT in 229 lung cancer patients in this study. Image alignment and tumor quantification were analyzed in 216 of these patients. Image misalignment was observed in 68% of the 216 routine PET/CTs, which was completely removed (86.21%) or reduced (13.79%) with PET and motion averaged CT registration. Among 120 PET/CTs in which the GTV can be delineated, alignment correction with motion averaged CT was associated with changes in the maximum SUV and GTV of up to 73 and 1950% between PET registered with regular CT and PET registered with motion averaged CT. The largest variation was observed in small lesions <50 cm³ in the vicinity of the diaphragm. Thus, demonstrating the potential for PET attenuated/registered with motion averaged CT to enhance tumor quantification on PET, which is also suggested in a study of 80 patients with NSCLC by Cheng et al. (15).

An alternative approach to reducing respiratory motion-related PET/CT image degradation is PET/CT acquisition through repeated imaging during breath holding (16, 17). However, this method may be limited by patient compliance if used for tumor volume delineation in patients with NSCLC due to their poor pulmonary function.

On the other hand, such image degradation can be more easily reduced by the generation of a respiratory motion corrected or 4D PET/CT during which the PET data are acquired in synchronization with respiratory motion, which can also minimize the poor image quality of PET/motion averaged CT in the vicinity of soft tissue, such as the diaphragm and the chest wall (11, 18, 19). 4D PET/CT is done through tracking an external tracer block that is placed on a patient's abdomen at the time of image acquisition as observed in 4D CT. Through 4D PET/CT imaging, prominent increase in FDG intensity of the tumor and reduction of tumor size due to decreased smearing effect have been observed (11, 20–22).

This may potentially increase the accuracy of GTV delineation on FDG-PET/CT and decrease the amount of normal tissue included in the GTV. As a result, increased accuracy for tumor localization and radiation dose escalation with IGRT for NSCLC may be possible.

4D FDG-PET IN TARGET VOLUME DELINEATION FOR IGRT

A very high degree of accuracy is required in the target volume delineation to optimize accurate tumor localization and maximal margin reduction in the delivery of image guided, intensity-modulated radiotherapy (IMRT) for lung cancer. Respiratory motion-related image degradation observed in FB PET/CT may have an impact on the accuracy of target volume delineation for sophisticated treatments, such as IGRT. In the planning of stereotactic ablative radiotherapy (SABR) for early-stage NSCLC, FB PET-target volumes often do not entirely encompass tumor motion, as FB-PET tumor volumes are often smaller than ITVs generated from the maximum intensity projections (MIP) obtained from 4D CT (23). Thus, target volumes delineated on FB-PET may increase the risk of geometric misses. This is especially problematic for image guided SABR, because of the high reliance on accurate tumor localization and the potential consequences of severe toxicity due to such misses. However, this problem may be corrected by 4D PET/CT imaging (22).

With the utilization of 4D FDG-PET or PET/CT, the most PET active subvolumes within the tumor may be more consistently identified for dose painting (24). In addition, missing disease undetectable on FB PET due to image degradation may be prevented with 4D PET/CT in the planning of thoracic IGRT in order to achieve the maximal TCP (25). 4D PET MIP for ITV delineation was described in detail by Lam et al. (18). ITV generated from 4D PET MIP was found to better correlate with that generated from 4D CT MIP than FB-PET-based ITV in this study. Furthermore, better definition of the extent of tumor in the vicinity of mobile structures, such as the diaphragm, the heart, and the chest wall with 4D PET was demonstrated, which can potentially improve the accuracy of tumor target definition and the sparing of normal tissue that is of similar density to the tumor.

Similarly, 4D PET-based ITV generation may improve the identification of tumor motion in the hilar and mediastinal regions over CT alone. Respiratory motion has been known to affect mediastinal and hilar lymph nodes (26). However, the similar tissue density between nodal disease and surrounding normal tissue in the mediastinal region may pose a challenge to ITV definition based on 4D CT alone. In a comparison of ITV generation based on 3D PET and 4D PET, a 1.3 cm expansion was required for ITV_{3D} to include 91% of the nodal disease (27). Further analysis of the ITV_{3D} with 4D PET demonstrated the inclusion of 45 ± 34 cm³ non-PET-avid tissues in the 3D PET volume. Therefore, 4D PET-based nodal ITV may further improve the accuracy of nodal disease definition, leading to the sparing of additional normal tissue adjacent to regional nodal disease. This may further improve the therapeutic ratio, especially with IGRT in the treatment of lung cancer.

The current evidence, described above, suggests that target volume delineation based on 4D PET/CT information may be the best

approach currently available for the delineation of tumor volumes for lung cancer. It warrants further investigation in future prospective studies, especially in the setting of dose escalation. In our opinion, its use in the clinical setting whenever possible is strongly encouraged, as it may improve patient treatment outcome in the setting of IGRT for lung cancer.

REFERENCES

- Greco C, Rosenzweig K, Cascini GL, Tamburini O. Current status of PET/CT for tumour volume definition in radiotherapy treatment planning for non-small cell lung cancer (NSCLC). *Lung Cancer* (2007) **57**:125–34.
- Van Loon J, van Baardwijk A, Boersma L, Öllers M, Lambin P, De Ruysscher D. Therapeutic implications of molecular imaging with PET in the combined modality treatment of lung cancer. *Cancer Treat Rev* (2011) **37**:331–43. doi:10.1016/j.ctrv.2011.01.005
- Cheebsumon P, Boellaard R, de Ruysscher D, van Elmpt W, van Baardwijk A, Yaqub M, et al. Assessment of tumour size in PET/CT lung cancer studies: PET- and CT-based methods compared to pathology. *EJNMMI Res* (2012) **2**:56. doi:10.1186/2191-219X-2-56
- Wanet M, Lee JA, Weynand B, De Bast M, Poncelet A, Lacroix V, et al. Gradient-based delineation of the primary GTV on FDG-PET in non-small cell lung cancer: a comparison with threshold-based approaches, CT and surgical specimens. *Radiother Oncol* (2011) **98**:117–25. doi:10.1016/j.radonc.2010.10.006
- Goerres GW, Kamel E, Heidelberg TH, Schwitzer MR, Burger C, von Schulthess GK, et al. PET-CT image co-registration in the thorax: influence of respiration. *Eur J Nucl Med Mol Imaging* (2002) **29**:351–60. doi:10.1007/s00259-001-0710-4
- Goerres GW, Kamel E, Seifert B, Burger C, Buch A, Hany TF, et al. Accuracy of image coregistration of pulmonary lesions in patients with non-small cell lung cancer using an integrated PET/CT system. *J Nucl Med* (2002) **43**:1469–75.
- Cohade C, Osman M, Marshall LT, Wahl RL. PET-CT: accuracy of PET and CT spatial registration of lung lesions. *Eur J Nucl Med Mol Imaging* (2003) **30**:721–6. doi:10.1007/s00259-002-1055-3
- Osman MM, Cohade C, Nakamoto Y, Marshall LT, Leal JP, Wahl RL. Clinically significant inaccurate localization of lesions with PET/CT: frequency in 300 patients. *J Nucl Med* (2003) **44**:240–3.
- Goerres GW, Burger C, Kamel E, Seifert B, Kaim AH, Buck A, et al. Respiration-induced attenuation artifact at PET/CT: technical considerations. *Radiology* (2003) **226**:906–10. doi:10.1148/radiol.2263011732
- Erdi YE, Nehmeh SA, Pan T, Pevsner A, Rosenzweig KE, Mageras G, et al. The CT motion quantitation of lung lesions and its impact on PET-measured SUVs. *J Nucl Med* (2004) **45**:1287–92.
- Nehmeh SA, Erdi YE, Ling CC. Effect of respiratory gating on reducing lung motion artifacts in PET imaging of lung cancer. *Med Phys* (2002) **29**:366–71. doi:10.1118/1.1448824
- Liu C, Pierce LA II, Alessio AM, Kinahan PE. The impact of respiratory motion on tumor quantification and delineation in static PET/CT imaging. *Phys Med Biol* (2009) **54**:7345–62. doi:10.1088/0031-9155/54/24/007
- Adams MC, Turkington TG, Wilson JM, Wong TZ. A systematic review of the factors affecting accuracy of SUV measurements. *AJR Am J Roentgenol* (2010) **195**:310–20. doi:10.2214/AJR.10.4923
- Chi PC, Mawlawi O, Luo D, Liao Z, MacApinlac HA, Pan T. Effects of respiration-averaged computed tomography on positron emission tomography/computed tomography quantification and its potential impact on gross tumor volume delineation. *Int J Radiat Oncol Biol Phys* (2008) **71**:890–9. doi:10.1016/j.ijrobp.2008.02.064
- Cheng NM, Yu CT, Ho KC, Wu YC, Liu YC, Wang CW, et al. Respiration-averaged CT for attenuation correction in non-small-cell lung cancer. *Eur J Nucl Med Mol Imaging* (2009) **36**:607–15. doi:10.1007/s00259-008-0995-7
- Meirelles GS, Erdi YE, Nehmeh SA, Squire OD, Larson SM, Humm JL, et al. Deep-inspiration breath-hold PET/CT: clinical findings with a new technique for detection and characterization of thoracic lesions. *J Nucl Med* (2007) **48**:712–9. doi:10.2967/jnumed.106.038034
- Yamaguchi T, Ueda O, Hara H, Sakai H, Kida T, Suzuki K, et al. Usefulness of a breath-holding acquisition method in PET/CT for pulmonary lesions. *Ann Nucl Med* (2009) **23**:65–71. doi:10.1007/s12149-008-0206-4
- Lamb JM. Generating lung tumor internal target volumes from 4D-PET maximum intensity projections. *Med Phys* (2011) **38**:5732–7. doi:10.1118/1.3633896
- Wolthaus JW, van Herk M, Muller SH, Belderbos JS, Lebesque JV, de Bois JA, et al. Fusion of respiration-corrected PET and CT scans: correlated lung tumour motion in anatomical and functional scans. *Phys Med Biol* (2005) **50**:1569–83.
- Lupi A, Zaroccolo M, Salgarello M, Malfatti V, Zanco P. The effect of 18F-FDG-PET/CT respiratory gating on detected metabolic activity in lung lesions. *Ann Nucl Med* (2009) **23**:191–6. doi:10.1007/s12149-008-0225-1
- Garcia Vicente AM, Soriano Castrejón AM, Talavera Rubio MP, León Martín AA, Palomar Muñoz AM, Pilkington Woll JP, et al. (18)F-FDG PET-CT respiratory gating in characterization of pulmonary lesions: approximation towards clinical indications. *Ann Nucl Med* (2010) **24**:207–14. doi:10.1007/s12149-010-0345-2
- Park SJ, Ionascu D, Killoran J, Mamede M, Gerbaudo VH, Chin L, et al. Evaluation of the combined effects of target size, respiratory motion and background activity on 3D and 4D PET/CT images. *Phys Med Biol* (2008) **53**:3661–79. doi:10.1088/0031-9155/53/13/018
- Hanna GG, van Sörnsen de Koste JR, Dahele MR, Carson KJ, Haasbeek CJ, Michielsen R, et al. Defining target volumes for stereotactic ablative radiotherapy of early-stage lung tumours: a comparison of three dimensional 18F-fluorodeoxyglucose positron emission tomography and four-dimensional computed tomography. *Clin Oncol* (2012) **24**:e71–80. doi:10.1016/j.clon.2012.03.002
- Aristophanous M, Yap JT, Killoran JH, Chen AB, Berbeco RI. Four-dimensional positron emission tomography: implications for dose painting of high-uptake regions. *Int J Radiat Oncol Biol Phys* (2011) **80**:900–8. doi:10.1016/j.ijrobp.2010.08.028
- Aristophanous M, Berbeco RI, Killoran JH, Yap JT, Sher DJ, Allen AM, et al. Clinical utility of 4D FDG-PET/CT scans in radiation treatment planning. *Int J Radiat Oncol Biol Phys* (2012) **82**:e99–105. doi:10.1016/j.ijrobp.2010.12.060
- Sher DJ, Wolfgang JA, Niemierko A, Choi NC. Quantification of mediastinal and hilar lymph node involvement using four-dimensional computed tomography scan: implications for radiation treatment planning. *Int J Radiat Oncol Biol Phys* (2007) **69**:1402–8. doi:10.1016/j.ijrobp.2007.05.022
- Lamb JM, Robinson CG, Bradley JD, Low DA. Motion-specific internal target volumes for FDG-avid mediastinal and hilar lymph nodes. *Radiother Oncol* (2013) **109**:112–6. doi:10.1016/j.radonc.2013.07.015

Conflict of Interest Statement: The authors declare that the research was conducted in the absence of any commercial or financial relationships that could be construed as a potential conflict of interest.

Received: 31 March 2014; paper pending published: 19 June 2014; accepted: 16 July 2014; published online: 04 August 2014.

*Citation: Chi A and Nguyen NP (2014) 4D PET/CT as a strategy to reduce respiratory motion artifacts in FDG-PET/CT. *Front. Oncol.* **4**:205. doi: 10.3389/fonc.2014.00205*

*This article was submitted to Radiation Oncology, a section of the journal *Frontiers in Oncology*.*

Copyright © 2014 Chi and Nguyen. This is an open-access article distributed under the terms of the Creative Commons Attribution License (CC BY). The use, distribution or reproduction in other forums is permitted, provided the original author(s) or licensor are credited and that the original publication in this journal is cited, in accordance with accepted academic practice. No use, distribution or reproduction is permitted which does not comply with these terms.



The potential role of respiratory motion management and image guidance in the reduction of severe toxicities following stereotactic ablative radiation therapy for patients with centrally located early stage non-small cell lung cancer or lung metastases

Alexander Chi^{1*}, Nam Phong Nguyen² and Ritsuko Komaki³

¹ Department of Radiation Oncology, Mary Babb Randolph Cancer Center of West Virginia University, Morgantown, WV, USA

² International Geriatric Radiotherapy Group, Tucson, AZ, USA

³ Department of Radiation Oncology, University of Texas MD Anderson Cancer Center, Houston, TX, USA

Edited by:

Ulf Lennart Karlsson, Marshfield Clinic, USA

Reviewed by:

Terence Tai Weng Sio, Mayo Clinic, USA

Yidong Yang, University of Miami Miller School of Medicine, USA

***Correspondence:**

Alexander Chi, Mary Babb Randolph Cancer Center of West Virginia University, PO Box 9234, 1 Medical Center Drive, Morgantown, WV 26505, USA

e-mail: achiaz2010@gmail.com

Image guidance allows delivery of very high doses of radiation over a few fractions, known as stereotactic ablative radiotherapy (SABR). This treatment is associated with excellent outcome for early stage non-small cell lung cancer and metastases to the lungs. In the delivery of SABR, central location constantly poses a challenge due to the difficulty of adequately sparing critical thoracic structures that are immediately adjacent to the tumor if an ablative dose of radiation is to be delivered to the tumor target. As of current, various respiratory motion management and image guidance strategies can be used to ensure accurate tumor target localization prior and/or during daily treatment, which allows for maximal and safe reduction of set up margins. The incorporation of both may lead to the most optimal normal tissue sparing and the most accurate SABR delivery. Here, the clinical outcome, treatment related toxicities, and the pertinent respiratory motion management/image guidance strategies reported in the current literature on SABR for central lung tumors are reviewed.

Keywords: stereotactic ablative radiotherapy, SABR, central location, non-small cell lung cancer, metastases

INTRODUCTION

In the past, thoracic radiotherapy has constantly been limited by toxicity to the normal tissue, such as the lungs and the esophagus, which hinders dose escalation to the gross disease to a desired therapeutic level (1–3). This is mainly due to the utilization of large planning target volume (PTV) margins to compensate uncertainties from respiratory motion and/or in daily patient set up (4, 5). In recent years, advances in imaging technology have enabled us to not only more accurately delineate the gross tumor volume (GTV) and the clinical target volume (CTV), but also given us more information on the location of tumor in relation to critical structures throughout the entire respiratory cycle (1, 2, 4–7). Thus, a PTV margin reduction is possible through accurate delineation of the internal target volume (ITV), which allows for dose escalation to the gross tumor. Tumor localization can be further verified with additional in-room imaging prior to daily treatment to ensure accurate radiation delivery (8). With image-guided radiotherapy (IGRT), ablative doses of radiation can be delivered to treat early stage non-small cell lung (T1–3, N0, M0) or lung metastases, a technique known as stereotactic ablative radiotherapy (SABR) or stereotactic body radiation therapy (SBRT), with excellent clinical outcome consistently observed (9), while local control of over 80% at 3 years have been observed following SABR for oligometastases to the lungs (10, 11).

Despite the rapid clinical adaptation of SABR worldwide, the feasibility of SABR in the treatment of centrally located lung lesions continues to be controversial. The central location is defined as a region that is within 2 cm of the proximal bronchial tree (12). In a phase II prospective study on SABR for T1–2, N0, M0 NSCLC, 60–66 Gy was delivered in three fractions to the tumor target, and the 2-year freedom from severe toxicity was much higher for peripheral lesions when compared to that for central lesions (83 vs. 54%) (13). A total of 12 Grade 3–5 treatment related toxicities were reported at 4 years in this study of 70 patients (14), 5 of which were Grade 5 toxicities. These consisted of pneumonia (three cases), hemoptysis (one case), and respiratory failure (one case). On the contrary, excellent clinical outcome with reasonable toxicity profile has also been reported by others who used dose fractionation regimens with lower fractional dose and increased number of fractions (9). However, treatment related lethal toxicity following SABR for central lung lesions, such as hemoptysis from SABR-related necrosis in the major airway, is still observed when the organ at risk (OAR) was in the high dose volume even when moderate fractionation schedules have been used (15). Therefore, not only lower fractional dose with increased number of fractions is necessary, but geometric accuracy and avoidance of immediately adjacent OARs from being included in the high dose volume are also critical in achieving optimal target volume dose coverage

and OAR sparing in the treatment of central lung lesions with SABR (16). These objectives are further complicated by breathing motion, which leads to variation in tumor location relative to adjacent critical organs throughout the entire respiratory cycle. As a result, a high level of image guidance is required to ensure accurate delivery of ablative doses to the tumor target with the smallest treatment margin possible for optimal OAR sparing. In this situation, a sharp dose gradient at the edge of the PTV to spare the immediately adjacent normal organs from receiving an ablative dose of radiation is also strongly desired. In the following sections, the key components of image-guided SABR will be discussed in relation to clinical experience on SABR for central lung lesions. Furthermore, how currently available respiratory motion management and image guidance techniques are used for safe delivery of SABR for central lung lesions, and how to select patients for SABR in this setting will be explored.

CLINICAL EXPERIENCE WITH SABR FOR CENTRAL LUNG TUMORS

The clinical experience in delivering SABR for central lung tumors has been reported together with that for peripheral lung tumors in multiple studies (12–14, 17–29). In general, no statistically significant difference in the clinical outcome based on tumor location was observed following SABR for early stage NSCLC (14, 18, 21, 24, 25, 27–30). As shown previously, the biologically effective dose (BED) appears to be a direct predictor of local control following SABR with increased failures observed when a lower BED is delivered to the tumor target irrespective of tumor location (12, 23, 26). In recent years, a number of studies have reported the clinical experience with SABR for central lung lesions alone (30–36). As shown in **Table 1**, the local control and overall survival following SABR for centrally located early stage NSCLC appear to be very similar to what has been observed following SABR for early stage NSCLC in general (12). Again, BED appears to be a significant predictor of local control favoring a BED of ≥ 100 Gy₁₀ [Gy calculated using an $\alpha/\beta = 10$ Gy, $BED = \text{total dose} \times (1 + \text{fractional dose}/(\alpha/\beta))$] to the tumor target (37). These findings corroborate with what have been observed in the studies including both peripheral and central lung tumors as mentioned above. Also suggested by studies listed in **Table 1**, poorer clinical outcome may be observed in advanced stage/recurrent NSCLC or metastases to the lungs when compared with that for early stage NSCLC.

Severe toxicities and deaths following SABR for centrally located lung lesions have been reported in many studies, which brought great concern regarding the feasibility of SABR for centrally located lung tumors (13, 14, 17–21, 30, 32–35). In these studies, large fractional dose, and/or failure to exclude OARs immediately adjacent to the tumor target from the high dose volume were frequently observed. Both often associated with deaths due to pulmonary injury or bleeding in areas of necrosis in the immediately adjacent organs, such as the esophagus, or the major airways (**Tables 2** and **3**). As shown in the Indiana phase II study, which included both peripherally and centrally located NSCLC (T1–2, N0, M0), 8 patients with Grade 3–4 toxicities, and 6 SABR-related deaths were identified among 70 patients after a median follow up of 17.5 months when 60–66 Gy was delivered in three fractions (13). The toxicities were mostly cardio-pulmonary in

nature. The rate of severe toxicity (Grade 3–5, CTCAE version 2.0.) significantly correlated with tumor location initially with an 11-fold increase in the risk of severe toxicity associated with central location (13). It suggests that centrally located lesions need to be treated differently even when this correlation lost statistical significance after a median follow up of 50.2 months due mostly to the small number of patients included. Death following treatment of central lung lesions with much lower dose per fraction was initially reported by Onimaru et al. (17). This occurred when the esophagus was not excluded from the high dose volume. It ultimately resulted in death due to hemoptysis as a result of an unhealing esophageal ulcer 5 months after SABR. A hot spot above the prescribed dose on the esophagus was later discovered, which may have contributed to esophageal ulceration.

Treatment related toxicities causing death have also been observed in other studies (18–21). As shown in **Table 2**, death due to bleeding/hemoptysis has been frequently observed following primary or repeat treatments of central lung lesions with SABR. Bronchial strictures and tissue necrosis have also been frequently encountered following SABR for lesions that were adjacent to or within the airways (18, 19). In one study, partial or complete bronchial strictures have been observed in 8/9 patients with centrally located stage I NSCLC after doses from 40–48 Gy/4 to 60 Gy/3 fractions were delivered (18). In their study, severe pulmonary toxicities associated with partial bronchial stricture were observed after 40 Gy/4 fractions were delivered. In a different study, death due to hemoptysis related to bronchial stenosis was observed after a peri-bronchial lesion was treated with 60 Gy/4 fractions (21). These findings demonstrate the risk for severe toxicity due to SABR-related bronchial stricture, which should be avoided whenever possible.

In studies that evaluated SABR for central lesions only (30–36), the incidence of severe toxicities was low among the patients reported. This may be related to lower fractional dose in the dose fractionation schedules used, patient selection, availability of cutting-edge technology for image guidance, and respiratory motion control, as well as many other factors. Among these studies, 9 deaths were reported following SABR in a total of 287 patients (**Table 3**). Again, bleeding due to tissue necrosis of the immediately adjacent OARs appears to be a common cause of death. Five deaths occurred after multiple courses of radiotherapy to single or multiple peri-bronchial lesions (33, 35), while one death occurred after SABR was delivered to an endobronchial lesion (34). One potential treatment related death due to a cardiac cause occurred in a patient with underlying cardiac conditions for whom the PTV and the heart overlapped (30). One death due to bronchial necrosis related hemorrhage occurred 10.5 months after SABR to a 5.7-cm metastasis abutting the left mainstem bronchus (32). The area of bronchial necrosis was retrospectively found to have received a maximum dose above the dose prescribed.

Stereotactic ablative radiotherapy for central lung tumors has been shown to be feasible without any treatment related severe toxicities by many as well (22–29). No fractional dose of over 12.5 Gy was used among them, which further supports the need to lower the fractional dose when treating centrally located lesions to avoid severe late toxicities (**Table 4**). However, SABR may not be the best treatment option for endobronchial lesions as it was

Table 1 | Clinical outcome following SABR for centrally located lung tumors alone.

Reference	No. of patients	Median age	Histology	Median FU (months)	Dose	Local control	DFS/PFS/CSS	OS	Severe toxicities
Haasbeek et al. (30)	63	74 (47–87)	NSCLC: T1–3, N0, M0	35	60 Gy/8 frx	5 years: 92.6%	5 years-DFS: 71%	5 years: 49.5%	Acute: 1 Grade 3 chest wall pain Late: 2 Grade 3 dyspnea 1 Grade 3 chest wall pain 1 Grade 3 rib fracture 2/9 Deaths potentially related to SABR
Nuyttens et al. (31)	56	73 (34–88)	NSCLC: 69.6%; metastases: 30.4%	23	45–60 Gy/5 frx 48 Gy/6 frx	2 years: 76% (early stage NSCLC: 85%)	3 years-CSS (early stage NSCLC): 80%	2 years: 60% (early stage NSCLC: 53%)	Acute: 4 Grade 3 pneumonitis Late: 6 Grade 3 pneumonitis
Rowe et al. (32)	47	72 (41–90)	NSCLC: 59%; metastases: 41%	11.3	50 Gy/4 frx (57%)	Two local failures observed			4 Grade 3 dyspnea within 2–4 months after SABR One SABR-related death
Oshiro et al. (33)	21	71 (35–89)	Recurrent/metastatic NSCLC: 95% Stage IA: 1 Stage IV: 8 Recurrent rI: 4 rIIA: 1	19.8	25–35 Gy/1 frx 40–48 Gy/4 frx 40–50 Gy/5 frx 48 Gy/8 frx 50–60 Gy/10 frx 39 Gy/3 frx	2 years: 59.6%	2 years-PFS: 23.8%	2 years-OS: 62.2%	Acute: none Late: 1 Grade 3 productive cough due to bronchial stenosis requiring dilatation 1 year after treatment 1 Grade 3 dyspnea 18 months after SABR, which was preceded by three courses of RT to bilateral tumors One SABR-related death
Unger et al. (34)	20	~(23–82)	Hilar lesions abutting or invading the mainstem bronchus. Metastases: 85%	10	30–40 Gy/5 frx	1 year: 63%		1 year: 54%	Acute: 1 Grade 3 radiation pneumonitis 8 months after SABR One SABR-related death

(Continued)

Table 1 | Continued

Reference	No. of patients	Median age	Histology	Median FU (months)	Dose	Local control	DFS/PFS/CSS	OS	Severe toxicities
Milano et al. (35)	53	67 (37–88)	NSCLC: 66.04% Stage I: 7 Stage II–III: 10 Stage IV (oligometastases): 15	10	20 Gy/4 frx 12.5–20 Gy/5 frx 40 Gy/8 frx 30–50 Gy/10 frx 49.5–55 Gy/11 frx 42–48 Gy/12 frx 52 Gy/13 frx 45–54 Gy/18 frx	2 years: 73%	2 years: 44% NSCLC Stage I: 72% Stage II–III: 12% Oligomet: 50%	Acute: none Late: 1 Grade 3 pneumonia 10 months after SABR Four SABR-related deaths	
Chang et al. (36)	27	~	NSCLC Stage I: 48.15% Recurrent: 51.85%	17	40–50 Gy/4 frx following 40 Gy delivered; no failures in the 50 Gy group	Three failures			One brachial plexopathy with partial arm paralysis after significant volume of the brachial plexus received 40 Gy

DFS, disease-free survival; PFS, progression-free survival; CSS, cause-specific survival; OS, overall survival; SABR, stereotactic ablative radiotherapy; oligomet, oligometastasis; frx, fraction.

frequently found to result in bronchial necrosis related complications, causing death (18, 19, 34). In addition, re-irradiating central lung lesions with hypofractionated dose fractionation regimens needs to be considered very carefully given the already increased risk of normal tissue injury from prior treatment (20, 33, 35).

As suggested by the clinical experience summarized above, the following are of pertinent importance in minimizing the risk of severe toxicities following SABR for central lung tumors: the use of dose fractionation schedules with relatively lower fractional dose while increasing the number of fractions accordingly to maintain an adequate BED; carefully respecting the dose constraints for the immediately adjacent OARs during treatment planning; and validation of accurate tumor localization through daily image guidance to ensure that the immediately adjacent structures are kept outside of the high dose region in the context of respiratory motion. Furthermore, sharp dose gradient at the PTV's edge through intensity modulation is strongly desired to optimize conformal avoidance of the immediately adjacent OARs when treating central lesions with SABR (12). This makes image guidance even more critical in the delivery of daily treatments. In the following sections, the current available respiratory motion management/image guidance techniques that can be used to optimize the safe and accurate delivery of SABR to treat central lung lesions in the context of the clinical studies described above will be further described and assessed.

RESPIRATORY MOTION MANAGEMENT IN LUNG SABR

Patient immobilization, respiratory motion management, and appropriate image guidance are closely integrated in thoracic IGRT. Multiple image guidance techniques are currently in use to ensure accurate tumor localization during lung SABR and these are closely related to the strategy for respiratory motion management that is used in conjunction with them. Tumor motion due to respiration in various locations of the lungs has been previously described by Seppenwoolde et al. (4). The greatest motion was observed in lower lobe tumors that were not attached to rigid structures in the cranio-caudal direction (12 ± 2 mm), while the lateral motion appears to be much less (2 ± 1 mm). The tumors were found to be more stable and spending more time in the expiratory phase of respiration. In addition, hysteresis of 1–5 mm has been observed commonly (4).

A more detailed description of respiratory motion can be found in a report by AAPM task group 76 (38), which further illustrates that patients' breathing patterns are irregular, and are highly variable in magnitude, and period. They not only vary intra- and inter-fractionally, but also vary between different patients. As shown by Wulf et al., a uniform ITV margin of 5 mm in transverse and 10 mm crano-caudally still led to partial misses of tumor targets in 12–16% of the patients even in the setting of stereotactic body frame usage (39). Therefore, individually accounting for respiratory motion with patients breathing in a repeatable fashion is essential for the most accurate and precise capturing of internal organ motion. Furthermore, tumor location needs to be verified under daily image guidance to ensure appropriate dose distribution during actual treatment to justify small PTV margins for the most optimal OAR sparing.

Table 2 | Deaths following SABR for central lung tumors in studies including both peripheral and central lesions.

Reference	Median FU (months)	No of central lesions/study	Lesions associated with death	Dose schedule associated with death	Cause of death/time of death
Fakiris et al. (14)	50.2	22	A pericardial and a pericardial NSCLC	60–66 Gy/3 frx	Hemoptysis (19.5 months after SABR) and pericardial effusion
Onimaru et al. (17)	18	9	A 3.5-cm metastasis from melanoma posterior to the R mainstem bronchus Esophageal dose parameters Maximum dose: 50.5 Gy Mean dose: 10.6 Gy 1 cc dose: 42.5 Gy	48 Gy/8 frx	Bleeding from an unhealing esophageal ulcer 5 months after SABR
Song et al. (18)	26.5	9	Endobronchial NSCLC in the mainstem bronchus	48 Gy/4 frx	Hemoptysis, aspiration, and pneumonia from treatment induced complete bronchial stricture 13 months after SABR
Stauder et al. (19)	15.8	47	A recurrent NSCLC that is obstructing the L mainstem bronchus (pneumonectomy on the contralateral side 17 years ago)	48 Gy/4 frx	Pulmonary failure caused by progressive bronchial obstruction due to tumor necrosis 7.5 months after SABR
Peulen et al. (20)	12	11	Bilateral hilar metastases from RCC, then R hilar recurrence 3 years later L hilar NSCLC encasing a lobar bronchus Carinal recurrence from esophageal cancer	40 Gy/4 frx, then 40 Gy/5 frx 40 Gy/4 frx to the primary disease followed by 33 Gy/3 frx 13 months later 40 Gy/5 frx following chemotherapy followed by 40 Gy/5 frx 29 months later	Hemoptysis 10 months after second course of SABR Hemoptysis/hemorrhage 6 weeks after second course of SABR A fistula between G-tube and trachea developed 10 months after second course of SABR; local progression 13 months after second SABR was treated with 40 Gy/5 frx, then again 42 Gy/7 frx 8 months later; The patient was found to have developed SVC syndrome due to severe RT induced fibrosis 7 months after third course of SABR and died of an MI during stent placement
Bral et al. (21)	16	17	Peri-bronchial early stage NSCLC	60 Gy/4 frx	Hemoptysis related to Grade 3 dyspnea due to bronchial stenosis. The patient died during stenting

Frx, fractions; RCC, renal cell carcinoma.

Respiratory motion management strategies currently in use are usually separated into five different categories: motion encompassing, respiratory gating, breath hold, forced shallow breathing with abdominal compression and breath-synchronized, or real time tumor tracking techniques (38). Among them, motion encompassing techniques to estimate the range of tumor motion have been most commonly used in the treatment of central lesions with SABR (**Table 5**). These include slow CT scanning, ITV generation with inhalation and exhalation breath hold CTs combined with free-breathing CT, and 4D or respiration corrected CT. A slow CT

is generated with a speed that would allow multiple respiratory cycles to be captured per slice to generate a tumor encompassing volume, which depicts tumor location throughout the entire respiratory cycle. This approach is limited by the lack of contrast between tumor from normal tissue when it is located in the vicinity of the mediastinum, the diaphragm, or the chest wall as a result of respiration related blurring. Alternatively, FDG PET registered to the planning CT has been used by some to aid target volume delineation due to the enhanced resolution of tumor in areas of soft tissue associated with image registration; and the

Table 3 | Deaths reported in studies on SABR for central lung tumors only.

Reference	Dose prescribed	Immediately adjacent organs	Dose to critical organs	Cause of death/time of death
Haasbeek et al. (30)	60 Gy/8 frx	Pericardium overlapping the target volume R hilum	Unknown	Cardiac event 2.5 years after SABR Respiratory failure
Rowe et al. (32)	50 Gy/4 frx to a metastasis from melanoma	L mainstem bronchus	Airway point dose: 54.2 Gy Airway _{5cc} dose: 12.7 Gy (overall: 14.7 Gy)	Hemorrhage with bronchial necrosis in the region of the maximum point dose 10.5 months after SABR
Oshiro et al. (33)	25 Gy/1 frx ^a	Hilum of unknown side	Unknown	Hemoptysis 18 months after SABR
Unger et al. (34)	30–40 Gy/5 frx to an endobronchial lesion from mesothelioma	Unknown mainstem bronchus	Maximum point dose: 49 Gy	Bronchial fistula related, 7 months after SABR
Milano et al. (35)	49.5 Gy/11 frx to one central NSCLC followed by 48 Gy/4 frx 15 months later 50 Gy/10 frx to one central and one peripheral NSCLC followed by 50 Gy/10 frx to three new central lesions and one bulky recurrence of the previously treated peripheral lesion 11 months later 35–50 Gy/10 frx to five central NSCLC 35 Gy/14 frx then 18 Gy/6 frx to three central NSCLC and 50 Gy/10 frx to one peripheral NSCLC	Bronchus Bronchus and trachea Bronchus and trachea Bronchus (0.5 cm from tumor) and trachea (1 cm from tumor)	Bronchus received 98 Gy cumulatively Unknown Unknown	Hemoptysis 6.5 months after second course of SABR Dyspnea 2 weeks after second course of SABR Bronchitis 6 months after second course of SABR Dyspnea 4 months after SABR

^aAfter previous intra-tracheobronchial brachytherapy to bilateral hilar lesions and SABR to the apical area of the same lobe.

volume encompassing effect associated with the relatively slower speed of a PET scan (**Table 5**). The inhalation and exhalation breath hold CTs have been used to estimate the extremes of breathing motion. Respiration monitoring may be used in this setting to confirm that the breathing range is constant and the ITV generated adequately encompasses the tumor at the time of actual treatment. Both methods provide less detail on tumor motion than 4D CT. As shown in **Table 5**, 4D CT was used for motion management in 7/14 studies in which motion encompassing techniques were used (19, 23, 25, 29, 30, 32, 36). It can estimate the mean tumor position and the range of tumor motion in relation to adjacent normal thoracic organs with increased sophistication when compared to the other two approaches, which is critical for target volume delineation in central locations of the thorax. The use of 4D CT in the treatment planning of lung SABR has been described in detail by Slotman et al. (40). As shown by Wang et al., 4D CT based target volume delineation consistently resulted in smaller PTV volume in lung SABR, which may potentially lead to an increase in normal tissue sparing (41).

Other respiratory motion management techniques are also used in the treatment of central lung tumors with SABR. The breath hold technique has been used by Song et al. and Milano et al. in the delivery of SABR, while respiratory gating has been used by Song et al. and Oshiro et al. in their patients (18, 33, 35). Forced shallow breathing with abdominal compression has been commonly used to reduce respiratory motion in the pre-4D CT era, when SABR began to become a treatment option for early stage NSCLC (14, 39, 42). Both deep inspiration breath hold (DIBH) and end expiratory breath hold (EEBH) can be used for the breath hold technique while the DIBH approach can potentially improve the sparing of the normal lung tissue (35, 38). However, breath holding requires a high degree of patient cooperation and is often limited to the delivery of 3D-CRT and step-and-shoot IMRT due to the short duration of breath holding of ≤ 30 s.

Respiratory gating refers to the delivery of radiation within a particular portion of a patient's respiratory cycle. The respiratory cycle can be monitored through external respiratory signal or internal fiducial markers, while the gating criteria can be set

Table 4 | Studies on lung SABR reporting no severe toxicity associated with central location.

Reference	Median FU (months)	No of central lesions/total lesions	Dose fractionation schedule used	Severe toxicities
Xia et al. (22)	27	9/43	50 Gy/10 frx	None
Guckenberger et al. (23)	14	22/159	48 Gy/8 frx ^a 26 Gy/1 frx 37.5 Gy/3 frx	None
Baba et al. (24)	26 ^b	29/124	44–52 Gy/4 frx	None
Olsen et al. (25) ^c	11 16 13	19/130	45–50 Gy/5 frx ^a 54 Gy/3 frx	None
Andratschke et al. (26)	21	24/92	35 Gy/5 frx ^a 40 Gy/4 frx ^a 30–45 Gy/3 frx	None
Takeda et al. (27)	OLTs from CRC 29 OLTs from other origins 15 NSCLC 24	33/232	50 Gy/5 frx	None
Stephans et al. (28)	15.3	7/94	50 Gy/5 frx ^a 60 Gy/3 frx	None
Janssen et al. (29)	13.8	29/65	40–48 Gy/8 frx ^a 37.5 Gy/3 frx	None

^aDose fractionation schedule for central lesions.

^bFor living patients only.

^cMedian FU based on dose fractionation schedule used.

OLTs, oligometastases; frx, fractions.

by either displacement (33), or phase based on a certain pre-set displacement distance or phase window, respectively. This technique requires respiration to be continuously monitored using surrogate markers of breathing motion (18, 33, 43). Although it can potentially spare more normal tissue compared to the motion encompassing method, it requires a high degree of quality assurance to validate the accurate representation of tumor motion by the external signal and the internal fiducial markers (38). In addition, treatment time is increased with gating as radiation is only delivered when the target is in the gated window.

Real time tumor tracking is different from the other techniques of respiratory motion management in that the radiation beam moves in synchrony with the tumor as the patient is breathing. The use of this technique is commonly observed with lung SABR delivery by the CyberKnife (CK, Accuray Corp.), a device that attaches a linear accelerator to a robotic arm to allow for beam adaptation to full three-dimensional motion of the tumor under close image guidance (31, 34). This is achieved through the intermittent monitoring of internal fiducial markers or the tumor itself, coupled with the continuous monitoring of external respiratory markers (44). Although the treated volume can potentially be reduced with this highly automated approach, the treatment time is usually long (60–90 min), and the localization of centrally located lung tumors on in-room x-rays may be difficult without the use of internal fiducial markers (44).

IMAGE GUIDANCE IN THE DELIVERY OF LUNG SABR

Regardless of the motion management strategy used, image guidance during daily treatment is essential in ensuring the accurate localization of the target volume in relation to adjacent normal structures. This allows for smaller PTV margins to be used, especially for centrally located lung tumors, with optimal dose volume coverage and OAR sparing. Image guidance strategies are on-board, peripheral, or integrated on various treatment delivery systems (1). Despite the ability to achieve very sharp dose gradient for normal structure sparing in SABR for central lung lesions, the clinical use of helical tomotherapy (a image-guided IMRT delivery system integrating a six MV linear accelerator with a helical CT) for this purpose has not been extensively reported (12). However, the first two strategies are widely adopted in SABR delivery.

On-board image guidance is conducted when the imaging device is attached to the actual treatment delivery system. The most commonly used on-board imaging device for the delivery of lung SABR is the cone beam CT (CBCT), which is re-constructed from a series of x-ray projections obtained in a single rotation of the source and detector around the patient (45). In the most commonly available CBCT systems, the imaging axis is chosen to be 90° to the treatment beam. CBCT provides 3D information of the tumor in relation to the critical normal structures for online verification of tumor localization prior to the delivery of daily treatment. It can be obtained with either MV or KV imaging. KV

Table 5 | Treatment planning, immobilization, and image guidance in SABR for central lung tumors.

Reference	Respiratory motion management	ITV	FDG PET for target definition	Dose calculation/TPS	Technique	Immobilization	Image guidance
Haasbeek et al. (30)	e	Y		-/BrainLab	3D	-	ExacTrac system
Nuyttens et al. (31)	RTT			-/CyberKnife	IMRT	-	Fiducial marker tracking per CyberKnife system
Rowe et al. (32)	e	Y		AAA/-	3D, IMRT	Full length vacuum cushion	CBCT
Oshiro et al. (33)	c			-/Eclipse (Varian)	3D	Individualized body casts	Gated KV-radiographs
Unger et al. (34)	RTT			Non-isocentric inverse planning algorithm with heterogeneity correction/CyberKnife	IMRT	-	IR emitting external markers and internal fiducial markers used for real time tumor tracking with CyberKnife
Milano et al. (35)	d	Y	Y	-/BrainLab	Arcs	-	ExacTrac system
Chang et al. (36)	e	Y		-/-	3D	-	CT-on-rail with orthogonal radiographs to confirm isocenter
Fakiris et al. (14)	a	Y		-/-	3D	SBF with abdominal compression	Daily treatment guided by external markers on SBF
Onimaru et al. (17)	b	Y		3D RTP with heterogeneity correction	3D	No immobilization cradles	Orthogonal radiographs on the first day
Song et al. (18)	a,c,d	Y		-/Render 3D system (Elekta) or Eclipse (Varian)	-	Vacuum fitted SBF	CBCT
Stauder et al. (19)	e	Y	Y	-/Eclipse (Varian)	3D	BodyFix vacuum system	CBCT
Peulen et al. (20)	a	Y		Pencil beam algorithm with heterogeneity correction/-	3D	SBF with abdominal compression	CT prior to each treatment
Bral et al. (21)	b,c	Y	Y	-/BrainLab	3D	Low density cradle with IR skin markers on the thorax	ExacTrac-like system using both external and internal markers
Xia et al. (22)	f	Y	N1 LN delineation	Body gamma knife planning system	MLC based gamma knife	Vacuum bag from head to pelvis	-
Guckenberger et al. (23)	e	Y		Collapsed cone algorithm/-	3D	SBF or BodyFix systems	CT, in-room CT, then CBCT since 2005
Baba et al. (24)	b	Y		? AAA/eclipse (Varian)	3D	BodyFix system	-
Olsen et al. (25)	e	Y		Superposition convolution algorithm with heterogeneity correction/-	3D	SBF system or alpha cradle	CBCT
Andratschke et al. (26)	f	Y		Unknown algorithm with heterogeneity correction/-	3D/arcs	Vacuum couch and low pressure foil	CT prior to each treatment, then CBCT since 2008

(Continued)

Table 5 | Continued

Reference	Respiratory motion management	ITV	FDG PET for target definition	Dose calculation/TPS	Technique	Immobilization	Image guidance
Takeda et al. (27)	f	Y	Superposition algorithm with heterogeneity correction/XIO (CMS)	DCMAT	Corset	–	–
Stephans et al. (28)	b	Y	Unknown with heterogeneity correction/BrainLab	IMRT	BodyFix system	ExactTrac system	–
Janssen et al. (29)	e	Y	–/–	–	SBF with abdominal compression	CBCT	–

^aForced shallow breathing with abdominal compression.^bInhalation and exhalation breath hold CTs used to generate ITV.^cRespiratory gating.^dBreath hold/active breathing control.^e4D CT.^fSlow CT.

^gSBF, stereotactic body frame; DCMAT, dynamic conformal/multiple arc therapy; RTT, real time tracking; Y, yes; ITV refers to that generated with motion encompassing technique or that accounted for when generating the PTV; –, unknown.

imaging is superior to MV imaging in providing better soft tissue resolution with low to moderate imaging doses, which potentially improves patient set up accuracy and alignment of tumor target volume in relation to adjacent critical structures (46). This may be especially helpful in the treatment of central lung lesions with SABR, as a high degree of anatomical information is necessary for the most optimal tumor localization. However, KV CBCT requires regular quality assurance for the alignment of the imaging and treatment beams (46).

Both 2D and 3D imaging are used in peripheral in-room image guidance strategies. The advantage of using imaging devices not directly attached to the treatment delivery system is that respiratory motion may be monitored during the delivery of radiation. However, they need to be carefully calibrated with the treatment beam's isocenter to minimize additional geometric uncertainties (1). CT-on-rails/in-room CT has been used for online image guidance with the treatment table moved to the imaging position after the patient is set up on the treatment table. Diagnostic quality CT images can be obtained with this approach for the best resolution of soft tissue structures prior to each treatment. However, additional set up errors may be introduced during patient movement between the imaging and treatment positions (46). Both CBCT and CT-on-rails/in-room CT have been used in image-guided SABR for central lung lesions. These strategies are frequently used with the motion encompassing method of respiratory motion management with low incidence of severe toxicities in the setting of primary irradiation, and tumor not directly involving the normal critical structure at risk (18, 19, 22, 23, 25–27, 29, 32, 36). As shown by Grills et al., small PTV margin accounting for systemic and random error may be consistently maintained when CBCT in conjunction with appropriate immobilization were used during SABR delivery for early stage NSCLC (47). In this study, the PTV margin may be reduced to <5 mm with the patient in a stereotactic body frame and to ~5 mm with a regular alpha cradle. Their findings were corroborated in a study by Guckenberger et al., which showed that the PTV margin can be reduced from 12 to <5 mm when KV CBCT is used in addition to a stereotactic body frame (48). In another study, the mean lung dose and the V₂₀ (volume of the normal lung receiving 20 Gy) were reduced by 47–77.3%; while the spinal cord dose was reduced by 55.2–58.5% for central lung lesions when CBCT image guidance was used with active breathing control (a breath hold technique) in the delivery of lung SABR as a result of reduction in treatment set up margins enabled by combining image guidance and respiratory motion management (49). In this study, pre-correction set up margins of 14.1 mm in the cranial–caudal direction was able to be reduced to 4.7 mm, while pre-correction set up margins of ~10 mm in the left–right and anterior–posterior directions were reduced to 3.2 and 3.5 mm, respectively. More recently, 4D CBCT has been under investigation to better capture tumor motion at the time of treatment, which may allow for small PTV margins of within 3 mm (50–52). Although fairly accurate with respiratory motion of <5 mm, 3D CBCT was shown to be less accurate in capturing respiratory motion than 4D CBCT as motion artifacts increase with increased tumor motion (53, 54). In addition, accurate localization of the target volume during daily treatment may provide information for adaptive adjustment of the PTV margin

and adaptive planning daily. Further exploration in this area is definitely warranted.

Commonly used 2D-imaging based peripheral strategies, such as the Novalis ExacTrac and Synchrony for CK, usually monitor external markers of respiration continuously with periodical verification of tumor location through x-rays of internal tumor markers. With the Novalis ExacTrac system, respiratory motion can be captured by continuous monitoring of infra-red (IR) reflecting markers attached to the patient's abdomen, while KV x-rays can be matched to digitally re-constructed radiographs for localization verification of internal tumor markers (43, 54). This system can be used for respiratory gating, which may potentially limit the amount of normal tissue irradiated as the gating window can be limited to as small as 2 mm (43). When used to delivery SABR for central lung tumors (21, 28, 30, 35), low incidence of severe toxicities have been observed when re-irradiation was excluded in general (14, 17–21, 30, 32–35). However, Grade 5 toxicities related or potentially related to SABR for lesions in close proximity to the major airway and the heart were reported with this approach of image guidance (21, 30). This suggests that online correction with 3D imaging may be beneficial in certain situations due to the increased amount of 3D geometric detail of critical normal structures in relation to the PTV it provides to avoid non-intended inclusion of critical structures in the high dose volume.

Real time tumor tracking of the CK system is accomplished in a way that is very similar to the ExacTrac system (43, 44). With the Synchrony system, the internal and external marker motions appear to be highly correlated (55). However, external marker based tumor motion prediction are influenced by multiple factors, and its correlation with tumor motion may deteriorate with prolonged treatment duration (56). In addition, a high rate of pneumothorax has been observed after thoracic fiducial marker placement with frequent marker migration (57, 58). Clinically, CK-based SABR has been correlated with excellent clinical outcome (59). It was used to deliver SABR for central lung tumors with only one Grade 5 toxicity encountered when an endobronchial lesion in the mainstem bronchus was treated to the prescribed dose among a total of 76 patients reported in two studies (31, 34). The safe delivery of SABR with CK for central lesions, and especially hilar lesions with relative low incidence of severe toxicity may be due to the fact that relatively smaller PTV can be used with real time tumor tracking as no ITV is needed in this situation (60, 61). When compared with linac-based systems, CK may also be associated with improvement in the sparing of the normal lungs from low dose irradiation for anteriorly located tumors (60, 61). This location-based difference was mostly due to the system's inability to deliver radiation from underneath the patient. However, these findings suggest that it may provide an advantage in the delivery of SABR for relatively more anterior central lung tumors.

CONCLUSION AND FUTURE DIRECTIONS

As shown above, image guidance techniques integrated with respiratory motion management enhances tumor localization in the delivery of SABR for central lung tumors, which are mobile as a result of respiration. As result, very small PTV margin can be

safely used to achieve optimal dose coverage of the tumor target and sparing of the adjacent critical normal structures. This makes SABR for central lung lesions feasible when the following criteria are met: primary irradiation of a limited number of lung lesions; dose constraints of the critical structures are strictly respected; and no direct overlap between the PTV and any immediately adjacent OARs. Therefore, the integration of respiratory motion management and image guidance is warranted in future clinical trials on SABR for centrally located lung tumors.

Particle therapy, such as proton therapy, has been increasingly investigated and utilized for the treatment of lung cancer in recent years due to the finite range of charged particles, which may provide an advantage over photon therapy in normal tissue sparing (62). Clinical experience in the delivery of stereotactic body proton therapy has been excellent without any severe toxicity reported in the treatment of central lesions (63, 64). Large smearing margins may be necessary to achieve the most optimal dose distribution in the delivery of passively scattered beams (PT), which may impair OAR sparing in situations of complex geometry (65). Active spot scanning, or intensity modulated proton therapy (IMPT) has been shown to provide a dosimetric advantage in the treatment of central lung lesions over PT and photon therapy (66, 67). However, dose distribution in IMPT is very sensitive to beam and tumor motion, as well as set up uncertainties. Methods to minimize interplay uncertainties have been proposed, which warrants further investigation in the future (65, 68, 69).

REFERENCES

- Verellen D, De Ridder M, Linthout N, Tournel K, Soete G, Storme G. Innovations in image-guided radiotherapy. *Nat Rev Cancer* (2007) 7:949–60. doi:10.1038/nrc2288
- van Herk M. Different styles of image-guided radiotherapy. *Semin Radiat Oncol* (2007) 17:258–67. doi:10.1016/j.semradonc.2007.07.003
- Fowler JF, Tomé WA, Fenwick JD, Mehta MP. A challenge to traditional radiation oncology. *Int J Radiat Oncol Biol Phys* (2004) 60:1241–56. doi:10.1016/j.ijrobp.2004.07.691
- Seppenwoode Y, Shirato H, Kitamura K, Shimizu S, van Herk M, Lebesque JV, et al. Precise and real-time measurement of 3D tumor motion in lung due to breathing and heartbeat, measured during radiotherapy. *Int J Radiat Oncol Biol Phys* (2002) 53:822–34. doi:10.1016/S0360-3016(02)02803-1
- van Herk M, Remeijer P, Rasch C, Lebesque JV. The probability of correct target dosage: dose-population histograms for deriving treatment margins in radiotherapy. *Int J Radiat Oncol Biol Phys* (2000) 47:1121–35. doi:10.1016/S0360-3016(00)00518-6
- Mageras GS, Pevsner A, Yorke ED, Rosenzweig KE, Ford EC, Hertanto A, et al. Measurement of lung tumor motion using respiration-correlated CT. *Int J Radiat Oncol Biol Phys* (2004) 60:933–41. doi:10.1016/S0360-3016(04)01078-8
- Redmond KJ, Song DY, Fox JL, Zhou J, Rosenzweig CN, Ford E. Respiratory motion changes of lung tumors over the course of radiation therapy based on respiration-correlated four-dimensional computed tomography scans. *Int J Radiat Oncol Biol Phys* (2009) 75:1605–12. doi:10.1016/j.ijrobp.2009.05.024
- Balter JM, Kessler ML. Imaging and alignment for image-guided radiation therapy. *J Clin Oncol* (2007) 25:8931–7. doi:10.1200/JCO.2006.09.7998
- Chi A, Liao Z, Nguyen NP, Xu J, Stea B, Komaki R. Systemic review of the patterns of failure following stereotactic body radiation therapy in early-stage non-small-cell lung cancer: clinical implications. *Radiother Oncol* (2010) 94:1–11. doi:10.1016/j.radonc.2009.12.008
- Ricardi U, Filippi AR, Guarneri A, Ragona R, Mantovani C, Giglioli F, et al. Stereotactic body radiation therapy for lung metastases. *Lung Cancer* (2012) 75:77–81. doi:10.1016/j.lungcan.2011.04.021
- Baschnagel AM, Mangona VS, Robertson JM, Welsh RJ, Kestin LL, Grills IS. Lung metastases treated with image-guided stereotactic body radiation therapy. *Clin Oncol* (2013) 25:236–41. doi:10.1016/j.clon.2012.12.005

12. Chi A, Jang SY, Welsh JS, Nguyen NP, Ong E, Gobar L, et al. Feasibility of helical tomotherapy in stereotactic body radiation therapy for centrally located early stage non-small-cell lung cancer or lung metastases. *Int J Radiat Oncol Biol Phys* (2011) **81**:856–62. doi:10.1016/j.ijrobp.2010.11.051
13. Timmerman R, McGarry R, Yiannoutsos C, Papiez L, Tudor K, DeLuca J, et al. Excessive toxicity when treating central tumors in a phase II study of stereotactic body radiation therapy for medically inoperable early-stage lung cancer. *J Clin Oncol* (2006) **24**:4833–9. doi:10.1200/JCO.2006.07.5937
14. Fakiris AJ, McGarry RC, Yiannoutsos CT, Papiez L, Williams M, Henderson MA, et al. Stereotactic body radiation therapy for early-stage non-small-cell lung carcinoma: four-year results of a prospective phase II study. *Int J Radiat Oncol Biol Phys* (2009) **75**:677–82. doi:10.1016/j.ijrobp.2008.11.042
15. Corradetti MN, Haas AR, Rengan R. Central-airway necrosis after stereotactic body-radiation therapy. *N Engl J Med* (2012) **366**:2327–9. doi:10.1056/NEJMMc1203770
16. Nagata Y, Wulf J, Lax I, Timmerman R, Zimmermann F, Stojkovski I, et al. Stereotactic radiotherapy of primary lung cancer and other targets: results of consultant meeting of the international atomic energy agency. *Int J Radiat Oncol Biol Phys* (2011) **79**:660–9. doi:10.1016/j.ijrobp.2010.10.004
17. Onimaru R, Shirato H, Shimizu S, Kitamura K, Xu B, Fukumoto S, et al. Tolerance of organs at risk in small-volume, hypofractionated, image-guided radiotherapy for primary and metastatic lung cancers. *Int J Radiat Oncol Biol Phys* (2003) **56**:126–35. doi:10.1016/S0360-3016(03)00095-6
18. Song SY, Choi W, Shin SS, Lee SW, Ahn SD, Kim JH, et al. Fractionated stereotactic body radiation therapy for medically inoperable stage I lung cancer adjacent to central large bronchus. *Lung Cancer* (2009) **66**:89–93. doi:10.1016/j.lungcan.2008.12.016
19. Stauder MC, Macdonald OK, Olivier KR, Call JA, Lafata K, Mayo CS, et al. Early pulmonary toxicity following lung stereotactic body radiation therapy delivered in consecutive daily fractions. *Radiother Oncol* (2011) **99**:166–71. doi:10.1016/j.radonc.2011.04.002
20. Peulen H, Karlsson K, Lindberg K, Tullgren O, Baumann P, Lax I, et al. Toxicity after reirradiation of pulmonary tumours with stereotactic body radiotherapy. *Radiother Oncol* (2011) **101**:260–6. doi:10.1016/j.radonc.2011.09.012
21. Bral S, Gevaert T, Linthout N, Versmessen H, Collen C, Engels B, et al. Prospective, risk-adapted strategy of stereotactic body radiotherapy for early-stage non-small-cell lung cancer: results of a phase II trial. *Int J Radiat Oncol Biol Phys* (2011) **80**:1343–9. doi:10.1016/j.ijrobp.2010.04.056
22. Xia T, Li H, Sun Q, Wang Y, Fan N, Yu Y, et al. Promising clinical outcome of stereotactic body radiation therapy for patients with inoperable stage I/II non-small-cell lung cancer. *Int J Radiat Oncol Biol Phys* (2006) **66**:117–25. doi:10.1016/j.ijrobp.2006.04.013
23. Guckenberger M, Wulf J, Mueller G, Krieger T, Baier K, Gabor M, et al. Dose-response relationship for image-guided stereotactic body radiotherapy of pulmonary tumors: relevance of 4D dose calculation. *Int J Radiat Oncol Biol Phys* (2009) **74**:47–54. doi:10.1016/j.ijrobp.2008.06.1939
24. Baba F, Shibamoto Y, Ogino H, Murata R, Sugie C, Iwata H, et al. Clinical outcomes of stereotactic body radiotherapy for stage I non-small cell lung cancer using different doses depending on tumor size. *Radiat Oncol* (2010) **5**:81. doi:10.1186/1748-717X-5-81
25. Olsen JR, Robinson CG, El Naqa I, Creach KM, Drzymala RE, Bloch C, et al. Dose-response for stereotactic body radiotherapy in early-stage non-small-cell lung cancer. *Int J Radiat Oncol Biol Phys* (2011) **81**:e299–303. doi:10.1016/j.ijrobp.2011.01.038
26. Andratschke N, Zimmermann F, Boehm E, Schill S, Schoenknecht C, Thamm R, et al. Stereotactic radiotherapy of histologically proven inoperable stage I non-small cell lung cancer: patterns of failure. *Radiother Oncol* (2011) **101**:245–9. doi:10.1016/j.radonc.2011.06.009
27. Takeda A, Kunieda E, Ohashi T, Aoki Y, Koike N, Takeda T. Stereotactic body radiotherapy (SBRT) for oligometastatic lung tumors from colorectal cancer and other primary cancers in comparison with primary lung cancer. *Radiother Oncol* (2011) **101**:255–9. doi:10.1016/j.radonc.2011.05.033
28. Stephans KL, Djemil T, Reddy CA, Gajdos SM, Kolar M, Mason D, et al. A comparison of two stereotactic body radiation fractionation schedules for medically inoperable stage I non-small cell lung cancer: the Cleveland clinic experience. *J Thorac Oncol* (2009) **4**:976–82. doi:10.1097/JTO.0b013e3181adf509
29. Janssen S, Dickgreber NJ, Koenig C, Bremer M, Werner M, Karstens JH, et al. Image-guided hypofractionated small-volume radiotherapy of non-small cell lung cancer – feasibility and clinical outcome. *Oncologie* (2012) **35**:408–12. doi:10.1159/000340064
30. Haasbeek CJ, Lagerwaard FJ, Slotman BJ, Senan S. Outcomes of stereotactic ablative radiotherapy for centrally located early-stage lung cancer. *J Thorac Oncol* (2011) **6**:2036–43. doi:10.1097/JTO.0b013e31822e71d8
31. Nuyttens JJ, van der Voort van Zyp NC, Praag J, Aluwini S, van Klaveren RJ, Verhoef C, et al. Outcome of four-dimensional stereotactic radiotherapy for centrally located lung tumors. *Radiother Oncol* (2012) **102**:383–7. doi:10.1016/j.radonc.2011.12.023
32. Rowe BP, Boffa DJ, Wilson LD, Kim AW, Detterbeck FC, Decker RH. Stereotactic body radiotherapy for central lung tumors. *J Thorac Oncol* (2012) **7**:1394–9. doi:10.1097/JTO.0b013e3182614bf3
33. Oshiro Y, Aruga T, Tsuoboi K, Marino K, Hara R, Sanayama Y, et al. Stereotactic body radiotherapy for lung tumors at the pulmonary hilum. *Strahlenther Onkol* (2010) **186**:274–9. doi:10.1007/s00066-010-2072-y
34. Unger K, Ju A, Oermann E, Suy S, Yu X, Vahdat S, et al. CyberKnife for hilar lung tumors: report of clinical response and toxicity. *J Hematol Oncol* (2010) **3**:39. doi:10.1186/1756-8722-3-39
35. Milano MT, Chen Y, Katz AW, Philip A, Schell MC, Okunieff P. Central thoracic lesions treated with hypofractionated stereotactic body radiotherapy. *Radiother Oncol* (2009) **91**:301–6. doi:10.1016/j.radonc.2009.03.005
36. Chang JY, Balter PA, Dong L, Yang Q, Liao Z, Jeter M, et al. Stereotactic body radiation therapy in centrally and superiorly located stage I or isolated recurrent non-small-cell lung cancer. *Int J Radiat Oncol Biol Phys* (2008) **72**:967–71. doi:10.1016/j.ijrobp.2008.08.001
37. Grills IS, Hope AJ, Guckenberger M, Kestin LL, Werner-Wasik M, Sonke JJ, et al. A collaborative analysis of stereotactic lung radiotherapy outcomes for early-stage non-small-cell lung cancer using daily online cone-beam computed tomography image-guided radiotherapy. *J Thorac Oncol* (2012) **7**:1382–93. doi:10.1097/JTO.0b013e318260e00d
38. Keall PJ, Mageras GS, Balter JM, Emery RS, Forster KM, Jiang SB, et al. The management of respiratory motion in radiation oncology report of AAPM Task Group 76. *Med Phys* (2006) **33**:3874–900. doi:10.1118/1.2349696
39. Wulf J, Hadinger U, Oppitz U, Olshausen B, Flentje M. Stereotactic radiotherapy of extracranial targets: CT simulation and accuracy of treatment in the stereotactic body frame. *Radiother Oncol* (2000) **57**:225–36. doi:10.1016/S0167-8140(00)00226-7
40. Slotman BJ, Lagerwaard FJ, Senan S. 4D imaging for target definition in stereotactic radiotherapy for lung cancer. *Acta Oncol* (2006) **45**:966–72. doi:10.1080/02841860600902817
41. Wang L, Hayes S, Paskalev K, Jin L, Buyyounouski MK, Ma CC, et al. Dosimetric comparison of stereotactic body radiotherapy using 4D CT and multiphase CT images for treatment planning of lung cancer: evaluation of the impact on daily dose coverage. *Radiother Oncol* (2009) **91**:314–24. doi:10.1016/j.radonc.2008.11.018
42. Timmerman R, Papiez L, McGarry R, Likes L, DesRosiers C, Frost S, et al. Extracranial stereotactic radioablation: results of a phase I study in medically inoperable stage I non-small cell lung cancer. *Chest* (2003) **124**:1946–55. doi:10.1378/chest.124.5.1946
43. Verellen D, Depuydt T, Gevaert T, Linthout N, Tournel K, Duchateau M, et al. Gating and tracking, 4D in thoracic tumours. *Cancer Radiother* (2010) **14**:446–54. doi:10.1016/j.canrad.2010.06.002
44. Gibbs IC, Loo BW Jr. CyberKnife stereotactic ablative radiotherapy for lung tumors. *Technol Cancer Res Treat* (2010) **9**:589–96.
45. Dawson LA, Jaffray DA. Advances in image-guided radiation therapy. *J Clin Oncol* (2007) **25**:938–46. doi:10.1200/JCO.2006.09.9515
46. Korreman S, Rasch C, McNair H, Verellen D, Oelfke U, Maingon P, et al. The European society of therapeutic radiology and oncology-European institute of radiotherapy (ESTRO-EIR) report on 3D CT-based in-room image guidance systems: a practical and technical review and guide. *Radiother Oncol* (2010) **94**:129–44. doi:10.1016/j.radonc.2010.01.004
47. Grills IS, Hugo G, Kestin LL, Galerani AP, Chao KK, Wloch J, et al. Image-guided radiotherapy via daily online cone-beam CT substantially reduces margin requirements for stereotactic lung radiotherapy. *Int J Radiat Oncol Biol Phys* (2008) **70**:1045–56. doi:10.1016/j.ijrobp.2007.07.2352

48. Guckenberger M, Krieger T, Richter A, Baier K, Wilbert J, Sweeney RA, et al. Potential of image-guidance, gating and real-time tracking to improve accuracy in pulmonary stereotactic body radiotherapy. *Radiother Oncol* (2009) **91**:288–95. doi:10.1016/j.radonc.2008.08.010
49. Shen Y, Zhang H, Wang J, Zhong R, Jiang X, Xu Q, et al. Hypofractionated radiotherapy for lung tumors with online cone beam CT guidance and active breathing control. *Radiat Oncol* (2010) **5**:19. doi:10.1186/1748-717X-5-19
50. Purdie TG, Moseley DJ, Bissonnette JP, Sharpe MB, Franks K, Bezjak A, et al. Respiration correlated cone-beam computed tomography and 4DCT for evaluating target motion in stereotactic lung radiation therapy. *Acta Oncol* (2006) **45**:915–22. doi:10.1080/02841860600907345
51. Sonke JJ, Lebesque J, van Herk M. Variability of four-dimensional computed tomography patient models. *Int J Radiat Oncol Biol Phys* (2008) **70**:590–8. doi:10.1016/j.ijrobp.2007.08.067
52. Sonke JJ, Rossi M, Wolthaus J, van Herk M, Damen E, Belderbos J. Frameless stereotactic body radiotherapy for lung cancer using four-dimensional cone beam CT guidance. *Int J Radiat Oncol Biol Phys* (2009) **74**:567–74. doi:10.1016/j.ijrobp.2008.08.004
53. Sweeney RA, Seubert B, Stark S, Homann V, Müller G, Flentje M, et al. Accuracy and inter-observer variability of 3D versus 4D cone-beam CT based image-guidance in SBRT for lung tumors. *Radiat Oncol* (2012) **7**:81. doi:10.1186/1748-717X-7-81
54. Jin JY, Yin FF, Tenn SE, Medin PM, Solberg TD. Use of the BrainLab ExacTrac X-Ray 6D system in image-guided radiotherapy. *Med Dosim* (2008) **33**:124–34. doi:10.1016/j.meddos.2008.02.005
55. Hoogeman M, Prévost JB, Nuyttens J, Pöll J, Levendag P, Heijmen B. Clinical accuracy of the respiratory tumor tracking system of the CyberKnife: assessment by analysis of log files. *Int J Radiat Oncol Biol Phys* (2009) **74**:297–303. doi:10.1016/j.ijrobp.2008.12.041
56. Malinowski KT, McAvoy TJ, George R, Dieterich S, D'Souza WD. Mitigating errors in external respiratory surrogate-based models of tumor position. *Int J Radiat Oncol Biol Phys* (2012) **82**:e709–16. doi:10.1016/j.ijrobp.2011.05.042
57. Pennathur A, Luketich JD, Heron DE, Abbas G, Burton S, Chen M, et al. Stereotactic radiosurgery for the treatment of stage I non-small cell lung cancer in high-risk patients. *J Thorac Cardiovasc Surg* (2009) **137**:597–604. doi:10.1016/j.jtcvs.2008.06.046
58. Bhagat N, Fidelman N, Durack JC, Collins J, Gordon RL, LaBerge JM, et al. Complications associated with the percutaneous insertion of fiducial markers in the thorax. *Cardiovasc Intervent Radiol* (2010) **33**:1186–91. doi:10.1007/s00270-010-9949-0
59. van der Voort van Zyp NC, Prévost JB, Hoogeman MS, Praag J, van der Holt B, Levendag PC, et al. Stereotactic radiotherapy with real-time tumor tracking for non-small cell lung cancer: clinical outcome. *Radiother Oncol* (2009) **91**:296–300. doi:10.1016/j.radonc.2009.02.011
60. Atalar B, Aydin G, Gungor G, Caglar H, Yapici B, Ozyar E. Dosimetric comparison of robotic and conventional linac-based stereotactic lung irradiation in early-stage lung cancer. *Technol Cancer Res Treat* (2012) **11**:249–55. doi:10.7785/tcr.2012.500293
61. Ding C, Chang CH, Haslam J, Timmerman R, Solberg T. A dosimetric comparison of stereotactic body radiation therapy techniques for lung cancer: robotic versus conventional linac-based systems. *J Appl Clin Med Phys* (2010) **11**:3223.
62. Liao Z, Lin SH, Cox JD. Status of particle therapy for lung cancer. *Acta Oncol* (2011) **50**:745–56. doi:10.3109/0284186X.2011.590148
63. Hata M, Tokuyama K, Kagei K, Sugahara S, Nakayama H, Fukumitsu N, et al. Hypofractionated high-dose proton beam therapy for stage I non-small cell lung cancer: preliminary results of a phase I/II clinical study. *Int J Radiat Oncol Biol Phys* (2007) **68**:786–93. doi:10.1016/j.ijrobp.2006.12.063
64. Fujii O, Demizu Y, Hashimoto N, Araya M, Takaqi M, Terashima K, et al. A retrospective comparison of proton therapy and carbon ion therapy for stage I non-small cell lung cancer. *Radiother Oncol* (2013) **109**:32–7. doi:10.1016/j.radonc.2013.08.038
65. Kang Y, Zhang X, Chang JY, Wang H, Wei X, Liao Z, et al. 4D proton treatment planning strategy for mobile lung tumors. *Int J Radiat Oncol Biol Phys* (2007) **67**:906–14. doi:10.1016/j.ijrobp.2006.10.045
66. Register SP, Zhang X, Mohan R, Chang JY. Proton stereotactic body radiation therapy for clinically challenging cases of centrally and superiorly located stage I non-small-cell lung cancer. *Int J Radiat Oncol Biol Phys* (2011) **80**:1015–22. doi:10.1016/j.ijrobp.2010.03.012
67. Seco J, Gu G, Marcelos T, Kooy H, Willers H. Proton arc reduces range uncertainty effects and improves conformality compared with photon volumetric modulated arc therapy in stereotactic body radiation therapy for non-small cell lung cancer. *Int J Radiat Oncol Biol Phys* (2013) **87**:188–94. doi:10.1016/j.ijrobp.2013.04.048
68. Seco J, Robertson D, Trofimov A, Paganetti H. Breathing interplay effects during proton beam scanning: simulation and statistical analysis. *Phys Med Biol* (2009) **54**:N283–94. doi:10.1088/0031-9155/54/14/N01
69. Santiago A, Jelen U, Ammazzalorso F, Engenhart-Cabillic R, Fritz P, Mühlnickel W, et al. Reproducibility of target coverage in stereotactic spot scanning proton lung irradiation under high frequency jet ventilation. *Radiother Oncol* (2013) **109**:45–50. doi:10.1016/j.radonc.2013.09.013

Conflict of Interest Statement: The Guest Associate Editor, Ulf Karlsson, declares that, despite having collaborated with authors Alexander Chi and Nam Nguyen, the review process was handled objectively and no conflict of interest exists. The authors declare that the research was conducted in the absence of any commercial or financial relationships that could be construed as a potential conflict of interest.

Received: 02 January 2014; paper pending published: 30 January 2014; accepted: 30 May 2014; published online: 25 June 2014.

Citation: Chi A, Nguyen NP and Komaki R (2014) The potential role of respiratory motion management and image guidance in the reduction of severe toxicities following stereotactic ablative radiation therapy for patients with centrally located early stage non-small cell lung cancer or lung metastases. *Front. Oncol.* **4**:151. doi:10.3389/fonc.2014.00151

This article was submitted to Radiation Oncology, a section of the journal *Frontiers in Oncology*.

Copyright © 2014 Chi, Nguyen and Komaki. This is an open-access article distributed under the terms of the Creative Commons Attribution License (CC BY). The use, distribution or reproduction in other forums is permitted, provided the original author(s) or licensor are credited and that the original publication in this journal is cited, in accordance with accepted academic practice. No use, distribution or reproduction is permitted which does not comply with these terms.



Strategies of dose escalation in the treatment of locally advanced non-small cell lung cancer: image guidance and beyond

Alexander Chi^{1*}, Nam Phong Nguyen², James S. Welsh³, William Tse⁴, Manish Monga⁴, Olusola Oduntan⁵, Mohammed Almubarak⁴, John Rogers⁴, Scot C. Remick⁴ and David Gius⁶

¹ Department of Radiation Oncology, Mary Babb Randolph Cancer Center of West Virginia University, Morgantown, WV, USA

² The International Geriatric Radiotherapy Group, Tucson, AZ, USA

³ Northern Illinois University Institute for Neutron Therapy at Fermilab, Batavia, IL, USA

⁴ Division of Hematology and Oncology, Mary Babb Randolph Cancer Center of West Virginia University, Morgantown, WV, USA

⁵ Thoracic Surgery, Mary Babb Randolph Cancer Center of West Virginia University, Morgantown, WV, USA

⁶ Department of Radiation Oncology, Robert H. Lurie Comprehensive Cancer Center of Northwestern University, Chicago, IL, USA

Edited by:

William Small, Stritch School of Medicine Loyola University Chicago, USA

Reviewed by:

Peter B. Schiff, NYU School of Medicine, USA

Kathryn Huber, Tufts Medical Center, USA

***Correspondence:**

Alexander Chi, Mary Babb Randolph Cancer Center of West Virginia University, PO Box 9234, 1 Medical Center Drive Morgantown, WV 26505, USA
e-mail: achiazz2010@gmail.com

Radiation dose in the setting of chemo-radiation for locally advanced non-small cell lung cancer (NSCLC) has been historically limited by the risk of normal tissue toxicity and this has been hypothesized to correlate with the poor results in regard to local tumor recurrences. Dose escalation, as a means to improve local control, with concurrent chemotherapy has been shown to be feasible with three-dimensional conformal radiotherapy in early phase studies with good clinical outcome. However, the potential superiority of moderate dose escalation to 74 Gy has not been shown in phase III randomized studies. In this review, the limitations in target volume definition in previous studies; and the factors that may be critical to safe dose escalation in the treatment of locally advanced NSCLC, such as respiratory motion management, image guidance, intensity modulation, FDG–positron emission tomography incorporation in the treatment planning process, and adaptive radiotherapy, are discussed. These factors, along with novel treatment approaches that have emerged in recent years, are proposed to warrant further investigation in future trials in a more comprehensive and integrated fashion.

Keywords: image guidance, intensity-modulated radiotherapy, NSCLC, adaptive radiotherapy, proton therapy

INTRODUCTION

Concurrent chemo-radiation is the standard of care in the management of non-small cell lung cancer (NSCLC) after its superiority over radiotherapy alone or sequential chemo-radiation has been demonstrated in multiple phase III randomized trials (1–5). In a meta-analysis of 1205 patients with locally advanced NSCLC from six randomized studies, concurrent chemo-radiation decreased loco-regional progression by 6.1% at 5 years when compared with sequential chemo-radiation (28.9 vs. 35.0%, $p = 0.01$) (6). This resulted in an improvement in overall survival of 4.5% at 5 years (15.1 vs. 10.6%, $p = 0.004$) and as suggested by the authors of this study, survival may be directly related to loco-regional control. The risk of regional failure, i.e., in the mediastinum, is relatively low after chemo-radiation to a dose of approximately 60 Gy with conventional fractionation (5, 7); in contrast, the rate of local failure remains relatively high. As such, it seems reasonable to propose that techniques to improve primary tumor control through dose escalation may be one strategy to improve treatment outcome in locally advanced NSCLC.

Dose escalation in the treatment of stage I–III NSCLC has been shown to be feasible in multiple institutional and early phase prospective studies (8–11). Among them, the radiation dose has been found to be a significant predictor of local control and survival by many (8–10). Based on the clinical outcome from a

University of Michigan study, 84.5 Gy was found to be required to achieve a local progression free survival (LPFS) of 50% at 30 months in patients with NSCLC (12). Further radiobiological modeling has suggested that a biologically effective dose (BED) of over 100 Gy₁₀ is required to achieve a LPFS of $\geq 80\%$ at 30 months in the treatment of NSCLC (13). This has been validated clinically in the treatment of early stage NSCLC with stereotactic ablative radiotherapy (SABR), which is also referred to as stereotactic body radiation therapy (SBRT) (14–16). In locally advanced NSCLC, every 1 Gy₁₀ in dose escalation was found to be associated with a 4% increase in survival and a 3% increase *in loco-regional* control in past chemo-radiation trials conducted by the Radiation Therapy Oncology Group (RTOG) (17). When combined with weekly carboplatin and paclitaxel, a maximally tolerated dose (MTD) of 74 Gy delivered with three-dimensional (3D) technique was found in a phase I/II RTOG study, RTOG 0117 (18). Inoperable patients with stage I–III NSCLC were included in this study, and a median survival of 21.6 months was observed in stage III patients. In a similar phase II study, a median survival of 24.3 months in stage III NSCLC patients was observed after induction carboplatin/paclitaxel followed by concurrent carboplatin/paclitaxel and radiation to 74 Gy (19).

Based on early clinical evidence, a phase III randomized dose escalation trial (RTOG 0617) was conducted by the RTOG. In

this study, patients were randomized to chemo-radiation to 60 vs. 74 Gy, and with or without Cetuximab (four arms) (20). Despite the anticipated improvement in clinical outcome with dose escalation, it actually resulted in inferior median survival (19.5 vs. 28.7 months, $p = 0.0007$) and an increase in local failure at 18 months (34.3 vs. 25.1%, $p = 0.0319$). In addition, dose escalation also resulted in an increase in grade 3 esophagitis (20.9 vs. 7.0%, $p = 0.0003$). The causes of poorer outcome in the 74-Gy arms remain to be discerned. However, several factors may potentially contribute to this finding, such as, larger-than-necessary planning target volume (PTV) in patients receiving 3D conformal radiotherapy (3D-CRT), which potentially leads to increased normal tissue toxicity; suboptimal target volume delineation when ¹⁸F-fluorodeoxyglucose (FDG) positron emission tomography (PET) information is not incorporated in the treatment planning process; failure to account for tumor shrinkage during the course of radiotherapy; and delayed tumor cell repopulation associated with prolonged overall treatment time. These can potentially be minimized with image-guided, intensity-modulated radiotherapy (IG-IMRT), and adaptive radiotherapy (ART), which may improve the efficacy of dose escalation in the treatment of locally advanced NSCLC in future clinical trials.

TARGET VOLUME IN RELATION TO CLINICAL OUTCOME AND TOXICITIES

In the treatment of locally advanced NSCLC with chemo-radiation, large tumor margins are often used to account for respiratory motion and set up uncertainties in the era of conventional and 3D radiotherapy (Table 1). With the addition of elective nodal irradiation (ENI), an even larger volume of normal tissue is included within the treated volume. As shown in Table 1, multiple clinical trials investigating the efficacy of sequential and concurrent chemo-radiation frequently used margins of 1.5–2 cm for the primary tumor. ENI was often carried out in these studies with inclusion of the bilateral hilum, mediastinum, and the ipsilateral supra-clavicular fossa in the initial radiation field, which extended 4–5 cm below the carina (3–5, 21–23). In these studies, dose to the gross disease has been limited to approximately 60 Gy with poor clinical outcome and fatal treatment related toxicities reported. Concurrent chemo-radiation prior to RTOG 0617 often led to a local control of 60–83%, while the median survival with concurrent chemo-radiation often increased to >15 months (3–5). Among them, seven late fatal pulmonary toxicities were observed in RTOG 9410, which demonstrated no significant improvement in local control and only marginal improvement in median survival with concurrent chemo-radiation over sequential chemo-radiation (5). These findings suggest that the large tumor volumes treated in the past not only precludes dose escalation to the primary tumor, but also increase the risk of severe treatment related toxicity.

Elective nodal irradiation, which for the most part involves treating areas of mediastinum that do not exhibit tumor as determined by imaging, has been shown to be unnecessary in the era of 3D-CRT. For example, a study by Rosenzweig et al. only identified a 6.1% elective nodal failure among 524 NSCLC patients who underwent radiotherapy to a mean dose of 66 Gy after a median follow up of 41 months (24). In a randomized prospective study by Yuan et al.

no statistically significant difference in the rate of elective nodal failure at 5 years following ENI (4%) and involved field irradiation (7%) was observed in stage III NSCLC patients who received concurrent chemo-radiation (25). However, involved field irradiation led to a reduction in radiation pneumonitis (RP) (mainly grade 2–3) from 29 to 17% ($p = 0.044$), and dose escalation from 60–64 to 68–74 Gy. This dose escalation led to statistically significant improvement in local control (55 vs. 38%, $p = 0.016$) and median survival (20.0 vs. 15.0 months, $p = 0.048$). With omission of ENI, dose escalation to 74 Gy with 3D techniques was found to be feasible in RTOG 0117 and CALGB 30105 (18, 19). However, a high rate of severe toxicity was still observed (Table 1). In this regard, the increased toxicity associated with dose escalation was corroborated by findings in RTOG 0617. This may be associated with the limitations of 3D techniques as 3D-CRT without image guidance was allowed in RTOG 0617, which often resulted in sizable gross tumor volume (GTV) to PTV expansion margins (26). Based on these studies, it is proposed that increasing expansion size may also increase the risk of severe treatment related toxicity in the high dose arm of RTOG 0617, which could potentially contribute to the observed decrease in patient survival.

STRATEGIES TO IMPROVE TARGET VOLUME DEFINITION THROUGH ADAPTIVE IMAGE-GUIDED IMRT

RESPIRATORY MOTION AND IMRT

The high incidence of loco-regional failures in NSCLC following radiotherapy may be associated with a high rate of tumor localization error during treatment (27). Such geometric errors may be minimized when respiratory motion is taken into consideration. Lung tumor motion associated with respiration has been well illustrated in multiple studies. In this regard, Seppenwoolde et al. showed that lower lobe tumors, not attached to any rigid thoracic structures, had increased cranial-caudal motion, as compared to upper lobe tumors or tumors attached to rigid structures during treatment (12 ± 6 vs. 2 ± 2 mm, $p = 0.005$) (28). In addition, anterior-posterior tumor motion of >5 mm could be observed in tumors located in the anterior or middle thorax and tumor motion was further complicated by hysteresis. In another study by Liu et al., cranial-caudal motion of >5 mm and ≥ 1 cm can be observed in 30 and 10% of patients with stage III NSCLC, which is associated with diaphragmatic movement of 1.53 cm on average (29). In a report by the AAPM task group 76, several strategies have been recommended to account for and control respiratory motion, which may be distinct for each individual patient (30).

One commonly used strategy to account for respiratory motion in the treatment of locally advanced NSCLC is 4D CT based treatment planning. Through 4D CT based planning, the range of tumor motion and changes in tumor volume through the entire breathing cycle can be more appropriately and reliably accounted for (29, 31–33). Also, it can potentially decrease the volume of normal tissue included in the PTV and this might be one technique to safely allow for dose escalation to the primary tumor (31). As such, it seems reasonable to suggest that improved accuracy in tumor localization throughout the respiratory cycle could improve tumor control probability (TCP) as “geometric tumor miss” is reduced. In this regard, the maximum intensity projections (MIP) reconstructed from a 4D data set, which reflects the brightest object

Table 1 | Target volume, toxicity, and clinical outcome in selected phase III randomized trials and phase I/II dose escalation trials combining chemotherapy and radiation for locally advanced NSCLC.

References	Radiotherapy technique	Tumor margin/ target volume expansion	ENI	Radiation dose	Severe RT related toxicity	Local control	Median survival (months)
PHASE III							
Dillman et al. (21)	2D	1.5 cm	Yes	60 Gy	1% (esophagitis, pneumonitis) in each arm	OR: ChemoRT 56% RT 43% ($p = 0.092$)	ChemoRT 13.7 ($p = 0.034$) RT 9.6
Sause et al. (22)	2D	2 cm	Yes	60, 69.6 Gy (bid)	Two radiation related deaths on ChemoRT and hyperfrx arms (1 on each arm)		RT 11.4 ChemoRT 13.2 ($p = 0.04$) Hyperfrx RT 12
Le Chevalier et al. (23)	2D	1–1.5 cm	Yes	65 Gy	Eight treatment related fatal toxicities	At 1 year: RT 17% ChemoRT 15%	RT 10 ChemoRT 12 ($p = 0.02$)
Furuse et al. (3)	2D	1.5 cm	Yes	56 Gy	No >grade 3 esophagitis, 1 grade 4 pulmonary toxicity on each arm	OR: concurrent 84.0% Sequential 66.4% ($p = 0.0002$)	Concurrent 16.5 ($p = 0.03998$) Sequential 13.3
Zatloukal et al. (4)	3D	1.5–2 cm	Yes	60 Gy	Severe acute esophagitis ($p = 0.009$): sequential 4% Concurrent 18%	Local only ($p = \text{NS}$): sequential 42% Concurrent 60%	Sequential 12.9 Concurrent 16.6
Curran et al. (5)	2D	2–2.5 cm	Yes	63; 69.6 Gy (bid)	Acute esophagitis ($p < 0.001$): sequential 4% Concurrent 22% Concurrent hyperfrx 45% Late severe pulmonary toxicities: no difference between three arms (13–17%) Seven late fatal pulmonary toxicities observed in this study	Sequential 61% Concurrent 70% Concurrent hyperfrx 71% ($p = \text{NS}$)	Sequential 14.6 Concurrent 17.0 Concurrent hyperfrx 15.6
Nyman et al. (7)	3D	CTV: 1.5–2 cm	No	64.6 Gy (bid); 60 Gy	Severe esophagitis: concurrent hyperfrx 20% Concurrent, daily 8% Concurrent, weekly 19% Severe pneumonitis: concurrent hyperfrx 0 Concurrent, daily 3% Concurrent, weekly 3%	Concurrent Hyperfrx 78% Concurrent, daily 78% 17.68 Concurrent, weekly 83%	Concurrent Hyperfrx 17.69 Concurrent, daily 17.68 Concurrent, weekly 20.63
Bradley et al. (20)	3D/IMRT	CTV: 0.5–1 cm; ITV (no 4D): 0.5–1 cm PTV: 0.5–1 cm	No	60 Gy; 74 Gy	Increased grade 5 toxicity observed with 74 Gy	18-month local failure: 60 Gy 25.1% 74 Gy 34.3% ($p = 0.0319$)	60 Gy 28.7 74 Gy 19.5

(Continued)

Table 1 | Continued

References	Radiotherapy technique	Tumor margin/ target volume expansion	ENI	Radiation dose	Severe RT related toxicity	Local control	Median survival (months)
PHASE I, II							
Bradley et al. (18)	3D	GTV-PTV: 1–1.5 cm	No	74 Gy	Grade 5 acute toxicity 4% Late grade 3–4 toxicities 20%		21.6 (stage III)
Socinski et al. (19)	3D	CTV 0.5–2 cm; PTV: 1 cm	No	74 Gy	Grade 3 acute esophagitis 16% Grade 3–5 pulmonary toxicity 16%	54%	24.3

NSCLC: non-small cell lung cancer; ENI: elective nodal irradiation; 2D: two-dimensional; 3D: three-dimensional; IMRT: intensity modulated radiotherapy; Hyperfrx: hyperfractionated; bid: twice daily; RT: radiotherapy; ChemoRT: chemo-radiation; OR: objective response.

along each ray on the projection image, may be used for the generation of the internal target volume (ITV) (34) that includes tumor motion into the radiation planning process. However, the outer excursion of respiratory motion may be underestimated by MIP in more advanced tumors and in the setting of irregular breathing patterns by approximately 20% as reported in previous studies (35–37). Thus, the ITV should be generated based on all available 4D CT data.

The utility of 4D CT combined with thoracic IMRT in the treatment of locally advanced NSCLC with chemo-radiation was shown to lower treatment related toxicity and improve patient survival when compared to 3D-CRT in a study from MD Anderson Cancer Center (38). This may be associated with dosimetric advantages of IMRT over 3D-CRT in dose conformity and the sparing of normal organs at risk (OARs) (39–41). As shown by Lievens et al., IMRT can result in significant reduction in the dose to the normal lungs and the spinal cord when compared to 3D-CRT (41). This led to the safe escalation of the prescribed dose (66 Gy in 33 daily fractions) by 8.6–14.2 Gy. Therefore, IMRT may be a strategy for dose escalation in the treatment of locally advanced NSCLC in selected patients through its ability to control radiation dose to critical OARs. This is also suggested by a quality of life (QoL) analysis of RTOG 0617, which demonstrated that the use of IMRT in the setting of dose escalation may improve patients' QoL, which has been correlated with overall survival (42). Dose escalation with the use of IMRT alone remains to be further investigated in future studies.

IMAGE GUIDANCE WITH CONE-BEAM CT (CBCT)

Intensity modulated radiotherapy can be used to achieve highly conformal dose distribution with sharp dose gradients and careful daily tumor localization should ensure accurate dose delivery with maximal reduction of treatment margins used for target volume delineation (43–45). This is especially important for dose escalation as radiotherapy often requires 6 weeks or greater to complete in the setting of chemo-radiation for locally advanced NSCLC. In this regard, various image guidance strategies have been proposed and are in clinical use currently (30, 46). Tumor volume,

its geometric relation to surrounding OARs, and any anatomical changes during a course of radiotherapy are best imaged with volumetric imaging techniques such as kV or MV cone-beam CT (CBCT). KV CBCT often provides superior soft tissue resolution with compared with MV CBCT due to the prevalence of photoelectric absorption interactions associated with lower beam energies (47). However, MV CBCT may be more helpful in the imaging of regions with high density materials, which produce artifacts in kV CT images (46, 47). As shown by Bissonnette et al., kV CBCT can reduce the set up margin for geometric uncertainties to 3 mm for locally advanced NSCLC patients (48). Such small margin can be safely used under daily image guidance, which reduce set up errors of ≥ 5 mm from 20–43 to 6% when compared with less-than-daily image guidance (49). Thus, daily image guidance is critical for the safe maximal reduction of set up margins when IGRT, or IG-IMRT is delivered; which will also maximize the possibility of safe dose escalation to the highest dose possible. When compared to other forms of image guidance, kV CBCT was found to be associated with more reliable tumor localization and smaller set up errors (50, 51) and this advantage appears to be most prominent with image registration based on soft tissue in addition to rigid bony registration (51, 52). However, tissue resolution and motion artifacts continue to be a concern for the use of CBCT in the setting of locally advanced NSCLC. These issues may be minimized by 4D CBCT, which remains to be further investigated in the clinical setting (53). One caveat for the clinical adaptation of image-guided IMRT is that there is always a risk for underestimating the range of tumor motion at the time of CT simulation due to the random occurrence of irregular breathing patterns (e.g., random deep inspiration) during the actual delivery of a course of conventionally fractionated radiotherapy. This may potentially lead to the under-dosing of the gross tumor in selected situations of dose painting as very sharp dose gradients are generated at the edge of the tumor targets with intensity modulation. Respiration motion management strategies, such as forced shallow breathing with abdominal compression, may reduce the risk for such geometric misses by limiting diaphragmatic motion to within 5 mm during daily treatment.

THE ROLE OF FDG-PET IN TARGET VOLUME DELINEATION

FDG-PET/CT has been increasingly incorporated into the treatment planning process to further increase the accuracy of target volume delineation in recent years. FDG-PET imaging is achieved through the detection of a pair of γ rays (511 keV each) that are produced in positron annihilation, which are emitted in 180° to each other (54). FDG-PET is associated with superior sensitivity and specificity (83 and 91%) for tumor detection when compared to CT (64 and 74%) (55). Therefore, PET may provide information for target volume delineation that may be otherwise not available with CT alone.

When compared with CT based treatment planning, PET registered to the planning CT was shown to alter tumor staging in 31% of the patients with stage I–III NSCLC by Bradley et al. (56). In this study, the addition of FDG-PET information resulted in alterations of the treatment volumes in 58% of the patients who were planned for 3D-CRT. Such alterations resulted from the identification of additional regional or parenchymal disease; and the improved tumor definition in the setting of atelectasis, which decreases the unnecessary inclusion of normal lung tissue in the GTV and these findings were corroborated in other studies (57, 58). Also, increased PTV volume, due to the additional nodal disease found with FDG-PET, does not necessarily increase the normal tissue complication probability; while PET data may improve the chance of local control by reducing the likelihood of geometric misses (57). Therefore, the inclusion of FDG-PET information in the treatment planning improves the accuracy of tumor volume delineation, which is critical in the optimization of TCP through IG-IMRT. In addition, PET may lead to nodal GTV reduction and lower doses to the OARs for stage III NSCLC when compared with treatment planning with CT alone, possibly leading to significant iso-toxic dose escalation (59, 60). Based on the evidence illustrated above, FDG-PET inclusion in the treatment planning process may be required in future dose escalation trials for locally advanced NSCLC.

ADAPTIVE IMAGE-GUIDED IMRT

Tumor shrinkage through a course of conventionally fractionated radiotherapy has been well characterized in multiple studies (61–64). In one study, a median GTV reduction of 24.7% after 30 Gy, and 44.3% after 50 Gy was observed in 22 patients with stage I–III NSCLC (78% stage III, 68% squamous cell carcinoma, and 68% underwent concurrent chemo-radiation) (63). In an analysis of 4D CT data collected before and during radiotherapy of at least 6 weeks from patients with stage I–III NSCLC, tumor shrinkage of $\geq 40\%$ by the end of radiotherapy was observed in 50% of the patients (mainly stage III) (64). Also, increased tumor motion in the crano-caudal direction increased in half of the patients as tumors shrunk. The observed changes may have an impact on PTV dose coverage and OAR sparing in the treatment of locally advanced NSCLC (62, 65). Therefore, re-planning or ART based on changes observed through daily image guidance is warranted in the treatment of locally advanced NSCLC, which may further maximize safe dose escalation to the gross disease. This may be especially important for IG-IMRT due to the sharp dose gradient generated and small margins for geometric uncertainties used.

Altered fractionation has been previously shown to improve local control and overall survival in the treatment of locally advanced NSCLC (66). This is also supported by the observed clinical outcome following hypo-fractionated radiotherapy for early stage NSCLC (16, 67). Altered fractionation is especially appealing in the setting of dose escalation, as prolonged course of radiotherapy can lead to increased geometric uncertainties, and impairment of local control due to accelerated tumor cell repopulation, which may partially explain the results observed in RTOG 0617 (13, 65). This is also supported by previous RTOG studies on concurrent chemo-radiation, which demonstrated a 2% increase in the risk of death for each day in the prolongation of therapy (68). A dose-per-fraction escalation strategy has been previously proposed to overcome the negative impact of tumor cell repopulation encountered when the total tumor dose is escalated with conventional fractionation. As modeled by Welsh et al., the TCP can be increased to $> 80\%$ with this strategy in approximately 5 weeks, which would require 100 Gy to be delivered over 10 weeks with conventional fractionation (69).

Early phase and retrospective studies on altered fractionation for radiotherapy alone or combined with chemotherapy in the treatment of stage III NSCLC have shown the feasibility of this strategy (70–78). This is especially true for chemo-radiation delivered with IGRT (74–78). As shown in Table 2, excellent median survival and local control have been frequently observed when hypofractionated, image-guided IMRT was delivered with concurrent chemotherapy. However, severe RP may occur with this approach if low dose irradiation of the normal lungs was not carefully constrained (74, 75). This was shown by Song et al., who observed four RP related deaths following image-guided IMRT delivered with helical tomotherapy (HT) (75). In this study, the rate of \geq grade 3 RP increased from 0 to 35%, when the volume of the contralateral lung receiving 5 Gy (V_5) was increased to above 60% ($p = 0.010$). This is corroborated in a study by Kim et al., which identified the ipsilateral V_5 , V_{10} , V_{15} , and the contralateral V_5 to be significant predictors of RP following HT based IGRT (79). This observation may be partially due to the fan-beam nature of IMRT delivery with HT, which leads to increased low dose irradiation of the normal tissue (80). However, the importance of normal lung sparing from low dose irradiation was observed following linac based IMRT as well, suggesting this to be independent from methods of radiation delivery (81).

One strategy to reduce treatment related toxicities associated with hypo-fractionated radiotherapy may be simultaneously integrated boost (SIB) to the gross tumor through FDG-PET based dose painting and the utility of adaptive IG-IMRT. This is suggested in a dosimetric study of 13 patients with stage III NSCLC (82). In this study, IMRT was shown to reduce the mean lung dose; furthermore, adaptive IMRT with SIB was shown to be superior to 3D-CRT or IMRT alone in dose escalation for larger GTVs, and was able to achieve maximal iso-toxic dose escalation of $17.1 \pm 10.1\%$, which increased TCP by 17.2% on average. This is consistent with image-guided IMRT with the SIB technique that has been previously shown to be feasible by Song et al. (75), and the utilization of adaptive IG-IMRT with SIB in the treatment of locally advanced NSCLC warrants further investigation in future dose escalation trials.

Table 2 | Chemo-IGRT for locally advanced NSCLC.

Reference	RT technique	Dose	Clinical outcome	Toxicity
Bral et al. (75)	HT	PTV 70.5 Gy/30 fractions	MS: Stage IIIA vs. III B (21 vs. 12 months, $p = 0.03$). 2-year LPFS: 50%	Late lung toxicity Grade 2 23% Grade 3 16% Two deaths due to grade 5 RP
Song et al. (76)	SIB with HT	GTV: 60–70.4 Gy (2–2.4 Gy/fraction) PTV: 50–64 Gy (1.8–2 Gy/fraction)	Stage III 2 year LC 62% (78% with C-Ch) MS not reached 2 year OS 59% (75% with C-Ch) Only 1 in-field failure was observed	Acute: 14% with grade 3 esophagitis Late: 11% with grade 5 treatment related pneumonitis V_5 of contralateral lung is a significant predictor of severe RP ($p = 0.029$)
Osti et al. (77)	3D-CRT under kV CBCT image guidance	PTV 60 Gy/20 fractions	Local failure: 37% MS (stage III): 13 months	No patient with >grade 3 treatment related toxicities
Bearz et al. (78)	HT	60 Gy/25 fractions	ORR: 84% MS: 24 months ^a	No RP reported No >grade 3 esophagitis
Donato et al. (79)	HT	67.5–68.4 Gy/30 fractions	Progression in 26% MS 24.1 months (C-Ch)	Acute grade 3 RP 10% Late grade 3 RP 5% No >grade 3 toxicity observed

^aInduction + concurrent chemotherapy; SIB, simultaneously integrated boost; HT, helical tomotherapy; 3D-CRT, 3D conformal radiotherapy; C-Ch, concurrent chemotherapy; LC, local control; OS, overall survival; MS, median survival; LPFS, local progression free survival; RP, radiation pneumonitis.

NOVEL USE OF A STEREOTACTIC BOOST AND PROTON THERAPY

Tumor shrinkage after a course of conventionally fractionated radiotherapy may allow for the delivery of a stereotactic boost to the primary tumor in selected patients. In a study by Feddock et al., 10 Gy \times 2 fractions, or 6.5 Gy \times 3 fractions were delivered following chemo-radiation to a median dose of 59.4 Gy in the treatment of stage II–III NSCLC (83). Although well tolerated in patients with peripheral primary tumors, two deaths due to fatal pulmonary hemorrhage occurred in patients with central lesions. Six local recurrences were observed among 35 patients after a median follow up of 13 months, which corresponds to an actuarial local control of 82.9%. These preliminary results suggest the feasibility of this treatment approach in selected patients, however, patient selection and the most optimal dose fractionation schedule to be used in this setting remains to be further investigated.

Proton therapy has been increasingly investigated in the treatment of lung cancer in recent years due to its advantage in normal tissue sparing over photon therapy (84). In the interaction with tissue, protons enter with lower dose than photon, and deposit the majority of their energy at a certain depth (Bragg peak) with very little exit dose. To be clinically useful, several Bragg peaks can be super-positioned to create a spread-out Bragg peak (SOBP) to cover a specific tumor volume with a desired dose. When compared with photon therapy (3D-CRT or IMRT), proton therapy was shown to significantly reduce the dose to the thoracic OARs, which allowed dose escalation from 63 to 74 Gy within the boundaries of accepted normal tissue dose constraints in stage III NSCLC (85). Intensity-modulated proton therapy

(IMPT) may further improve OAR sparing in stage IIIB NSCLC patients, which increases the possibility of dose escalation when compared to IMRT (63–83.5 Gy), and passive scattering proton therapy (PSPT) (74–84.4 Gy) (86). ART may also be indicated in the delivery of PT to improve OAR sparing and target volume coverage (87). In a retrospective study of PT for patients with stage II–III NSCLC, local control of 88.6% was achieved following a median follow up of 16.9 months (88). In this study, a median dose of 78.3 Gy was delivered without any \geq grade 3 toxicity observed. In a phase II study of concurrent chemotherapy and PSPT (74 Gy) for stage III NSCLC, local control of 79.5% and a median overall survival of 29.4 months were observed after a median follow up of 19.7 months (89). In this study, isolated local failure was observed in only 9.1% of the patients, while no grade 4–5 toxicity was observed. While comparable to what is observed in the standard arm of RTOG 0617 in median survival, this may be further improved with adaptive IG-IMPT, which needs to be further investigated in future studies. Due to the unique physical properties of protons, dose distribution in IMPT is very sensitive to tumor motion in relation to the treatment beam scanning motion, which is known as the interplay effect (90). Range uncertainties produced by the interplay effect may lead to under-dosing of the tumor or increased dose to the OARs immediately beyond the range of the proton beam. To account for interplay uncertainties, 4D treatment planning, larger spot size, and fractionated dose schedules have been advocated (91–93). Recently, image guidance for range verification during proton therapy has been shown to be feasible with in-room PET imaging (94). This along with strategies to overcome interplay uncertainties in proton therapy warrants further

investigation. However, early clinical experience with proton therapy in the setting of dose escalation for locally advanced NSCLC appears promising.

Although not widely studied, delivering SABR to small peripheral primary tumors and conventionally fractionated radiotherapy combined with concurrent chemotherapy to regional nodal disease in selected cases of locally advanced NSCLC has been endorsed and clinically used by many thoracic Radiation Oncologists. The local control of the primary tumor may be potentially improved as suggested by clinical outcome from SABR for early stage NSCLC (16). At the same time, the regional disease can be addressed with concurrent chemo-radiation. SABR combined with concurrent chemo-radiation, as definitive treatment or a boost to the primary disease, will be suitable for a selected group of patients only. As the mediastinum contains many critical normal structures, which may be at a risk for overdosing along with the lungs if the primary tumor is in their proximity.

CHEMOTHERAPY IN THE SETTING OF DOSE ESCALATION

Combining chemotherapy with radiotherapy has been shown to improve local control and patients' overall survival in previous trials (1, 95). However, chemotherapy, especially taxane-based regimens, has been associated with increased incidence of severe RP (96–99). Severe RP was observed in 47% of the patients treated with concurrent weekly docetaxel and conventionally fractionated radiotherapy to 60–66 Gy delivered with 2D techniques in a phase II study (96). This observation was dose independent, but correlated with the size of initial radiation portals. Consolidation docetaxel was also found to be correlated with increased risk of grade 2–5 RP (14.6 vs. 3.6%, $p = 0.015$) following concurrent chemo-radiation in the retrospective review of the dosimetric data from a randomized prospective study (97). In this study, the mean lung dose was also significantly correlated with the incidence of RP. Furthermore, the increased risk of RP with chemotherapy may be more prominent in patients who are older (98, 99). Therefore, special attention may be necessary to keep the treated volume to as small as possible to minimize the amount of normal lung tissue irradiated to the full dose, which may be especially important in patients who are older than 65 years (99). For the purpose of dose escalation in the setting of chemo-radiation, this may be best accomplished with modern techniques of respiratory motion management and image guidance used in the context of various emerging treatment strategies discussed above.

CONCLUSION

Adaptive, image-guided IMRT, when delivered with appropriate respiratory motion management strategies, can effectively reduce the tumor target volume while accurately localize the tumor during a course of chemo-radiation. This allows for dose escalation to the gross disease in the treatment of locally advanced NSCLC as less normal tissue is being irradiated to the prescribed dose. This strategy can be further enhanced with the incorporation of FDG-PET in target volume definition. The utility of stereotactic ablative therapy as a boost or definitive treatment for the primary tumor appears to be feasible in selected patients, while proton therapy, and especially IMPT, appears to be promising and may be superior to photon therapy in dose escalation for

the treatment of locally advanced NSCLC. These new treatment approaches remain to be further studied in future clinical trials. Here, we propose the following strategies to be further investigated in selected patients in future trials with respiratory motion management and the incorporation of FDG-PET in the treatment planning required:

- (1) Adaptive image-guided IMRT or IMPT delivered in a simultaneously integrated fashion with concurrent chemotherapy.
- (2) Stereotactic boost to the primary tumor to be delivered prior or after a standard course of concurrent chemo-radiation to 60 Gy, or given in between a split course of concurrent chemo-radiation that is hypofractionated, image-guided, and intensity modulated.
- (3) Stereotactic ablative radiotherapy to the primary tumor to be followed by concurrent chemotherapy and image-guided IMRT to the regional nodal disease.

REFERENCES

1. Schaake-Konning C, Van Den Bogaert W, Dalesio O, Festen J, Hoogenhout J, van Houtte P, et al. Effects of concomitant cisplatin and radiotherapy on inoperable non-small-cell lung cancer. *N Engl J Med* (1992) **326**:524–30. doi:10.1056/NEJM199202203260805
2. Jeremic B, Shibamoto Y, Acimovic L, Milisavljevic S. Hyperfractionated radiation therapy with or without concurrent low-dose daily carboplatin/etoposide for stage III non-small-cell lung cancer: a randomized study. *J Clin Oncol* (1996) **14**:1065–70.
3. Furuse K, Fukuoka M, Kawahara M, Nishikawa H, Takada Y, Kudoh S, et al. Phase III study of concurrent versus sequential thoracic radiotherapy in combination with mitomycin, vindesine, and cisplatin in unresectable stage III non-small cell lung cancer. *J Clin Oncol* (1999) **17**:2692–9.
4. Zatloukal P, Petruzelka L, Zemanova M, Havel I, Janku F, Judas L, et al. Concurrent versus sequential chemoradiotherapy with cisplatin and vinorelbine in locally advanced non-small cell lung cancer: a randomized study. *Lung Cancer* (2004) **46**:87–98. doi:10.1016/j.lungcan.2004.03.004
5. Curran WJ Jr, Paulus R, Langer CJ, Komaki R, Lee JS, Hauser S, et al. Sequential vs. concurrent chemoradiation for stage III non-small cell lung cancer: randomized phase III trial RTOG 9410. *J Natl Cancer Inst* (2011) **103**:1452–60. doi:10.1093/jnci/djr325
6. Aupérin A, Le Péchoux C, Rolland E, Curran WJ, Furuse K, Fournel P, et al. Meta-analysis of concomitant versus sequential radiochemotherapy in locally advanced non-small-cell lung cancer. *J Clin Oncol* (2010) **28**:2181–90. doi:10.1200/JCO.2009.26.2543
7. Nyman J, Friesland S, Hallqvist A, Seke M, Bergström S, Thaning L, et al. How to improve loco-regional control in stages IIIa-b NSCLC? Results of a three-armed randomized trial from the Swedish Lung Cancer Study Group. *Lung Cancer* (2009) **65**:62–7. doi:10.1016/j.lungcan.2008.10.021
8. Kong FM, Ten Haken RK, Schipper MJ, Sullivan MA, Chen M, Lopez C, et al. High-dose radiation improved local control and overall survival in patients with inoperable/unresectable non-small-cell lung cancer: long-term results of a radiation dose escalation study. *Int J Radiat Oncol Biol Phys* (2005) **63**:324–33. doi:10.1016/j.ijrobp.2005.02.010
9. Rosenzweig KE, Fox JL, Yorke E, Amols H, Jackson A, Rusch V, et al. Results of a phase I dose-escalation study using three-dimensional conformal radiotherapy in the treatment of inoperable nonsmall cell lung carcinoma. *Cancer* (2005) **103**:2118–27. doi:10.1002/cncr.21007
10. Willner J, Baier K, Caragiani E, Tschammler A, Flentje M. Dose, volume, and tumor control predictions in primary radiotherapy of non-small-cell lung cancer. *Int J Radiat Oncol Biol Phys* (2002) **52**:382–9. doi:10.1016/S0360-3016(01)01823-5
11. Bradley J, Graham MV, Winter K, Purdy JA, Komaki R, Roa WH, et al. Toxicity and outcome results of RTOG 9311: a phase I-II dose-escalation study using three-dimensional conformal radiotherapy in patients with inoperable non-small-cell lung carcinoma. *Int J Radiat Oncol Biol Phys* (2005) **61**:318–28. doi:10.1016/j.ijrobp.2004.06.260

12. Martel MK, Ten Haken RK, Hazuka MB, Kessler ML, Strawderman M, Turrisi AT, et al. Estimation of tumor control probability model parameters from 3-D dose distributions of non-small cell lung cancer patients. *Lung Cancer* (1999) **24**:31–7. doi:10.1016/S0169-5002(99)00019-7
13. Fowler JF, Tomé W, Fenwick JD, Mehta MP. A challenge to traditional radiation oncology. *Int J Radiat Oncol Biol Phys* (2004) **60**:1241–56. doi:10.1016/j.ijrobp.2004.07.691
14. Onishi H, Shirato H, Nagata Y, Hiraoka M, Fujino M, Gomi K, et al. Hypofractionated stereotactic radiotherapy (HypoFXSRT) for stage I non-small cell lung cancer: updated results of 257 patients in a Japanese multi-institutional study. *J Thorac Oncol* (2007) **2**:S94–100. doi:10.1097/JTO.0b013e318074de34
15. Grills IS, Hope AJ, Guckenberger M, Kestin LL, Werner-Wasik M, Yan D, et al. A collaborative analysis of stereotactic lung radiotherapy outcomes for early-stage non-small-cell lung cancer using daily online cone-beam computed tomography image-guided radiotherapy. *J Thorac Oncol* (2012) **7**:1382–93. doi:10.1097/JTO.0b013e318260e00d
16. Chi A, Liao Z, Nguyen NP, Xu J, Stea B, Komaki R. Systemic review of the patterns of failure following stereotactic body radiation therapy in early-stage non-small-cell lung cancer: clinical implications. *Radiother Oncol* (2010) **94**:1–11. doi:10.1016/j.radonc.2009.12.008
17. Machtay M, Bae K, Movsas B, Paulus R, Gore EM, Komaki R, et al. Higher biologically effective dose of radiotherapy is associated with improved outcomes for locally advanced non-small cell lung carcinoma treated with chemoradiation: an analysis of the Radiation Therapy Oncology Group. *Int J Radiat Oncol Biol Phys* (2012) **82**:425–34. doi:10.1016/j.ijrobp.2010.09.004
18. Bradley JD, Bae K, Graham MV, Byhardt R, Govindan R, Fowler J, et al. Primary analysis of the phase II component of a phase I/II dose intensification study using three-dimensional conformal radiation therapy and concurrent chemotherapy for patients with inoperable non-small-cell lung cancer: RTOG 0117. *J Clin Oncol* (2010) **28**:2475–80. doi:10.1200/JCO.2009.27.1205
19. Socinski MA, Blackstock AW, Bogart JA, Wang X, Munley M, Rosenman J, et al. Randomized phase II trial of induction chemotherapy followed by concurrent chemotherapy and dose-escalated thoracic conformal radiotherapy (74 Gy) in stage III non-small-cell lung cancer: CALGB 30105. *J Clin Oncol* (2008) **26**:2457–63. doi:10.1200/JCO.2007.14.7371
20. Bradley JD, Paulus R, Komaki R, Masters GA, Forster K, Schild SE, et al. A randomized phase III comparison of standard-dose (60 Gy) versus high-dose (74 Gy) conformal chemoradiotherapy with or without cetuximab for stage III non-small cell lung cancer. Results on radiation dose in RTOG 0617. *J Clin Oncol* (2013) **31**:(Suppl 7501).
21. Dillman RO, Seagren SL, Propert KJ, Guerra J, Eaton WL, Perry MC, et al. A randomized trial of induction chemotherapy plus high-dose radiation versus radiation alone in stage III non-small-cell lung cancer. *N Engl J Med* (1990) **323**:940–5. doi:10.1056/NEJM199010043231403
22. Sause W, Kolesar P, Taylor S, Johnson D, Livingston R, Komaki R, et al. Final results of phase III trial in regionally advanced unresectable non-small cell lung cancer: Radiation Therapy Oncology Group, Eastern Cooperative Oncology Group, and Southwest Oncology Group. *Chest* (2000) **117**:358–64. doi:10.1378/chest.117.2.358
23. Le Chevalier T, Arriagada R, Quoix E, Ruffie P, Martin M, Douillard JY, et al. Radiotherapy alone versus combined chemotherapy and radiotherapy in unresectable non-small cell lung carcinoma. *Lung Cancer* (1994) **10**:S239–44. doi:10.1016/0169-5002(94)91687-X
24. Rosenzweig KE, Sura S, Jackson A, Yorke E. Involved-field radiation therapy for inoperable non-small-cell lung cancer. *J Clin Oncol* (2007) **25**:5557–61. doi:10.1200/JCO.2007.13.2191
25. Yuan S, Sun X, Li M, Yu J, Ren R, Yu Y, et al. A randomized study of involved-field irradiation versus elective nodal irradiation in combination with concurrent chemotherapy for inoperable stage III nonsmall cell lung cancer. *Am J Clin Oncol* (2007) **30**:239–44. doi:10.1097/01.coc.0000256691.27796.24
26. Available from: [http://www.rtg.org/ClinicalTrials/ProtocolTable/StudyDetails.aspx?study=0617](http://www.rtog.org/ClinicalTrials/ProtocolTable/StudyDetails.aspx?study=0617)
27. Rosenman JG, Halle JS, Socinski MA, Deschesne K, Moore DT, Johnson H, et al. High-dose conformal radiotherapy for treatment of stage IIIA/IIIB non-small-cell lung cancer: technical issues and results of a phase I/II trial. *Int J Radiat Oncol Biol Phys* (2002) **54**:348–56. doi:10.1016/S0360-3016(02)02958-9
28. Seppenwoolde Y, Shirato H, Kitamura K, Shimizu S, van Herk M, Lebesque JV, et al. Precise and real-time measurement of 3D tumor motion in lung due to breathing and heartbeat, measured during radiotherapy. *Int J Radiat Oncol Biol Phys* (2002) **53**:822–34. doi:10.1016/S0360-3016(02)02803-1
29. Liu HH, Balter P, Tutt T, Choi B, Zhang J, Wang C, et al. Assessing respiration-induced tumor motion and internal target volume using four-dimensional computed tomography for radiotherapy of lung cancer. *Int J Radiat Oncol Biol Phys* (2007) **68**:531–40. doi:10.1016/j.ijrobp.2006.12.066
30. Keall PJ, Mageras GS, Balter JM, Emery RS, Forster KM, Jiang SB, et al. The management of respiratory motion in radiation oncology report of AAPM Task Group 76. *Med Phys* (2006) **33**:3874–900. doi:10.1118/1.2349696
31. Rietzel E, Liu AK, Doppke KP, Wolfgang JA, Chen AB, Chen GT, et al. Design of 4D treatment planning target volumes. *Int J Radiat Oncol Biol Phys* (2006) **66**:287–95. doi:10.1016/j.ijrobp.2006.05.024
32. Pantarotto JR, Piet AH, Vincent A, van Sörsen de Koste JR, Senan S. Motion analysis of 100 mediastinal lymph nodes: potential pitfalls in treatment planning and adaptive strategies. *Int J Radiat Oncol Biol Phys* (2009) **74**:1092–9. doi:10.1016/j.ijrobp.2008.09.031
33. Redmond KJ, Song DY, Fox JL, Zhou J, Rosenzweig CN, Ford E. Respiratory motion changes of lung tumors over the course of radiation therapy based on respiration-correlated four-dimensional computed tomography scans. *Int J Radiat Oncol Biol Phys* (2009) **75**:1605–12. doi:10.1016/j.ijrobp.2009.05.024
34. Underberg RW, Lagerwaard FJ, Slotman BJ, Cuypers JP, Senan S. Use of maximum intensity projections (MIPs) for target volume generation in 4DCT scans for lung cancer. *Int J Radiat Oncol Biol Phys* (2005) **63**:253–60. doi:10.1016/j.ijrobp.2005.05.045
35. Muirhead R, McNee SG, Featherstone C, Moore K, Muscat S. Use of maximum intensity projections (MIPs) for target outlining in 4DCT radiotherapy planning. *J Thorac Oncol* (2008) **3**:1433–8. doi:10.1097/JTO.0b013e3181e5db7
36. Cai J, Read PW, Baisden JM, Larner JM, Benedict SH, Sheng K. Estimation of error in maximal intensity projection-based internal target volume of lung tumors: a simulation and comparison study using dynamic magnetic resonance imaging. *Int J Radiat Oncol Biol Phys* (2007) **69**:895–902. doi:10.1016/j.ijrobp.2007.07.2322
37. Park K, Huang L, Gagne H, Papiez L. Do maximum intensity projection images truly capture tumor motion? *Int J Radiat Oncol Biol Phys* (2009) **73**:618–25. doi:10.1016/j.ijrobp.2008.10.008
38. Liao ZX, Komaki RR, Thames HD, Liu HH, Tucker SL, Mohan R, et al. Influence of technologic advances on outcomes in patients with unresectable, locally advanced non-small-cell lung cancer receiving concomitant chemoradiotherapy. *Int J Radiat Oncol Biol Phys* (2010) **76**:775–81. doi:10.1016/j.ijrobp.2009.02.032
39. Liu HH, Wang X, Dong L, Wu Q, Liao Z, Stevens CW, et al. Feasibility of sparing lung and other thoracic structures with intensity-modulated radiotherapy for non-small-cell lung cancer. *Int J Radiat Oncol Biol Phys* (2004) **58**:1268–79. doi:10.1016/j.ijrobp.2003.09.085
40. Christian JA, Bedford JL, Webb S, Brada M. Comparison in inverse-planned three-dimensional conformal radiotherapy and intensity-modulated radiotherapy for non-small-cell lung cancer. *Int J Radiat Oncol Biol Phys* (2007) **67**:735–41. doi:10.1016/j.ijrobp.2006.09.047
41. Lievens Y, Nulens A, Gaber MA, Defraene G, De Wever W, Stroobants S, et al. Intensity-modulated radiotherapy for locally advanced non-small-cell lung cancer: a dose-escalation planning study. *Int J Radiat Oncol Biol Phys* (2011) **80**:306–13. doi:10.1016/j.ijrobp.2010.06.025
42. Movsas B, Hu C, Sloan J, Bradley JD, Kavadi VS, Narayan S, et al. Quality of life (QOL) analysis of the randomized radiation (RT) dose-escalation NSCLC trial (RTOG 0617): the rest of the story. *Int J Radiat Oncol Biol Phys* (2013) **87**:S1–2. doi:10.1016/j.ijrobp.2013.06.012
43. Verellen D, De Ridder M, Linthout N, Tournel K, Soete G, Storme G. Innovations in image-guided radiotherapy. *Nat Rev Cancer* (2007) **7**:949–60. doi:10.1038/nrc2288
44. Jaffray DA. Image-guided radiotherapy: from current concept to future perspectives. *Nat Rev Clin Oncol* (2012) **9**:688–99. doi:10.1038/nrclinonc.2012.194
45. Yeung AR, Li JG, Shi W, Newlin HE, Chvetsov A, Liu C, et al. Tumor localization using cone-beam CT reduces setup margins in conventionally fractionated radiotherapy for lung tumors. *Int J Radiat Oncol Biol Phys* (2009) **74**:1100–7. doi:10.1016/j.ijrobp.2008.09.048
46. Dawson LA, Jaffray DA. Advances in image-guided radiation therapy. *J Clin Oncol* (2007) **25**:938–46. doi:10.1200/JCO.2006.09.9515

47. Korreman S, Rasch C, McNair H, Verellen D, Oelfke U, Maingon P, et al. The European Society of Therapeutic Radiology and Oncology-European Institute of Radiotherapy (ESTRO-EIR) report on 3D CT-based in-room image guidance systems: a practical and technical review and guide. *Radiat Oncol* (2010) **94**:129–44. doi:10.1016/j.radonc.2010.01.004
48. Bissonnette JP, Purdie TG, Higgins JA, Li W, Bezjak A. Cone-beam computed tomographic image guidance for lung cancer radiation therapy. *Int J Radiat Oncol Biol Phys* (2009) **73**:927–34. doi:10.1016/j.ijrobp.2008.08.059
49. Higgins J, Bezjak A, Hope A, Panzarella T, Li W, Cho JB, et al. Effect of image-guidance frequency on geometric accuracy and setup margins in radiotherapy for locally advanced lung cancer. *Int J Radiat Oncol Biol Phys* (2011) **80**:1330–7. doi:10.1016/j.ijrobp.2010.04.006
50. Borst GR, Sonke JJ, Betgen A, Remeijer P, van Herk M, Lebesque JV. Kilo-voltage cone-beam computed tomography setup measurements for lung cancer patients; first clinical results and comparison with electronic portal-imaging device. *Int J Radiat Oncol Biol Phys* (2007) **68**:555–61. doi:10.1016/j.ijrobp.2007.01.014
51. Roman NO, Shepherd W, Mukhopadhyay N, Hugo GD, Weiss E. Interfractional positional variability of fiducial markers and primary tumors in locally advanced non-small-cell lung cancer during audiovisual biofeedback radiotherapy. *Int J Radiat Oncol Biol Phys* (2012) **83**:1566–72. doi:10.1016/j.ijrobp.2011.10.051
52. Sonke JJ, Lebesque J, van Herk M. Variability of four-dimensional computed tomography patient models. *Int J Radiat Oncol Biol Phys* (2008) **70**:590–8. doi:10.1016/j.ijrobp.2007.08.067
53. Sonke JJ, Zijp L, Remeijer P, van Herk M. Respiratory correlated cone beam CT. *Med Phys* (2005) **32**:1176–86. doi:10.1111/1.1869074
54. Nestle U, Kremp S, Grosu AL. Practical integration of [¹⁸F]-FDG-PET and PET-CT in the planning of radiotherapy for non-small cell lung cancer (NSCLC): the technical basis, ICRU-target volumes, problems, perspectives. *Radiat Oncol* (2006) **81**:209–25. doi:10.1016/j.radonc.2006.09.011
55. Gambhir SS, Czernin J, Schwimmer J, Silverman DH, Coleman RE, Phelps ME. A tabulated summary of the FDG PET literature. *J Nucl Med* (2001) **42**:S1–93.
56. Bradley J, Thorstad WL, Mutic S, Miller TR, Dehdashti F, Siegel BA, et al. Impact of FDG-PET on radiation therapy volume delineation in non-small-cell lung cancer. *Int J Radiat Oncol Biol Phys* (2004) **59**:78–86. doi:10.1016/j.ijrobp.2003.10.044
57. Erdi YE, Rosenzweig K, Erdi AK, Macapinlac HA, Hu YC, Brabian LE, et al. Radiotherapy treatment planning for patients with non-small cell lung cancer using positron emission tomography (PET). *Radiat Oncol* (2002) **62**:51–60. doi:10.1016/S0167-8140(01)00470-4
58. Mah K, Caldwell CB, Ung YC, Danjoux CE, Balogh JM, Ganguli SN, et al. The impact of (¹⁸)FDG-PET on target and critical organs in CT-based treatment planning of patients with poorly defined non-small-cell lung carcinoma: a prospective study. *Int J Radiat Oncol Biol Phys* (2002) **52**:339–50. doi:10.1016/S0360-3016(01)01824-7
59. van Der Wel A, Nijsten S, Hochstenbag M, Lamers R, Boersma L, Wanders R, et al. Increased therapeutic ratio by ¹⁸FDG-PET CT planning in patients with clinical CT stage N2-N3M0 non-small-cell lung cancer: a modeling study. *Int J Radiat Oncol Biol Phys* (2005) **61**:649–55. doi:10.1016/j.ijrobp.2004.06.205
60. Møller DS, Khalil AA, Knap MM, Muren LP, Hoffmann L. A planning study of radiotherapy dose escalation of PET-active tumour volumes in non-small cell lung cancer patients. *Acta Oncol* (2011) **50**:883–8. doi:10.3109/0284186X.2011.581694
61. Kupelian PA, Ramsey C, Meeks SL, Willoughby TR, Forbes A, Wagner TH, et al. Serial megavoltage CT imaging during external beam radiotherapy for non-small-cell lung cancer: observations on tumor regression during treatment. *Int J Radiat Oncol Biol Phys* (2005) **63**:1024–8. doi:10.1016/j.ijrobp.2005.04.046
62. Ramsey CR, Langen KM, Kupelian PA, Scaperoth DD, Meeks SL, Mahan SL, et al. A technique for adaptive image-guided helical tomotherapy for lung cancer. *Int J Radiat Oncol Biol Phys* (2006) **64**:1237–44. doi:10.1016/j.ijrobp.2005.11.012
63. Fox J, Ford E, Redmond K, Zhou J, Wong J, Song DY. Quantification of tumor volume changes during radiotherapy for non-small-cell lung cancer. *Int J Radiat Oncol Biol Phys* (2009) **74**:341–8. doi:10.1016/j.ijrobp.2008.07.063
64. Britton KR, Starkschall G, Tucker SL, Pan T, Nelson C, Chang JY, et al. Assessment of gross tumor volume regression and motion changes during radiotherapy for non-small-cell lung cancer as measured by four-dimensional computed tomography. *Int J Radiat Oncol Biol Phys* (2007) **68**:1036–46. doi:10.1016/j.ijrobp.2007.01.021
65. Britton KR, Starkschall G, Liu H, Chang JY, Bilton S, Ezhil M, et al. Consequences of anatomic changes and respiratory motion on radiation dose distributions in conformal radiotherapy for locally advanced non-small-cell lung cancer. *Int J Radiat Oncol Biol Phys* (2009) **73**:94–102. doi:10.1016/j.ijrobp.2008.04.016
66. Saunders M, Dische S, Barrett A, Harvey A, Griffiths G, Palmer M. Continuous, hyperfractionated, accelerated radiotherapy (CHART) versus conventional radiotherapy in non-small cell lung cancer: mature data from the randomised multicentre trial. CHART Steering committee. *Radiat Oncol* (1999) **52**:137–48. doi:10.1016/S0167-8140(99)00087-0
67. Bogart JA, Hodgson L, Seagren SL, Blackstock AW, Wang X, Lenox R, et al. Phase I study of accelerated conformal radiotherapy for stage I non-small-cell lung cancer in patients with pulmonary dysfunction: CALGB 39904. *J Clin Oncol* (2010) **28**:202–6. doi:10.1200/JCO.2009.25.0753
68. Machay T, Hsu C, Komaki R, Sause WT, Swann S, Langer CJ, et al. Effect of overall treatment time on outcomes after concurrent chemoradiation for locally advanced non-small-cell lung carcinoma: analysis of the Radiation Therapy Oncology Group (RTOG) experience. *Int J Radiat Oncol Biol Phys* (2005) **63**:667–71. doi:10.1016/j.ijrobp.2005.03.037
69. Welsh JS, Lock M, Harari PM, Tomé WA, Fowler J, Mackie TR, et al. Clinical implementation of adaptive helical tomotherapy: a unique approach to image-guided intensity modulated radiotherapy. *Technol Cancer Res Treat* (2006) **5**:465–79.
70. Kepka L, Tyc-Szczepaniak D, Bujko K. Dose-per-fraction escalation of accelerated hypofractionated three-dimensional conformal radiotherapy in locally advanced non-small cell lung cancer. *J Thorac Oncol* (2009) **4**:853–61. doi:10.1097/JTO.0b013e3181a97dda
71. Cho KH, Ahn SJ, Pyo HR, Kim KS, Kim YC, Moon SH, et al. A phase II study of synchronous three-dimensional conformal boost to the gross tumor volume for patients with unresectable stage III non-small-cell lung cancer: results of Korean Radiation Oncology Group 0301 study. *Int J Radiat Oncol Biol Phys* (2009) **74**:1397–404. doi:10.1016/j.ijrobp.2008.10.020
72. Cannon DM, Mehta MP, Adkinson JB, Khuntia D, Traynor AM, Tomé W, et al. Dose-limiting toxicity after hypofractionated dose-escalated radiotherapy in non-small-cell lung cancer. *J Clin Oncol* (2013) **31**:4343–8. doi:10.1200/JCO.2013.51.5353
73. Zhu ZF, Fan M, Wu KL, Zhao KL, Yang HJ, Chen GY, et al. A phase II trial of accelerated hypofractionated three-dimensional conformal radiation therapy in locally advanced non-small cell lung cancer. *Radiat Oncol* (2011) **98**:304–8. doi:10.1016/j.radonc.2011.01.022
74. Bral S, Duchateau M, Versmessen H, Engels B, Tournel K, Vinh-Hung V, et al. Toxicity and outcome results of a class solution with moderately hypofractionated radiotherapy in inoperable stage III non-small cell lung cancer using helical tomotherapy. *Int J Radiat Oncol Biol Phys* (2010) **77**:1352–9. doi:10.1016/j.ijrobp.2009.06.075
75. Song CH, Pyo H, Moon SH, Kim TH, Kim DW, Cho KH. Treatment-related pneumonitis and acute esophagitis in non-small cell lung cancer patients treated with chemotherapy and helical tomotherapy. *Int J Radiat Oncol Biol Phys* (2010) **78**:651–8. doi:10.1016/j.ijrobp.2009.08.068
76. Osti MF, Agolli L, Valeriani M, Falco T, Bracci S, De Sanctis V, et al. Image guided hypofractionated 3-dimensional radiation therapy in patients with inoperable advanced stage non-small cell lung cancer. *Int J Radiat Oncol Biol Phys* (2013) **85**:e157–63. doi:10.1016/j.ijrobp.2012.10.012
77. Bearz A, Minatel E, Rumeileh IA, Borsatti E, Talamini R, Franchin G, et al. Concurrent chemoradiotherapy with tomotherapy in locally advanced non-small cell lung cancer: a phase I, docetaxel dose-escalation study with hypofractionated radiation regimen. *BMC Cancer* (2013) **13**:513. doi:10.1186/1471-2407-13-513
78. Donato V, Arcangeli S, Monaco A, Caruso C, Cianciulli M, Boboc G, et al. Moderately escalated hypofractionated (chemo) radiotherapy delivered with helical intensity-modulated technique in stage III unresectable non-small cell lung cancer. *Front Oncol* (2013) **3**:286. doi:10.3389/fonc.2013.00286
79. Kim Y, Hong SE, Kong M, Choi J. Predictive factors for radiation pneumonitis in lung cancer treated with helical tomotherapy. *Cancer Res Treat* (2013) **45**:295–302. doi:10.4143/crt.2013.45.4.295
80. Chi A, Jang SY, Welsh JS, Nguyen NP, Ong E, Gobar L, et al. Feasibility of helical tomography in stereotactic body radiation therapy for centrally located early stage non-small-cell lung cancer or lung metastases. *Int J Radiat Oncol Biol Phys* (2011) **81**:856–62. doi:10.1016/j.ijrobp.2010.11.051

81. Shi A, Zhu G, Wu H, Yu R, Li F, Xu B. Analysis of clinical and dosimetric factors associated with severe acute radiation pneumonitis in patients with locally advanced non-small cell lung cancer treated with concurrent chemotherapy and intensity-modulated radiotherapy. *Radiat Oncol* (2010) **5**:35. doi:10.1186/1748-717X-5-35
82. Guckenberger M, Kavanagh A, Patridge M. Combining advanced radiotherapy technologies to maximize safety and tumor control probability in stage III non-small cell lung cancer. *Strahlenther Onkol* (2012) **188**:894–900. doi:10.1007/s00066-012-0161-9
83. Feddock J, Arnold SM, Shelton BJ, Sinha P, Conrad G, Chen L, et al. Stereotactic body radiation therapy can be used safely to boost residual disease in locally advanced non-small cell lung cancer: a prospective study. *Int J Radiat Oncol Biol Phys* (2013) **85**:1325–31. doi:10.1016/j.ijrobp.2012.11.011
84. Liao Z, Lin SH, Cox JD. Status of particle therapy for lung cancer. *Acta Oncol* (2011) **50**:745–56. doi:10.3109/0284186X.2011.590148
85. Chang JY, Zhang X, Wang X, Kang Y, Riley B, Bilton S, et al. Significant reduction of normal tissue dose by proton radiotherapy compared with three-dimensional conformal or intensity-modulated radiation therapy in stage I or stage III non-small-cell lung cancer. *Int J Radiat Oncol Biol Phys* (2006) **65**:1087–96. doi:10.1016/j.ijrobp.2006.01.052
86. Zhang X, Li Y, Pan X, Li X, Mohan R, Komaki R, et al. Intensity-modulated proton therapy reduces the dose to normal tissue compared with intensity-modulated radiation therapy or passive scattering proton therapy and enables individualized radical radiotherapy for extensive stage IIIB non-small-cell lung cancer: a virtual clinical study. *Int J Radiat Oncol Biol Phys* (2010) **77**:357–66. doi:10.1016/j.ijrobp.2009.04.028
87. Koay EJ, Legg D, Mohan R, Komaki R, Cox JD, Chang JY. Adaptive/nonadaptive proton radiation planning and outcomes in a phase II trial for locally advanced non-small cell lung cancer. *Int J Radiat Oncol Biol Phys* (2012) **84**:1093–100. doi:10.1016/j.ijrobp.2012.02.041
88. Nakayama H, Satoh H, Sugahara S, Kurishima K, Tsuboi K, Sakurai H, et al. Proton beam therapy of stage II and III non-small-cell lung cancer. *Int J Radiat Oncol Biol Phys* (2011) **81**:979–84. doi:10.1016/j.ijrobp.2010.06.024
89. Chang JY, Komaki R, Lu C, Wen HY, Allen PK, Tsao A, et al. Phase 2 study of high-dose proton therapy with concurrent chemotherapy for unresectable stage III nonsmall cell lung cancer. *Cancer* (2011) **117**:4707–13. doi:10.1002/cncr.26080
90. Bert C, Durante M. Motion in radiotherapy: particle therapy. *Phys Med Biol* (2011) **56**:R113–44. doi:10.1088/0031-9155/56/16/R01
91. Engelsman M, Rietzel E, Kooy HM. Four-dimensional proton treatment planning for lung tumors. *Int J Radiat Oncol Biol Phys* (2006) **64**:1589–95. doi:10.1016/j.ijrobp.2005.12.026
92. Kang Y, Zhang X, Chang JY, Wang H, Wei X, Liao Z, et al. 4D proton treatment planning strategy for mobile lung tumors. *Int J Radiat Oncol Biol Phys* (2007) **67**:906–14. doi:10.1016/j.ijrobp.2006.10.045
93. Grassberger C, Dowdell S, Lomax A, Sharp G, Shackleford J, Choi N, et al. Motion interplay as a function of patient parameters and spot size in spot scanning proton therapy for lung cancer. *Int J Radiat Oncol Biol Phys* (2013) **86**:380–6. doi:10.1016/j.ijrobp.2013.01.024
94. Min CH, Zhu X, Winey BA, Grogg K, Testa M, El Fakhri G, et al. Clinical application of in-room positron emission tomography for in vivo treatment monitoring in proton radiation therapy. *Int J Radiat Oncol Biol Phys* (2013) **86**:183–9. doi:10.1016/j.ijrobp.2012.12.010
95. Aupérin A, Le Péchoux C, Pignon JP, Koning C, Jeremic B, Clamon G, et al. Concomitant radio-chemotherapy based on platin compounds in patients with locally advanced non-small cell lung cancer (NSCLC): a meta-analysis of individual data from 1764 patients. *Ann Oncol* (2006) **17**:473–83. doi:10.1093/annonc/mdj117
96. Onishi H, Kuriyama K, Yamaguchi M, Komiyama T, Tanaka S, Araki T, et al. Concurrent two-dimensional radiotherapy and weekly docetaxel in the treatment of stage III non-small cell lung cancer: a good local response but no good survival due to radiation pneumonitis. *Lung Cancer* (2003) **40**:79–84. doi:10.1016/S0169-5002(02)00532-9
97. Barriger RB, Fakiris AJ, Hanna N, Yu M, Mantravadi P, McGarry RC. Dose-volume analysis of radiation pneumonitis in non-small-cell lung cancer patients treated with concurrent cisplatin and etoposide with or without consolidation docetaxel. *Int J Radiat Oncol Biol Phys* (2010) **78**:1381–6. doi:10.1016/j.ijrobp.2009.09.030
98. Dang J, Li G, Ma L, Diao R, Zang S, Han C, et al. Predictors of grade ≥ 2 and grade ≥ 3 radiation pneumonitis in patients with locally advanced non-small cell lung cancer treated with three-dimensional conformal radiotherapy. *Acta Oncol* (2013) **52**:1175–80. doi:10.3109/0284186X.2012.747696
99. Palma DA, Senan S, Tsujino K, Barriger RB, Rengan R, Moreno M, et al. Predicting radiation pneumonitis after chemoradiation therapy for lung cancer: an international individual patient data meta-analysis. *Int J Radiat Oncol Biol Phys* (2013) **85**:444–50. doi:10.1016/j.ijrobp.2012.04.043

Conflict of Interest Statement: The authors declare that the research was conducted in the absence of any commercial or financial relationships that could be construed as a potential conflict of interest.

Received: 13 March 2014; paper pending published: 24 April 2014; accepted: 04 June 2014; published online: 20 June 2014.

*Citation: Chi A, Nguyen NP, Welsh JS, Tse W, Monga M, Oduntan O, Almubarak M, Rogers J, Remick SC and Gius D (2014) Strategies of dose escalation in the treatment of locally advanced non-small cell lung cancer: image guidance and beyond. *Front. Oncol.* **4**:156. doi: 10.3389/fonc.2014.00156*

*This article was submitted to Radiation Oncology, a section of the journal *Frontiers in Oncology*.*

Copyright © 2014 Chi, Nguyen, Welsh, Tse, Monga, Oduntan, Almubarak, Rogers, Remick and Gius. This is an open-access article distributed under the terms of the Creative Commons Attribution License (CC BY). The use, distribution or reproduction in other forums is permitted, provided the original author(s) or licensor are credited and that the original publication in this journal is cited, in accordance with accepted academic practice. No use, distribution or reproduction is permitted which does not comply with these terms.



Moderately escalated hypofractionated (chemo) radiotherapy delivered with helical intensity-modulated technique in stage III unresectable non-small cell lung cancer

Vittorio Donato¹, Stefano Arcangeli^{1*}, Alessia Monaco¹, Cristina Caruso¹, Michele Cianciulli¹, Genoveva Boboc¹, Cinzia Chiostrini¹, Roberta Rauco² and Maria Cristina Pressello²

¹ Department of Radiotherapy, Azienda Ospedaliera S.Camillo-Forlanini, Rome, Italy

² Department of Medical Physics, Azienda Ospedaliera S. Camillo-Forlanini, Rome, Italy

Edited by:

Nam Phong Nguyen, International Geriatric Radiotherapy Group, USA

Reviewed by:

Jaroslaw T. Hepel, Brown University, USA

Michael Andrew Samuels, Yale University, USA

***Correspondence:**

Stefano Arcangeli, Department of Radiotherapy, Azienda Ospedaliera S. Camillo-Forlanini, Circonvallazione Gianicolense 87, Rome 00152, Italy
e-mail: stefano.arcangeli@yahoo.it

Purpose: To assess clinical outcomes and toxicities in patients with stage III unresectable non-small cell lung cancer (NSCLC) treated with a moderately escalated hypofractionated radiotherapy delivered with Helical Intensity-Modulated Technique in combination with sequential or concurrent chemotherapy.

Materials and Methods: Sixty-one consecutive patients considered non-progressive after two cycles of induction chemotherapy were treated with a moderately escalated hypofractionated radiation course of 30 daily fractions of 2.25–2.28 Gy each administered in 6 weeks up to a total dose of 67.5–68.4 Gy (range, 64.5–71.3 Gy). Thirty-two received sequential RT after two more cycles (total = 4 cycles) of chemotherapy, while 29 were treated with concurrent chemo-radiation. The target was considered the gross tumor volume and the clinically proven nodal regions, without elective nodal irradiation.

Results: With a median follow up of 27 months (range 6–40), 1-year and 2-year OS rate for all patients was 77 and 53%, respectively, with a median survival duration of 18.6 months in the sequential group and 24.1 months in the concomitant group. No Grade ≥ 4 acute and late toxicity was reported. Acute Grade 3 treatment-related pneumonitis was detected in 10% of patients. Two patients, both receiving the concurrent schedule, developed a Grade 3 acute esophagitis. The overall incidence of late Grade 3 lung toxicity was 5%. No patients experienced a Grade 3 late esophageal toxicity.

Conclusion: A moderately hypofractionated radiation course delivered with a Helical Intensity-Modulated Technique is a feasible treatment option for patients with unresectable locally advanced NSCLC receiving chemotherapy (sequentially or concurrently). Hypofractionated radiotherapy with a dedicated technique allows safely dose escalation, minimizing the effect of tumor repopulation that may occur with prolonged treatment time.

Keywords: dose escalation, hypofractionated radiotherapy, chemo-radiation, unresectable NSCLC, helical tomotherapy

INTRODUCTION

More than two third of the patients with non-small-cell lung cancer (NSCLC) in the Western Countries are found to have locally advanced or metastatic disease at the time of diagnosis (1). Improving outcomes for patients with stage III disease still remains a major challenge. Concurrent chemo-radiation is the current mainstay of treatment for unresectable NSCLC, since two meta-analyses have confirmed the benefit of concomitant approach using platinum-based therapy (2, 3). Nevertheless, local control is achieved in 40% and 5-year survival is 15%. Other than systemic failures, these poor clinical results can be partly attributed to the still high rates of thoracic failures with traditional radiation doses and techniques that cannot allow to deliver the radiation doses

beyond a certain threshold in order to avoid the risk of unacceptable toxicities. Indeed, while huge research have been devoted on improving systemic therapy options for patients with advanced lung cancer, less efforts have been placed on the importance of increasing the delivered radiation dose beyond 60 Gy, which has been the standard for over 20 years (4). Martel et al. (5) at the end of 1990s estimated that the dose to achieve a 50% local control at 2 years should be above 70 Gy. Soon after, improvements in radiation delivery techniques that have the potential to better sparing of normal tissues as well as advances in tumor volume definition have focused the attention in the investigation of dose escalation. By using a conventional fractionation regimen, however, dose escalation is obtained by increasing the number of daily treatments,

thus resulting in a prolongation of the overall time. Unfortunately in NSCLC such a long duration of the radiation course has been shown to be detrimental to tumor control and survival, resulting in a significantly shortened survival ($p=0.016$) in four Radiation Therapy Oncology Group (RTOG) prospective randomized trials (6), with a loss of survival rate of 1.6% per day of prolongation beyond 6 weeks (7). Therefore, both total radiation dose and treatment duration (or overall time) should be considered crucial factors affecting the outcome of radiotherapy in the management of NSCLC. Relying on a better conformal avoidance of normal healthy tissues obtained with image-guided rotational IMRT (8), we applied an alternative strategy that has already been shown (9) to effectively escalate the dose by increasing dose per day while reducing the number of treatment fractions and duration of the treatment course, thus avoiding the risk of lessening the benefit of the extra dose due to tumor cell repopulation during treatment (6, 10). In this article we retrospectively analyzed data from 61 consecutive patients with stage III unresectable NSCLC treated with a moderately escalated hypofractionated radiotherapy delivered with Helical Intensity-Modulated Technique in combination with sequential or concurrent chemotherapy.

MATERIALS AND METHODS

POPULATION

The analysis included 61 patients with stage III unresectable NSCLC who were considered non-progressive after two cycles of induction platinum-based chemotherapy, basing on a contrast-enhanced computed tomography (CT) scan of the chest, brain, and upper abdomen. The treatment policy was reviewed and approved by the IRB and carried out in compliance with the Helsinki Declaration of 1975, as revised in 2000. Written informed consent was obtained from each patient.

PRETREATMENT EVALUATION

Initial workup included bronchoscopy, CT of the lung and upper abdomen through the adrenal glands, an MRI of the brain with contrast, and a bone scan. A whole body 18F-deoxyglucose (FDG) – Positron Emission Tomography (PET) scan was performed in 33 patients (54%). All patients had a Forced Expiratory Volume in the first second (FEV1) and DLCO (Carbon Monoxide Diffuse Capacity) at least 40% of predicted value, adequate blood tests, consisting in absolute neutrophil count $>1500/\text{mL}$, hemoglobin count $\geq 10 \text{ g/dL}$, platelet count $\geq 100,000/\text{mL}$, serum creatinine level $<1.6 \text{ mg/dL}$, serum bilirubin <1.5 times normal institutional limits, serum aspartate aminotransferase, and alanine aminotransferase <2.5 normal institutional limits, and a World Health Organization Performance Status (WHO-PS) ≤ 2 . None of them experienced a weight loss of more than 10% in the last 6 months.

TREATMENT

Treatment plan – chemotherapy

Induction chemotherapy consisted of cisplatin (80 mg/m^2) or carboplatin (AUC 5) on day 1 and gemcitabine 1250 mg/m^2 on day 1 and 8, for a total of two cycles repeated every 21 days. Thereafter, patients candidates for chemo-radiotherapy with curative intent were those considered non-progressive (RECIST criteria) (11).

In a first phase, the treatment schedule consisted in a sequential approach, with radiation course intended to start at the end of two more cycles of chemotherapy following the same rules described above, within 7 days from day 21 of the cycle 4. After a first report (12) showing only minor complications, all non-progressive patients after induction chemotherapy were treated with concurrent chemoradiation. In the concurrent schedule cisplatin-vinorelbine (cisplatin 40 mg/m^2 day 2 and 9, vinorelbine 15 mg/m^2 day 2 and 9, cisplatin 40 mg/m^2 day 23, vinorelbine 15 mg/m^2 day 23 and 30) was used, and radiotherapy began within 7 days after the completion of induction chemotherapy (within 7 days from day 21 of the cycle 2).

Treatment plan – radiotherapy

Simulation. All patients were positioned supine on a wing board and immobilized by means of thermoplastic frames. CT scan for planning from the level of the cricoid cartilage through the whole liver volume was acquired in shallow breathing mode at 3 mm slice thickness, ensuring that the amplitude of respiration, that was checked under fluoroscopy, was kept within maximum 15 mm. The gross tumor volume (GTV) included the primary tumor and the pretreatment involved lymph nodes as defined on CT imaging (short axis $> 1 \text{ cm}$ or necrosis) or on FDG-PET. For the clinical target volume (CTV) a margin of 5 mm incorporating microscopic disease around GTV was used (13). Depending on the tumor location, the planning target volume (PTV) included the CTV plus a total margin of at least 1 cm to the superior-inferior dimensions and at least 0.8 cm in the axial plane, unless the PTV expansion extended outside of the skin, or into the spinal canal. In this case, PTV margins were limited. Automatic contouring of the lungs and heart was performed using the Pinnacle3 treatment planning system (version 8.0 h; Philips Radiation Oncology Systems, Fitchburg, MA, USA), with manual corrections allowed. Planning risk volumes (PRV) were constructed with a 3-mm margin for the spinal cord and 5-mm for the esophagus.

Dose schedule, constraints, and treatment delivery. Dose prescription to the median dose point of the entire PTV was 30 fractions of 2.25–2.28 Gy each up to a total dose of 67.5–68.4 Gy (range, 64.5–71.3 Gy). According to the linear-quadratic model, the corresponding normalized total dose at 2 Gy per fraction (EQD2) is approximately 70 and 72 Gy, considering an alfa/beta ratio of 10 Gy for tumor and acutely responding normal tissues and 3 Gy for late complications, respectively. The optimization was driven with the aim of delivering the prescribed dose to at least 95% of the PTV, according to ICRU 50/62 guidelines (14). DVH's points and penalties were setted to best meet the constraints for organs at risk (OARs) without compromising PTV coverage. Specific dosimetric guidelines for OARs in accordance to the Quantec (15) dose-volume model were applied and rescaled on fractionation's change as follows: V19 for lungs $<30\%$, MLD (volume of both lungs minus GTV) $<19 \text{ Gy}$; a maximal dose (D_{\max}) of 47 Gy on the spinal cord; mean esophageal volume $<32 \text{ Gy}$, V33 $<50\%$, V47 $<40\%$; mean heart volume $<33 \text{ Gy}$, V38 $<80\%$, V57 $<30\%$. Dose computation and treatment delivery were performed on the TomoTherapy HiArt II system (TomoTherapy Inc., Madison, WI, USA). Image-Guided Radiotherapy (IGRT) was performed

by means of a Megavolt Computed Tomography (MVCT) before each daily session in the same shallow breathing modality adopted on CT simulation, and positioning was done using the integrated registration with the planning CT to account for set-up uncertainties. The delivery parameters usually used for treatment planning and optimization were: 2.5 cm (field width); 0.287 (pitch); 2.5 (modulation factors); 0.215 cm × 0.215 cm; (dose calculation grid). Treatment replanning was never performed considering that tumor shrinkage during the radiation course is small and might be counteracted by the risk of delivering inadequate dose to the tumor rind, where residual cancer clonogens may still be present (16).

RESPONSE AND TOXICITY EVALUATION

Patients were seen weekly during treatment and at a 3-monthly interval during the first 2 years of follow up and every 6 months thereafter. Toxicity monitoring was focused on treatment-related esophageal and pulmonary adverse events and assessed by the RTOG grading system (17). Any increase in grade from baseline was considered toxicity related to the treatment and calculated for the acute (90 days from start of RT) and late phase (beyond 90 days). Assessment of tumor response relied upon RECIST criteria (11). Progressive disease that developed within or at the margin of the PTV, as well as recurrences in another lobe of the ipsilateral lung, was scored as loco-regional failure, whereas progression in the contralateral lung or extrathoracic sites was defined as distant failure. Overall survival was calculated by the Kaplan-Meier method from the initiation of treatment and patients were censored at the time of the specific event.

RESULTS

This report includes 61 enrolled patients with locally advanced stage III unresectable NSCLC treated between 2008 and 2011, with a median follow up of 27 months (range 6–40). All patients were considered non-progressive after two cycles of induction platinum-based chemotherapy. Among them, 32 received sequential RT after two more cycles (total = 4 cycles) of chemotherapy, while 29 were treated with concurrent chemoradiation. All patients but one, who discontinued treatment due to a decline in performance status, finished the scheduled course, with a median of 42 days (range, 42–45 days). One patient died prematurely from non-cancer and non-treatment-related causes within 3 months after completion of the radiation course. Details on the baseline disease, patients, and treatment characteristics are summarized in Table 1.

TOXICITY

No Grade ≥4 acute and late toxicity was reported. Acute Grade 3 treatment-related pneumonitis was detected in 10%. In all cases, acute lung toxicity developed 2–4 months after the completion of treatment and resolved within 7 months. Two patients, both receiving the concurrent schedule, developed a Grade 3 acute esophagitis. The overall incidence of late Grade 3 lung toxicity was 5%. No patients experienced a Grade 3 late esophageal toxicity.

LOCAL CONTROL AND SURVIVAL

Among 59 patients evaluable for local control, the overall response rate was 54% (6% CR, 48% PR). Stable disease was observed in

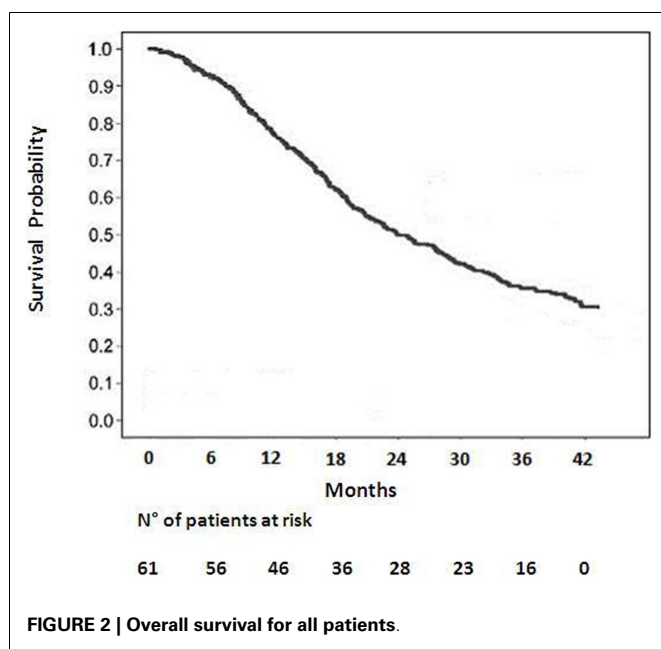
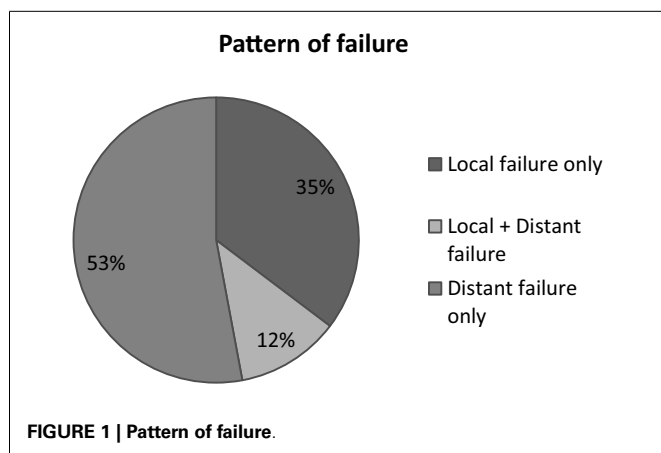
Table 1 | Baseline characteristics.

	Value
PATIENTS CHARACTERISTICS	
N Patients	61
Age (year)	67 (Range 40–78)
Sex	
Male	46 (75.4%)
Female	15 (24.6%)
COPD	
Yes	39 (64%)
No	22 (36%)
WHO-PS	
0	22 (36%)
1	31 (50.8%)
2	8 (13.2%)
Smokers	
Never	7 (11.4%)
Quit	46 (75.4%)
Current	8 (13.2%)
DISEASE CHARACTERISTICS	
Type of carcinoma	
Adenocarcinoma	31 (50.8%)
Squamous cell	23 (37.8%)
Unspecified NSCLC	7 (11.4%)
Stage (TNM sixth edition)	
IIIA	35 (57.4%)
IIIB	26 (42.6%)
Median GTV size (cc)	81.8 (5.9–598.8)
Tumor location	
Upper-middle lobes	47 (77%)
Inferior lobes	14 (23%)
TREATMENT CHARACTERISTICS	
Chemotherapy timing	
Induction	All (100%)
Sequential	32 (52.5%)
Concurrent	29 (47.5%)
Drugs in sequential schedule	
Cisplatin-gemcitabine	28 (87.5%)
Carboplatin based	4 (12.5%)
Drugs in concurrent schedule	
Cisplatin-vinorelbine	29 (100%)
Total radiation dose	67.95 Gy (64.5–71.3 Gy)
Median OTT (days)	42 (42–45)

20%. Progression was documented in the remaining patients. The median survival duration was 18.6 months in the sequential group and 24.1 months in the concomitant group. A summary of the analysis of patterns of failure is provided in Figure 1. One-year and 2-year OS rate was 77 and 53% respectively for all patients (Figure 2), 43% of whom were stage IIIB.

DISCUSSION

The renewed interest in the adoption of dose escalated regimens has recently prompted the RTOG to open a randomized Phase III trial, RTOG 0617 (18), to determine whether chemo-radiotherapy with a higher radiation dose (74 Gy) improved overall survival



compared with the current standard dose (60 Gy). Unexpectedly, early findings (19), demonstrated that the higher dose of radiation did not improve overall survival, and the study was closed to further participant enrollment in the high-dose arm. In absence of a difference between the toxicity rates between the two groups, it can be speculatively argued that at least two factors may be advocated for this disappointing outcome: (1) a higher risk of death related to the effects on the normal lungs and perhaps the heart from high-dose three dimensional conformal radiotherapy (3D-CRT) and IMRT; (2) the protraction of the overall treatment time beyond 6 weeks in the high-dose arm, that might have favored tumor repopulation. These poor results warrant the radioncological community to move a step backwards in the dose escalated approach. However the path for dose escalation should not be abandoned since local failure following concurrent chemotherapy and normo-fractionated radiation therapy for patients with stage III NSCLC approximates 85% (20), and the effect of higher radiation doses on survival is shown to be independent of whether chemotherapy is

given (21). Thus, RT dose intensity remains important despite the establishment of chemotherapy in Stage III NSCLC, ensuring a 4% relative improvement in survival and 3% relative improvement *in loco*-regional control for every 1 Gy BED increase (22). Over last decade, radiotherapy schedules other than conventional fractionation have been explored for dose intensification in unresectable NSCLC: hyperfractionation has been investigated with promising results and its efficacy has been substantiated in a Meta-Analysis of Radiotherapy in Lung Cancer (MAR-LC) (23) conducted on 2000 patients affected with NSCLC that found that modified fractionation (accelerated or hyperfractionated radiotherapy) improved overall survival as compared to conventional radiotherapy, resulting in an absolute benefit of 2.5% (8.3–10.8%) at 5 years. Although increasing the RT dose intensity by accelerating the time may represent a suitable strategy, its application in the clinical practice may be challenging and limited by the logistic difficulties of treating patients multiple times in a day and an expected rates of greater acute esophageal toxicity. On the other hand, the administration of higher daily doses (hypofractionated RT) would be certainly be more attractive, allowing to complete the treatment in fewer fractions, but has long been discouraged given some concerns on the potentially increased late adverse effects. Mehta et al. (9) have developed a dose per fraction escalation schedule in NSCLC using advanced radiotherapy delivery technologies. The strength of this approach is the capability of escalating the dose by moderately increasing the dose per fraction without prolonging the duration of the treatment course beyond 6 weeks – which might counteract the benefit of dose escalation allowing time for the tumor to begin re-growing. We implemented this alternative strategy in the context of combined chemo-radiotherapy and we reported 10% Grade 3 acute lung toxicity, which is consistent with the 8 and 11% encountered by others (24–26) and even lower than major treatment-related pneumonitis rates observed in some recent trials that have assessed hypofractionated RT regimens in association with chemotherapy (27, 28). Our findings confirm that moderate hypofractionation using IGRT techniques, that help to reduce the total irradiated volume, might not actually increase the risk of radiation pneumonitis in typical “parallel” organs such as the healthy lungs – with an expected marked volume effect – despite the tumor fractionation sensitivity is smaller than that of the critical normal tissue (29). The time course of acute lung toxicity reflected the typical pattern of behavior of the classical radiation pneumonitis, having developed 2–4 months after the completion of radiation and resolved without sequelae within 7 months (30). Then, in two patients who experienced a Grade 3 acute esophagitis, the maximum time of discontinuation of treatment did not exceed 3 days, thus resulting in a very short treatment break. Late toxicity was mild, with no patients experiencing a >G2 esophagitis. Outcomes in terms of local tumor control and survival seem to compare favorably with prospective data from phase II trials (25, 31, 32) addressing the role of concurrent chemotherapy either in combination with modern radiotherapy techniques, or in the setting of dose escalation for various hypofractionation schemes in locally advanced inoperable NSCLC (33–36) (Table 2). This study does not lead to any definitive conclusion on the correlation between overall survival and dose level, but a strong relationship would be expected given that higher dose is known to improve local control.

Table 2 | Comparison of reported series of dose escalation or dose escalated hypofractionated radiotherapy in inoperable non-small cell lung cancer.

Author	Patients with stage III NSCLC	RT dose	Fraction	Toxicity	Outcomes
Kong (33)	60	63–103 Gy	2.15 Gy	–	5-Years OS, 13% Median survival, 19 months
Bradley (34)	83	71–90 Gy	2.10 Gy	No Group 3–4 acute esophagitis Acute Group ≥3 pneumonitis 6% Late Group ≥3 esophagitis 0–8% Late Group ≥3 pneumonitis 0–16%	3-Years OS, 26% (IIIA) 15% (IIB)
Belderbos (35)	42	60–94 Gy	2.25 Gy	No Group 3–4 acute esophagitis Acute Group ≥3 pneumonitis 35% Late Group ≥3 pneumonitis 57% 1 Case of late Group 5 esophagitis	2-Years OS, 24–40% (GTV </≥75 cm ³) Median survival, 17 months
Bral (36)	40	70.5 Gy	2.35 Gy	Acute Group 5 pneumonitis 5% Acute Group 3 esophagitis 2.5% Late Group 3 pneumonitis 16% No Group 3–4 late esophagitis	1-Year OS, 65% 2-Years OS, 27% Median survival, 17 months
Adkison (24)	36	57–80.5 Gy	2.28–3.22 Gy	No Group 3–4 acute toxicities Acute Group 2 esophagitis 13% Acute Group 2 pneumonitis 13%	2-Years OS, 46.8% Median survival, 18 months
Current	61	67.5–68.4 Gy	2.25–2.28 Gy	Acute Group 3 esophagitis 3% Acute Group 3 pneumonitis 12% Late Group 3 pneumonitis 7% No Group 3–4 late esophagitis	1-Year OS, 77% 2-Years OS, 53% Median survival:18.6 months (seq Group) 24.1 Months (conc group)

Notwithstanding its retrospective nature and a potential bias due to the accrual of selected (responders-only) patients to the induction chemotherapy, our findings show that high biologically effective dose delivered in a standard time frame may be safely administered with or without chemotherapy, provided that highly conformal radiotherapy techniques are used. More robust clinical trials are needed to confirm this strategy.

REFERENCES

- Jemal A, Siegel R, Ward E, Hao Y, Xu J, Murray T, et al. Cancer statistics, 2008. *CA Cancer J Clin* (2008) **58**:71–96. doi:10.3322/CA.2007.0010
- Non-Small Cell Lung Cancer Collaborative Group. Chemotherapy in non-small cell lung cancer: a meta-analysis using updated data on individual patients from 52 randomized trials. *BMJ* (1995) **311**:899–909. doi:10.1136/bmj.311.7010.899
- Aupérin A, Le Péchoux C, Rolland E, Curran WJ, Furuse K, Fournel P, et al. Meta-analysis of concomitant versus sequential radiochemotherapy in locally advanced non-small-cell lung cancer. *J Clin Oncol* (2010) **28**(13):2181–90. doi:10.1200/JCO.2009.26.2543
- Perez CA, Stanley K, Rubin P, Kramer S, Brady L, Perez-Tamayo R, et al. A prospective randomized study of various irradiation doses and fractionation schedules in the treatment of inoperable non-oat-cell carcinoma of the lung. Preliminary report by the Radiation Therapy Oncology Group. *Cancer* (1980) **45**:2744–53. doi:10.1002/1097-0142(19800601)45:11<2744::AID-CNCR2820451108>3.0.CO;2-U
- Martel MK, Ten Haken RK, Hazuka MB, Kessler ML, Strawderman M, Turrisi AT, et al. Estimation of tumor control probability model parameters from 3-D dose distributions of non-small cell lung cancer patients. *Lung Cancer* (1999) **24**(1):31–7. doi:10.1016/S0169-5002(99)00019-7
- Machtay M, Hsu C, Komaki R, Sause WT, Swann RS, Langer CJ, et al. Effect of overall treatment time on outcomes after concurrent chemoradiation for locally advanced non-small-cell lung carcinoma: analysis of the Radiation Therapy Oncology Group (RTOG) experience. *Int J Radiat Oncol Biol Phys* (2005) **63**(3):667–71. doi:10.1016/j.ijrobp.2005.03.037
- Fowler JF, Chappell R. Non-small cell lung tumors repopulate rapidly during radiation therapy. *Int J Radiat Oncol Biol Phys* (2000) **46**(2):516–7. doi:10.1016/S0360-3016(99)00364-8
- Aldridge JS, Mackie TR. Conformal avoidance radiotherapy. *Radiother Oncol* (1998) **48**(Suppl1):S76.
- Mehta M, Scrimger R, Mackie R, Paliwal B, Chappell R, Fowler J. A new approach to dose escalation in non small cell lung cancer. *Int J Radiat Oncol Biol Phys* (2001) **49**:23–33. doi:10.1016/S0360-3016(00)01374-2
- Cox JD, Pajak TF, Asbell S, Russell AH, Pederson J, Byhardt RW, et al. Interruptions of high-dose radiation therapy decrease long-term survival of favorable patients with unresectable non-small cell carcinoma of the lung: analysis of 1244 cases from 3 Radiation Therapy Oncology Group (RTOG) trials. *Int J Radiat Oncol Biol Phys* (1993) **27**(3):493–8. doi:10.1016/0360-3016(93)90371-2
- Therasse P, Arbuck SG, Eisenhauer EA, Wanders J, Kaplan RS, Rubinstein L, et al. New guidelines to evaluate the response to treatment in solid tumors. European Organization for Research and Treatment of Cancer, National Cancer Institute of the United States, National Cancer Institute of Canada. *J Natl Cancer Inst* (2000) **92**:205–16. doi:10.1093/jnci/92.3.205
- Monaco A, Caruso C, Giammarino D, Cianciulli M, Pressello MC, Donato V. Radiotherapy for inoperable non-small cell lung cancer using helical tomotherapy. *Tumori* (2012) **98**(1):86–9. doi:10.1700/1053.11504
- Yuan S, Meng X, Yu J, Mu D, Chao KS, Zhang J, et al. Determining optimal clinical target volume margins on the basis of microscopic extracapsular extension of metastatic nodes in patients with non-small-cell lung cancer. *Int J Radiat Oncol Biol Phys* (2007) **67**(3):727–34. doi:10.1016/j.ijrobp.2006.08.057
- Prescribing, Recording and Reporting Photon Beam Therapy (Report 62); Supplement to ICRU Report 50. In Book Prescribing, Recording and Reporting Photon Beam Therapy Report 62; Supplement to ICRU Report 50. City: International Commission on Radiation Units and Measurements; 1999.

15. Jackson A, Marks LB, Bentzen SM, Eisbruch A, Yorke ED, Ten Haken RK, et al. The lessons of QUANTEC: recommendations for reporting and gathering data on dose-volume dependencies of treatment outcome. *Int J Radiat Oncol Biol Phys* (2010) **76**(3 Suppl):S155–60. doi:10.1016/j.ijrobp.2009.08.074
16. Siker ML, Tomé WA, Mehta MP. Tumour volume changes on serial imaging with megavoltage CT for non-small cell lung cancer during intensity modulated radiotherapy: how reliable, consistent and meaningful is the effect? *Int J Radiat Oncol Biol Phys* (2006) **66**(1):135–41. doi:10.1016/j.ijrobp.2006.03.064
17. Cox JD, Stetz J, Pajak TF. Toxicity criteria of the Radiation Therapy Oncology Group (RTOG) and the European Organization for Research and Treatment of Cancer (EORTC). *Int J Radiat Oncol Biol Phys* (1995) **31**(5):1341–6. doi:10.1016/0360-3016(95)00060-C
18. Bradley J, Schild S, Bogart J, Dobelbower MC, Choy H, Adjei A, et al. RTOG 0617/NCCTG N0628/CALGB 30609/ECOG R0617: a randomized phase III comparison of standard dose (60 Gy) versus High-Dose (74 Gy) conformal radiotherapy with concurrent and consolidation carboplatin/paclitaxel ± cetuximab (IND #103444) in patients with stage IIIa/IIIb non-small cell lung cancer. Available from: <http://www.rtog.org> 2009.
19. Bradley J, Paulus R, Komaki R, Masters GA, Forster K, Schild SE, et al. A randomized phase III comparison of standard dose (60 Gy) versus High-Dose (74 Gy) conformal radiotherapy with or without cetuximab in patients with cetuximab for stage III non-small cell lung cancer. Results on radiation dose in RTOG 0617. *J Clin Oncol* (2013) **31**. (Abstr.7501)
20. Le Chevallier T, Arriagada R, Tarayre M, Lacombe-Terrier MJ, Laplanche A, Quoix E, et al. Significant effect of adjuvant chemotherapy in survival in locally advanced non-small cell lung carcinoma. *J Natl Cancer Inst* (1992) **84**:58. doi:10.1093/jnci/84.1.58
21. Wang L, Correa CR, Zhao L, Hayman J, Kalemkerian GP, Lyons S, et al. The effect of radiation dose and chemotherapy on overall survival in 237 patients with Stage III non-small-cell lung cancer. *Int J Radiat Oncol Biol Phys* (2009) **73**(5):1383–90. doi:10.1016/j.ijrobp.2008.06.1935
22. Machtay M, Bae K, Movsas B, Paulus R, Gore EM, Komaki R, et al. Higher biologically effective dose of radiotherapy is associated with improved outcomes for locally advanced non small cell lung carcinoma treated with chemoradiation: an analysis of the Radiation Therapy Oncology Group. *Int J Radiat Oncol Biol Phys* (2012) **82**(1):425–34. doi:10.1016/j.ijrobp.2010.09.004
23. Mauguen A, Le Péchoux C, Saunders MI, Schild SE, Turrisi AT, Baumann M, et al. Hyperfractionated or accelerated radiotherapy in lung cancer: an individual patient data meta-analysis. *J Clin Oncol* (2012) **30**(22):2788–97. doi:10.1200/JCO.2012.41.6677
24. Adkison JB, Cannon GM, Khuntia D, Jaradat H, Tomé WA, Walker W, et al. Image-guided, intensity-modulated hypofractionated radiotherapy for inoperable non-small cell lung cancer: preliminary results of a phase I dose escalation study. *Int J Radiat Oncol Biol Phys* (2007) **69**:S88. doi:10.1016/j.ijrobp.2007.07.160
25. Sura S, Gupta V, Yorke E, Jackson A, Amols H, Rosenzweig KE. Intensity-modulated radiation therapy (IMRT) for inoperable non-small cell lung cancer: the Memorial Sloan-Kettering Cancer Center (MSKCC) experience. *Radiat Oncol* (2008) **87**:17–23. doi:10.1016/j.radonc.2008.02.005
26. Yom SS, Liao Z, Liu HH, Tucker SL, Hu CS, Wei X, et al. Initial evaluation of treatment related pneumonitis in advanced-stage non-small-cell lung cancer patients treated with concurrent chemotherapy and intensity-modulated radiotherapy. *Int J Radiat Oncol Biol Phys* (2007) **68**:94–102. doi:10.1016/j.ijrobp.2006.12.031
27. Song CH, Pyo H, Moon SH, Kim TH, Kim DW, Cho KH. Treatment-related pneumonitis and acute esophagitis in non-small-cell lung cancer patients treated with chemotherapy and helical tomotherapy. *Int J Radiat Oncol Biol Phys* (2010) **78**(3):651–8. doi:10.1016/j.ijrobp.2009.08.068
28. Uytterlinde W, Chen C, Kwint M, de Bois J, Vincent A, Sonke JJ, et al. Prognostic parameters for acute esophagus toxicity in Intensity Modulated Radiotherapy and concurrent chemotherapy for locally advanced non-small cell lung cancer. *Radiat Oncol* (2013) **107**(3):392–7. doi:10.1016/j.radonc.2013.04.012
29. Vogelius IS, Westerly DC, Cannon GM, Bentzen SM. Hypofractionation does not increase radiation pneumonitis risk with modern conformal radiation delivery techniques. *Acta Oncol* (2010) **49**:1052e1057. doi:10.3109/0284186X.2010.498835
30. Rosiello RA, Merrill WW. Radiation-induced lung injury. *Clin Chest Med* (1990) **11**:65–71.
31. Govaert S, Troost E, Schuurmans O, de Geus-Oei L, Termeer A, Span PN, et al. Treatment outcome and toxicity of Intensity modulated (chemo) radiotherapy in stage III non small cell lung cancer patients. *Radiat Oncol* (2012) **7**:150. doi:10.1186/1748-717X-7-150
32. Liao ZX, Komaki RR, Thames HD Jr, Liu HH, Tucker SL, Mohan R, et al. Influence of technologic advances on outcomes in patients with unresectable, locally advanced non-small-cell lung cancer receiving concomitant chemoradiotherapy. *Int J Radiat Oncol Biol Phys* (2010) **76**:775–81. doi:10.1016/j.ijrobp.2009.02.032
33. Kong FM, Ten Haken RK, Schipper MJ, Sullivan MA, Chen M, Lopez C, et al. High-dose radiation improved local tumor control and overall survival in patients with inoperable/unresectable non-small-cell lung cancer: long-term results of a radiation dose escalation study. *Int J Radiat Oncol Biol Phys* (2005) **63**:324–33. doi:10.1016/j.ijrobp.2005.02.010
34. Bradley J, Graham MV, Winter K, Purdy JA, Komaki R, Roa WH, et al. Toxicity and outcome results of RTOG 9311: a Phase I-II dose-escalation study using three-dimensional conformal radiotherapy in patients with Inoperable non-small-cell lung carcinoma. *Int J Radiat Oncol Biol Phys* (2005) **61**:318–328. doi:10.1016/j.ijrobp.2004.06.260
35. Belderbos JS, Heemsbergen WD, De Jaeger K, Baas P, Lebesque JV. Final results of a Phase I/II dose escalation trial in non-small-cell lung cancer using three-dimensional conformal radiotherapy. *Int J Radiat Oncol Biol Phys* (2006) **66**:126–34. doi:10.1016/j.ijrobp.2006.04.034
36. Bral S, Duchateau M, Versmessen H, Engels B, Tournel K, Vinh-Hung V, et al. Toxicity and outcome results of a class solution with moderately hypofractionated radiotherapy in inoperable stage III non-small cell lung cancer using helical tomotherapy. *Int J Radiat Oncol Biol Phys* (2010) **77**(5):1352–9. doi:10.1016/j.ijrobp.2009.06.075

Conflict of Interest Statement: The authors declare that the research was conducted in the absence of any commercial or financial relationships that could be construed as a potential conflict of interest.

Received: 25 July 2013; accepted: 04 November 2013; published online: 18 November 2013.

*Citation: Donato V, Arcangeli S, Monaco A, Caruso C, Cianciulli M, Boboc G, Chiostrini C, Rauco R and Pressello MC (2013) Moderately escalated hypofractionated (chemo) radiotherapy delivered with helical intensity-modulated technique in stage III unresectable non-small cell lung cancer. *Front. Oncol.* **3**:286. doi:10.3389/fonc.2013.00286*

*This article was submitted to Radiation Oncology, a section of the journal *Frontiers in Oncology*.*

Copyright © 2013 Donato, Arcangeli, Monaco, Caruso, Cianciulli, Boboc, Chiostrini, Rauco and Pressello. This is an open-access article distributed under the terms of the Creative Commons Attribution License (CC BY). The use, distribution or reproduction in other forums is permitted, provided the original author(s) or licensor are credited and that the original publication in this journal is cited, in accordance with accepted academic practice. No use, distribution or reproduction is permitted which does not comply with these terms.



Feasibility of tomotherapy-based image-guided radiotherapy for small cell lung cancer

Nam P. Nguyen^{1*}, Wei Shen², Sarah Kratz³, Jacqueline Vock⁴, Paul Vos⁵, Vinh-Hung Vincent⁶, Gabor Altdorfer⁷, Lars Ewell¹, Siyoung Jang¹, Ulf Karlsson⁸, Juan Godinez⁹, Melissa Mills¹, Thomas Sroka¹⁰, Suresh Dutta¹¹, Alexander Chi¹² and The International Geriatric Radiotherapy Group

¹ Department of Radiation Oncology, University of Arizona, Tucson, AZ, USA

² Division of Pulmonary Medicine, University of Arizona, Tucson, AZ, USA

³ Division of Hematology Oncology, University of Arizona, Tucson, AZ, USA

⁴ Department of Radiation Oncology, Lindenhofspital, Bern, Switzerland

⁵ Department of Biostatistics, East Carolina University, Greenville, NC, USA

⁶ Department of Radiation Oncology, University of Geneva, Geneva, Switzerland

⁷ Department of Radiation Oncology, Camden Clark Medical Center, Parkersburg, WV, USA

⁸ Department of Radiation Oncology, Marshfield Clinic, Marshfield, WI, USA

⁹ Department of Radiation Oncology, Florida Radiation Oncology, Jacksonville, FL, USA

¹⁰ Department of Radiation Oncology, Darmouth College, New Lebanon, NH, USA

¹¹ Medicine and Radiation Oncology PA, San Antonio, TX, USA

¹² Department of Radiation Oncology, West Virginia University, Morgantown, WV, USA

Edited by:

Kwan-Hwa Chi, Shin-Kong Memorial Hospital, Taiwan

Reviewed by:

Kwan-Hwa Chi, Shin-Kong Memorial Hospital, Taiwan

Daniel Grant Peterait, Rapid City Regional Hospital, USA

*Correspondence:

Nam P. Nguyen, Department of Radiation Oncology, University of Arizona, 1501 North, Campbell Avenue, Tucson, AZ 85724-5081, USA
e-mail:
namphong.nguyen@yahoo.com

Background: To assess the tolerance of patients with small cell lung cancer undergoing chemoradiation with tomotherapy-based image-guided radiotherapy (IGRT).

Materials and Methods: A retrospective review of the toxicity profile for nine patients with small cell lung cancer of the limited stage who underwent chemoradiation delivered with helical tomotherapy (HT) has been conducted.

Results: Acute grade 3–4 hematologic and esophagitis toxicities developed in two and three patients respectively. One patient developed a pulmonary embolism during radiotherapy. Seven patients had weight loss ranging from 0 to 30 pounds (median: 4 pounds). Three patients had treatment breaks ranging from 2 to 12 days. At a median follow-up of 11 months (range: 2–24 months), no patients developed any radiation related toxicities such as grade 3–4 pneumonitis or other long-term complications. The median survival was estimated to be 15 months. There were two local recurrences, three mediastinal recurrences, and six distant metastases.

Conclusion: Grade 3–4 toxicities remained significant during chemoradiation when radiation was delivered with tomotherapy-based IGRT. However, the absence of grade 3–4 pneumonitis is promising and the use of HT needs to be investigated in future prospective studies.

Keywords: small cell lung cancer, limited stage, chemoradiation, IGRT

INTRODUCTION

Standard of care for small cell lung cancer of limited stage is concurrent chemotherapy and radiotherapy (1–7). Radiotherapy usually starts within 30 days of the initiation of chemotherapy to ensure an optimal outcome (5). Treatment toxicity of the combined modality is significant because of the volume of the normal organs irradiated (esophagus and lungs) and the bone marrow suppression from chemotherapy. Grade 3–4 esophagitis, pneumonitis, and hematologic toxicity occurred frequently (1–7). Although there are still controversies about the technique of radiation delivery and the most optimal dose of radiotherapy, most institutions treated the gross tumor and mediastinum, which is followed by a cone down to the gross tumor with the three-dimensional conformal radiotherapy technique (3-D CRT). Some institutions choose to treat the gross tumor and involved lymph

nodes only to decrease normal tissue toxicity with the risk of recurrence in the non-irradiated mediastinal lymph nodes (4). Recently, new techniques of radiotherapy such as image-guided radiotherapy (IGRT) has been introduced to help reduce the treatment margins used to create the planning target volume through more precise image guidance. This potentially decreases normal tissue toxicity through reducing the volume of normal tissue included in the high dose volume. It also allows improved tumor coverage and the delivery of higher radiation to the target volume which potentially improves loco-regional control without increasing the risk of normal tissue complications. Preliminary results of IGRT in head and neck and gastrointestinal cancers have been promising because of significant sparing of normal organs at risk for radiotherapy complications (8–12). This has prompted us to conduct this retrospective study on the feasibility of delivering IGRT with helical

tomotherapy (HT) in the setting of concurrent chemoradiation for limited-stage small cell lung cancers.

MATERIALS AND METHODS

The medical records of nine patients with limited-stage small cell lung cancers who underwent concurrent chemoradiation delivered with HT between September 2009 and February 2012 were retrospectively reviewed. The University of Arizona Institutional Review Board (IRB) approved the study and waived the requirement for patient consent because of the retrospective nature of the study. All but one patient underwent platinum-based chemotherapy with cisplatin and etoposide (7) or carboplatin and etoposide (1). One patient refused chemotherapy because of the fear of treatment-related toxicities. All patients had mediastinal nodal involvement (8 N2, 1 N3) at presentation. Six patients had stage IIIA and three patients had stage IIIB disease. **Table 1** summarizes patient characteristics. All patients underwent positron emission tomography (PET) with computed tomography (CT) as part of the staging. The PET-CT was also incorporated into the planning CT to outline the target volume. All patients underwent simulation and treatment in the supine position with their arms raised above their heads and were immobilized using a custom-made Vac-Lok cradle (Medtec, Orange City, IA, USA). For the actual simulation, a CT scan of the chest with and without intravenous (IV) contrast was performed in the treatment position. The thorax area from the neck to mid-abdomen was scanned with a slice thickness of 3 mm. The CT scan without contrast was used for planning to avoid possible interference of the contrast density on radiotherapy isodose distribution. The gross tumor volume (GTV) was defined as the post-chemotherapy tumor volume after one cycle of chemotherapy. All patients underwent 4D simulation at the time of the CT simulation to outline the tumor internal target volume (ITV). Respiratory motion was accounted for by 4D CT which retrospectively sums of the CT images collected from evenly separated time points (10 phases) throughout one breathing cycle. The clinical target volume (CTV) was created by expansion of the ITV, PET positive mediastinal lymph nodes, ipsilateral hilum, and mediastinum with a 0.8 cm margin. For tumor located in the upper lobes (8), the ipsilateral supraclavicular lymph node area was also treated prophylactically and the lower mediastinum was excluded. For tumor located in the lower lobe, the lower mediastinum was treated but the supraclavicular lymph node area was excluded. A margin of approximately 0.2 cm was added to create the final PTV. The PTV and ITV was treated to a total dose of 4500 cGy in 180 cGy/fraction and 5000 cGy in 200 cGy/fraction respectively. All target volumes were checked daily before each treatment and the isodose lines verified to ensure that no excessive radiation was delivered to the OARs. Patients were simulated and re-planned at 4000 cGy to account for tumor shrinkage, and/or expansion of the lungs from resolution of the atelectasis. The residual gross tumor ITV was boosted for an additional dose of 1000 cGy in 200 cGy/fraction (6) or 1500 cGy in 125 cGy/fraction twice a day (bid) (3) to achieve a tumor dose of 6000–6500 cGy. The bid fractionation was chosen when the tumor encased the blood vessels to decrease the risk of hemorrhage as the tumor may already invade into the adventitia of the blood vessels. Dose constraints for normal organs at risk for complications were the following: lungs

Table 1 | Patient characteristics.

Patient number	9
Median age	60 (46–84)
Sex	
Female	2
Male	7
Histology	Small cell
T stage	
T1	4
T2	3
T4	2
N stage	
N2	8
N3	1
Stage	
IIIA	6
IIIB	3
Tumor location	
RUL	4
LUL	3
RML	1
LLL	1
Follow-up	2–24 months (median: 11 months)

RUL: right upper lobe; LUL: left upper lobe; RML: right middle lobe; LLL: left lower lobe.

(V20 <30%, V5 <50%); spinal cord: $D_{\max} <40$ Gy; cardiac ventricles: V40 <10%, V20 <50%). Minimal target coverage was 95% for all targets with at least 99% of the prescribed dose delivered to the gross tumor and mediastinal lymph nodes. Radiotherapy started on the second cycle of chemotherapy. Weekly complete blood count (CBC) and blood chemistry to assess renal function were performed during chemoradiation.

Treatment breaks and weight loss were recorded during chemoradiation. Acute and long-term toxicities were graded according to Radiotherapy Oncology Group (RTOG) group severity scale (<http://ctep.cancer.gov>). All patients had a follow-up visit 1 month and regularly 3 months following treatment. Clinical examination was performed at each follow-up to detect recurrent disease and possible complications resulting from the treatment. Patients were asked specifically about their exercise tolerance, dysphagia, weight loss, and difficulty to breathe compared to their pre-treatment baseline. The patients were also monitored during and following treatment with a team of dietitians because of the expected grade 3–4 esophagitis. A PET-CT scan was performed 4, 10 months, and yearly after treatment if there was no clinical evidence of disease. Patient with a complete response (CR) on PET-CT will undergo prophylactic cranial irradiation (PCI). Survival data was analyzed using Kaplan–Meier estimation.

RESULTS

PTV target coverage ranged from 96 to 98% (median: 97%). Maximum spinal cord dose ranged from 3300 to 4100 cGy (median: 3500 cGy). V20 and V5 for both lungs combined ranged from 6 to 25% (median: 22%) and 30 to 67% (median: 53%) respectively.

Table 2 | Treatment toxicity.

Weight loss	0–30 pounds (median: 4 pounds)
Treatment break	Three patients had treatment breaks ranging from 2 to 12 days
Grade 3–4 toxicities	
Hematologic	2/9 (22%)
Esophagitis	3/9 (30%)
Pulmonary embolism	1/9 (11%)

Because of the tumor location in the upper lobes in eight patients, the cardiac ventricles doses were insignificant. Except for one patient, all patients had significant shrinkage of the GTV during treatment (30% or more of the pre-treatment tumor volume). For one patient, tumor size increased during treatment and he developed loco-regional failure later.

Two patients (22%) developed grade 3–4 hematologic toxicity. Three patients (33%) had grade 3–4 esophagitis and one patient (11%) had pulmonary embolism. Median weight loss was 4 pounds (range: 0–30 pounds). Three patients (33%) had treatment breaks ranging from 2 to 12 days (Table 2). Four patients (44%) had a CR on PET-CT post treatment. However, only one patient with a CR underwent PCI. The other three declined PCI because of the fear of late neurotoxicity. Two of these patients developed multiple brain metastases later and died. Two patients developed local recurrences (22%) and three patients had mediastinal recurrences (33%). Six patients (66%) developed distant metastasis (brain: 2, liver: 2, bones: 2, adrenals: 1). At a median follow-up of 11 months (range: 2–24 months), the median and 2-year survival was estimated to be 15 months and 28% respectively. No patients developed grade 3–4 acute or late pneumonitis. The acute esophagitis resolved by 6 weeks following treatment completion and all patients recovered from their weight loss. No patient noticed a change of their breathing pattern or physical activity compared the pre-treatment baseline.

DISCUSSION

Randomized studies of small cell lung cancer with limited stages revealed poor survival with a high rate of loco-regional recurrences and distant metastases (2, 6, 13–17). Radiation therapy dose ranged from 4500 cGy in 150 cGy bid to 4500–5000 cGy in 25 daily fractions. Despite a low dose of radiation, patients still experienced grade 3–4 pneumonitis ranging from 3.2 to 6.2% (2, 13, 15, 16). In severe cases death may occur (2, 13, 15). Among long-term survivors, grade 3–4 pulmonary fibrosis has been reported in 37–39% of the patients (17). Radiation-induced lung injury was most likely due to irradiation of a large volume of the normal lungs with the conventional radiotherapy technique when the ipsilateral mediastinum was included in the treatment volume. Preliminary data indicated that by limiting the target volume to the GTV and adjacent lymph nodes, radiation dose escalation was feasible to improve local control. With this approach, Bogard et al. reported that the GTV dose may be increased to 7000 cGy with grade 3 pneumonitis observed in only 5% of the patients (18). Thus, a new radiation technique that allows radiation dose escalation without increasing lung toxicity may potentially improve local

control and survival while preserving patient quality of life. The introduction of intensity-modulated radiotherapy (IMRT) may allow for decrease normal tissue toxicity because of the rapid dose fall-off away from the target volume (19). However, when IMRT was used for elective nodal irradiation in patients with limited-stage small cell lung cancer, 7% of the patients still experienced grade 3 pneumonitis despite the fact that two-third of the patients was treated to 4500 cGy in 30 bid fractions and the target was limited to the GTV and lymph nodes involved on PET scan (20). Thus, our study is the first to demonstrate the feasibility of adaptive IGRT delivered with HT-based image to spare the normal lungs from excessive irradiation as the GTV was treated to a higher dose of radiation (6000–6500 cGy) and the ipsilateral mediastinum was included in the treatment field. The absence of grade 3–4 pneumonitis and long-term lung injury in our study may be attributed to multiple factors. We outlined the GTV post-chemotherapy as a target volume as Hu et al. (3) observed no difference in local control if the post-chemotherapy GTV was treated instead of the pre-chemotherapy GTV. As the tumor shrinks during radiotherapy, re-planning and boosting to the residual tumor may allow for sparing of the normal lungs without compromise of target coverage (21). All but one of the patients had significant decreased in size of the tumor which is in agreement with other studies. Hugo et al (22) reported that the GTV volume decreased by 23% after 5 weeks of radiotherapy in patients with non-small cell lung cancer. In addition, compared to conventional IMRT, HT provides comparable target coverage with a significant reduction of the lungs V20 (23). We also set high priority to limit the V5 for normal lung as the patients received concurrent chemotherapy which may increase radiosensitization of the normal lungs and the risks of severe pneumonitis (23). The low V5 and V20 in our study indicated that the normal lungs may be preserved from excessive irradiation with HT-based IGRT in the treatment of patients with small cell lung cancer of limited stage. This is true even if elective nodal irradiation is administered. Thus, dose escalation to the gross disease with reduced margins may be feasible with HT-based IGRT. This hypothesis warrants further validation in future prospective trials with larger number of patients.

We do observe a high rate of grade 3–4 esophagitis which is unavoidable because the esophagus is included in the ipsilateral mediastinum. However, all patients recovered following treatment and resumed a normal physical activity. The addition of a radiation protector such as amifostine may be an option to decrease the severity of esophagitis and improve patient quality of life during treatment (24).

The study is limited by the fact that it only includes a small number of patients and a short follow-up after treatment. Thus, it can only serve as a preliminary report which warrant further validation in future prospective studies.

CONCLUSION

Image-guided radiotherapy delivered with HT may potentially reduce the risk of radiation related severe toxicities, and especially lung toxicities in the setting of concurrent chemoradiation for limited-stage small cell lung cancer. This may allow for further radiation dose escalation to the gross tumor to improve treatment outcome. Prospective studies with a large number of

patients should be conducted in the future to further validate this hypothesis.

REFERENCES

- Scullier JP, Lafitte JJ, Efremidis A, Florin MC, Lecomte J, Berchier MC. A phase III randomized study of concomitant induction radiochemotherapy testing two modalities of radiosensitization by cisplatin (standard versus daily) for limited small-cell lung cancer. *Ann Oncol* (2008) **19**:1691–7. doi:10.1093/annonc/mdn354
- Bonner JA, Sloan JA, Shanahan TG, Brooks BJ, Marks RS, Krook JE. Phase III comparison of twice-daily split course irradiation versus once-daily irradiation for patients with limited stage small-cell lung carcinoma. *J Clin Oncol* (1999) **17**:2681–91.
- Hu X, Bao Y, Zhang L, Guo Y, Chen YY, Li KX, et al. Chemotherapy tumor extent for limited-stage small cell lung cancer. *Cancer* (2012) **118**:278–87. doi:10.1002/cncr.26119
- Colaco R, Sheikh H, Lorigan P, Blackhall F, Hulse P, Califano R, et al. Omitting elective nodal irradiation in limited-stage small cell lung cancer—Evidence from a phase II trial. *Lung Cancer* (2012) **76**:72–7. doi:10.1016/j.lungcan.2011.09.015
- Pijls-Johannesma M, De Ruyscher D, Vansteenkiste J, Kester A, Rutten I, Lambin P. Timing of chest radiotherapy in patients with limited stage small cell lung cancer: a systemic review and meta-analysis of randomized controlled trials. *Cancer Treat Rev* (2007) **33**:461–73. doi:10.1016/j.ctrv.2007.03.002
- Takada M, Fukuoka M, Kawahara M, Sugiura T, Yokohama A, Yokota S, et al. Phase III study of concurrent versus sequential thoracic radiotherapy in combination with cisplatin and etoposide for limited stage small cell lung cancer: results of the Japan Clinical Oncology Group Study 9104. *J Clin Oncol* (2002) **20**:3054–60. doi:10.1200/JCO.2002.12.071
- Spiro SG, James LE, Rudd RM, Trask CW, Tobias JS, Snee M, et al. Early compared with late radiotherapy in combined modality treatment for limited disease small cell lung cancer: a London Lung Cancer Group Multicenter randomized clinical trial and meta-analysis. *J Clin Oncol* (2006) **24**:3823–30. doi:10.1200/JCO.2005.05.3181
- Nguyen NP, Vock J, Vinh-Hung V, Ceizyk M, Smith-Raymond L, Stevie M, et al. Feasibility of image-guided radiotherapy based on helical tomotherapy to reduce contralateral parotid dose in head and neck cancer. *BMC Cancer* (2012) **12**:175. doi:10.1186/1471-2407-12-175
- Nguyen NP, Chi A, Betz M, Almeida F, Vos P, Davis R, et al. Feasibility of intensity-modulated and image-guided radiotherapy for functional organ preservation in locally advanced laryngeal cancer. *PLoS One* (2012) **7**:e42729. doi:10.1371/journal.pone.0042729
- Nguyen NP, Smith-Raymond L, Vinh-Hung V, Sloan D, Davis R, Vos P, et al. Feasibility of tomotherapy to spare the cochlea from excessive radiation in head and neck cancer. *Oral Oncol* (2011) **47**:414–9. doi:10.1016/j.oraloncology.2011.03.011
- Nguyen NP, Ceizyk M, Almeida F, Chi A, Betz M, Modarresifar H, et al. Effectiveness of image-guided radiotherapy for locally advanced rectal cancer. *Ann Surg Oncol* (2011) **18**:380–5. doi:10.1245/s10434-010-1329-0
- Nguyen NP, Vock J, Sroka T, Khan R, Jang S, Chi A, et al. Feasibility of image-guided radiotherapy based on tomotherapy for the treatment of locally advanced anal carcinoma. *Anticancer Res* (2011) **31**:4393–6.
- Turrisi AT, Kim K, Blum R, Sause WT, Livingston RB, Komaki R, et al. Twice-daily compared with once-daily thoracic radiotherapy in limited small-cell lung cancer treated concurrently with cisplatin and etoposide. *N Engl J Med* (1999) **340**:265–71. doi:10.1056/NEJM199901283400403
- Hu X, Bao Y, Zhang L, Guo Y, Chen YY, Li KX, et al. Omitting elective nodal irradiation and irradiating postinduction versus preinduction chemotherapy tumor extent for limited stage small cell lung cancer. *Cancer* (2012) **118**:278–87. doi:10.1002/cncr.26119
- Schild SE, Bonner JA, Shanahan TG, Brooks BJ, Marks RS, Geyer SM, et al. Long-term results of a phase III trial comparing once-daily radiotherapy with twice daily radiotherapy in limited-stage small cell lung cancer. *Int J Radiat Oncol Biol Phys* (2004) **59**:943–51. doi:10.1016/j.ijrobp.2004.01.055
- Murray N, Coy P, Pater JL, Hodson I, Arnold A, Zee BC, et al. Importance of timing for thoracic irradiation in the combined modality treatment of limited-stage small cell lung cancer. *J Clin Oncol* (1993) **11**:336–44.
- Gregor A, Drings P, Burghouts J, Postmus PE, Morgan D, Sahmoud T, et al. Randomized trial of alternating versus sequential radiotherapy/chemotherapy in limited disease patients with small cell lung cancer. *J Clin Oncol* (1997) **15**:2840–9.
- Bogard JA, Herndon JE, Lyss AP, Watson D, Miller AA, Lee ME, et al. 70 Gy thoracic radiotherapy is feasible concurrent with chemotherapy for limited-stage small cell lung cancer: analysis of cancer and leukemia group B study 39802. *Int J Radiat Oncol Biol Phys* (2004) **59**:460–8. doi:10.1016/j.ijrobp.2003.10.021
- Bezjak A, Rumble RB, Rodrigues G, Hope A, Warde P. Members of the IMRT indication panel. *Clin Oncol* (2012) **24**:508–20. doi:10.1016/j.clon.2012.05.007
- Shirvani SM, Komaki R, Heymach JV, Fossella SV, Chang JY. Positron emission tomography/computed-tomography-guided intensity-modulated radiotherapy for limited-stage small cell lung cancer. *Int J Radiat Oncol Biol Phys* (2012) **82**:91–7. doi:10.1016/j.ijrobp.2010.12.072
- Guckenberger M, Wilbert J, Richter A, Baier K, Flentje M. Potential of adaptive radiotherapy to escalate radiation dose in combined radiochemotherapy for locally advanced non-small cell lung cancer. *Int J Radiat Oncol Biol Phys* (2011) **79**:901–8. doi:10.1016/j.ijrobp.2010.04.050
- Hugo GD, Weiss E, Badawi A, Orton M. Localization accuracy of the clinical target volume during image-guided radiotherapy of lung cancer. *Int J Radiat Oncol Biol Phys* (2011) **81**:560–7. doi:10.1016/j.ijrobp.2010.11.032
- Song CH, Pyo H, Moon SH, Kim TH, Cho KH. Treatment-related pneumonitis and acute esophagitis in non-small cell lung cancer patients treated with chemotherapy and radiotherapy. *Int J Radiat Oncol Biol Phys* (2010) **78**:651–8. doi:10.1016/j.ijrobp.2009.08.068
- Garces YI, Okuno SH, Schild SE, Mandrekar SJ, Bot BM, Martens JM, et al. Phase I North Central Cancer Treatment Group trial N9923 of escalating doses of twice daily thoracic radiotherapy with amifostine and with alternating chemotherapy in limited stage small-cell lung cancer. *Int J Radiat Oncol Biol Phys* (2007) **67**:995–1001. doi:10.1016/j.ijrobp.2006.10.034

Conflict of Interest Statement: The authors declare that the research was conducted in the absence of any commercial or financial relationships that could be construed as a potential conflict of interest.

Received: 04 October 2013; accepted: 12 November 2013; published online: 26 November 2013.

Citation: Nguyen NP, Shen W, Kratz S, Vock J, Vos P, Vincent V-H, Altdorfer G, Ewell L, Jang S, Karlsson U, Godinez J, Mills M, Sroka T, Dutta S, Chi A and The International Geriatric Radiotherapy Group (2013) Feasibility of tomotherapy-based image-guided radiotherapy for small cell lung cancer. Front. Oncol. 3:289. doi:10.3389/fonc.2013.00289

*This article was submitted to Radiation Oncology, a section of the journal *Frontiers in Oncology*.*

Copyright © 2013 Nguyen, Shen, Kratz, Vock, Vos, Vincent, Altdorfer, Ewell, Jang, Karlsson, Godinez, Mills, Sroka, Dutta, Chi and The International Geriatric Radiotherapy Group. This is an open-access article distributed under the terms of the Creative Commons Attribution License (CC BY). The use, distribution or reproduction in other forums is permitted, provided the original author(s) or licensor are credited and that the original publication in this journal is cited, in accordance with accepted academic practice. No use, distribution or reproduction is permitted which does not comply with these terms.



The potential role of magnetic resonance spectroscopy in image-guided radiotherapy

Mai Lin Nguyen¹, Brooke Willows², Rihan Khan³, Alexander Chi⁴, Lyndon Kim⁵, Sherif G. Nour⁶, Thomas Sroka⁷, Christine Kerr⁸, Juan Godinez⁹, Melissa Mills¹⁰, Ulf Karlsson¹¹, Gabor Altdorfer¹², Nam Phong Nguyen^{13*}, Gordon Jendrasiak¹⁴ and The International Geriatric Radiotherapy Group

¹ Department of Psychology, Stanford University, Palo Alto, CA, USA

² School of Medicine, University of Arizona, Phoenix, AZ, USA

³ Department of Radiology, University of Arizona, Tucson, AZ, USA

⁴ Department of Radiation Oncology, University of West Virginia, Morgantown, WV, USA

⁵ Division of Neuro-Oncology, Department of Neurosurgery and Medical Oncology, Thomas Jefferson University, Philadelphia, PA, USA

⁶ Department of Radiology, Emory University, Atlanta, GA, USA

⁷ Department of Radiation Oncology, Dartmouth College, New Lebanon, NH, USA

⁸ Department of Radiation Oncology, Centre Val d'Aurelle, Montpellier, France

⁹ Department of Radiation Oncology, Florida Radiation Oncology Group, Jacksonville, FL, USA

¹⁰ Department of Radiation Oncology, University of Arizona, Tucson, AZ, USA

¹¹ Department of Radiation Oncology, Marshfield Clinic, Marshfield, WI, USA

¹² Department of Radiation Oncology, Camden Clark Cancer Center, Parkersburg, WV, USA

¹³ Department of Radiation Oncology, Howard University Hospital, Washington DC, USA

¹⁴ Department of Radiation Oncology, East Carolina University, Greenville, NC, USA

Edited by:

Kwan-Hwa Chi, Shin-Kong Memorial Hospital, Taiwan

Reviewed by:

Sean Collins, Georgetown University Hospital, USA

William Small, Robert H. Lurie Comprehensive Cancer Center of Northwestern University, USA

*Correspondence:

Nam Phong Nguyen, Department of Radiation Oncology, Howard University Hospital, 2401 Georgia Avenue N.W., Washington DC 20060, USA

e-mail: namphong.nguyen@yahoo.com

Magnetic resonance spectroscopy (MRS) is a non-invasive technique to detect metabolites within the normal and tumoral tissues. The ability of MRS to diagnose areas of high metabolic activity linked to tumor cell proliferation is particularly useful for radiotherapy treatment planning because of better gross tumor volume (GTV) delineation. The GTV may be targeted with higher radiation dose, potentially improving local control without excessive irradiation to the normal adjacent tissues. Prostate cancer and glioblastoma multiforme (GBM) are two tumor models that are associated with a heterogeneous tumor distribution. Preliminary studies suggest that the integration of MRS into radiotherapy planning for these tumors is feasible and safe. Image-guided radiotherapy (IGRT) by virtue of daily tumor imaging and steep dose gradient may allow for tumor dose escalation with the simultaneous integrated boost technique (SIB) and potentially decrease the complications rates in patients with GBM and prostate cancers.

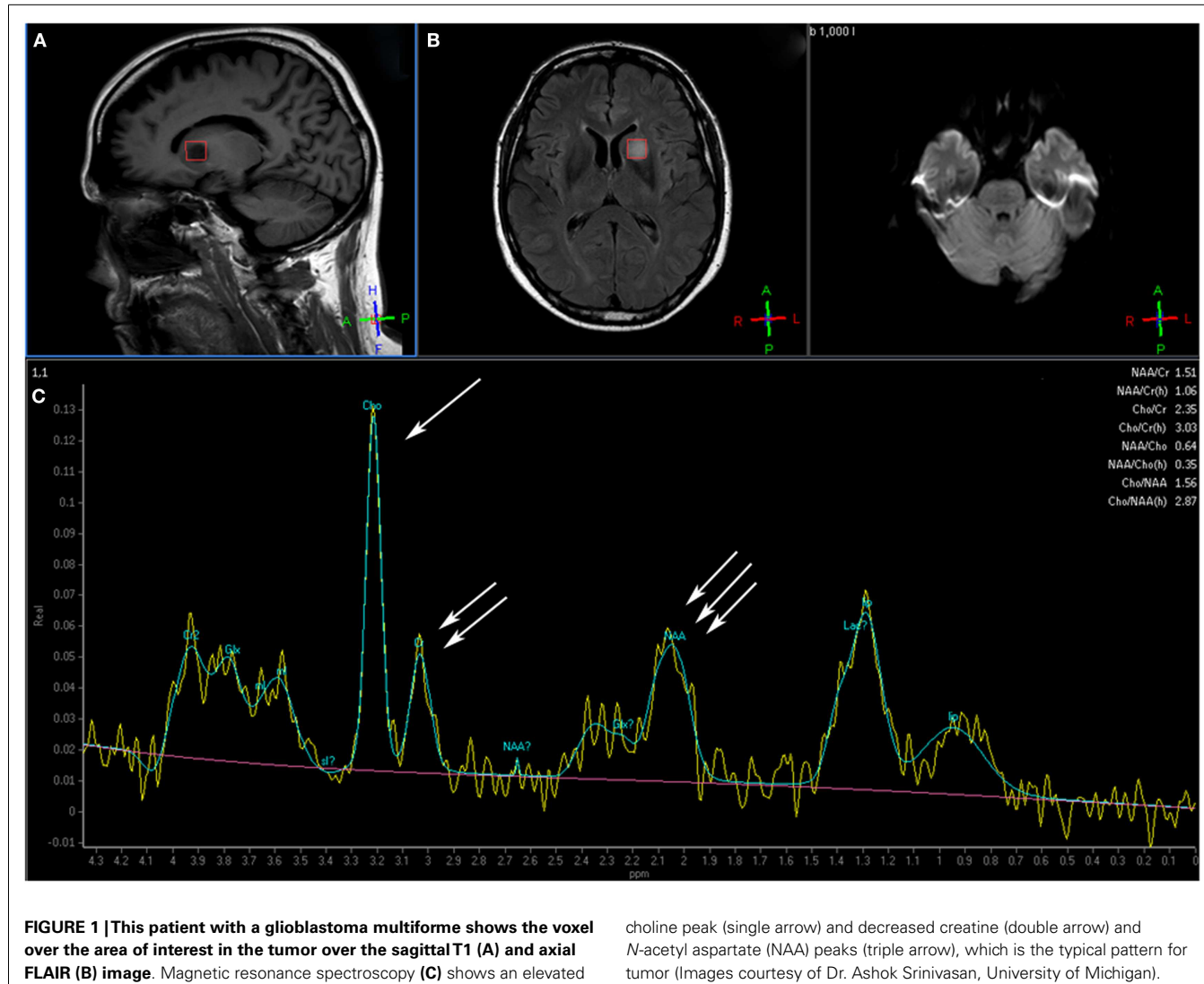
Keywords: MRS, IGRT, prostate cancer, GBM

POTENTIAL ADVANTAGES OF MAGNETIC RESONANCE SPECTROSCOPY FOR FUNCTIONAL TUMOR IMAGING

Magnetic resonance spectroscopy (MRS) is based on nuclear magnetic resonance technique to investigate the metabolism of chemicals in the body. Different chemicals containing the same nucleus exhibit characteristic chemical shifts in resonance frequency, allowing the chemical form of the element to be identified. Since the most abundant atom in the body is hydrogen (H), ¹H MRS estimates the concentration of different metabolites within normal tissues of the body, which are displayed as a spectrum of resonances (peaks) along the *x*-axis as parts per million (ppm) and the amplitude of resonances is measured on the *y*-axis using an arbitrary scale. Depending on the clinical question, many major metabolites can be measured with MRS. In the brain, *N*-acetyl aspartate (NAA) is a marker for neuronal and axonal integrity. A decrease in NAA level is usually associated with neuronal loss or damage. Choline (Cho) represents the constituents of cell membrane. Increased Cho is associated with increased concentration of cells and/or cell membrane synthesis such as cancer. Creatinine (Cr) is a marker for cell energy metabolism. Decreased in

Cr is associated with tissue death or necrosis. Lactate is a marker for anaerobic glycolysis. Increased lactate is associated with hypoxemia and tumors because of their anaerobic metabolism. Increased lipids concentration is observed in necrotic areas of the tumor. In gliomas, NAA is reduced because of neurons destruction by the tumor and Cho is increased because of tumor cell proliferation. Thus, abnormal Cho/NAA ratio is observed in areas of tumor infiltration such as the area of vasogenic edema around the gross tumor. **Figure 1** illustrates the potential of MRS to outline the gross tumor volume (GTV) in a patient with glioblastoma multiforme (GBM).

Magnetic resonance spectroscopy is particularly helpful to distinguish radiation injury from tumor recurrence after radiotherapy as both may have similar magnetic resonance imaging (MRI) appearances (1). Decreased in Cho, NAA, and Cr are usually observed with radiation injury and high Cho/NAA ratio is suggestive of tumor recurrence (2). In the prostate, Citrate (Cit) is produced by the normal prostate epithelium. The prostate has a high concentration of mitochondrial Zinc (Zn), which inhibits aconitase, the first enzyme of the Krebs cycle, which normally



converts citrate to isocitrate leading to a high concentration of citrate in the prostatic epithelium (3). Cit is often decreased in area of prostate adenocarcinoma because of the low Zn concentration. High Cho and Cr are also observed in tumor areas because of cancer cells proliferation. Thus, higher Cho + Cr/Cit ratio is observed in areas of high tumor concentration compared to normal prostate tissue. **Figure 2** illustrates the potential of MRS to outline the GTV in a patient with biopsy-proven adenocarcinoma of the prostate. Interestingly, areas of high Gleason score (4 + 3 or above) associated with tumor poor differentiation may be associated with high Cho + Cr/Cit ratio suggesting that MRS may be useful to guide prostate biopsy (4, 5). A high Cho + Cr/Cit ratio is also associated with a large tumor volume and advanced tumor stage (6, 7). As a result, MRS is very accurate to detect high grade tumors within the prostate gland, which may be useful for treatment planning because of the high recurrence rates of these tumors (8). As prostate cancer has a heterogeneous distribution within the prostate gland, MRS is particularly helpful to guide a second biopsy if the

initial biopsy was negative among patients with a high PSA level suspicious for prostate cancer (9). MRS can also be used to assess radiotherapy response or recurrence following prostate irradiation. As Cit level decreases following prostate cancer irradiation at a faster rate than Cho or Cr, the Cho level, or Cho/Cr ratio are often used for radiation response.

A low normalized Cho following radiotherapy may predict a low PSA (0.5 ng/ml or less) at 1 year following prostate cancer treatment (10). Conversely, high Cho level or Cho/Cr ratio may detect local recurrences in patients with rising PSA following prostate cancer irradiation (11–13). The pattern of local recurrence following external beam irradiation of prostate cancer is predominantly within the dominant intra-prostatic tumors suggesting that radiation dose escalation of these focal tumor masses may improve local control (14).

PRINCIPLES OF IMAGE-GUIDED RADIOTHERAPY

Conventional treatment with three-dimensional conformal radiotherapy (3D-CRT) has been associated with a higher rate of toxicity

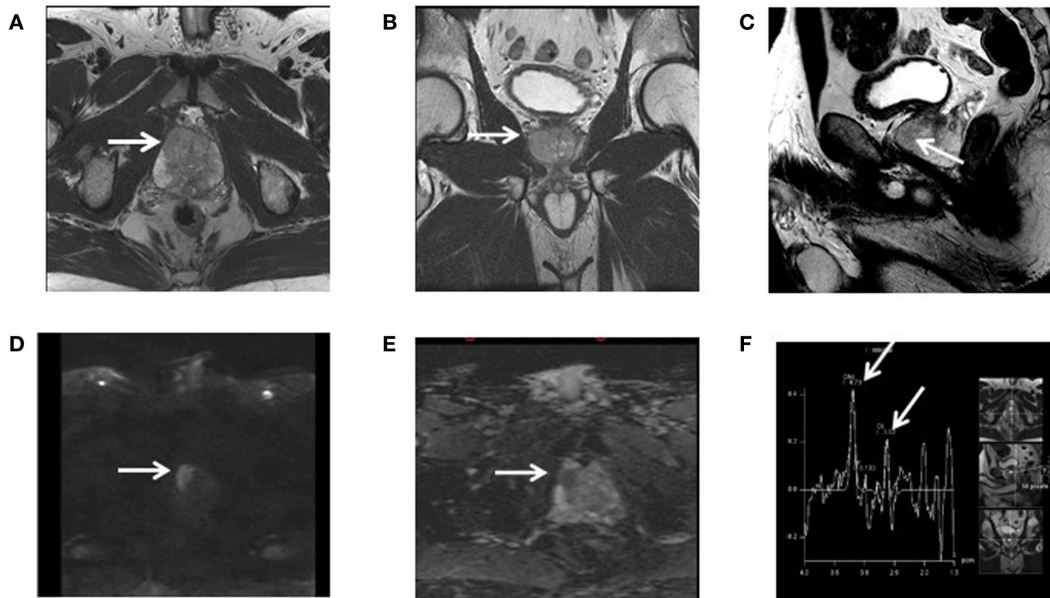


FIGURE 2 | This patient has a biopsy-proven adenocarcinoma of the prostate in the magnetic resonance spectroscopy area suspicious for malignancy. Axial (A), Coronal (B), and sagittal (C) high-resolution

T2-weighted images. Axial diffusion weighted, $b = 2000$ (D) and ADC map (E). ^1H -spectroscopy demonstrating elevated choline/creatinine-to-citrate ratio (F).

with radiation dose escalation because of irradiation of a large volume of normal tissues (15). The introduction of intensity-modulated radiotherapy (IMRT) has led to significant reduction of normal tissue irradiation because of the steep radiation dose gradient away from the target volume compared to 3D-CRT (16). However, a significant amount of normal tissues is still irradiated because the inclusion of the tumor and areas at high risk for invasion with a large rim of normal tissue called planning target volume or PTV to avoid marginal miss. Recently, image-guided radiotherapy (IGRT) by combining the steep dose gradient of IMRT with daily imaging may further improve treatment toxicity because of the PTV reduction provided that the gross tumor and area at risk for tumor invasion can be accurately outlined with proper diagnostic imaging (17). Functional tumor imaging such as MRS in combination with conventional diagnostic studies such as MRI may allow the radiation oncologist to develop a treatment plan that covers the PTV with a curative radiation dose while sparing the normal organs with the simultaneous integrated boost (SIB) technique, which delivers different dose levels within the PTV (18). Thus, the intra-prostatic or GBM GTV outlined by MRS may be treated with a higher radiation dose than the PTV for improved local control while the IMRT steep dose gradient decreases radiation dose to the normal adjacent organs and potentially reduces long-term complications. The success of functional imaging for accurate radiation delivery with IGRT requires a close collaboration between the diagnostic radiologist and radiation oncologist as MRS is not easy to interpret because of its limitations even for experienced diagnostic radiologist. As radiation dose escalation with IGRT may be associated with significant toxicity, it is imperative to outline the GTV accurately.

POTENTIAL APPLICATION OF MRS FOR IGRT OF GLIOBLASTOMA MULTIFORME

Multiple studies of radiation dose escalation for GBM have failed to demonstrate an improvement in survival or local control (19). However, these studies were based on 3D conformal radiotherapy (3D-CRT) and MRI imaging. One possible explanation is whether the high radiation dose was actually delivered to the areas of high cancer concentration to be effective because of the heterogeneity of the tumor distribution within the target volume. Another possible explanation is the protracted treatment time may not be effective for local control because of the accelerated repopulation of cancer stem cells, which may be radio-resistant (20). Thus, a treatment course that delivers a high radiation dose to the GTV within a short time may be more effective for tumor control and potentially improve patient quality of life as they will have more time to spend with their family. Functional imaging with MRS may allow the radiation oncologist to outline the target volume accurately and spare the normal brain from unnecessary irradiation. The potential of IGRT to decrease the planning target volume (PTV) because of daily imaging coupled with the steep dose gradient of IMRT may further reduce treatment toxicity. As a result, the combination of precise tumor targeting and planning with MRS and effective radiotherapy delivery through IGRT may improve local control without excessive neurotoxicity. The feasibility of MRS for radiotherapy treatment planning of GBM has been investigated. The choline to creatinine ratio as an indice of the tumor activity (3 or higher) was converted on a gray scale, fused to the MRI images and transferred to the computer tomography (CT) scan as GTV in 12 patients with glioma (21). Among the patients in the study who had GBM, an IMRT plan was developed to delivered 5940 cGy in 180 cGy to the PTV while limiting

radiation to the critical radiosensitive structures such as the optic chiasm and brain stem. Radiotherapy treatment was well tolerated by all patients without complications. A SIB plan was also generated but not used for treatment to increase the GTV dose to 7000 cGy based on the choline/creatinine ratio. Despite a higher GTV dose, the dose to the radiosensitive structures did not increase and highlighted the safety of radiation dose escalation with the SIB technique. Another study corroborated the feasibility of MRS for radiation dose escalation. Thirty-five GBM patients underwent surgical resection and had MRS to outline the tumor bed after surgery (22). The voxels within the post-operative T2 MRI that contained acholine/*N*-acetylaspartate ratio of 2 or above were treated with stereotactic radiosurgery (SRS) to a dose determined by the Radiation Therapy Oncology Group (RTOG) SRS guidelines followed by an additional dose of 6000 cGy with 3D-CRT. Among the 16 patients of the study who received temozolomide (TMZ) in addition to the radiotherapy protocol, median survival was 20.8 months compared to the historical control of 14.6 months for the ones treated with conventional radiotherapy and TMZ of the European Organization for Research and Treatment of Cancer (EORTC) (23). Grade 3–4 toxicity of the protocol treatment was acceptable suggesting that radiation dose-escalation based on MRS for GTV delineation may improve local control without excessive toxicity. Preliminary studies of MRI-based IMRT treatment of GBM also suggest that radiation dose escalation may be safe when combined with TMZ. Thirty-eight GBM patients were treated to a dose ranging from 6600 to 8100 cGy to the GTV with the IMRT technique. Only three patients with radiation dose exceeding 7500 cGy developed radionecrosis. Among the 22 patients who had functional imaging with C¹¹ methionine positron emission tomography (MET-PET) before treatment, seven out of eight patients recurred because of inadequate coverage of the GTV as defined by MET-PET (24). This study highlights the potential of MRS to avoid marginal miss and possibly decreasing complications rates with PTV reduction. IMRT-based IGRT for GBM has been investigated to shorten the treatment course with promising results (25–27). Thus, MRS-based IGRT treatment for GBM merits further investigations in the future to improve local control and reduce toxicity.

POTENTIAL APPLICATION OF MRS FOR IGRT OF PROSTATE CARCINOMA

On line IGRT in prostate cancer allows for immediate correction of daily movement of the prostate secondary to bladder and rectum filling. The ability to increase radiation delivery accurately avoids unnecessary irradiation of the bladder and rectum and may decrease radiation side effects. In a study of 275 patients with prostate cancer treated to a tumor dose of 74–78 Gy, patients who had IGRT experienced significantly less diarrhea, urinary frequency, and fatigue compared to the ones without IGRT. The margins and planning constraints were the same for both groups (28). The reduced morbidity of radiation with daily imaging was also corroborated in another study of 282 patients with prostate cancer. Among 154 patients treated with IGRT, rectal pain and diarrhea were significantly less even though they were treated to a higher dose compared to the ones who did not have IGRT (29). Inpatients with intermediate to high risk prostate cancer,

a higher radiation dose may be required to improve local control and biochemical-free survival if dose escalation does not lead to increased risk of complications (15). However, in patients with multiple co-morbidity factors such as the elderly, increasing radiation dose to the prostate may further increase the risk of rectal damage because the close proximity of the rectum to the prostate (30). Thus, increasing radiation dose to the intra-prostatic GTV may offer the ideal solution of limiting rectal dose while delivering a curative tumor dose. The feasibility of this treatment strategy was demonstrated in a dosimetric study of eight patients with prostate cancer (31). The intra-prostatic GTV as outlined with ¹⁸F Choline PET-CT, a cell proliferation marker with intense accumulation in prostatic cancer cell, was treated up to 90 Gy without exceeding the dose constraints to the bladder and rectum with the IMRT technique. Other dosimetric studies corroborated the feasibility of PET-based GTV dose escalation up to 100 Gy with IGRT for patients with prostate cancer (32, 33). The potential of MRS for potential intra-prostatic GTV dose escalation with IMRT was highlighted in one dosimetric study where the prostate was treated to 70 Gy at 1.8 Gy/fraction while the GTV was treated to 90 Gy at 2.25 Gy (34). Compared to an IMRT plan that conventionally treated the prostate to 70 Gy, the rectal dose was 40 and 48 Gy for the GTV dose escalation plan and conventional plan respectively. Thus, using MRS for potential GTV boost allows for a higher radiobiologic dose to the tumor while decreasing radiation dose to the rectum.

The safety of intra-prostatic GTV dose escalation was illustrated in a clinical study of 118 patients with intra-prostatic GTV defined either on MRI or MRS (35). The GTV and PTV were treated to 81–82 and 78 Gy, respectively with IMRT. No patient developed grade 3–4 gastrointestinal toxicity. **Figure 3** illustrates the potential of MRS for GTV boost in a patient with prostate adenocarcinoma treated with radical prostatectomy (36). The patient had two intra-prostatic nodules suggestive of malignancy on pre-operative MRS and confirmed pathologically after surgery. These two GTV could have been treated to a high radiation dose to improve local control while sparing the rectum if the patient had definitive irradiation instead of surgery. In fact, this patient may be a good candidate for high dose rate prostate brachytherapy as these two foci can be treated to a higher dose by increasing the dwell time of the radioactive source (37). Preliminary clinical study of PET-based intra-prostatic GTV dose escalation with IGRT has been very promising because of minimal toxicity (38). As ¹⁸F-choline PET-CT may not be available in most centers, MRS-based GTV may be a practical method for IGRT dose escalation of prostate cancer. MRS may also play a significant role in the future because of its ability to detect recurrence following external beam prostate irradiation and for possible salvage (39).

LIMITATIONS OF MAGNETIC RESONANCE SPECTROSCOPY

Multiple factors can potentially limit MRS. Inhomogeneities in the magnetic field can cause peak overlap and poor quantification. This can be limited if the magnetic field is shimmed prior to the MRS study, which helps to correct for magnetic field inhomogeneities. Susceptibility artifact can degrade the study if the area of interest is in a part of the brain close to bone or air, such as in the paranasal sinuses. Iron and other minerals built up in the

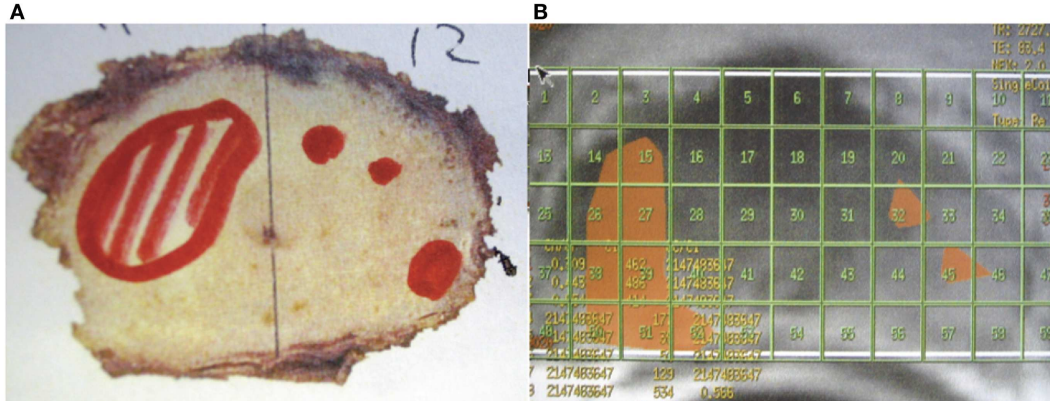


FIGURE 3 | This patient had a radical prostatectomy demonstrating two intra-prostatic adenocarcinoma in the pre-operative magnetic resonance spectroscopy areas suspicious for malignancy. These two gross tumor volumes could have been treated to a higher radiation dose (81 Gy) while the prostate received only 78 Gy with the image-guided radiotherapy technique, thus improving the chance for local control and decreasing the risk of

long-term rectal damage. **(A)** The areas outlined in red showed the cancerous tissue in the right and left lobe in the prostate. **(B)** The areas outlined in orange had an abnormal CCr (choline+creatinine/citrate) ratio suspicious for malignancy on pre-operative magnetic resonance spectroscopy. (Images courtesy of Dr. Shigeo Horie, Teikyo University, and Dr. John G. Delinasios, International Institute of Anticancer Research.)

paranasal ganglia can also cause susceptibility artifact that causes distortion. In a similar fashion, if the spectrum is obtained in an area of the brain close to the scalp, scalp lipids can degrade the spectrum. Each box in an MRS exam called a voxel, is limited in spatial selectivity, and when using multivoxel MRS technique, there is a certain degree of overlap within each voxel from the adjacent voxels. In general, spatial resolution is also limited due to a low signal to noise ratio.

CONCLUSION

Functional imaging with MRS may allow radiation dose escalation with IGRT for GBM and prostate carcinoma while sparing the adjacent normal organs. MRS should be integrated in future prospective studies to assess its potential to reduce long-term complications and possibly improving local control in patients with GBM and prostate cancers.

REFERENCES

- Huang J, Wang AM, Shetty A, Maitz AH, Yan D, Doyle D, et al. Differentiation between intra-axial metastatic tumor progression and radiation injury following fractionated radiation therapy or stereotactic radiosurgery using MR spectroscopy, perfusion MR imaging or volume progression modeling. *Magn Reson Imag* (2011) **29**:993–1001. doi:10.1016/j.mri.2011.04.004
- Elias AE, Carlos RC, Smith EA, Frechting D, George B, Maly P, et al. MR spectroscopy using normalized and non-normalized metabolite ratios for differentiating recurrent brain tumor from radiation injury. *Acad Radiol* (2011) **18**:1101–8. doi:10.1016/j.acra.2011.05.006
- Costello LC, Franklin RB. Concepts of citrate production and secretion by prostate: hormonal relationships in normal and neoplastic prostate. *Prostate* (1991) **19**:181–205. doi:10.1002/pros.2990190302
- Brames R, Zaider M, Zakian KL, Koutcher JA, Shukla-Dave A, Reuter VE, et al. Regarding the focal treatment of prostate cancer: inference of the Gleason grade from magnetic resonance spectroscopic imaging. *Int J Radiat Oncol Biol Phys* (2009) **74**:110–4. doi:10.1016/j.ijrobp.2008.07.055
- Kobus T, Vos PC, Hambrick T, De Rooj M, Hulsbergen-Van de Kaa CA, Barantsz JO, et al. Prostate cancer aggressiveness: in vivo assessment of MR spectroscopy and diffusion-weighted imaging at 3T. *Radiology* (2012) **265**:457–67. doi:10.1148/radiol.12111744
- Creange G, Parfait S, Liegard M, Maingon P, Ben Salem D, Cochet A, et al. Tumor volume and metabolism of prostate cancer determined by proton magnetic resonance spectroscopic imaging at 3T without endorectal coil reveal potential clinical implications in the context of radiation oncology. *Int J Radiat Oncol Biol Phys* (2011) **80**:1087–94. doi:10.1016/j.ijrobp.2010.03.007
- Shukla-Dave A, Hricak H, Ishill NM, Moskowitz CS, Drobniak M, Reuter VE, et al. Correlation of MR imaging and MR spectroscopic imaging findings with Ki-67, phospho-AKT, and androgen receptor expression in prostate cancer. *Radiology* (2009) **250**:803–12. doi:10.1148/radiol.2503080473
- Villeirs GM, de Meerleer GO, de Visschere PJ, Fonteyne VH, Verbaey AC, Oosterlinck W. Combined magnetic resonance imaging and spectroscopy in the assessment of high grade prostate carcinoma in patients with elevated PSA: a single institution experience of 356 patients. *Int J Radiat Oncol Biol Phys* (2009) **77**:340–5. doi:10.1016/j.ejrad.2009.08.007
- Panebianco V, Sciarra A, Ciccarello M, Lisi D, Bernardo S, Cattarino S, et al. Role of magnetic resonance spectroscopic imaging ($[^1\text{H}]$ MRSI) and dynamic contrast-enhanced MRI (DCE-MRI) in identifying prostate cancer foci in patients with negative biopsy and high levels of prostate specific antigens. *Radiol Med* (2010) **115**:1314–29. doi:10.1007/s11547-010-0575-3
- Menard C, Smith ICP, Somorjai RL, Leboldus L, Patel R, Littman C, et al. Magnetic resonance spectroscopy of the malignant prostate gland after radiotherapy: a histopathologic study of diagnostic validity. *Int J Radiat Oncol Biol Phys* (2001) **50**:317–23. doi:10.1016/S0360-3016(01)01480-8
- Pucar D, Shukla D, Hricak H, Moskowitz CS, Kuroiwa K, Olgac S, et al. Prostate cancer: correlation of MR imaging and MR spectroscopy with pathologic findings after radiation therapy-initial experience. *Radiology* (2005) **236**:545–53. doi:10.1148/radiol.2362040739
- Valentini AL, Gui B, d'Agostino GR, Mattiuci G, Clementi V, di Molfetta IV, et al. Locally advanced prostate cancer: three-dimensional magnetic resonance spectroscopy to monitor prostate response to radiotherapy. *Int J Radiat Biol Phys* (2011) **84**:719–24. doi:10.1016/j.ijrobp.2011.12.089
- Westphalen AC, Coakley FV, Roach M, McCulloch CE, Kurhanewicz J. Locally recurrent prostate cancer after external beam radiation therapy. *Radiology* (2010) **256**:485–92. doi:10.1148/radiol.10092314
- Arrayeh E, Westphalen AC, Kurhanewicz J, Roach M, Jung AJ, Carrrol PR, et al. Does local recurrence of prostate cancer after radiation therapy occur at the site of the primary tumor? Results of a longitudinal MRI and MRS study. *Int J Radiat Oncol Biol Phys* (2011) **82**:e787–93. doi:10.1016/j.ijrobp.2011.11.030
- Kuban DA, Tucker SL, Dong L, Stark-Schall G, Huang EH, Cheung MR, et al. Long-term results of the M.D.Anderson randomized dose-escalation trial for

- prostate cancer. *Int J Radiat Oncol Biol Phys* (2008) **70**:67–74. doi:10.1016/j.ijrobp.2007.06.054
16. Gupta T, Agarwall J, Jain S, Phurailatpam R, Kannan S, Ghosh-Laskar S, et al. Three-dimensional conformal radiotherapy (3D-CRT) versus intensity-modulated radiotherapy (IMRT) in squamous cell carcinoma of the head and neck: a randomized controlled trial. *Radiother Oncol* (2012) **104**:343–8. doi:10.1016/j.radonc.2012.07.001
 17. Louvel G, Cazoulat G, Chazon E, Le Maitre A, Simon A, Henry O, et al. Image-guided and adaptive radiotherapy. *Cancer Radiother* (2012) **16**:423–9. doi:10.1016/j.canrad.2012.07.177
 18. Leclerc M, Maingon P, Hamoir P, Dalban C, Calais G, Nuyts S, et al. A dose escalation study with intensity modulated radiotherapy (IMRT) in T2N0, T2N1, T3N0 squamous cell carcinomas (SCC) of the oropharynx, larynx and hypopharynx using a simultaneous integrated boost (SIB) approach. *Radiother Oncol* (2013) **106**:333–40. doi:10.1016/j.radonc.2013.03.002
 19. Souhami L, Seiferheld W, Brachman D, Podgorsack EB, Werner-Wasik M, Lustig R, et al. Randomized comparison of stereotactic radiosurgery with Carmustine for patients with glioblastoma multiforme: report of radiation therapy oncology group 93-05 protocol. *Int J Radiat Oncol Biol Phys* (2004) **60**:856–60. doi:10.1016/j.ijrobp.2004.04.011
 20. Gao X, McDonald JT, Hlatky L, Enderling H. Acute and fractionated irradiation differentially modulate glioma stem cell division kinetics. *Cancer Res* (2013) **73**:1481–90. doi:10.1158/0008-5472.CAN-12-3429
 21. Narayana A, Chang J, Thakur S, Huang W, Karimi S, Hou B, et al. Use of MR spectroscopy and functional imaging in the treatment of glioma. *Br J Radiol* (2007) **80**:347–54. doi:10.1259/bjr/65349468
 22. Einstein DB, Wessels B, Bangert B, Fu P, Nelson AD, Cohen M, et al. Phase II trial of radiosurgery to magnetic resonance spectroscopy-defined high risk tumor volumes in patients with glioblastoma multiforme. *Int J Radiat Oncol Biol Phys* (2012) **84**:668–74. doi:10.1016/j.ijrobp.2012.01.020
 23. Stupp R, Hegi ME, Mason WP, van den Bent MJ, Taphoom MJ, Janger RC, et al. Effect of radiotherapy with concomitant and adjuvant temozolamide versus radiotherapy alone on survival in glioblastoma in a randomized phase III study: 5-year analysis of the EORTC-NCIC trial. *Lancet Oncol* (2009) **10**:459–66. doi:10.1016/S1470-2045(09)70025-7
 24. Tsien CI, Brown D, Normolle D, Schipper M, Piert M, Junck L, et al. Concurrent temozolamide and dose-escalated intensity-modulated radiation therapy in newly diagnosed glioblastoma. *Clin Cancer Res* (2012) **18**:273–9. doi:10.1158/1078-0432.CCR-11-2073
 25. Lipani JD, Jackson PS, Soltys SG, Sato K, Adler JR. Survival following Cyberknife radiosurgery and hypofractionated radiotherapy for newly diagnosed glioblastoma multiforme. *Technol Cancer Res Treat* (2008) **7**:249–55.
 26. Sato K, Baba Y, Inoue M, Omori R. Radiation necrosis and brain edema associated with cyberknife treatment. *Acta Neurochir Suppl* (2003) **86**:513–6.
 27. Yoshikawa K, Saito K, Kajiwara K, Nomura S, Ishihara H, Suzuki M. Cyberknife stereotactic radiotherapy for patients with malignant glioma. *Min Invasive Neurosurg* (2006) **49**:110–5. doi:10.1055/s-2006-932183
 28. Gill S, Thomas J, Fox C, Kron T, Rolfo A, Leahy M, et al. Acute toxicity in prostate cancer patients treated with and without image-guided radiotherapy. *Radiat Oncol* (2011) **6**:145. doi:10.1186/1748-717X-6-145
 29. Singh J, Greer PB, White MA, Parker J, Patterson JP, Tang CI, et al. Treatment-related morbidity in prostate cancer: a comparison of 3-dimensional conformal radiotherapy with and without image guidance using implanted fiducial markers. *Int J Radiat Oncol Biol Phys* (2012) **85**:1018–23. doi:10.1016/j.ijrobp.2012.07.2376
 30. Hamstra DA, Stenmark MH, Ritter T, Litzenberg D, Jackson W, Johnson S, et al. Age and comorbid illness are associated with late rectal toxicity following dose-escalated radiation therapy for prostate cancer. *Int J Radiat Oncol Biol Phys* (2013) **85**:1246–53. doi:10.1016/j.ijrobp.2012.10.042
 31. Chang JH, Joon DL, Lee ST, Gong SV, Anderson NJ, Scott AM, et al. Intensity modulated radiation dose painting for localized prostate cancer using ¹¹C choline positron emission tomography plan. *Int J Radiat Oncol Biol Phys* (2012) **83**:e691–6. doi:10.1016/j.ijrobp.2012.01.087
 32. Hardcastle N, Tome WA. Risk-adaptive volumetric modulated arc therapy using biologic objective functions for subvolume boosting in radiotherapy. *Comput Math Methods Med* (2012) **2012**:348471. doi:10.1155/2012/348471
 33. Maggio A, Fiorino C, Mangili P, Cozzarini C, de Cobelli F, Cattaneo GM, et al. Feasibility of safe ultra-high (EQD2>100 Gy) dose escalation on dominant intra-prostatic lesions by helical tomotherapy. *Acta Oncol* (2011) **50**:25–34. doi:10.3109/0284186X.2010.530688
 34. Pickett B, Vigneaut E, Kurhanewicz J, Verhey L, Roach M. Static field intensity modulation to treat a dominant intra-prostatic lesion to 90 Gy compared to seven fields 3-dimensional radiotherapy. *Int J Radiat Oncol Biol Phys* (1999) **43**:921–9. doi:10.1016/S0360-3016(98)00502-1
 35. Fonteyne V, Villeirs G, Speelers B, de Neve W, de Wagter C, Lumen N, et al. Intensity-modulated radiotherapy as primary therapy for prostate cancer: report on acute toxicity after dose escalation with simultaneous integrated boost to intraprostatic lesion. *Int J Radiat Oncol Biol Phys* (2008) **72**:799–807. doi:10.1016/j.ijrobp.2008.01.040
 36. Saito K, Kaminaga T, Muto S, Ide H. Clinical efficacy of proton magnetic resonance spectroscopy (¹H-MRS) in the diagnosis of prostate cancer. *Anticancer Res* (2008) **28**:1899–904.
 37. Kazi A, Godwin G, Simpson J, Sasso G. MRS-guided HDR brachytherapy boost to the dominant intraprostatic lesion in high risk localized prostate cancer. *BMC Cancer* (2010) **10**:472. doi:10.1186/1471-2407-10-472
 38. Pinkawa M, Piroth MD, Holy R, Klotz J, Djukic V, Corral NE, et al. Dose-escalation using intensity-modulated radiotherapy for prostate cancer—evaluation of quality of life with and without (¹⁸F)-choline PET-CT detected simultaneous integrated boost. *Radiat Oncol* (2012) **7**:14. doi:10.1186/1748-717X-7-14
 39. Hsu CC, Hsu H, Pickett B, Crehange G, Hsu IG, Dea R, et al. Feasibility of MRI imaging/MR-spectroscopy-planned focal partial salvage permanent prostate implant (PPI) for localized recurrence after initial PPI for prostate cancer. *Int J Radiat Oncol Biol Phys* (2012) **85**:370–7. doi:10.1016/j.ijrobp.2012.04.028

Conflict of Interest Statement: The authors declare that the research was conducted in the absence of any commercial or financial relationships that could be construed as a potential conflict of interest.

Received: 10 October 2013; accepted: 14 April 2014; published online: 05 May 2014.

Citation: Nguyen ML, Willows B, Khan R, Chi A, Kim L, Nour SG, Sroka T, Kerr C, Godinez J, Mills M, Karlsson U, Altdorfer G, Nguyen NP, Jendrasik G and The International Geriatric Radiotherapy Group (2014) The potential role of magnetic resonance spectroscopy in image-guided radiotherapy. Front. Oncol. 4:91. doi:10.3389/fonc.2014.00091

*This article was submitted to Radiation Oncology, a section of the journal *Frontiers in Oncology*.*

Copyright © 2014 Nguyen, Willows, Khan, Chi, Kim, Nour, Sroka, Kerr, Godinez, Mills, Karlsson, Altdorfer, Nguyen, Jendrasik and The International Geriatric Radiotherapy Group. This is an open-access article distributed under the terms of the Creative Commons Attribution License (CC BY). The use, distribution or reproduction in other forums is permitted, provided the original author(s) or licensor are credited and that the original publication in this journal is cited, in accordance with accepted academic practice. No use, distribution or reproduction is permitted which does not comply with these terms.



Potential applications of imaging and image-guided radiotherapy for brain metastases and glioblastoma to improve patient quality of life

Nam P. Nguyen^{1*}, Mai L. Nguyen², Jacqueline Vock³, Claire Lemanski⁴, Christine Kerr⁴, Vincent Vinh-Hung⁵, Alexander Chi⁶, Rihan Khan⁷, William Woods⁸, Gabor Altdorfer⁹, Mark D'Andrea¹⁰, Ulf Karlsson¹¹, Russ Hamilton¹ and Fred Ampil¹²

¹ Department of Radiation Oncology, The University of Arizona, Tucson, AZ, USA

² Department of Psychology, Stanford University, Palo Alto, CA, USA

³ Department of Radiation Oncology, Lindenhoftspital, Bern, Switzerland

⁴ Department of Radiation Oncology, Centre Val d'Aurelle, Montpellier, France

⁵ Department of Radiation Oncology, University Hospitals of Geneva, Geneva, Switzerland

⁶ Department of Radiation Oncology, University of West Virginia, Morgantown, WV, USA

⁷ Department of Radiology, The University of Arizona, Tucson, AZ, USA

⁸ Department of Radiation Oncology, Richard A. Henson Cancer Institute, Salisbury, MD, USA

⁹ Department of Radiation Oncology, Camden Clark Cancer Center, Parkersburg, WV, USA

¹⁰ Department of Radiation Oncology, Southeast Treatment Center, Houston, TX, USA

¹¹ Department of Radiation Oncology, Marshfield Clinic, Marshfield, WI, USA

¹² Department of Radiation Oncology, Louisiana State University, Shreveport, LA, USA

Edited by:

Felipe A. Calvo, Hospital General Universitario Gregorio Marañón, Spain

Reviewed by:

Anuja Jhingran, MD Anderson Cancer Center, USA

Kara Leonard, Rhode Island Hospital, USA

*Correspondence:

Nam P. Nguyen, Department of Radiation Oncology, The University of Arizona, 1501 N. Campbell Avenue, Tucson, AZ 85724-5081, USA
e-mail: namphong.nguyen@yahoo.com

Treatment of glioblastoma multiforme (GBM) and brain metastasis remains a challenge because of the poor survival and the potential for brain damage following radiation. Despite concurrent chemotherapy and radiation dose escalation, local recurrence remains the predominant pattern of failure in GBM most likely secondary to repopulation of cancer stem cells. Even though radiotherapy is highly effective for local control of radio-resistant tumors such as melanoma and renal cell cancer, systemic disease progression is the cause of death in most patients with brain metastasis. Preservation of quality of life (QOL) of cancer survivors is the main issue for patients with brain metastasis. Image-guided radiotherapy (IGRT) by virtue of precise radiation dose delivery may reduce treatment time of patients with GBM without excessive toxicity and potentially improve neurocognitive function with preservation of local control in patients with brain metastasis. Future prospective trials for primary brain tumors or brain metastasis should include IGRT to assess its efficacy to improve patient QOL.

Keywords: glioblastoma, brain metastases, image-guided radiotherapy, neurotoxicity

INTRODUCTION

Treatment of glioblastoma multiforme (GBM) and brain metastasis remains a challenge because the poor survival and potential for brain damage. Despite the fact that GBM is a primary glioma and brain metastasis represents dissemination to the brain of solid malignant tumors, median survival for both conditions remains similar because of the lack of treatment efficacy. Prognosis factors for both GBM and brain metastasis are age and performance status based on the recursive partitioning analysis (1, 2). Thus, given the remote chance for long-term survival, the goal of treatment should be the improvement of quality of life (QOL) for GBM and brain metastasis patients. New radiotherapy techniques such as image-guided radiotherapy (IGRT) provides the clinician with an unique opportunity to shorten the length of treatment without increasing treatment toxicity by virtue of normal tissue sparing. Magnetic resonance imaging (MRI) is now integrated into of radiotherapy planning to improve treatment accuracy. New imaging modalities such as positron emission tomography (PET) and diffusion tensor imaging (DTI) may also accurately

delineate the gross tumor volume (GTV) and the areas of radiation brain damage respectively, and complement MRI to decrease normal tissue toxicity. In the following sections, we will review the literature to determine how to best combine new diagnostic technology with advanced radiation treatment to improve patient QOL.

TREATMENT OF GLIOBLASTOMA

Standard treatment for GBM is surgical resection if feasible followed by concurrent chemotherapy with temozolomide (TMZ) and radiation (3). Despite the addition of TMZ, only 9.8% of the patients survived at 5 years. The predominant pattern of recurrence is local failure suggesting that improving local control may improve survival. Many institutions have attempted to increase radiation dose to the tumor bed for better local control. However, a randomized study using radiosurgery as a boost dose to the tumor bed prior to chemoradiation did not demonstrate any improvement of survival. Two hundred and three patients with supratentorial GBM were randomized between carmustine

(BCNU) and standard radiation to 60 Gy or radiosurgery boost followed by standard radiation. Local failures occurred in 90% for both groups causing patient death (4). These clinical results suggest that GBM is both chemo- and radio-resistant. Recent studies in molecular biology have demonstrated the existence of cancer stem cells (CSCs) in GBM responsible for treatment failure. Despite high doses of radiation of 30–60 Gy in a single fraction, these CSCs continued to proliferate in cell cultures following radiation (5). The radio-resistance of GBM cells suggests that radiation dose escalation alone is not feasible to control tumor growth in the clinical setting because of the excessive neurotoxicity associated with such a high dose. The mechanism of chemo-resistance of CSCs is complex but one of the principal mechanisms is the presence of transporters that actively pump the drugs out of the cells preventing their tumoricidal actions (6). Thus, unless new therapies are directed toward the control of CSCs, conventional postoperative chemotherapy and radiation is doomed to fail. A reasonable alternative to the standard fractionation schedule would be shortening the course of radiotherapy which may allow the patient to spend quality time with their family provided that the accelerated course does not increase toxicity. A randomized trial of TMZ versus standard radiotherapy versus hypo-fractionated radiotherapy in elderly patients showed a better survival in patients above 70 years treated by hypo-fractionated radiotherapy or TMZ as compared to standard radiotherapy (7).

TREATMENT OF BRAIN METASTASES

Even though the optimal treatment for brain metastasis remains controversial, radiation therapy is very effective to prevent disease progression even for radio-resistant tumors such as renal cell cancer and melanoma. The delivery of a very high radiation dose with radiosurgery provides excellent local control (8). However, when there are multiple metastases or when there is evidence of tumor progression after radiosurgery, whole brain radiotherapy (WBRT) is required. In patients who had tumor regression following whole brain irradiation, neurocognitive function, and survival improve suggesting that local control of the tumor in the brain remains the most important factor to prevent deterioration of mental status (9). Even though ultimately all patients experienced deterioration of their neurocognitive function following radiosurgery alone or radiosurgery with WBRT, improvement of local control with the addition of WBRT delayed the time to deterioration emphasizing the importance of local control on mental status (10). There are still controversies whether WBRT should be added to radiosurgery for brain metastasis at initial diagnosis. In one study, the poor survival observed with WBRT and radiosurgery compared to radiosurgery alone is most likely due to the delay to initiate chemotherapy in patients who received WBRT (11). Most of the patients treated for brain metastasis ultimately died from systemic disease progression emphasizing the fact that while local control remains important, chemotherapy remains the main treatment and should not be delayed unnecessarily (12). Thus, future studies should focus on decreasing the overall treatment time and the neurotoxicity of WBRT while optimizing local control of brain metastases.

RADIATION-INDUCED NEUROTOXICITY

Animal experiments demonstrate normal brain injury following WBRT. Adult rats exposed to single fraction whole brain irradiation to 25 Gy developed decreased cognitive function compared to sham-irradiated rats (13). Autopsy of the irradiated rat brains revealed demyelination with or without necrosis mainly in the corpus callosum. Increased gliosis was also observed similar to the one reported in human brains affected by accelerated aging such as Alzheimer's disease and multiple sclerosis. Damage to the normal brain is dose-dependent as adults rats exposed to whole brain fractionated irradiation to 30 Gy in 10 fractions developed memory loss without observed microscopic damage (14). The mechanism of brain injury at the molecular level is complex and is postulated secondary to depletion of oligodendrocytes leading to demyelination, deletion of neural stem cells (NSCs) in the hippocampus, cerebral cortex, vascular injury, and more recently vasculitis (15, 16). The use of MRI-based techniques such as DTI allows for monitoring of human brain damage following irradiation. DTI measures water molecule diffusion in the brain which varies with the direction, density, and myelination of white matter fibers. Diffusion of water perpendicular and parallel to white fibers is termed radial diffusivity (RD) and axial diffusivity (AD) respectively. Increased RD and decreased AD has been correlated to decreased myelination and increased gliosis respectively. Using DTI prior to and 1 month post WBRT in 14 patients with brain metastases, increased RD was observed in all brain structures but more prominent in the cingula and fornix suggesting demyelination of the limbic structures responsible for memory and behavior (17). Radiation-induced demyelination of the white matter tract was also corroborated in another study also showing a heterogeneous extent of injury despite a uniform radiation dose suggesting that some white matter tracts are more sensitive than others (18). An autopsy case report of a patient dying following radiation myopathy also demonstrated extensive demyelination and axonal loss without vascular damage corroborating the DTI report (19). In addition, WBRT or partial brain irradiation damages the NSCs which usually remain dormant within the subventricular zone. Following a moderate radiation dose of 4 Gy, NSCs start to proliferate exposing them to death from apoptosis with higher radiation doses (20, 21). Animal experiments demonstrated a direct relationship between radiation damage to NSCs and neurocognitive dysfunction. Rats receiving WBRT developed cognitive dysfunction but if they were transplanted with NSCs in the hippocampus after radiation, the ones who received NSCs recovered their cognitive function compared to the ones who had sham surgery (22). The transplanted NSCs migrated extensively and differentiated into glial and neuronal lineages of the rat brain even though they were from human species suggesting that 1 day, human NSC transplants may be used to treat neurocognitive damage following brain irradiation (22). In another mouse model delivering a high radiation dose to the whole brain (20 Gy in 4 Gy/fraction) similar to the clinical whole brain treatment, the mice developed short term memory loss associated with decreased granular layer of the dentate gyrus of the hippocampus. However, if the irradiated mice received NSCs administered intravenously following each radiation treatment, they preserved both

brain structure and function (23). Autopsy of patients who had WBRT also demonstrated depletion of neuronal cells in the hippocampus (24). Thus, protecting the limbic system from excessive radiation may reduce neurocognitive damage following WBRT.

CURRENT IMPACT OF MRI ON RADIOTHERAPY TREATMENT PLANNING

Because of the non-ionizing technique that uses a strong magnetic field to provide high resolution anatomic information, MRI is now integrated into the radiotherapy planning for brain tumors. The accuracy of MRI to demonstrate tumor invasion of the normal organs has led to the development of MRI-based linear accelerators. Institutional preference dictates the choice of either T2-weighted MRI or FLAIR MRI to outline the GTV and surrounding edema as CTV. Traditionally T2-weighted MRI has been used as GTV delineation because biopsy of the area of MRI T2 abnormality demonstrated tumor cells outside of contrast enhanced CT abnormality. However, T2 weighting causes cranial spinal fluid (CSF) to be brighter which may potentially impair visualization of the GTV. The FLAIR sequence nullifies the CSF signal and may provide better GTV delineation. An expansion of 2 cm of the CTV is used to outline PTV. The FLAIR PTV is usually larger than the T2 PTV and may potentially increase normal tissue toxicity (25). On the other hand FLAIR images provides better tumor-to-CSF contrast compared to T2 and T1 weighted sequences and may be valuable for stereotactic planning of brain gliomas and metastases (26). Thus, incorporating FLAIR sequence into radiotherapy planning may potentially improve tumor targeting for radiation dose escalation.

The introduction of higher field strength MRI (3.0 T) (3T MRI) compared to the conventional 1.5 T (1.5T MRI) may potentially increase radiotherapy delivery accuracy because of higher image resolution. In a study of 138 patients with brain metastases, 22% were found to have a higher number of metastases with 3 T MRI compared to 1.5 T MRI. All patients were treated with radiosurgery with the radiotherapy planning based on 3 T MRI and would have had geographic miss if 1.5 T MRI was used for treatment planning (27). Patients with multiple brain metastases are more likely to have additional lesions seen on 3 T MRI (28). The superiority of 3 T MRI for radiosurgery planning compared to 1.5 T MRI was also corroborated in another study (29). Thus, even though these studies are only preliminary, 3 T MRI may have an increasing importance in the future for radiotherapy planning.

POTENTIAL ROLE OF O-(2-[¹⁸F]-FLUOROETHYL-L-TYROSINE POSITRON EMISSION TOMOGRAPHY IN RADIOTHERAPY PLANNING AND TREATMENT OF GBM

Accurate tumor delineation is the first step in radiotherapy planning to avoid marginal miss and to decrease excessive radiation dose to the critical structures adjacent to the tumor. Standard imaging for neurologic oncology has been MRI with gadolinium contrast. The extent of contrast enhancement on MRI is used to determine the GTV or as an indicator of therapeutic response. However, contrast enhancement due to the transient blood brain barrier breakdown following surgery, may mimic tumor progression and interfere with the GTV delineation. O-(2-[¹⁸F]-fluoroethyl-L-tyrosine (FET) is an amino acid analog

radiolabeled with fluorine 18. After crossing the blood brain barrier, FET is taken by LAT2 transporters located on the membranes of the GBM cells. Thus, high uptake of FET by the tumor cells allows for better visualization of the tumor compared to the normal brain. The advantages of FET include its long half-life (110 min), its ease for synthesis, its fast brain and tumor uptake kinetics, and low accumulation in non-tumor tissues making this radiotracer an ideal imaging technique in the outpatient setting (30). Because the tumor uptake of FET is independent of blood brain barrier disruption, FET-PET may be complementary to MRI to outline the exact extension of the tumor and serve as functional imaging for IGRT. In a study of 17 patients with biopsy proven GBM, FET-PET was compared to MRI for GTV delineation. The GTV based on FET-PET was larger in 10 patients, smaller in three, and the same in the remaining four (31). Perhaps, the major advantage of FET-PET over conventional MRI for radiotherapy planning is its ability to detect areas of high tumor activity within the GTV which manifest as a high standard uptake value (SUV) (32). These high SUV areas can be targeted with a higher radiation dose compared to the dose delivered to the GTV, thus potentially increasing tumor control without increasing radiation dose to the normal brain tissue. The main weaknesses of the clinical studies which failed to demonstrate a survival benefit for dose escalation in GBM are their reliance on MRI for target delineation and the radiotherapy technique employed which delivered a uniform dose across the GTV. The tumor concentration within the GTV is heterogeneous and areas with high concentration of actively dividing tumor cells may have residual tumor cells after radiation. On the other hand, increasing tumor dose to improve local control may lead to severe complications because of excessive irradiation of the adjacent normal brain tissue. Thus, a radiation technique that allows radiation dose escalation within the tumor without increasing the dose to the normal brain would be ideal. Integrating FET-PET into IGRT planning may be a solution to avoid neurotoxicity. As an illustration, the dosimetric advantage of IGRT with the simultaneous integrated boost (SIB) technique to spare the normal brain compared to the conventional sequential (SEQ) boost technique for primary brain tumors was reported recently (33). Other advantages of FET-PET are its better accuracy compared to MRI allowing better local control because of decreased risk of marginal miss and better ability to detect tumor after radiation (31, 34). FET-PET will likely play a prominent role in future IGRT studies for brain tumors.

TECHNOLOGIES OF IGRT DELIVERY

There are currently two systems for IGRT delivery which are grouped into radiation-based (kV and MV) and non-radiation based (ultrasound, electromagnetic) (35). Visualization of the tumor is either direct or through fiducial markers inserted into the tumor. The images acquired before the treatment are then compared to the ones acquired during radiotherapy planning. A shift in patient position is performed if there is any discrepancy in the set up and another set of images is obtained to verify treatment accuracy. Thus, daily imaging minimizes the risk for marginal miss due to positioning and patient movement during treatment. It is unclear which imaging modality is optimal for IGRT delivery. The choice of the IGRT technology most likely depends on clinician

preference, the types of tumors most commonly treated at the radiation oncology institution, and budget constraints.

In the radiation based system, the image acquired prior to treatment are either 2-dimensional (2D) or 3-dimensional (3D). The quality of image is superior with kV imaging compared to MV imaging. Image acquisition in the 2D system relies on electronic portal imaging devices (EPIDs) where the treatment beam is captured on a flat panel behind the patient (Clinac, Elekta Oncology Primus) and stereotactic imaging. The stereotactic imaging relies on two kV X-ray sources mounted on ceiling or floor which provides orthogonal images and real time imaging (CyberKnife, Novalis TX, BrainLab). Even though the image quality is excellent, stereotactic imaging relies on bony landmarks or surrogate markers and does not provide soft tissue information. The kVCT (fan beam) imaging uses a diagnostic CT scan along side the linear accelerator (CT on rails, Siemens Medical Systems; ExaCT, Varian Medical Systems). Soft tissue information is excellent with the kVCT fan beam but the couch needs to be displaced between imaging and treatment which may lead to positioning error. The kVCT (cone beam) uses a gantry mounted kV source and a flat panel detector. A series of kV X-rays are taken when the gantry rotates and a 3D image is reconstructed. Even though the soft tissue special resolution is good, the image quality is inferior to fan beam kV CT (Synergy, Elekta; On Board Imager, Varian Medical Systems; Artiste, Siemens Medical Systems). In the MV CT fan beam system, the imaging is performed by the treatment beam which rotates around the patient while the couch moves (Helical Tomotherapy). There is no metal artifacts but the image quality is inferior to kV CT.

In the non-radiation based system, an ultrasound is performed before the treatment for target localization (usually prostate). The system is simple, non-invasive, inexpensive but operator dependent (Varian Medical Systems, B Mode Acquisition, and Targeting; Nomos, Elekta Oncology). Another non-radiation based system relies on the implantation of electromagnetic transponders inserted in the target (usually prostate) which provides tracking of the tumor motion (Calypso). The last non-radiation based system which is just approved by the US Food and Drug Administration involves a hybrid MRI and Cobalt linear accelerator (ViewRay) may have promising potential for brain tumors because of the imaging quality but needs to be confirmed in future clinical trials.

CLINICAL STUDIES DEMONSTRATING THE POTENTIAL ROLE OF IGRT IN THE TREATMENT OF GBM

The combination of better tumor delineation, daily treatment imaging, and sharp dose gradient makes IGRT an ideal tool for radiotherapy because of the potential for dose escalation and reduced toxicity to the normal brain compared to 3-dimensional conformal radiotherapy (3D-CRT). As most studies failed to demonstrate an improvement in local control and survival in GBM patients with radiation dose escalation because of the tumor radio-resistance, accelerated radiation treatment may provide the patient with a better QOL and more quality time with their loved ones if the shortened treatment is equally effective compared to the conventional fractionation (30 days of radiotherapy). Preliminary studies of intensity-modulated radiotherapy (IMRT) for GBM demonstrated the feasibility of this treatment alternative.

A total of 24 patients with resected GBM received postoperative hypo-fractionated IMRT to the surgical cavity and residual tumor to 60 Gy in 10 fractions (6 Gy/fraction) and concurrent TMZ. The median survival was 16 months comparable to historic control in patients treated with conventional fractionation (36). Other studies also corroborated the efficacy and safety of hypo-fractionated IMRT for GBM (37). Compared to IMRT, IGRT may allow for reduction of the planning target volume because of daily pre-treatment imaging and the accuracy of the technique. Thus, IGRT is particularly useful when the tumor is located close to critical radiosensitive structures such as the optic chiasm, optic nerves, and brain stem. IGRT has been used as a boost dose for these indications to deliver a high dose to the tumor bed without increasing the risk of complications (38). Patients with GBM close to radiosensitive structures can also be treated with IGRT through the whole course of treatment with the SIB technique delivering a higher dose to the tumor (66 Gy instead of 60 Gy) without any complications (39). The course of radiotherapy can also be reduced to three to six treatments with IGRT without excessive toxicity (40). Other studies also corroborated the efficacy and safety of hypo-fractionated IGRT for GBM with fractionation ranging from one to eight treatments (41, 42).

The best illustration of the indication for IGRT in the treatment of GBM may be its role in the re-irradiation of recurrent tumor following standard chemoradiotherapy. Depending on tumor size, a single or multiple fractions may be delivered with IGRT for salvage. The steep dose gradient between the tumor and surrounding tissues decreases the risk of brain necrosis. Median survival following salvage IGRT ranges from 7 to 11 months with or without chemotherapy (43–47). Toxicity of IGRT for re-irradiation remains acceptable. As most IGRT studies for recurrent GBM were based on MRI for tumor delineation, it would be interesting to see if integrating FET-PET into radiotherapy planning would improve local control and survival. A preliminary study PET study using ¹¹C Methionine, a radiolabeled amino acid with a shorter half-life compared to FET, suggests that the median survival of patients with recurrent GBM undergoing molecular imaging for radiotherapy planning is superior to the ones of patients who had conventional MRI (48). Median survival was respectively 9 and 5 months for IGRT with and without biological imaging. The data is intriguing and merits further investigation.

CLINICAL STUDIES DEMONSTRATING THE POTENTIAL ROLE OF IGRT IN THE TREATMENT OF BRAIN METASTASIS

As survival of patients with brain metastasis depends on the control of systemic disease, it would be logical to provide radiotherapy within a short time frame to avoid delay in initiating chemotherapy. Radiosurgery would be one option because treatment would be delivered in one fraction. The caveat of radiosurgery is the high risk of recurrence in the non-treated areas of the brain. Adding WBRT may decrease the risk of recurrence in other areas of the normal brain but may worsen neurocognitive function and delay chemotherapy. The ideal treatment for brain metastases would be a combination of high radiation to the tumor, a reasonable treatment time to allow chemotherapy initiation, and preservation of neurocognitive function if feasible.

Preliminary studies of whole brain IGRT with SIB to the brain metastases have been very encouraging. A phase I study of 48 patients with one to three brain metastases reported no increased toxicity when the whole brain was treated to 30 Gy in 3 Gy/fraction while the brain metastases were treated on a dose escalation schedule ranging from 35 Gy (3.5 Gy/fraction) to 60 Gy (6 Gy/fraction). Only 8 out of 48 patients (14%) developed progressive disease in the brain (49). A later pooled analysis of 120 patients with brain metastasis confirmed the safety of this approach. Seventy patients with one to three brain metastases were treated according to the previous protocol of 30 Gy in 3 Gy/fraction to the whole brain and 50 patients with one to six brain metastases were treated to 20 Gy in 4 Gy/fraction to the whole brain and 40 Gy in 8 Gy/fraction to the brain metastases (50). Twenty-one patients (23%) died from intracranial disease progression. Three patients developed tumor necrosis but there was no death from treatment toxicity. Thus, whole brain IGRT with SIB seemed to achieve good local control for patients with one to six brain metastases within 1–2 weeks of radiotherapy. The absence of toxicity of whole brain IGRT with SIB was also corroborated in another study. Twenty-nine patients with one to four brain metastases were treated to 30 Gy in 3 Gy/fraction to the whole brain and 40 Gy in 4 Gy/fraction to the brain metastases (51). QOL and neurocognitive function were also tested. Three patients (13%) developed local failures. There was no impairment of neurocognitive function but QOL deteriorated 3 months after treatment. The cause of death in all three IGRT whole brain studies were predominantly systemic disease progression emphasizing the need for systemic disease control in patients with brain metastasis.

To protect long-term survivors from neurocognitive dysfunction following WBRT, sparing of the limbic system from excessive radiation should be considered. Technically, it is feasible to spare the hippocampus and NSCs compartment with IGRT without under-dosing the target volume (52, 53). Animal experiments demonstrated the feasibility of NSC sparing IMRT. Mice receiving NSC sparing IMRT developed less damage to the NSC compared to a non-sparing NSC technique (54). Thus, it would be interesting to combine whole brain IGRT with SIB and hippocampus sparing in patients with brain metastases to improve local control and preserve neurocognitive function in future clinical trials.

We emphasize that radiation dose escalation for brain tumors and brain metastasis should not be performed without appropriate image guidance because of the potential for increased neurotoxicity. Preliminary evidence suggests that when combined with advanced tumor imaging such as PET scan, IGRT may provide excellent loco-regional control while sparing normal organs from excessive radiation toxicity in patients with locally advanced head and neck cancer (55, 56). As an illustration, even a small organ such as the cochlea can be shielded from radiation when the gross neck nodes were treated to a curative dose of radiation (70 Gy). This may potentially decrease the risk of hearing loss (57). Similarly, IGRT, when applied intracranially, may potentially maximize normal neuro-tissue sparing, and potentially improves the patient's QOL in patient with primary brain tumors and brain metastasis and needs to be investigated in future prospective studies.

CONCLUSION

Image-guided radiotherapy is a promising technique to reduce treatment time in patients with GBM. In the future FET-PET may further improve treatment accuracy of IGRT and potentially improve local control. In patients with brain metastases, whole brain IGRT with SIB may allow improvement of local control and early initiation of systemic therapy for better survival. Sparing of the hippocampus with whole brain IGRT is intriguing and merits further investigation to preserve neurocognitive function. Prospective studies should be performed to investigate the feasibility of IGRT to improve QOL in patients with GBM or brain metastasis.

REFERENCES

- Gaspar LE, Scott C, Murray K, Curran W. Validation of the RTOG recursive partitioning analysis (RPA) classification for brain metastases. *Int J Radiat Oncol Biol Phys* (1993) **41**:1001–6.
- Curran WJ, Scott CB, Horton J, Nelson JS, Weinstein AS, Fischbach AJ, et al. Recursive partitioning analysis of prognostic factors in three Radiation Therapy Oncology Group malignant glioma trials. *J Natl Cancer Inst* (1993) **85**:704–10. doi:10.1093/jnci/85.9.704
- Stupp R, Heqi ME, Mason WP, van den Bent MJ, Taphoom MJ, Janger RC, et al. Effect of radiotherapy with concomitant and adjuvant temozolomide versus radiotherapy alone on survival in glioblastoma in a randomized phase III study: 5-year analysis of the EORTC-NCIC trial. *Lancet Oncol* (2009) **10**:459–66. doi:10.1016/S1470-2045(09)70025-7
- Souhami L, Seiferheld W, Brachman D, Podgorsack EB, Werner-Wasik M, Lustig R, et al. Randomized comparison of stereotactic radiosurgery with carmustine for patients with glioblastoma multiforme: Report of Radiation Therapy Oncology Group 93-05 protocol. *Int J Radiat Oncol Biol Phys* (2004) **60**:853–60. doi:10.1016/j.ijrobp.2004.04.011
- Sasaki A, Nakajo T, Tsunoda Y, Yamamoto G, Kobayashi Y, Tsuji M, et al. Gene analysis and dynamics of tumor stem cells after radiation. *Hum Cell* (2013) **26**(2):73–9. doi:10.1007/s13577-013-0060-0
- Warrier S, Pavanram P, Raina D, Arvind N. Study of chemoresistant CD 133+ cancer stem cells from human glioblastoma cell line U138MG using multiple assays. *Cell Biol Int* (2012) **36**:1137–43. doi:10.1042/CBI20110539
- Malmstrom A, Gronberg BH, Marosi C, Stupp R, Frappaz D, Schultz H, et al. Temozolomide versus standard week radiotherapy versus hypofractionated radiotherapy in patients older than 60 years with glioblastoma: the Nordic randomised phase 3 trial. *Lancet Oncol* (2012) **13**:916–26. doi:10.1016/S1470-2045(12)70265-6
- Hara W, Tran P, Li G, Su Z, Puataweepong P, Adler JR, et al. CyberKnife for brain metastases of malignant melanoma and renal cell carcinoma. *Neurosurgery* (2009) **64**:A26–32. doi:10.1227/01.NEU.0000339118.55334.EA
- Li J, Bentzen SM, Renschler M, Mehta MP. Regression after whole brain radiation for brain metastases correlates with survival and improved cognitive function. *J Clin Oncol* (2007) **25**:1260–6. doi:10.1200/JCO.2006.09.2536
- Aoyama H, Tago M, Kato N, Toyoda T, Kenjyo M, Hirota S, et al. Neurocognitive function of patients with brain metastasis who received either whole brain radiotherapy plus stereotactic radiosurgery or radiosurgery alone. *Int J Radiat Oncol Biol Phys* (2007) **68**:1388–95. doi:10.1016/j.ijrobp.2007.03.048
- Chang EL, Wefel JS, Hess KS, Allen PK, Lang FF, Kornguth DG, et al. Neurocognition in patients with brain metastases treated with radiosurgery or radiosurgery plus whole brain irradiation: a randomized controlled trial. *Lancet Oncol* (2009) **10**:1037–44. doi:10.1016/S1470-2045(09)70263-3
- Khuntia D, Brown P, Li J, Mehta M. Whole brain radiotherapy in the management of brain metastasis. *J Clin Oncol* (2006) **24**:1295–304. doi:10.1200/JCO.2005.04.6185
- Akiyama K, Tanaka R, Sato M, Takeda N. Cognitive dysfunction and histological finding in adult rats one year after whole brain irradiation. *Neurol Med Chir (Tokyo)* (2001) **41**:590–98. doi:10.2176/nmc.41.590
- Lambroglu I, Chen QM, Boissiere G, Mazeron JJ, Poisson M, Baillet F, et al. Radiation-induced cognitive function: an experimental model in the old rat. *Int J Radiat Oncol Biol Phys* (1995) **31**:65–70. doi:10.3174/ajnr.A2643

15. Greene-Schloesser D, Robbins ME, Pfeiffer AM, Shaw EG, Wheeler KT Chan MD. Radiation-induced brain injury, a review. *Front Oncol* (2012) **2**:73. doi:10.3389/fonc.2012.00073
16. Rauch PJ, Park HS, Knisely JPS, Chiang VL, Vortmeyer AO. Delayed radiation-induced vasculitic leukoencephalopathy. *Int J Radiat Oncol Biol Phys* (2011) **83**:369–75. doi:10.1016/j.ijrobp.2011.06.1982
17. Chapman CH, Nazem-Zadeh M, Lee OE, Schipper MJ, Tsien CI, Lawrence TS, et al. Regional variation in brain white matter diffusion index changes following radiation. *PLoS One* (2013) **8**:e57768. doi:10.1371/journal.pone.0057768
18. Uh J, Merchant TE, Li Y, Feng T, Gajjar A, Ogg RJ, et al. Difference in brain stem fiber tract response to radiation: a longitudinal diffusion tensor imaging study. *Int J Radiat Oncol Biol Phys* (2013) **86**(2):292–7. doi:10.1016/j.ijrobp.2013.01.028
19. Lengyel Z, Reko G, Majtenyi K, Pisch J, Csornai M, Lesznyak J, et al. Autopsy verifies demyelination and lack of vascular damage in partially reversible radiation myopathy. *Spinal Cord* (2003) **41**:577–85. doi:10.1038/sj.sc.3101480
20. Daynac M, Chicheportiche A, Pineda JR, Gauthier LR, Boussin FD, Mouthon MA. Quiescent neural stem cells exit dormancy upon alteration of GABAAR signaling following radiation damage. *Stem Cell Res* (2013) **11**:516–28. doi:10.1016/j.scr.2013.02.008
21. Acharya MM, Lan ML, Kan VH, Patel NH, Giedzinski E. Consequences of ionizing radiation-induced damage in human neural stem cells. *Free Radic Biol Med* (2010) **49**:1846–55. doi:10.1016/j.freeradbiomed.2010.08.021
22. Acharya MM, Christie LA, Lan ML, Giedzinski E, Fike JR, Rosi S, et al. Human neural stem cell transplantation ameliorates radiation-induced cognitive dysfunction. *Cancer Res* (2011) **71**:4834–45. doi:10.1158/0008-5472.CAN-11-0027
23. Joo KM, Jin J, Kang BG, Lee SJ, Kim KH, Yang H, et al. Transdifferentiation of neural stem cells: a therapeutic mechanism against the radiation-induced brain damage. *PLoS One* (2012) **7**:e25936. doi:10.1371/journal.pone.0025936
24. Monge ML, Vogel H, Masek M, Ligon KL, Fisher PG, Palmer TD. Impaired human hippocampal neurogenesis after treatment for central nervous system malignancies. *Ann Neurol* (2007) **62**:515–20. doi:10.1002/ana.21214
25. Stall B, Zach L, Ning H, Ondos J, Arora B, Shankavaram U, et al. Comparison of T2 and FLAIR imaging for target delineation in high grade gliomas. *Radiat Oncol* (2010) **5**:5. doi:10.1186/1748-717X-5-5
26. Essig M, Debus J, Schlemmer HP, Hawighorst H, Wannenmacher M, van Kaick G. Improved tumor contrast and delineation in the stereotactic radiotherapy planning of cerebral gliomas and metastases with contrast media supported FLAIR imaging. *Strahlenther Onkol* (2000) **176**:84–94. doi:10.1007/PL00002333
27. Sacon PA, Shaw EG, Chan MD, Squire SE, Johnson AJ, McMullen KP, et al. Use of 3.0-T MRI for stereotactic radiosurgery planning for treatment of brain metastases: a single institution retrospective review. *Int J Radiat Oncol Biol Phys* (2010) **78**:1142–6. doi:10.1016/j.ijrobp.2010.05.049
28. Loganathan AG, Chan MD, Alphonse N, Peiffer AM, Johnson AJ, McMullen KP, et al. Clinical outcomes of brain metastases treated with gamma knife radiosurgery with 3.0T versus 1.5T MRI-based treatment planning: have we finally optimized detection of occult brain metastases? *J Med Imaging Radiat Oncol* (2012) **56**:554–60. doi:10.1111/j.1754-9485.2012.02429.x
29. MacFadden D, Zhang B, Brock KK, Hodaic M, Laperriere N, Schwartz M, et al. Clinical evaluation of stereotactic target localization using 3-Tesla MRI for radiosurgery planning. *Int J Radiat Oncol Biol Phys* (2010) **76**:1472–79. doi:10.1016/j.ijrobp.2009.03.020
30. Benouach-Amiel A, Lubrano V, Tafani M, Uro-coste E, Gantet P, Sol JC, et al. Evaluation of O-(2-[¹⁸F]-fluoroethyl)-L-tyrosine in the diagnosis of glioblastoma. *Arch Neurol* (2010) **67**:370–2. doi:10.1001/archneurol.2010.22
31. Niyazi M, Geisler J, Sieferl A, Schwarz SB, Ganswindt U, Garry S, et al. FET-PET for malignant glioma treatment planning. *Radiother Oncol* (2011) **99**:44–8. doi:10.1016/j.radonc.2011.03.001
32. Rickhey M, Koelbl O, Eilles C, Bogner L. A biologically adapted dose-escalation approach, demonstrated for ¹⁸F-FET-PET in brain tumors. *Strahlenther Onkol* (2008) **184**:536–42. doi:10.1007/s00066-008-1883-6
33. Baisden JM, Sheehan J, Reish AG, McIntosh AF, Sheng K, Read PW, et al. Helical tomotherapy simultaneous integrated boost provides a dosimetric advantage in the treatment of primary intracranial tumor. *Neurol Res* (2011) **33**:820–4. doi:10.1179/1743132811Y.0000000035
34. Rachinger W, Goetz C, Popperl G, Gildehaus FJ, Kreth FW, Holtmannspotter M, et al. Positron emission tomography with O-(2-[¹⁸F] fluoroethyl)-L-tyrosine versus magnetic resonance imaging in the diagnosis of recurrent gliomas. *Neurosurgery* (2005) **57**:505–11. doi:10.1227/01.NEU.0000171642.49553.B0
35. De Los Santos J, Popple R, Agazaryan N, Bayouth JE, Bissonette JP, Bucci MK, et al. Image-Guided Radiation Therapy (IGRT) technologies for radiation therapy localization and delivery. *Int J Radiat Oncol Biol Phys* (2013) **87**:33–45. doi:10.1016/j.ijrobp.2013.02.021
36. Reddy K, Damek D, Gaspar LE, Ney D, Waziri A, Lillehei K, et al. Phase II trial of hypofractionated IMRT with temozolamide for patients with newly diagnosed glioblastoma multiforme. *Int J Radiat Oncol Biol Phys* (2012) **84**:655–60. doi:10.1016/j.ijrobp.2012.01.035
37. Hingorani M, Colley VP, Dixit S, Beavis AM. Hypofractionated radiotherapy for glioblastoma: strategy for poor risk patients or hope for the future? *Br J Radiol* (2011) **65**:e770–81. doi:10.1259/bjr/83827377
38. Oermann E, Collins BT, Erickson KT, Yu X, Lei S, Suy S, et al. CyberKnife enhanced conventionally fractionated chemoradiation for high grade glioma in close proximity to critical structures. *J Hematol Oncol* (2010) **3**:22. doi:10.1186/1756-8722-3-22
39. Donato V, Caruso C, Bressi C, Pressello MC, Salvati M, Dalitala A, et al. Evaluation of helical tomotherapy in the treatment of high grade gliomas near critical structures. *Tumori* (2012) **98**:636–42. doi:10.1700/1190.13206
40. Sato K, Baba Y, Inoue M, Omori R. Radiation necrosis and brain edema associated with CyberKnife treatment. *Acta Neurochir Suppl* (2003) **86**:513–7.
41. Lipani JD, Jackson PS, Soltys SG, Sato K, Adler JR. Survival following CyberKnife radiosurgery and hypofractionated radiotherapy for newly diagnosed glioblastoma multiforme. *Technol Cancer Res Treat* (2008) **7**:249–55.
42. Yoshikawa K, Saito K, Kajiwara K, Nomura S, Ishihara H, Suzuki M. CyberKnife stereotactic radiotherapy for patients with malignant glioma. *Minim Invasive Neurosurg* (2006) **49**:110–5. doi:10.1055/s-2006-932183
43. Conti A, Pontoriero A, Arpa D, Siragusa C, Tomasello C, Romanelli P, et al. Efficacy and toxicity of CyberKnife re-irradiation and dose-dense temozolomide for recurrent gliomas. *Acta Neurochir* (2012) **154**:203–9. doi:10.1007/s00701-011-1184-1
44. Fogh SE, Andrews DW, Glass J, Curran W, Glass C, Champ C, et al. Hypofractionated stereotactic radiotherapy: an effective therapy for recurrent high grade gliomas. *J Clin Oncol* (2010) **28**:3048–53. doi:10.1200/JCO.2009.25.6941
45. Koga T, Maruyama K, Tanaka M, Ino Y, Saito N, Nakagawa K, et al. Extended field stereotactic radiosurgery for recurrent glioblastoma. *Cancer* (2012) **118**:4193–200. doi:10.1002/cncr.27372
46. Minniti G, Armosini V, Salvati M, Lanzetta G, Caporello P, Mei M, et al. Fractionated stereotactic reirradiation and concurrent temozolomide in patients with recurrent glioblastoma. *J Neurooncol* (2011) **103**:683–91. doi:10.1007/s11060-010-0446-8
47. Villavicencio AT, Burneikiene S, Romanelli P, Fariselli L, McNeely L, Lipani JD, et al. Survival following stereotactic radiosurgery for newly diagnosed and recurrent glioblastoma multiforme: a multicenter experience. *Neurosurg Rev* (2009) **32**:417–24. doi:10.1007/s10143-009-0212-6
48. Grosu AL, Weber WA, Franz M, Stark S, Piert M, Thamm R, et al. Reirradiation of recurrent high grade gliomas using amino-acid PET (SPECT)/CT/MRI image fusion to determine gross tumor volume for stereotactic fractionated radiotherapy. *Int J Radiat Oncol Biol Phys* (2005) **63**:511–9. doi:10.1016/j.ijrobp.2005.01.056
49. Rodrigues G, Yartsev S, Yaremko B, Perera F, Dar AR, Hammond A, et al. Phase I trial of simultaneous in-field boost with helical tomotherapy for patients with one to three brain metastasis. *Int J Radiat Oncol Biol Phys* (2011) **80**:1128–33. doi:10.1016/j.ijrobp.2010.03.047
50. Rodrigues G, Eppinga W, Lagerwaard F, de Haan P, Haasbeek C, Perera F, et al. A pooled analysis of arc-based image-guided simultaneous integrated boost radiation therapy for oligometastatic brain metastases. *Radiat Oncol* (2012) **102**:180–6. doi:10.1016/j.radonc.2011.05.032
51. Weber DC, Caparotti F, Laouiti M, Malek K. Simultaneous-in-field boost for patients with 1 to 4 brain metastasis/es treated with volumetric arc therapy: a prospective study on quality of life. *Radiother Oncol* (2011) **6**:79. doi:10.1186/1748-717X-6-79
52. Marsh JC, Godbole RH, Herskovic AM, Giedla BT, Turian JV. Sparing of the neural stem cell compartment during whole brain radiotherapy: a dosimetric study using helical tomotherapy. *Int J Radiat Oncol Biol Phys* (2010) **78**:946–54. doi:10.1016/j.ijrobp.2009.12.012

53. Gondi V, Tolakanahalli R, Mehta MP, Tewatia D, Rowley H, Kuo JS, et al. Hippocampal-sparing whole brain radiotherapy: a how to technique to use helical tomotherapy and linear accelerator based intensity-modulated radiotherapy. *Int J Radiat Oncol Biol Phys* (2010) **78**:1244–52. doi:10.1016/j.ijrobp.2010.01.039
54. Redmont KJ, Achanta P, Grossman SA, Armour M, Reyes J, Kleinberg L, et al. A radiotherapy technique to limit dose to neural progenitor cell niches without compromising tumor coverage. *J Neurooncol* (2011) **104**:579–87. doi:10.1007/s11060-011-0530-8
55. Nguyen NP, Ceizyk M, Vos P, Betz M, Chi A, Almeida F, et al. Feasibility of tomotherapy-based image-guided radiotherapy for locally advanced oropharyngeal cancer. *PLoS One* (2013) **8**:e60268. doi:10.1371/journal.pone.0060268
56. Nguyen NP, Smith-Raymond L, Vinh-Hung V, Vos P, Davis R, Desai A, et al. Feasibility of tomotherapy-based image-guided radiotherapy to reduce aspiration risk in patients with non-laryngeal and non-hypopharyngeal head and neck cancer. *PLoS One* (2013) **8**:e56290. doi:10.1371/journal.pone.0056290
57. Nguyen NP, Smith-Raymond L, Vinh-Hung V, Sloan D, Davis R, Vos P, et al. Feasibility of tomotherapy to spare the cochlea from excessive radiation in head and neck cancer. *Oral Oncol* (2011) **47**:414–9. doi:10.1016/j.oraloncology.2011.03.011

Conflict of Interest Statement: The authors declare that the research was conducted in the absence of any commercial or financial relationships that could be construed as a potential conflict of interest.

Received: 24 May 2013; accepted: 04 November 2013; published online: 19 November 2013.

Citation: Nguyen NP, Nguyen ML, Vock J, Lemanski C, Kerr C, Vinh-Hung V, Chi A, Khan R, Woods W, Altdorfer G, D'Andrea M, Karlsson U, Hamilton R and Ampil F (2013) Potential applications of imaging and image-guided radiotherapy for brain metastases and glioblastoma to improve patient quality of life. Front. Oncol. 3:284. doi:10.3389/fonc.2013.00284

This article was submitted to Radiation Oncology, a section of the journal Frontiers in Oncology.

Copyright © 2013 Nguyen, Nguyen, Vock, Lemanski, Kerr, Vinh-Hung, Chi, Khan, Woods, Altdorfer, D'Andrea, Karlsson, Hamilton and Ampil. This is an open-access article distributed under the terms of the Creative Commons Attribution License (CC BY). The use, distribution or reproduction in other forums is permitted, provided the original author(s) or licensor are credited and that the original publication in this journal is cited, in accordance with accepted academic practice. No use, distribution or reproduction is permitted which does not comply with these terms.



Five fraction image-guided radiosurgery for primary and recurrent meningiomas

Eric Karl Oermann^{1,2*}, **Rahul Bhandari**¹, **Viola J. Chen**², **Gabriel Lebec**², **Marie Gurka**², **Siyuan Lei**², **Leonard Chen**¹, **Simeng Suy**², **Norio Azumi**³, **Frank Berkowitz**⁴, **Christopher Kalhorn**¹, **Kevin McGrail**¹, **Brian Timothy Collins**², **Walter C. Jean**¹ and **Sean P. Collins**^{2*}

¹ Department of Neurosurgery, Georgetown University Hospital, Washington, DC, USA

² Department of Radiation Medicine, Georgetown University Hospital, Washington, DC, USA

³ Department of Pathology, Georgetown University Hospital, Washington, DC, USA

⁴ Department of Radiology, Georgetown University Hospital, Washington, DC, USA

Edited by:

Nam Phong Nguyen, International Geriatric Radiotherapy Group, USA

Reviewed by:

Michael Chan, Wake Forest University, USA

Christopher Schultz, Medical College of Wisconsin, USA

*Correspondence:

Eric Karl Oermann and Sean P. Collins,
Department of Radiation Medicine,
Georgetown University Medical Center,
3800 Reservoir Road NW,
Washington, DC 20007, USA
e-mail: eko@georgetown.edu;
spc9@georgetown.edu

Purpose: Benign tumors that arise from the meninges can be difficult to treat due to their potentially large size and proximity to critical structures such as cranial nerves and sinuses. Single fraction radiosurgery may increase the risk of symptomatic peritumoral edema. In this study, we report our results on the efficacy and safety of five fraction image-guided radiosurgery for benign meningiomas.

Materials/Methods: Clinical and radiographic data from 38 patients treated with five fraction radiosurgery were reviewed retrospectively. Mean tumor volume was 3.83 mm³ (range, 1.08–20.79 mm³). Radiation was delivered using the CyberKnife, a frameless robotic image-guided radiosurgery system with a median total dose of 25 Gy (range, 25–35 Gy).

Results: The median follow-up was 20 months. Acute toxicity was minimal with eight patients (21%) requiring a short course of steroids for headache at the end of treatment. Pre-treatment neurological symptoms were present in 24 patients (63.2%). Post treatment, neurological symptoms resolved completely in 14 patients (58.3%), and were persistent in eight patients (33.3%). There were no local failures, 24 tumors remained stable (64%) and 14 regressed (36%). Pre-treatment peritumoral edema was observed in five patients (13.2%). Post-treatment asymptomatic peritumoral edema developed in five additional patients (13.2%). On multivariate analysis, pre-treatment peritumoral edema and location adjacent to a large vein were significant risk factors for radiographic post-treatment edema ($p=0.001$ and $p=0.026$ respectively).

Conclusion: These results suggest that five fraction image-guided radiosurgery is well tolerated with a response rate for neurologic symptoms that is similar to other standard treatment options. Rates of peritumoral edema and new cranial nerve deficits following five fraction radiosurgery were low. Longer follow-up is required to validate the safety and long-term effectiveness of this treatment approach.

Keywords: radiosurgery, meningioma, toxicity, fractionation, treatment outcome

BACKGROUND

Meningiomas are commonly benign tumors with a generally favorable prognosis (1). However, without treatment they may progress locally, compressing adjacent structures and causing neurologic deficits. They pose a unique clinical challenge due to their large size and variable anatomical locations within the skull (1). Surgical resection of the entire tumor, when possible without neurologic injury, is the standard of care with a 10-year local control of 80% or higher (2–9). For subtotally resected or recurrent tumors, conventionally fractionated radiation therapy (1.8–2.0 Gy per fraction) to approximately 54 Gy improves local control (2, 4, 6–8).

More recent experience suggests a role for single fraction stereotactic radiosurgery (SRS) (12–18 Gy) as a primary treatment for well selected, small meningiomas or as adjuvant treatment for residual disease (10–12). In cases where single fraction SRS has

been appropriately utilized, results have been excellent, demonstrating equivalent local control to both conventional radiation therapy and surgical resection for select groups of meningioma patients (10, 11). Patients with large tumors (>7.5 cc) have a poor prognosis with this approach, and unacceptably high rates of local failure (10, 11).

Single fraction radiosurgery, however, may increase the risk of symptomatic peritumoral edema and/or cranial nerve injury (10, 12, 13). This risk of peritumoral edema may be increased in tumors that are large, recurrent, adjacent to large veins, and/or basally located (10, 13–19). Conventional fractionated radiation therapy has been employed to treat these patients. The gross tumor volume (GTV) is typically targeted with a margin of 2–5 mm to adjust for set-up inaccuracy. Due to these large planned treatment volumes (PTVs), treatment is generally fractionated over 25–30

sessions to limit toxicity to adjacent normal structures. Due to the long natural history of this disease, it is essential to maximize post-treatment quality of life by preventing treatment related adverse outcomes while minimizing neurological symptoms associated with tumor progression. It is possible that some of the adverse effects of single fraction radiosurgery for large tumors may be mitigated by limited fractionation.

The CyberKnife is an image-guided, frameless, SRS platform. The frameless configuration allows for staged treatment, and it has been successfully utilized to treat a wide variety of intracranial tumors including meningiomas (8, 9, 20). In this retrospective study, we report our preliminary results with five fraction image-guided radiosurgery as a treatment for meningiomas, either as monotherapy or as an adjuvant to surgical resection. This treatment was conducted with the belief that its accurate and highly conformal delivery would minimize peritumoral edema and cranial nerve toxicity.

MATERIALS AND METHODS

PATIENT SELECTION AND TREATMENT

We performed a retrospective review of patients with benign meningiomas treated with CyberKnife SRS from December 1st, 2007 to February 1st, 2011 by SPC and BTC. Patients who had undergone SRS for intracranial meningiomas with or without surgical resection were included in the present study. Patients with atypical or malignant meningiomas were excluded from this study. All patients were treated by an interdisciplinary team of radiation oncologists and neurosurgeons. High resolution CT images were obtained from all patients for pre-treatment planning with target volumes, and critical structures were manually delineated by the treating neurosurgeon (**Figure 1**). The treating isodose and prescription dose were determined by the treating radiation oncologist in consultation with the treating neurosurgeon, and took into account the target volume, proximity to critical structures, and previous treatment history. In most cases, the dose was prescribed to the isodose surface that encompassed the margin of the tumor. Treatment plans were generated using an inverse planning method by the CyberKnife treatment software (Multiplan, Accuray).

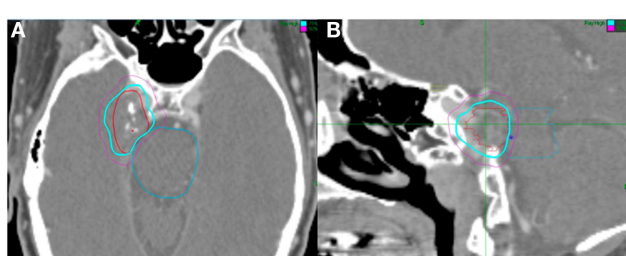


FIGURE 1 | Fifty-three-year-old man with a right Meckel cave meningioma. He presented with right facial pain. The decision was to proceed with radiosurgery. Treatment planning axial (**A**) and sagittal (**B**) computed tomography images demonstrating the GTV (red), brainstem (blue), and chiasm (yellow). Isodose lines shown as follows: blue 79% (prescription) and purple 50%. Note proximity of the meningioma to the brainstem. The tumor was treated with 2500 cGy in five fractions and his pain resolved.

OUTCOMES ASSESSMENT

Patients were tracked as part of routine clinical follow-up by the interdisciplinary team. MRI scans were obtained at pre-defined intervals, every 6 months for the first year, and then yearly thereafter, unless acute changes in neurological status warranted immediate imaging. Neurological symptoms were clinically assessed and recorded by the treating neurosurgeons. Peritumoral edema was assessed on T2 weighted and FLAIR MRI sequences. Patient steroid requirements were assessed at each clinical follow-up visit.

STATISTICAL ANALYSIS

All statistical analyses were performed utilizing SPSS Statistics v19 (IBM). Statistical analysis was performed in order to identify pre-treatment and treatment variables that correlated with post-treatment peritumoral edema. Due to the relatively small sample size, Fisher's Exact Test was used for categorical variables, while Spearman's Rho was employed for examining the interaction between continuous variables and post-treatment peritumoral edema. For analysis of volume and dose, due to the small sample sizes, patients were stratified as being over or under the median and a Chi-square test was employed. Alpha was set to 0.05 to yield a 95% confidence interval (CI) for all statistical tests.

RESULTS

PATIENT AND TREATMENT CHARACTERISTICS

Thirty-eight patients were identified as having undergone treatment for intracranial meningiomas and were subsequently included in the current study (**Table 1**). Twenty-nine (79%) of the patients were female and nine (24%) were male. The median age at time of treatment with radiosurgery was 64 years. Thirteen (34%) patients had undergone prior surgery, of which five were classified as gross total resection and eight were classified as subtotal resections. The remaining 24 patients had received no previous surgical or non-surgical interventions and were treated without pathologic confirmation. Twenty-seven (71%) of the tumors were primary, while 11 (29%) were recurrent. The tumors occurred

Table 1 | A summary of patient characteristics for patients included in the study.

Characteristic	N = 38	(%)
Race/ethnicity		
Caucasian	24	(63)
African American	11	(29)
Hispanic	1	(3)
Asian	2	(5)
Gender		
Female	29	(76)
Male	9	(24)
Age at radiosurgery		
Mean	62	
Median	64	
Extent of resection		
Gross total	5	(13)
Subtotal	8	(21)
No surgery	24	(63)

Table 2 | A summary of tumor characteristics for all tumors included within the study.

Characteristic	N = 38	(%)
Primary vs. recurrent		
Primary	27	(71)
Recurrent	11	(29)
Location: general		
Basal	22	(58)
Non-basal	16	(42)
Location: specific		
Bifrontal	1	(3)
Cavernous sinus	7	(18)
Cerebellopontine angle	5	(13)
Falcine	2	(5)
Falcotentorial	1	(3)
Lateral ventricle	1	(3)
Meckel's cave	2	(5)
Middle cranial fossa	1	(3)
Parafalcine	2	(5)
Parasagittal	5	(13)
Parietal convexity	1	(3)
Parietal lobe	1	(3)
Petroclival	2	(5)
Posterior fossa	1	(3)
Sphenoid wing	2	(5)
Suprasellar	1	(3)
Temporal lobe	3	(8)
Volume (cc)		
Min	1.08	
Max	20.79	
Mean	6.22	
Median	3.84	

at a variety of intracranial sites (**Table 2**), with an almost even number of basal and non-basal tumors, 22 (58%) and 16 (42%) respectively. The median tumor volume was 3.83 mm³ (range, 1.08–20.79 mm³). The median isodose was 82% (70–90%) which was treated with a median prescription dose of 2500 cGy (2500–3500 cGy) and resulted in a median percent tumor coverage of 99.5% (**Table 3**).

COMPLICATIONS AND NEUROLOGICAL SYMPTOMS AFTER SRS

Acute toxicity after SRS treatment included symptoms such as headaches, fatigue, and nausea. Headaches were the most common complication with nine patients (23.7%) complaining of headaches at the end of treatment. Four patients (10.5%) experienced fatigue, and only one patient (2.6%) complained of nausea. Twenty-four patients (63.2%) presented with neurological symptoms prior to therapy (**Table 4**). These neurological symptoms included facial pain, hearing loss, diplopia, proptosis, vertigo, facial numbness, and reduced visual acuity. After SRS, neurological examination revealed complete resolution of neurological symptoms in 14 patients (58.3%), continued symptoms in eight patients (33.3%), and recurrence of symptoms after initial improvement in two patients (8.3%). Only one patient (2.6%) developed a

Table 3 | A summary of treatment characteristics for patients treated on a frameless stereotactic radiosurgical system.

Characteristic	N = 38	Characteristic	N = 38
Rx dose (cGy)		Percent tumor covered	
Min	2500	Min	97.4
Max	3500	Max	99.9
Mean	2691	Mean	99.3
Median	2500	Median	99.5
Isodose line (%)		Non-zero beams	
Min	70	Min	88
Max	90	Max	259
Mean	82	Mean	175
Median	82	Median	174
Homogeneity index		Collimator (mm)	
Min	1	Min	5
Max	1.39	Max	15
Mean	1.22	Mean	11
Median	1.2	Median	10
New conformality index			
Min	1.32		
Max	2.25		
Mean	1.66		
Median	1.61		

Table 4 | A summary of changes in neurological deficits.

Deficit	Pre-SRS	Improved post-SRS	Recurrence after initial improvement	Continued Sx post-SRS
Facial pain	9	5	2	2
Hearing loss	1	0	0	1
Diplopia	4	4	0	0
Proptosis	2	0	0	2
Vertigo	2	2	0	0
Facial numbness	4	3	0	1
Reduced visual acuity	2	0	0	2

All neurological deficits were noted by the treatment team on either clinical exam or through direct questioning of the patient.

new deficit, facial numbness, immediately after radiation, which resolved after a few days. Otherwise, no new neurological deficits were observed after SRS.

Facial pain was the most common presenting neurological symptom pre-SRS treatment. Of the nine patients (37.5%) who presented with facial pain, five patients (55.6%) were asymptomatic after radiation, two patients (22.2%) had continued symptoms, and another two patients (22.2%) had recurrent facial pain after initial improvement. Diplopia, vertigo, and facial numbness improved in the majority of patients. Proptosis and reduced visual acuity did not improve with treatment.

LOCAL CONTROL RATE AND PERITUMORAL EDEMA

Twenty-four patients (63.2%) who underwent SRS showed no change in tumor size, while 14 patients (36.8%) showed a decrease

Table 5 | (A) A comprehensive table detailing individual patient outcomes with regards to pre-treatment therapies, radiation dosage, and subsequent clinical outcomes. (B) A summary of individual patient factors and whether patients had pre-treatment or post-treatment peritumoral edema.

(A)						
Patient	Location treated	Surgery	Cumulative dose	Local outcome	Acute toxicity	Post-radiation steroids
1	Temporal lobe	None	3000	Decreased	Headache	Yes
2	Tentorial	None	3500	Decreased	No	No
3	Posterior Temporal lobe	Subtotal	3000	Stable	No	No
4	Cavernous sinus	Subtotal	2500	Decreased	No	No
5	CPA	None	2750	Stable	No	No
6	CPA	None	2750	Stable	No	No
7	Cavernous sinus	None	2500	Stable	No	No
8	Cavernous sinus	None	2500	Stable	Headache	Yes
9	Parasagittal	Gross total	2500	Stable	Fatigue	No
10	Parietal falcine	Subtotal	2500	Stable	No	No
11	Parietal Parasagittal	Gross total	2500	Stable	Headache	No
12	Petroclival	Subtotal	2500	Stable	Fatigue	No
13	Medial sphenoid wing	Subtotal	2500	Stable	Fatigue and headache	No
14	Middle cranial fossa	None	3000	Stable	Headache	Yes
15	Petroclival	None	2500	Stable	Headache	Yes
16	Cavernous sinus	Subtotal	2500	Decreased	No	No
17	Frontal parafalcine	None	2500	Decreased	No	No
18	Sphenoid wing	None	2500	Decreased	No	No
19	CPA	None	2500	Stable	No	No
20	Parietal convexity	None	2500	Stable	No	No
21	CPA	None	2500	Stable	No	Yes
22	Anterior parafalcine	None	3000	Decreased	Headache and nausea	Yes
23	Bifrontal	None	3000	Stable	No	No
24	CPA	None	3000	Decreased	Headache	No
25	Anterior falcine	Gross total	3000	Decreased	No	No
26	Cavernous sinus	None	2500	Decreased	No	No
27	Falcotentorial	Subtotal	2500	Stable	No	No
28	Posterior fossa	Subtotal	3000	Stable	No	No
29	Posterior Parasagittal	Gross total	2500	Stable	No	No
30	Cavernous sinus	None	2500	Stable	No	No
31	Parafalcine	None	2500	Decreased	No	No
32	Anterior temporal	Gross total	3000	Decreased	Headache	Yes
33	Lateral ventricle	None	3000	Stable	No	No
34	Suprasellar	None	2500	Stable	Fatigue	Yes
35	Cavernous sinus	None	2500	Decreased	Hypesthesia	No
36	Meckel's cave	None	2500	Stable	No	No
37	Meckel's cave	None	2750	Decreased	No	No
38	Parietal lobe	Gross total	3000	Stable	No	No

(B)						
Patient	Anatomical classification	Volume (cc)	Recurrence	Adjacent to vein	Pre-treatment peritumoral edema	Post-treatment peritumoral edema
1	Non-basal	1.08	No	No	No	No
2	Non-basal	1.6	No	Yes	No	Yes
3	Non-basal	16.7	Yes	No	Yes	Yes
4	Basal	5.56	Yes	Yes	Yes	Yes
5	Basal	1.37	No	No	No	No
6	Basal	2.56	No	Yes	No	No

(Continued)

Table 5 | Continued

Patient	Anatomical classification	Volume (cc)	Recurrence	Adjacent to vein	Pre-treatment peritumoral edema	Post-treatment peritumoral edema
7	Basal	4.05	No	No	No	No
8	Basal	12.19	No	No	No	No
9	Non-basal	11.24	Yes	No	Yes	Yes
10	Non-basal	6.48	Yes	No	No	No
11	Non-basal	6.44	Yes	Yes	No	No
12	Basal	2.12	Yes	No	No	No
13	Basal	20.17	No	No	No	No
14	Basal	2.14	No	Yes	No	Yes
15	Basal	20.79	No	No	No	No
16	Basal	13.82	No	Yes	Yes	Yes
17	Non-basal	6.43	No	No	No	No
18	Basal	5.48	No	No	No	No
19	Basal	10.84	No	No	No	No
20	Non-basal	3.24	No	No	No	No
21	Basal	12.13	No	No	No	Yes
22	Non-basal	1.17	No	No	No	No
23	Non-basal	6.59	No	No	No	No
24	Basal	1.53	No	No	No	No
25	Non-basal	3.59	Yes	Yes	Yes	Yes
26	Basal	13.07	No	No	No	No
27	Non-basal	4.68	No	No	No	No
28	Basal	11.83	Yes	No	No	No
29	Non-basal	2.63	Yes	No	No	Yes
30	Basal	2.65	No	No	No	No
31	Non-basal	2.611	No	No	No	Yes
32	Non-basal	3.04	Yes	Yes	No	No
33	Non-basal	3.628	No	Yes	No	No
34	Basal	2.62	No	No	No	No
35	Basal	1.38	No	Yes	No	No
36	Basal	4.97	No	No	No	No
37	Basal	1.90	No	Yes	No	No
38	Non-basal	1.89	Yes	Yes	No	No

Table 6 | A statistical analysis of variables associated with peritumoral edema.

Pre-treatment characteristic	Likelihood ratio	p-Value
Pre-treatment peritumoral edema	15.77	0.001
Anatomical classification	1.28	0.293
Adjacent to vein	4.83	0.045
Volume (cc)	0	1
Recurrence	2.77	0.116
Cumulative dose	0.002	0.968

p-Values are for two-sided Fisher's Exact Test.

in tumor size resulting in a crude radiographic local control rate of 100% of the meningiomas treated with SRS (**Table 5**).

Intracranial edema is commonly managed with oral steroids, and oral steroid requirements were measured as a surrogate for post-radiation peritumoral edema. Symptomatic, acute, post-radiation edema requiring steroids occurred in six patients

(15.8%). In addition, two patients (5.3%) were given steroids due to evidence of post-radiation edema on MRI, but without any clinical signs of toxicity (**Table 5**).

Pre-SRS radiographic peritumoral edema continued to be observed in five patients (13.2%) on follow-up MRI imaging. Of these patients, four (10.5%) had recurrent tumors following a subtotal or gross resection, and three (7.9%) had a radiological tumor volume greater than 10.0 cc (**Table 5**). A total of 10 patients had post-treatment radiographic peritumoral edema, with new onset being observed in five patients (13.2%). On univariate statistical analysis, only pre-treatment peritumoral edema ($p = 0.001$) and adjacency to a large vein ($p = 0.045$) correlated with post-treatment peritumoral edema (**Table 6**).

DISCUSSION

Our results show that fractionated SRS may provide similar local control with minimal toxicity and excellent quality of life. Headaches, fatigue, and nausea were the only three acute complaints, all of which resolved over time. Headaches were the

most common complication, present in 23.7% of our patients, which is consistent with other studies (12). Nausea was the least common, present in only one patient. This trend has also been observed in previous studies (21, 22).

In this study several patients presented with neurological symptoms and the majority responded to treatment with minimal toxicity at 2 years of follow-up. The present response rate of neurological symptoms compares favorably to similar studies with Gamma Knife (17, 21). Kondziolka et al. noted that five patients in their series of 99 cases had new or worsened deficits occurring 3–31 months after radiosurgery, while Chang et al. reported two cases out of 140 experiencing worsened deficits. Most tellingly, Kondziolka et al. reported that 67 out of 70 patients reported that their treatments were subjectively “successful” on an outcomes questionnaire, indicative of a high preservation of quality of life post-SRS (21). Uniquely, we have found an excellent response of tumor-associated facial pain to five fraction radiosurgery. While documented in other studies involving single fraction radiosurgery, our results suggest that a five fraction approach can also yield a beneficial reduction in tumor-associated trigeminal neuralgia (23–25). Other studies have suggested that recurrence of these symptoms typically occurs within 2 years, and is more likely to recur for malignant skull base tumors, with the mechanism of relief being decompression of affected nerve roots (24, 25).

Stereotactic radiosurgery was well tolerated with few post-treatment complications. As previously mentioned, other studies have suggested a relationship between tumor volume and post-SRS edema and complications (26). However, we found no correlation found between tumor volume, margin dose, and the presence of complications, which is similar to findings in other studies (12, 14, 22). Furthermore, it may be that if such a relationship does exist between large tumor volume and complications, that it may be mitigated in part through dose fractionation like in the present study.

At roughly 2 years, none of the patients developed local failures, and 14 showed a decrease in tumor size that may be correlated

favorably with local control, although this has not been conclusively shown (27). There is a high degree of variability in volume reduction post-radiosurgery with studies reporting rates less than 20% and over 60%, ultimately the implications and the time course of post-radiosurgery volume reduction need to be further studied to ascertain its prognostic implications (21, 28). With regards to local control, control rates for meningiomas post-radiosurgery typically require longer follow-up for thorough assessment, with many studies placing the 10-year rate of local control at 84% (11, 22, 29).

Only 13% of the patients developed new onset post-SRS peritumoral edema, with 26% of patients developing it overall. In addition, only 2.6% of the patient group receiving five fraction radiosurgery had symptomatic peritumoral edema. These results are in agreement with other papers on the use of hypofractionated radiosurgery for meningiomas, and compares favorably to an average of 5–10% of patients developing symptomatic edema in other studies (12, 21, 30, 31). In one such study by Kollova et al. edema was more common in tumor volumes greater than 10 cm³ (26). However the present study and others have suggested that simple tumor volume is not a significant contributor to post-radiation peritumoral edema, which may be in fact more due to the interface between meningioma and cortical tissue rather than gross volume (21, 32).

CONCLUSION

Stereotactic radiosurgery is a safe and effective treatment for benign intracranial meningiomas with or without surgical resection. Dose fractionation is well tolerated, and may offer equivalent local control to single session SRS. Fractionation may offer particular benefit to patients with large tumors located in critical locations or in other high-risk patients. Further studies are warranted to fully ascertain the potential benefits and risks of dose fractionation for SRS therapy of meningiomas, and its ultimate impact on local control.

REFERENCES

- Alexiou GA, Gogou P, Markoula S, Kyritsis AP. Management of meningiomas. *Clin Neurol Neurosurg* (2010) **112**:177–82. doi:10.1016/j.clineuro.2009.12.011
- Simpson D. The recurrence of intracranial meningiomas after surgical treatment. *J Neurosurg Psychiatry* (1957) **20**:22–39. doi:10.1136/jnnp.20.1.22
- Mirimanoff RO, Dosoretz DE, Linggood RM, Ojemann RG, Martuzza RL. Meningioma: analysis of recurrence and progression following neurosurgical resection. *J Neurosurg* (1985) **62**:18–24. doi:10.3171/jns.1985.62.1.0018
- Barbaro NM, Gutin PH, Wilson CB, Sheline GE, Boldrey EB, Wara WM. Radiation therapy in the treatment of partially resected meningiomas. *Neurosurgery* (1987) **20**:525–8. doi:10.1227/00006123-198704000-00003
- Condra KS, Buatti JM, Mendenhall WM, Friedman WA, Marcus RB Jr, Rhoton AL. Benign meningiomas: primary treatment selection affects survival. *Int J Radiat Oncol Biol Phys* (1997) **39**:427–36. doi:10.1016/S0360-3016(97)00317-9
- Soyer S, Chang EL, Selek U, Shi W, Maor MH, Demonte F. Radiotherapy after surgery for benign cerebral meningioma. *Radiother Oncol* (2004) **71**:85–90. doi:10.1016/j.radonc.2004.01.006
- Rogers L, Mehta M. Role of radiation therapy in treating intracranial meningiomas. *Neurosurg Focus* (2007) **23**:E4. doi:10.3171/FOC-07/10/E4
- Colombo F, Casentini L, Cavedon C, Scalchi P, Cora S, Francescon P. Cyberknife radiosurgery for benign meningiomas: short-term results in 199 patients. *Neurosurgery* (2009) **64**:A7–13. doi:10.1227/01.NEU.0000338947.84636.A6
- Coppa ND, Raper DM, Zhang Y, Collins BT, Harter KW, Gagnon GJ, et al. Treatment of malignant tumors of the skull base with multi-session radiosurgery. *J Hematol Oncol* (2009) **2**:16. doi:10.1186/1756-8722-2-16
- Kondziolka D, Flickinger JC, Perez B. Judicious resection and/or radiosurgery for parasagittal meningiomas: outcomes from a multicenter review. Gamma Knife Meningioma Study Group. *Neurosurgery* (1998) **43**:405–13; discussion 413–4. doi:10.1097/00006123-199809000-00001
- Pollock BE, Stafford SL, Utter A, Giannini C, Schreiner SA. Stereotactic radiosurgery provides equivalent tumor control to Simpson Grade 1 resection for patients with small- to medium-size meningiomas. *Int J Radiat Oncol Biol Phys* (2003) **55**:1000–5. doi:10.1016/S0360-3016(02)04356-0
- DiBiase SJ, Kwok Y, Yovino S, Arena C, Naqvi S, Temple R, et al. Factors predicting local tumor control after gamma knife stereotactic radiosurgery for benign intracranial meningiomas. *Int J Radiat Oncol Biol Phys* (2004) **60**:1515–9. doi:10.1016/j.ijrobp.2004.05.073
- Ganz JC, Schrottner O, Pendl G. Radiation-induced edema after Gamma Knife treatment for meningiomas. *Stereotact Funct Neurosurg* (1996) **66**(Suppl 1):129–33. doi:10.1159/000099778
- Nakamura S, Hiyama H, Arai K, Nakaya K, Sato H, Hayashi M, et al. Gamma Knife radiosurgery for meningiomas: four cases of radiation-induced edema. *Stereotact Funct Neurosurg* (1996) **66**(Suppl 1):142–5. doi:10.1159/000099804

15. Vermeulen S, Young R, Li F, Meier R, Raisis J, Klein S, et al. A comparison of single fraction radiosurgery tumor control and toxicity in the treatment of basal and non-basal meningiomas. *Stereotact Funct Neurosurg* (1999) **72**(Suppl 1): 60–6.
16. Singh VP, Kansai S, Vaishya S, Julka PK, Mehta VS. Early complications following gamma knife radiosurgery for intracranial meningiomas. *J Neurosurg* (2000) **93**(Suppl 3):57–61.
17. Chang JH, Chang JW, Choi JY, Park YG, Chung SS. Complications after gamma knife radiosurgery for benign meningiomas. *J Neurol Neurosurg Psychiatry* (2003) **74**:226–30. doi:10.1136/jnnp.74.2.226
18. Conti A, Pontoriero A, Salamone I, Siragusa C, Midili F, La Torre D, et al. Protecting venous structures during radiosurgery for parasagittal meningiomas. *Neurosurg Focus* (2009) **27**:E11. doi:10.3171/2009.8. FOCUS09-157
19. Hasegawa T, Kida Y, Yoshimoto M, Iizuka H, Ishii D, Yoshida K. Gamma Knife surgery for convexity, parasagittal, and falcine meningiomas. *J Neurosurg* (2011) **114**:1392–8. doi:10.3171/2010.11. JNS10112
20. Oermann E, Collins BT, Erickson KT, Yu X, Lei S, Suy S, et al. CyberKnife enhanced conventionally fractionated chemoradiation for high grade glioma in close proximity to critical structures. *J Hematol Oncol* (2010) **3**:22. doi:10.1186/1756-8722-3-22
21. Kondziolka D, Levy EI, Nirajan A, Flickinger JC, Lunsford LD. Long-term outcomes after meningioma radiosurgery: physician and patient perspectives. *J Neurosurg* (1999) **91**:44–50. doi:10.3171/jns.1999.91.1.0044
22. Stafford SL, Pollock BE, Foote RL, Link MJ, Gorman DA, Schomberg PJ, et al. Meningioma radiosurgery: tumor control, outcomes, and complications among 190 consecutive patients. *Neurosurgery* (2001) **49**:1029–37; discussion 1037–28. doi:10.1097/00006123-200111000-00001
23. Chang JW, Kim SH, Huh R, Park YG, Chung SS. The effects of stereotactic radiosurgery on secondary facial pain. *Stereotact Funct Neurosurg* (1999) **72**(Suppl 1):29–37. doi:10.1159/000056436
24. Pollock BE, Julian BA, Foote RL, Gorman DA. Stereotactic radiosurgery for tumor-related trigeminal pain. *Neurosurgery* (2000) **46**:576–82; discussion 582–3. doi:10.1097/00006123-200003000-00010
25. Squire SE, Chan MD, Furr RM, Lowell DA, Tatter SB, Ellis TL, et al. Gamma knife radiosurgery in the treatment of tumor-related facial pain. *Stereotact Funct Neurosurg* (2012) **90**:145–50. doi:10.1159/000335873
26. Kollova A, Liscak R, Novotny J Jr, Vladyka V, Simonova G, Janouskova L. Gamma Knife surgery for benign meningioma. *J Neurosurg* (2007) **107**:325–36. doi:10.3171/JNS-07/08/0325
27. Kondziolka D, Mathieu D, Lunsford LD, Martin JJ, Madhok R, Nirajan A, et al. Radiosurgery as definitive management of intracranial meningiomas. *Neurosurgery* (2008) **62**:53–8; discussion 58–60. doi:10.1227/01.NEU.0000311061.72626.0D
28. Minniti G, Amichetti M, Enrichi RM. Radiotherapy and radiosurgery for benign skull base meningiomas. *Radiat Oncol* (2009) **4**:42. doi:10.1186/1748-717X-4-42
29. Zada G, Pagnini PG, Yu C, Erickson KT, Hirschbein J, Zelman V, et al. Long-term outcomes and patterns of tumor progression after gamma knife radiosurgery for benign meningiomas. *Neurosurgery* (2010) **67**:322–8; discussion 328–29. doi:10.1227/01.NEU.0000371974.88873.15
30. Santacroce A, Walier M, Regis J, Liscak R, Motti E, Lindquist C, et al. Long-term tumor control of benign intracranial meningiomas after radiosurgery in a series of 4565 patients. *Neurosurgery* (2012) **70**:32–9; discussion 39. doi:10.1227/NEU.0b013e31822d408a
31. Unger KR, Lominska CE, Chanyasukit J, Randolph-Jackson P, White RL, Aulisi E, et al. Risk factors for posttreatment edema in patients treated with stereotactic radiosurgery for meningiomas. *Neurosurgery* (2012) **70**:639–45. doi:10.1227/NEU.0b013e3182351ae7
32. Cai R, Barnett GH, Novak E, Chao ST, Suh JH. Principal risk of peritumoral edema after stereotactic radiosurgery for intracranial meningioma is tumor-brain contact interface area. *Neurosurgery* (2010) **66**:513–22. doi:10.1227/01.NEU.0000365366.53337.88

Conflict of Interest Statement: Brian Timothy Collins and Sean P. Collins have received honoraria from Accuray Inc. The other co-authors declare that the research was conducted in the absence of any commercial or financial relationships that could be construed as a potential conflict of interest.

Received: 23 June 2013; paper pending published: 17 July 2013; accepted: 03 August 2013; published online: 20 August 2013.

*Citation: Oermann EK, Bhandari R, Chen VJ, Lebec G, Gurka M, Lei S, Chen L, Suy S, Azumi N, Berkowitz F, Kalhorn C, McGrail K, Collins BT, Jean WC and Collins SP (2013) Five fraction image-guided radiosurgery for primary and recurrent meningiomas. *Front. Oncol.* **3**:213. doi: 10.3389/fonc.2013.00213*

This article was submitted to Radiation Oncology, a section of the journal Frontiers in Oncology.

Copyright © 2013 Oermann, Bhandari, Chen, Lebec, Gurka, Lei, Chen, Suy, Azumi, Berkowitz, Kalhorn, McGrail, Collins, Jean and Collins. This is an open-access article distributed under the terms of the Creative Commons Attribution License (CC BY). The use, distribution or reproduction in other forums is permitted, provided the original author(s) or licensor are credited and that the original publication in this journal is cited, in accordance with accepted academic practice. No use, distribution or reproduction is permitted which does not comply with these terms.



A multicenter retrospective study of frameless robotic radiosurgery for intracranial arteriovenous malformation

Eric K. Oermann¹*, Nikhil Murthy², Viola Chen³, Advaith Baimeedi¹, Deanna Sasaki-Adams⁴, Kevin McGrail², Sean P. Collins³, Matthew G. Ewend⁴ and Brian T. Collins³*

¹ Department of Neurological Surgery, Icahn School of Medicine at Mount Sinai, New York, NY, USA

² Department of Neurological Surgery, Georgetown University School of Medicine, Washington, DC, USA

³ Department of Radiation Medicine, Georgetown University School of Medicine, Washington, DC, USA

⁴ Department of Neurological Surgery, The University of North Carolina at Chapel Hill, Chapel Hill, NC, USA

Edited by:

Nam Phong Nguyen, International Geriatric Radiotherapy Group, USA

Reviewed by:

Wenyin Shi, Thomas Jefferson University, USA

Yidong Yang, University of Miami Miller School of Medicine, USA

*Correspondence:

Eric K. Oermann and Brian T. Collins,
1468 Madison Avenue, New York, NY,
USA

e-mail: eko@georgetown.edu;
collinsb@gunet.georgetown.edu

Introduction: CT-guided, frameless radiosurgery is an alternative treatment to traditional catheter-angiography targeted, frame-based methods for intracranial arteriovenous malformations (AVMs). Despite the widespread use of frameless radiosurgery for treating intracranial tumors, its use for treating AVM is not well described.

Methods: Patients who completed a course of single fraction radiosurgery at The University of North Carolina or Georgetown University between 4/1/2005–4/1/2011 with single fraction radiosurgery and received at least one follow-up imaging study were included. All patients received pre-treatment planning with CTA ± MRA and were treated on the CyberKnife (Accuray) radiosurgery system. Patients were evaluated for changes in clinical symptoms and radiographic changes evaluated with MRI/MRA and catheter-angiography.

Results: Twenty-six patients, 15 male and 11 female, were included in the present study at a median age of 41 years old. The Spetzler-Martin grades of the AVMs included seven Grade I, 12 Grade II, six Grade III, and one Grade IV with 14 (54%) of the patients having a pre-treatment hemorrhage. Median AVM nodal volume was 1.62 cm³ (0.57–8.26 cm³) and was treated with a median dose of 1900 cGy to the 80% isodose line. At median follow-up of 25 months, 15 patients had a complete closure of their AVM, 6 patients had a partial closure, and 5 patients were stable. Time since treatment was a significant predictor of response, with patients experiencing complete closure having on average 11 months more follow-up than patients with partial or no closure ($p=0.03$). One patient experienced a post-treatment hemorrhage at 22 months.

Conclusion: Frameless radiosurgery can be targeted with non-invasive MRI/MRA and CTA imaging. Despite the difficulty of treating AVM without catheter angiography, early results with frameless, CT-guided radiosurgery suggest that it can achieve similar results to frame-based methods at these time points.

Keywords: stereotactic radiosurgery, arteriovenous malformations, image guided radiation therapy, outcomes, CT angiography

INTRODUCTION

Intracranial arteriovenous malformations (AVMs) present one of the greatest clinical challenges for neurosurgeons, radiation oncologists, and neurointerventionalists. Classically, the treatment of these lesions involved careful patient selection followed by large, open surgical procedures, or more recently endovascular obliteration, radiosurgery, or a combination of these methods (1–3). This trend of utilizing increasingly less invasive options, endovascular, and radiosurgical, has led to the advent of frameless radiosurgical devices that do not require the traditional head frame for stereotactic guidance (4, 5). Despite the widespread adoption of these devices for treating both intracranial and extracranial pathologies, to the author's knowledge to date there has been only two reports on the results of frameless radiosurgical devices

for the treatment of intracranial AVM (5, 6). We report the retrospective results of two institutions with using CyberKnife frameless stereotactic radiosurgery (SRS) for the treatment of intracranial AVM.

METHODS

PATIENT SELECTION AND TREATMENT

We performed a retrospective review of patients with intracranial AVMs treated with CyberKnife SRS from December 1st, 2005 to February 1st, 2011 at Georgetown University Hospital and the University of North Carolina at Chapel Hill. Patients who had undergone single fraction SRS for intracranial AVM with or without endovascular embolization and had received at least one follow-up imaging study were included. All patients were

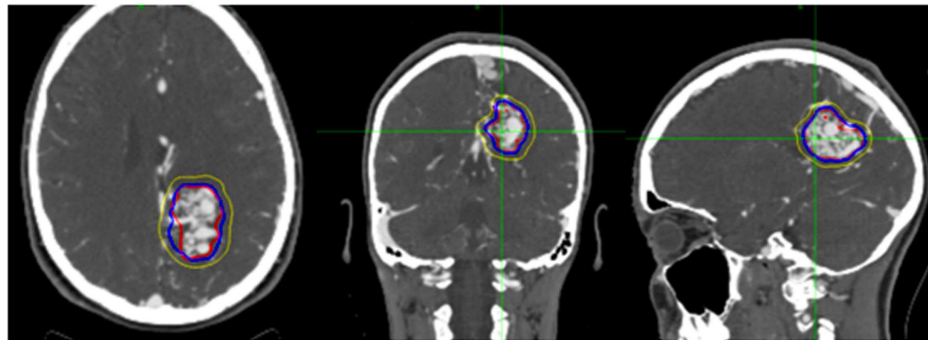


FIGURE 1 | Figure demonstrating treatment planning for a representative case. Planned treatment volume (red), 90% isodose (blue), and 50% isodose (yellow) can be seen in three planes on pre-treatment planning CTA.

treated by an interdisciplinary team of radiation oncologists and neurosurgeons. High resolution CTA images with or without MRA were obtained from all patients for pre-treatment planning. A planning target volume (PTV) and critical structures were manually delineated by the treating neurosurgeon with the PTV encompassing the contour of the AVM with a 1 mm margin (**Figure 1**). All treatment planning was performed on pre-treatment CTA imaging, and when available, using fused MRA/CTA imaging. The treating isodose and prescription dose were determined by the treating radiation oncologist in consultation with the treating neurosurgeon, and took into account the AVM nidus, overall volume, proximity to critical structures, and previous treatment history. Treatment plans were generated using an inverse planning method by the CyberKnife treatment software (Multiplan, Accuray).

OUTCOMES ASSESSMENT

Patients were tracked as part of routine clinical follow-up by the interdisciplinary team. MRA scans with or without catheter-angiography confirmation were obtained at pre-defined annual intervals unless acute changes in neurological status warranted immediate imaging. Neurological symptoms were clinically assessed and recorded by the treating neurosurgeons. Complete closure was defined as total resolution of the AVM nidus and draining veins on imaging, with partial closure being defined as a decrease in size of the nidus with the persistence of large draining veins.

STATISTICAL ANALYSIS

All statistical analyses were performed utilizing SPSS Statistics v19 (IBM). Statistical analysis was performed in order to identify pre-treatment and treatment variables that correlated with AVM closure. The Kruskal-Wallis test, a non-parametric equivalent to ANOVA, was utilized for comparison of continuous variables grouped by AVM closure outcomes. For analysis of volume and dose, Pearson Chi-square testing was employed. Alpha was set to 0.05 to yield a 95% confidence interval (CI) for all statistical tests. Averages were all reported as the median value and interquartile range (IQR), which is a more robust measure of dispersion than simple range.

RESULTS

PATIENT AND TREATMENT CHARACTERISTICS

Twenty-six patients were identified as having undergone treatment for intracranial AVM and met all criteria for inclusion in the current study (**Table 1**). Fifteen (58%) of the patients were male and 11 (42%) were female. The median age at time of treatment with radiosurgery was 41 years (IQR, 26–55 years). The AVMs had a range of Spetzler-Martin grades with 7 Grade I, 12 Grade II, 6 Grade III, and 1 Grade IV. Ten (38%) of the patients were either current smokers or had a history of smoking, and seven (23%) of the patients were hypertensive. Fourteen (54%) of the patients had a pre-treatment hemorrhage, and of the hypertensive patients, six out of seven (86%) experienced pre-treatment hemorrhage ($p = 0.027$). The median AVM nidus volume was 1.62 cm³ (IQR, 0.57–8.26 cm³). Pre-treatment embolization was performed in 11 patients (42%), with 9 patients being treated with Onyx and the others with *n*-butyl cyanoacrylate (NBCA). The median isodose was 80% (76–83%), which was treated with a median prescription dose of 1900 cGy (IQR, 1800–2175 cGy). Seventeen (65%) of the patients had SRS as monotherapy, while nine underwent a combination of SRS and embolization or, in one case, surgical resection.

AVM CLOSURE RATES

At median follow-up for the cohort of 25 months (IQR, 19–36 months), 15 patients had a complete closure of their AVM, 6 patients had a partial closure, and 5 patients were stable (**Figure 2**). Time since treatment was a significant predictor of response, fully closed AVM had, on average, 11 months more follow-up time than those with partial or no closure ($p = 0.03$) (**Table 2**). Nidal volume and dose did not correlate with AVM closure rate ($p = 0.63, 0.12$). Spetzler-Martin Grade did not correlate with AVM closure as well ($p = 0.26$).

NEUROLOGICAL DEFICITS AND TOXICITY

One patient experienced a post-treatment hemorrhage at 22 months requiring emergent surgical decompression (**Table 3**). No other significant post-treatment adverse events were reported. The most common pre-treatment neurological symptom was headaches (46%), which improved in most cases after treatment

Table 1 | Summary of AVM patient characteristics.

Variable	Value
Subjects, N	26
Median age, years (IQR)	41 (26–55)
Gender	
Male, n (%)	15 (58)
Female, n (%)	11 (42)
Smoking status	
Current/prior history, n (%)	10 (38)
Never, n (%)	12 (46)
Unknown, n (%)	4 (15)
Pre-treatment neurological symptoms	
Headache, n (%)	12 (46)
Seizures, controlled/uncontrolled, n/n (%/%)	2/2 (8/8)
Motor deficits, n (%)	9 (35)
Pre-treatment hemorrhage, n (%)	14 (54)
Hypertension (%)	7 (27)
Pre-treatment hemorrhage, n (%)	6 (86)
No pre-treatment hemorrhage, n (%)	1 (14)
Spetzler martin grade	
I, n (%)	7
II, n (%)	12
III, n (%)	6
IV, n (%)	1
Median Nidus volume, cm ³ (IQR)	1.62 (0.57–8.26)
Intervention	
SRS only, n (%)	17 (65)
SRS + embolization or surgery, n (%)	9 (35)
Isodose, median % (IQR)	80 (76–83%)
Dose, median cGy (IQR)	1900 (1800–2175)

with only four patients (15%) reporting them at the end of the study. Pre-treatment, controlled, and uncontrolled seizures were symptoms in 16% of the patients. By conclusion of the study, 12% of the patients had controlled seizures on oral medications, and no patients had uncontrolled seizures.

DISCUSSION

Our results show that frameless SRS is a safe and effective technique for the treatment of intracranial AVM. A large recent study by Ding et al. reported an obliteration rate of 30% at 10 years, and the present study with an obliteration rate of 58% at 3 years compares favorably to these results (7). The higher rate of closure in the present study may be due to generally smaller nodal volumes, and generally lower grades, yet roughly equivalent marginal doses (7). It is worth noting that Spetzler–Martin grading incorporates size into its calculation of grade (as well as draining veins and eloquence of cortex), and therefore is unsurprisingly correlated with obliteration rates. The results of this article with regards to obliteration rates and dependent factors are consistent with observations made in similar studies of radiosurgical outcomes for treatment of intracranial AVM with Gamma Knife

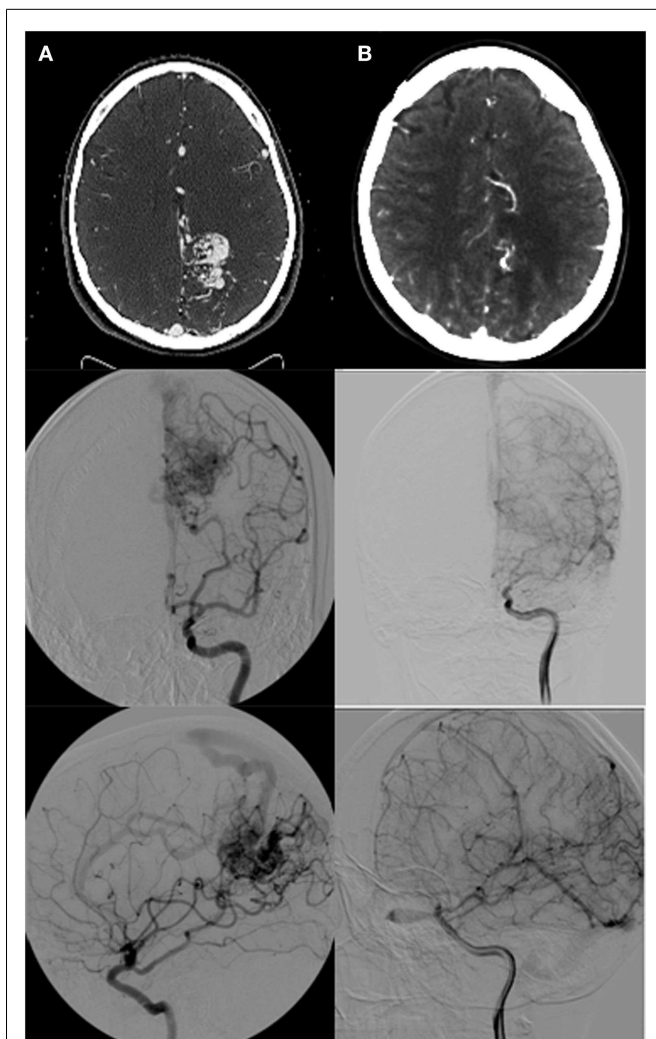


FIGURE 2 | (A) Pre-radiosurgery, and **(B)** post-radiosurgery CT angiograms and angiograms for a representative case with follow-up images taken at 2 years post-radiosurgery demonstrating complete nodal obliteration with no residual draining vein.

(7–10). While other studies have shown a consistent and expected dependence of AVM closure on dose, volume, grade, and follow-up time, the present study only demonstrated a dependence on follow-up time (8). This lack of dependence upon dose and volume may be attributable to a small sample size and the variance within these factors, and therefore are negative results due to lack of statistical power rather than truly negative results.

Our minimally invasive approach of obtaining CTA with or without MRA for planning purposes prior to frameless SRS does come with a notable drawback when treating AVM after embolization with Onyx. Onyx, an ethylene vinyl alcohol polymer which is solvated in dimethyl-sulfoxide (DMSO), is radio-opaque and can cause artifact on CTA, which can make it difficult to properly visualize the AVM nidus for treatment planning and follow-up.

The distribution of post-treatment neurological complications in the present group compared similarly to reported series within

Table 2 | Summary of AVM treatment characteristics and patient outcomes.

Variable	Endpoint			(p-Value)
	Complete closure (n = 15)	Partial closure (n = 6)	Stable (n = 5)	
Median follow-up, months (IQR)	31 (24–39)	17 (11–22)	25 (18–29)	0.03
Spetzler martin grade	–	–	–	0.26
I, n (%)	5 (33)	3 (50)	0 (0)	
II, n (%)	8 (53)	3 (50)	2 (40)	
III, n (%)	3 (20)	0 (0)	3 (60)	
IV, n (%)	1 (6)	0 (0)	0 (0)	
Median Nidus volume, cm ³ (IQR)	1.15 (0.54–4.66)	3.42 (0.71–10.24)	4.42 (1.96–9.07)	0.63
Intervention				0.64
SRS only, n (%)	8 (53)	5 (83)	4 (80)	
SRS + embolization or surgery, n (%)	7 (47)	1 (17)	1 (20)	
Isodose, median % (IQR)	80 (76–85%)	77 (72–80%)	81 (80–81%)	0.24
Dose, median Gy (IQR)	1800 (1750–1950)	2050 (2000–2175)	2000 (2000–2200)	0.12

Table 3 | Summary of post-treatment adverse events and symptoms.

Variable	Value
Post-treatment hemorrhage, n (%)	1 (4)
Post-treatment neurological symptoms	
Headache, n (%)	4 (15)
Seizures, controlled/uncontrolled, n/n (%/%)	3/0 (12/0)
Motor deficits, n (%)	3 (12)

the Gamma Knife literature as well, with a significant improvement occurring for major neurological symptoms including seizures and motor function compared to pre-operative symptoms (9, 11). For pre-treatment headaches, there was 66% rate of total resolution, identical to the results of Steiner et al. (11).

Approximately, half of the patients in the present series experienced pre-treatment hemorrhage. Pre-treatment hemorrhage can vary greatly between studies in the literature, with some cohorts consisting almost entirely of patients with hemorrhage, and others entirely without (7, 11). Recent studies have shown that post-radiosurgery hemorrhage can increase the time until AVM closure, and previous work by Flickinger demonstrated that pre-treatment hemorrhage can have a lasting impact on the resolution of neurologic sequelae, although this last finding has been disputed (7, 12, 13).

CONCLUSION

This small pilot series demonstrates that frameless SRS is a safe and effective measure for treating intracranial AVM in utilizing the traditional single fraction approach. Due to advanced imaging and motion tracking technologies, it can achieve equivalent results to traditional frame-based methods without the need for pins and a stereotaxic frame. With further research, we may be able to maximize the benefits of this novel technology for the treatment of intracranial AVM.

REFERENCES

- Spetzler RF, Martin NA. A proposed grading system for arteriovenous malformations. *J Neurosurg* (1986) **65**(4):476–83. doi:10.3171/jns.1986.65.4.0476
- Simon C, Chan MS, Lam JM, Tam PH, Poon WS. Complete obliteration of intracranial arteriovenous malformation with endovascular cyanoacrylate embolization: initial success and rate of permanent cure. *AJNR Am J Neuroradiol* (2004) **25**(7):1139–43.
- Viñuela F, Dion JE, Duckwiler G, Martin NA, Lylyk P, Fox A, et al. Combined endovascular embolization and surgery in the management of cerebral arteriovenous malformations: experience with 101 cases. *J Neurosurg* (1991) **75**(6):856–64. doi:10.3171/jns.1991.75.6.0856
- Adler JR Jr, Chang S, Murphy M, Doty J, Geis P, Hancock S. The Cyberknife: a frameless robotic system for radiosurgery. *Stereotact Funct Neurosurg* (1998) **69**(1–4):124–8. doi:10.1159/000099863
- Pedroso AG, De Salles AA, Tajik K, Golish R, Smith Z, Frighetto L, et al. Novalis shaped beam radiosurgery of arteriovenous malformations. *J Neurosurg* (2004) **101**:425–34.
- Colombo F, Cavedon C, Casentini L, Francescon P, Causin F, Pinna V. Early results of CyberKnife radiosurgery for arteriovenous malformations: clinical article. *J Neurosurg* (2009) **111**(4):807–19. doi:10.3171/2008.10.JNS08749
- Ding D, Yen C-P, Xu Z, Starke RM, Sheehan JP. Radiosurgery for patients with unruptured intracranial arteriovenous malformations: clinical article. *J Neurosurg* (2013) **118**(5):958–66. doi:10.3171/2013.2.JNS121239
- Karlsson B, Lindquist C, Steiner L. Prediction of obliteration after gamma knife surgery for cerebral arteriovenous malformations. *Neurosurgery* (1997) **40**(3):425–31. doi:10.1097/00006123-199703000-00001
- Pan DH-C, Guo W-Y, Chung W-Y, Shiau C-Y, Chang Y-C, Wang L-W. Gamma knife radiosurgery as a single treatment modality for large cerebral arteriovenous malformations. *J Neurosurg* (2000) **93**:113–9.
- Yamamoto M, Jimbo M, Hara M, Saito I, Mori K. Gamma knife radiosurgery for arteriovenous malformations: long-term follow-up results focusing on complications occurring more than 5 years after irradiation. *Neurosurgery* (1996) **38**(5):906–14. doi:10.1097/00006123-199605000-00010
- Steiner L, Lindquist C, Adler JR, Torner JC, Alves W, Steiner M. Clinical outcome of radiosurgery for cerebral arteriovenous malformations. *J Neurosurg* (1992) **77**(1):1–8. doi:10.3171/jns.1992.77.1.0001
- Flickinger JC, Kondziolka D, Lunsford LD, Pollock BE, Yamamoto M, Gorham DA, et al. A multi-institutional analysis of complication outcomes after arteriovenous malformation radiosurgery. *Int J Radiat Oncol Biol Phys* (1999) **44**(1):67–74. doi:10.1016/S0360-3016(98)00518-5
- Karlsson B, Lax I, Söderman M. Factors influencing the risk for complications following gamma knife radiosurgery of cerebral arteriovenous malformations. *Radiat Oncol* (1997) **43**(3):275–80. doi:10.1016/S0167-8140(97)00060-1

Conflict of Interest Statement: Brian T. Collins and Sean P. Collins have received honoraria from Accuray Inc. for previous work as consultants. The other co-authors declare that the research was conducted in the absence of any commercial or financial relationships that could be construed as a potential conflict of interest.

Received: 18 July 2014; accepted: 13 October 2014; published online: 04 November 2014.

Citation: Oermann EK, Murthy N, Chen V, Baimeedi A, Sasaki-Adams D, McGrail K, Collins SP, Ewend MG and Collins BT (2014) A multicenter retrospective study

of frameless robotic radiosurgery for intracranial arteriovenous malformation. *Front. Oncol.* **4**:298. doi: 10.3389/fonc.2014.00298

This article was submitted to Radiation Oncology, a section of the journal *Frontiers in Oncology*.

Copyright © 2014 Oermann, Murthy, Chen, Baimeedi, Sasaki-Adams, McGrail, Collins, Ewend and Collins. This is an open-access article distributed under the terms of the Creative Commons Attribution License (CC BY). The use, distribution or reproduction in other forums is permitted, provided the original author(s) or licensor are credited and that the original publication in this journal is cited, in accordance with accepted academic practice. No use, distribution or reproduction is permitted which does not comply with these terms.



Potential applications of image-guided radiotherapy for radiation dose escalation in patients with early stage high-risk prostate cancer

Nam P. Nguyen^{1*}, Rick Davis², Satya R. Bose¹, Suresh Dutta³, Vincent Vinh-Hung⁴, Alexander Chi⁵, Juan Godinez⁶, Anand Desai⁷, William Woods⁸, Gabor Altdorfer⁹, Mark D'Andrea¹⁰, Ulf Karlsson¹¹, Richard A. Vo¹², Thomas Sroka¹³ and the International Geriatric Radiotherapy Group

¹ Department of Radiation Oncology, Howard University, Washington, DC, USA

² Department of Radiation Oncology, Michael D. Wachtel Cancer Center, Oskosh, WI, USA

³ Department of Radiation Oncology, Medicine and Radiation Oncology PA, San Antonio, TX, USA

⁴ Department of Radiation Oncology, Martinique University Hospital, Martinique, France

⁵ Department of Radiation Oncology, University of West Virginia, Morgantown, WV, USA

⁶ Department of Radiation Oncology, Rochester Radiation Oncology Group, Rochester, NY, USA

⁷ Department of Radiation Oncology, Akron City Hospital, Akron, OH, USA

⁸ Department of Radiation Oncology, Richard A. Henson Institute, Salisbury, MD, USA

⁹ Department of Radiation Oncology, Camden Clark Cancer Center, Parkersburg, WV, USA

¹⁰ Department of Radiation Oncology, University Cancer Centers, Houston, TX, USA

¹¹ Department of Radiation Oncology, Marshfield Clinic, Marshfield, WI, USA

¹² University of Galveston School of Medicine, Galveston, TX, USA

¹³ Department of Radiation Oncology, Geisel School of Medicine at Dartmouth, Dartmouth College, Hanover, NH, USA

Edited by:

John Varlotta, University of Massachusetts Medical Center, USA

Reviewed by:

Joshua Silverman, New York University Medical Center, USA

Wenyin Shi, Thomas Jefferson University, USA

*Correspondence:

Nam P. Nguyen, Department of Radiation Oncology, Howard University Hospital, 2401 Georgia Avenue NW, Washington, DC 20060, USA

e-mail: namphong.nguyen@yahoo.com

Patients with early stage high-risk prostate cancer (prostate specific antigen > 20, Gleason score > 7) are at high risk of recurrence following prostate cancer irradiation. Radiation dose escalation to the prostate may improve biochemical-free survival for these patients. However, high rectal and bladder dose with conventional three-dimensional conformal radiotherapy may lead to excessive gastrointestinal and genitourinary toxicity. Image-guided radiotherapy (IGRT), by virtue of combining the steep dose gradient of intensity-modulated radiotherapy and daily pretreatment imaging, may allow for radiation dose escalation and decreased treatment morbidity. Reduced treatment time is feasible with hypo-fractionated IGRT and it may improve patient quality of life.

Keywords: prostate cancer, high-risk, image-guided radiotherapy, hypofractionation

INTRODUCTION

Prostate cancer is currently detected at an early stage because of routine screening for prostate specific antigen (PSA) in elderly males (1). Patients with low-risk early stage prostate cancer (PSA < 10, Gleason score < 5) demonstrate optimal results when treated with surgery or radiotherapy. However, in high-risk early stage prostate cancer patients (PSA > 20, Gleason score > 7), the current recommendation is androgen suppression therapy combined with radiotherapy because of potential for local recurrences and distant metastases (2). Increasing radiation dose to the prostate may improve local control and survival of these patients (3). However, normal organs adjacent to the prostate specifically the rectum, and bladder also receive a high radiation dose with dose escalation using the conventional three-dimensional conformal radiotherapy (3D-CRT) technique, which leads to a higher risk of complications (3). Thus, a radiotherapy technique that allows radiation dose escalation to the prostate while minimizing radiation to the rectum and bladder may improve the therapeutic ratio. Intensity-modulated radiotherapy (IMRT) has been introduced

recently to decrease excessive radiation dose to the normal organs near the prostate cancer because of the steep dose gradient away from the target (4). Compared to 3D-CRT, IMRT may increase survival rates in patients with high-risk disease because of reduced rectal volume irradiated over 70 Gy and significantly decreased gastrointestinal (GI) toxicity, thus allowing radiation dose escalation to the tumor (5). However, in radiation dose escalation trials for prostate cancer, patients who had higher rectal doses during IMRT were still at an increased risk of long-term rectal complications (6). Inclusion of a large rectal volume in the IMRT planning treatment volume (PTV) may be required to avoid a marginal miss and therefore lead to excessive rectal irradiation. The introduction of image-guided radiotherapy (IGRT), which combines the normal tissue sparing effect of IMRT and daily imaging, has been proven to decrease further radiation dose to the normal organs without compromising local control in head and neck cancer (7–9). Thus, IGRT may allow for radiation dose escalation in patients with early stage high-risk prostate cancer and improve biochemical-free survival while reducing treatment toxicity.

TECHNIQUES OF PROSTATE CANCER RADIATION THERAPY DELIVERY WITH IGRT

Currently, many systems are used for daily imaging and may be classified as invasive and non-invasive. In the invasive systems, metallic markers are implanted into the prostate as fiducial markers (FM) to guide radiation delivery. Usually, three seeds are implanted under ultrasound (US) guidance into the prostate before CT planning. Daily MV or kV CT are performed to align the seeds to the planning CT before each treatment. Alternatively, the seeds can be tracked in real time imaging with a robotic system (Cyberknife) or through electromagnetic waves emitted by the transponders (Calypso System), and allow accurate radiation delivery even though the prostate moves during treatment. In the non-invasive system, the prostate position before treatment can be detected either by US or by CT scan. The patient is shifted for set-up discrepancies and additional images are obtained to verify treatment accuracy. The US system is inexpensive, simple, and non-radiation-based, but is operator-dependent. The CT system provides either kV or MV imaging. Fan beam kV CT uses a diagnostic CT scan alongside the linear accelerator. Cone beam kV CT uses a gantry mounted kV source and a flat panel detector. A series of kV X-rays are taken when the gantry rotates and a 3D image is reconstructed. Image quality is superior with fan beam kV CT compared to cone beam CT, but the couch needs to be displaced between imaging and treatment, which may lead to positioning error. In the MV CT system, the imaging is performed by the treatment beam that rotates around the patient while the couch moves (helical Tomotherapy).

Image quality is inferior with MV CT compared to kV CT, but there are no metal artifacts, which may be helpful if the patient has hip prosthesis. The latest technology for tumor imaging is based on magnetic resonance imaging (MRI), which involves a hybrid Cobalt linear accelerator and an MRI (ViewRay). This is a promising technology for prostate cancer IGRT, as MRI provides better imaging of the prostate gland compared to CT scans. Furthermore, MRI allows visualization of gross tumor volume (GTV) inside the prostate and may enable a higher radiation dose using the simultaneous integrated boost (SIB) technique.

REDUCTION OF PROSTATE CANCER TREATMENT MORBIDITY ASSOCIATED WITH ACCURATE IMAGE GUIDANCE

Preliminary evidence suggests that better visualization of the prostate during radiotherapy leads to improved patient quality of life (QOL) because of the increased accuracy of radiation delivery. In a study of 282 prostate cancer patients treated with 3D-CRT with ($n = 154$) and without image guidance ($n = 128$), proctitis severity was significantly reduced with image guidance (10). Patients who had image guidance underwent prostate FM placement and MRI imaging before radiotherapy planning to outline the target volume. Rectal and urinary dysfunction during radiotherapy was assessed with QOL questionnaires. Despite a higher tumor dose to the prostate, patients treated with image guidance experienced less diarrhea and rectal pain compared to the ones who did not undergo IGRT. During radiotherapy, the prostate position changes daily depending on bladder and rectal filling. Accurate target localizing with intra-prostate FM instead of bony landmark fusion leads to a decreased volume of bladder and

rectum being irradiated to a high dose and therefore a reduction of acute morbidity. Gill et al. (11) reported significant reduction in severe urinary frequency, diarrhea, and fatigue in patients with prostate cancer who were treated with IGRT ($n = 265$) compared with patients not treated with IGRT ($n = 26$). Both groups were treated with IMRT using the same constraints and PTV margins. The prostate dose was higher for the group treated with IGRT (78 Gy) compared to those treated without IGRT (74 Gy). Thus, regardless of the radiotherapy technique, accurate localization of the prostate before treatment decreases treatment toxicity by eliminating the geographic miss of the prostate, which would lead to an excessive radiation dose to the adjacent non-involved normal structures. Other studies have corroborated the image guidance effects on sparing normal organs in patients with prostate cancer (12, 13).

RADIATION DOSE ESCALATION FOR HIGH-RISK PROSTATE CANCER PATIENTS TREATED WITH IGRT AND CONVENTIONAL FRACTIONATION

In patients with high-risk prostate cancer, long-term follow-up suggests that a radiation dose ≥ 80 –81 Gy to the tumor bed may be required for long-term biochemical control (14, 15). The effect of radiation dose escalation may be independent of hormonal therapy (15). Radiation doses up to 86.4 Gy were determined to be feasible with limited toxicity in prostate cancer patients treated with IMRT (16). In a study of 1,002 prostate cancer patients treated to 86.4 Gy with IMRT, late grade 3 GI and genitourinary (GU) toxicities were reported (0.7 and 2.2%, respectively). However, acute grade 3–4 toxicities were not reported in the study. Thus, IGRT may allow for radiation dose escalation and further reduction of normal tissue toxicity by combining IMRT and daily imaging. Indeed, preliminary evidence suggests that IGRT as a safe radiotherapy technique for radiation dose escalation in patients with prostate cancer. Takeda et al. (17) reported no acute grade 3–4 toxicities in 141 patients with intermediate or high-risk localized prostate cancer when the radiation dose was increased from 76 Gy ($n = 13$) to 80 Gy ($n = 128$). Only two patients developed long-term grade 3 toxicities. Kok et al. (18) compared late toxicities among 311 patients treated with IMRT for prostate cancer without image guidance (74 Gy) and with image guidance (78 Gy). Despite a higher radiation dose in this study, late GI toxicities were significantly reduced in patients with image guidance. In a similar study comparing IGRT (78 Gy) and 3D-CRT (76 Gy) for high-risk prostate cancer, late GI and GU toxicities were significantly decreased for patients treated with IGRT (19).

RADIATION DOSE ESCALATION FOR HIGH-RISK PROSTATE CANCER PATIENTS TREATED WITH IGRT AND HYPOFRACTIONATION

Prostate cancer cells are characterized by a low α/β ratio ranging from 0.8 to 2.2 Gy, suggesting that delivering a radiation dose higher than the conventional fractionation of 1.8–2 Gy/day may be more effective for cancer cell killing. On the opposite side is the risk of normal tissue injury associated with high dose hypofractionation. However, if the volume of rectal and bladder tissue exposed to a high radiation dose can be reduced with high precision radiation delivery, hypofractionation may be an

ideal radiation technique to reduce treatment time while potentially improving the biochemical control in patients with high-risk prostate cancer. Jerekzek-Fossa et al. (20) compared the acute toxicity of 179 prostate cancer patients treated with IGRT [70.2 Gy in 2.7 Gy/fraction (84.2 Gy dose equivalent in 2 Gy/fraction)] and 174 patients treated with 3D-CRT (80 Gy in 2 Gy fraction). There was no significant difference in toxicity between the two groups of patients. In a follow-up study, QOL of the patients treated with hypo-fractionated IGRT was not significantly affected long-term, thus illustrating that IGRT may be beneficial in patients with high-risk prostate cancer (21). A similar radiation dose escalation study was performed in 48 prostate cancer patients using regimens of 68.04 Gy at 2.52 Gy/fraction ($n = 32$), 70 Gy at 2.5 Gy/fraction ($n = 5$), and 70.2 Gy at 2.6 Gy/fraction. No patients developed grade 3–4 late toxicities (22). The safety of IGRT for hypofractionation was also corroborated in another study where patients with high-risk prostate cancer were treated up to 74.2 Gy in 2.65 Gy/fraction with the SIB technique. Only 1 out of 70 patients developed an acute grade 3 rectal reaction (23). A preliminary report from a randomized study comparing high dose hypofractionation to conventional fractionation with IGRT suggests that hypo-fractionation may allow for a higher radiobiologic dose without increasing treatment toxicity for high-risk prostate cancer patients. Patients ($n = 124$) were recruited and treated to 76 Gy in 2 Gy/fraction ($n = 57$) and 63 Gy in 3.15 Gy/fraction ($n = 67$) equivalent to 84 Gy in 2 Gy/fraction to the prostate with the SIB technique (24). There was no significant difference in acute toxicities between the two arms suggesting that IGRT may confer effective normal tissue sparing but long-term follow-up is needed as complications may develop later.

The extreme hypo-fractionation scheme for high-risk prostate cancer involves continuous tracking of the prostate with two orthogonal X-ray imagers that allow a tight PTV margin posteriorly (3 mm) while multiple non-coplanar beams improve the plan conformity compared to IMRT (Cyberknife) (25). Total treatment time can be reduced to 1 week instead of the conventional 8–9 weeks of treatment as the volume of rectum and bladder exposed to high radiation dose can be minimized. In addition, if treatment toxicity can be reduced, a high dose to the prostate may be feasible to improve local control. Oliai et al. (26) reported the acute toxicity and long-term complications of 70 patients with low- to high-risk prostate cancer treated with radiation dose escalation by Cyberknife (CK) ranging from 35 Gy in 7 Gy/fraction ($n = 5$), 36.25 Gy in 7.25 Gy/fraction ($n = 36$), and 37.5 Gy in 7.5 Gy/fraction ($n = 29$). Acute and late grade 3 GU toxicities were 4 and 3%, respectively. None of the patients experienced grade 3–4 toxicities at a median follow-up of 31 months. Katz et al. (27) also corroborated the low toxicity of CK for prostate cancer. Among 304 patients with low ($n = 211$), intermediate ($n = 81$), and high-risk ($n = 12$) prostate cancer treated with CK to 35 Gy in 7 Gy/fraction ($n = 50$) and 36.25 Gy in 7.25 Gy/fraction ($n = 254$), none of the patients developed acute grade 3–4 toxicity. At a median follow-up of 60 months, only 2% of the patients developed long-term grade 3 GU toxicity. A follow-up study suggested that prostate cancer patients treated with this fractionation on CK had QOL similar to that observed in conventional fractionation (28). Even though most patients treated with CK hypo-fractionation had low

to intermediate risk prostate cancer, late grade 3 GI and GU toxicities ranged from 0 to 3%, which confirmed the safety of CK for radiation dose escalation (29–34). The high radiobiologic equivalent dose of 92 Gy (corresponding to 35 Gy in 7 Gy/fraction with an α/β ratio of 1.5) or higher with hypo-fractionated CK suggests that this radiotherapy technique may be potentially effective for high-risk prostate cancer. However, this hypothesis will need to be tested in future prospective trials. It is encouraging that in a pooled analysis of patients with prostate cancer treated with hypo-fractionated CK, a 5-year PSA relapse-free survival of 81% was suggested for high-risk patients.

ROLE OF BRACHYTHERAPY IN RADIATION DOSE ESCALATION IN PATIENTS WITH HIGH-RISK PROSTATE CANCER

Brachytherapy may be the ideal modality of radiation dose escalation for prostate cancer either alone or as a boost. The radioactive seeds or high dose rate (HDR) brachytherapy catheters are inserted inside the prostate, thus prostate motion is not an issue for brachytherapy compared to external beam radiation. In addition, the radiation dose decreases proportionally to the square of the distance away from the radioactive sources and allows significant sparing of the rectum and bladder. Because of the risk of extracapsular extension of the tumor, brachytherapy is frequently given as a boost following external beam radiation, but brachytherapy without external beam radiation has been reported with excellent local control and survival in selected studies when combined with androgen deprivation therapy (35–37). A higher dose to the prostate ranging from 10,000 to 12,000 cGy may be achieved as a boost after external beam radiation with low dose rate (LDR) brachytherapy (38, 39). As a result, long-term biochemical-free survival has been observed with LDR brachytherapy boost for high-risk prostate cancer (40). Brachytherapy with HDR begins to play a prominent role in the management of high-risk prostate cancer because of the technical issues associated with LDR permanent seeds implant: discrepancy between planned and actual seeds distribution, inability to correct seeds position or to optimize the dose delivered once the seeds are in place, which may be related to the radiation oncologist technical skills. The HDR catheters are relatively easy to visualize with US and may be safely implanted outside the prostate capsule and into the seminal vesicles without the risk of seeds migration. Uncertainty over target dose associated with prostate volume changes, which occurs following LDR seeds implant is not an issue with HDR brachytherapy. Perhaps the most important advantage of HDR over LDR brachytherapy is the real time dose modulation, which provides immediate feedback to the physician and physicist for optimal catheter distribution and dwell time. Preliminary results of HDR monotherapy or combined with external beam radiotherapy were very encouraging with excellent biochemical-free survival and acceptable toxicity (35–37, 41, 42). Dose escalation with HDR boost after external beam radiotherapy was feasible and was reported to be associated with a higher biochemical-free survival in high-risk prostate cancer patients (43, 44). As most studies reported 3D-CRT with HDR brachytherapy, it would be interesting to combine IGRT and HDR brachytherapy for high-risk prostate cancer to decrease long-term complications in future prospective studies. Nevertheless,

brachytherapy is an invasive procedure with its complications and may not be indicated for all patients. The optimal radiation dose for disease control in high-risk prostate cancer has not been elucidated when combined with androgen deprivation therapy and needs to be investigated in future clinical trials.

CURRENT CONTROVERSIES IN THE MANAGEMENT OF HIGH-RISK PROSTATE CANCER

ROLE OF PELVIC RADIOTHERAPY IN THE TREATMENT OF HIGH RISK OF PROSTATE CANCER

As high-risk prostate cancer patients may have occult pelvic lymph nodes metastases that are not detected with current diagnostic technologies, pelvic lymph nodes irradiation may improve loco-regional control and survival. However, these patients also received androgen deprivation therapy that may affect micrometastases. On the other hand, treating the prostate and seminal vesicles only allows radiation dose escalation without the toxicity of pelvic irradiation. Radiation dose escalation from 64 to 74 Gy to a local field with 3D-CRT and neoadjuvant androgen deprivation has been reported to improve biochemical-free survival in a randomized study (45). Using the Roach formula to estimate the risk of pelvic lymph nodes metastases, a matched-pair analysis did not report the benefit of adding pelvic radiotherapy in patients at high risk (>15%) of lymph nodes metastases (46). Two randomized studies also corroborated the lack of survival benefit when the pelvis was radiated compared to irradiation of the prostatic bed only (47, 48). As an illustration, excellent local control and survival were observed in studies where HDR brachytherapy to the prostate were combined with hormonal therapy without pelvic irradiation (35–37, 49). The rate of distant metastases or pelvic failures did not increase in those studies. Thus, pelvic irradiation may not be necessary for high-risk prostate cancer when combined with androgen deprivation therapy and may increase treatment toxicity because of the increased volume of normal tissues in the radiation fields.

PROSTATE MOTION AND OPTIMAL PTV FOR IGRT

Prostate motion depends on rectal and bladder filling. In the supine position for treatment, prostate position is less affected by bladder filling because of bladder extension anteriorly. However, in the prone position, pressure on the bladder may push the prostate posteriorly and the prostate position is affected by the patient breathing pattern (50). Prostate motion ranged from 1.5 to 3.7 mm, 0.7 to 1.9 mm, and 1.4 to 3.6 mm in the antero-posterior (AP), left-to-right (LR), and superior-inferior (SI) dimension, respectively (51–55). The magnitude of prostate motion also depends on the individual patient. Choice of a PTV also depends on whether the institution includes pelvic lymph node irradiation or not as it would be difficult to tract the motion of two independent systems. In that sense, radiation dose escalation would be technically easier without pelvic irradiation. PTV margins for the lymph nodes may need to be enlarged to avoid under dosing the pelvic lymph nodes if the set up needs to change because of prostate motion secondary to rectal filling. The choice of the PTV margins also depends on the prostate tracking system used by the institution, either with FM or electromagnetic transponders (invasive method), or with soft tissue fusion based on CBCT or MVCT. For the non-invasive method, once an optimum PTV has been

selected by the institution, adaptive therapy performed for the first week or two of treatment based on observed prostate motion on an individual patient may allow the clinician to reduce the PTV for example if the established PTV may be too generous. These efforts may reduce interfraction motion but will not reduce intrafraction motion that occurs during treatment. Unless the institution uses an online tracking system for treatment delivery such as the robotic CK, PTV margins should take into account intrafraction motion, which may be dependent on treatment time. The use of an endorectal balloon may decrease intrafraction prostate motion and may reduce further rectal dose by pushing the posterior rectal wall away from the high dose area (56). Another factor to take into consideration is the deformation of the prostate, which may be related to peristalsis, degree of pelvic musculature contraction, and breathing pattern. Any prospective trial on radiation dose escalation should take into consideration the degree prostate deformation during treatment as under dosing of the prostate may occur in patients with a large degree of prostate deformation (more than 10% of prostate volume) (57).

In summary, PTV margins should be determined by the type of IGRT image tracking and radiation treatment delivery. For example, published recommended LR, AP, and SI margins ranged from 3.6, 3.7, and 3.7 mm and 2.46, 2.28, and 2.56 mm for FM and CBCT, respectively (58, 59).

DOSE PRESCRIPTION COMPARISON AMONG INSTITUTIONS USING PROSTATE IGRT

Currently, there is no standard recommendation on how to prescribe radiation dose for patients undergoing prostate IGRT. Each institution set up a specific protocol making dose comparison difficult among various institutions to assess long-term local control, and complications. In addition, there were different dose schedule fractionation, and various PTV margins based the technology used for image tracking. As an illustration, Norkus et al. (24) reported the following protocol in a randomized study of dose escalation using hypofractionation and CBCT for image guidance. The prostate PTV was treated to a total dose of 76 Gy at 2 Gy/fraction and 63 Gy at 3.15 Gy/fraction, respectively, with a PTV margin of 10 mm except posteriorly (7 mm). The dose was optimized so that 95–108% of the PTV received the prescribed dose. On the other hand, Takeda et al. (17) treated the prostate PTV to a total dose of 80 Gy in 2 Gy/fraction using FM with a PTV margin of 5 mm except posteriorly (3 mm). The dose was prescribed to cover 95% of the target volume. At another institution, even though FM was used for image guidance, the prostate PTV margin was 10 mm except posteriorly (6 mm). The prescribed dose was 86.4 Gy to a maximum isodose encompassing the PTV (60). As the preliminary results from these institutions are excellent for local control with acceptable toxicity, it would be very difficult to set up a standard recommendation for PTV margins and dose.

FUTURE DIRECTIONS OF IMAGE-GUIDED RADIOTHERAPY FOR RADIATION DOSE ESCALATION IN PATIENTS WITH HIGH-RISK PROSTATE CANCER

Patient with high-risk prostate cancer often have a heterogeneous tumor distribution within the prostate with areas of concentrated cancer cells responsible for disease recurrence following

radiotherapy (61). These intra-prostatic tumor nodules may require a higher dose to achieve local control. The conventional radiotherapy technique with IMRT or IGRT for prostate cancer consists of a homogeneous radiation dose distribution within the prostate. Thus, previous studies of radiation dose escalation increased the total dose to the prostate, which may account for the risk of late GI and GU complications. New imaging techniques such as diffusion-weighted (DW), MRI, magnetic resonance spectroscopy (MRS), and positron emission tomography (PET)-CT are more accurate for detection of these intra-prostatic tumor nodules and may allow for radiation dose escalation within the prostate (62–64). Dosimetric studies suggest that radiation dose escalation for intra-prostatic tumors nodules with IGRT is feasible and may allow significant reduction of the rectal dose (65). In a clinical study of 118 patients with prostate cancer, the GTV defined by MRI or MRS was treated to 80–81 Gy while the prostate dose was limited to 78 Gy with IMRT. No patients developed grade 3–4 GI toxicity (66). Thus, IGRT may be a promising technique for radiation dose escalation on intra-prostatic nodules as significant rectal toxicity has been observed in patients who had hypo-fractionated IGRT up to 50 Gy in 10 Gy/fraction (67).

CONCLUSION

Image-guided radiotherapy is a promising technique to reduce treatment toxicity in patients with early stage high-risk prostate carcinoma and may improve biochemical-free survival associated with radiation dose escalation. Reduced treatment time with hypo-fractionated IGRT may improve patient QOL as they will have more time to spend with their family. Future clinical trials focused on improving tumor imaging with MRI, MRS, and PET-CT to reduce long-term complications associated with high dose prostate irradiation are warranted.

REFERENCES

- DeSantis CE, Lin CC, Mariotto AB, Siegel RL, Stein KD, Kramer JL, et al. Cancer treatment and survivorship statistics, 2014. *CA Cancer J Clin* (2014) **64**(4):252–71. doi:10.3322/caac.21235
- Nguyen PL, Chen MH, Beard CJ, Suh WW, Renshaw AA, Lofredo AA, et al. Radiation with or without 6 months of androgen suppression therapy in intermediate and high-risk clinically localized prostate cancer: a postrandomization analysis by subgroup. *Int J Radiat Oncol Biol Phys* (2010) **77**:1046–52. doi:10.1016/j.ijrobp.2009.06.038
- Kuban DA, Tucker SL, Dong L, Starkshall G, Huang EH, Cheung MR, et al. Long-term results of the M. D. Anderson dose-escalation trial for prostate cancer. *Int J Radiat Oncol Biol Phys* (2008) **70**:67–74. doi:10.1016/j.ijrobp.2007.06.054
- Michalski JM, Yan Y, Watkins-Bruner D, Bosch WR, Winter K, Galvin JM, et al. Preliminary toxicity analysis of 3-dimensional conformal radiation therapy versus intensity-modulated radiation therapy on the high dose arm of the Radiation Therapy Oncology Group 0126 prostate cancer trial. *Int J Radiat Oncol Biol Phys* (2013) **87**:932–8. doi:10.1016/j.ijrobp.2013.07.041
- Gandaglia G, Karakiewicz PI, Briganti A, Trinh QD, Schiffmann J, Tian Z, et al. Intensity-modulated radiation therapy leads to survival benefit only in patients with high-risk prostate cancer: a population-based study. *Ann Oncol* (2014) **25**:979–86. doi:10.1093/annonc/mdu087
- Hoffman KE, Voong KR, Pugh TJ, Skinner H, Levy LB, Takiar V, et al. Risk of late toxicity in men receiving dose-escalated hypofractionated intensity modulated prostate radiation therapy: results from a randomized trial. *Int J Radiat Oncol Biol Phys* (2014) **88**:1074–84. doi:10.1016/j.ijrobp.2014.01.015
- Nguyen NP, Ceizyk M, Vos P, Vinh-Hung V, Davis R, Desai A, et al. Effectiveness of image-guided radiotherapy for laryngeal sparing in head and neck cancer. *Oral Oncol* (2010) **46**:283–6. doi:10.1016/j.oraloncology.2010.01.010
- Nguyen NP, Smith-Raymond L, Vinh-Hung V, Vos P, Davis R, Desai A, et al. Feasibility of tomotherapy-based image-guided radiotherapy to reduce aspiration risk in patients with non-laryngeal and non-hypopharyngeal head and neck cancer. *PLoS One* (2013) **3**:e56290. doi:10.1371/journal.pone.0056290
- Nguyen NP, Ceizyk M, Vos P, Betz M, Chi A, Almeida F, et al. Feasibility of tomotherapy-based image-guided radiotherapy for locally advanced oropharyngeal cancer. *PLoS One* (2013) **8**:e60268. doi:10.1371/journal.pone.0060268
- Singh J, Greer PB, White MA, Parker J, Patterson J, Tang CI, et al. Treatment related morbidity in prostate cancer: a comparison of 3-dimensional conformal radiation therapy with and without image guidance using implanted fiducial markers. *Int J Radiat Oncol Biol Phys* (2013) **85**:1018–23. doi:10.1016/j.ijrobp.2012.07.2376
- Gill S, Thomas J, Fox C, Kron T, Rolfo A, Leahy M, et al. Acute toxicity in prostate cancer treated with and without image-guided radiotherapy. *Radiat Oncol* (2011) **6**:145. doi:10.1186/1748-717X-6-145
- Lipps IM, Dehnad H, Van Gils CH, Kruger B, Arto E, Van der Heide UA, et al. High-dose intensity-modulated radiotherapy for prostate cancer using fiducial marker-based position verification: acute and late toxicity in 331 patients. *Radiat Oncol* (2008) **3**:35. doi:10.1186/1748-717X-3-15
- Soete G, Verellen D, Michielsen D, Rappe B, Keuppen F, Storme G. Image-guided conformal arc therapy for prostate cancer: early side-effects. *Int J Radiat Oncol Biol Phys* (2006) **66**:S141–4. doi:10.1016/j.ijrobp.2006.05.077
- Zeledsky MJ, Pei X, Chou JF, Schechter M, Kollmeier M, Cox B, et al. Dose escalation for prostate cancer radiotherapy: predictors of long-term biochemical tumor control and distant metastases-free survival outcomes. *Eur Urol* (2011) **60**:1133–9. doi:10.1016/j.eururo.2011.08.029
- Pahlajani N, Ruth KJ, Buyyounouski MK, Chen DYT, Horwitz EM, Hanks GE, et al. Radiotherapy doses of 80 Gy or higher are associated with lower mortality in men with Gleason score 8–10 prostate cancer. *Int J Radiat Oncol Biol Phys* (2012) **82**:1949–56. doi:10.1016/j.ijrobp.2011.04.005
- Spratt DE, Pei X, Yamada J, Kollmeier MA, Cox B, Zeledsky MJ. Long-term survival and toxicity in patients treated with high dose intensity-modulated radiation therapy for prostate cancer. *Int J Radiat Oncol Biol Phys* (2013) **85**:686–92. doi:10.1016/j.ijrobp.2012.05.023
- Takeda K, Takai Y, Narazaki K, Mitsuya M, Umezawa R, Kadoya N, et al. Treatment outcome of high-dose image-guided intensity-modulated radiotherapy using intra-prostatic fiducial markers for localized prostate cancer at a single institute in Japan. *Radiat Oncol* (2012) **7**:105. doi:10.1186/1748-717X-7-105
- Kok D, Gill S, Bressel M, Byrne K, Kron T, Fox C, et al. Late toxicity and biochemical control in 554 prostate cancer patients treated with and without dose escalated image guided radiotherapy. *Radiother Oncol* (2013) **107**:140–6. doi:10.1016/j.radonc.2013.04.007
- Sveistrup J, Rosenshield PM, Deasy JO, Oh JH, Pommer T, Peterson PM, et al. Improvement in toxicity in high risk prostate cancer patients treated with image-guided intensity-modulated radiation therapy compared to 3D conformal radiotherapy without daily image guidance. *Radiat Oncol* (2014) **9**:44. doi:10.1186/1748-717X-9-44
- Jereczek-Fossa BA, Zerini D, Fodor C, Santoro L, Cambria R, Garibaldi C, et al. Acute toxicity of image-guided hypofractionated radiotherapy for prostate cancer: non-randomized comparison with conventional fractionation. *Urol Oncol* (2011) **29**:523–32. doi:10.1016/j.urolonc.2009.10.004
- Jereczek-Fossa BA, Santoro L, Zerini D, Fodor C, Vischioni B, Dispignier M, et al. Image-guided hypofractionated radiotherapy and quality of life for localized prostate cancer: prospective longitudinal study in 337 patients. *J Urol* (2013) **189**:2099–103. doi:10.1016/j.juro.2013.01.005
- Guerra JLL, Isa N, Matute R, Russo M, Puebla F, Kim MM, et al. Hypofractionated helical tomotherapy using 2.5–2.6 Gy daily fractions for localized prostate cancer. *Clin Transl Oncol* (2013) **15**:271–7. doi:10.1007/s12094-012-0907-y
- Alongi F, Fogliata A, Navarría P, Tozzi A, Mancuso P, Lobefalo F, et al. Moderate hypofractionation and simultaneous integrated boost with volumetric modulated arc therapy (RapidArc) for prostate cancer. Report of feasibility and acute toxicity. *Strahlenther Onkol* (2012) **188**:990–6. doi:10.1007/s00066-012-0171-7
- Norkus D, Karkhelyte A, Engels B, Versmessen H, Griskevicius R, De Ridder M, et al. A randomized hypofractionation dose escalation trial for high risk prostate cancer patients: interim analysis of acute toxicity and quality of life in 124 patients. *Radiat Oncol* (2013) **8**:206. doi:10.1186/1748-717X-8-206
- Hossain S, Xia P, Huang K, Descovich M, Chuang C, Gottschalk AR, et al. Dose gradient near target-normal structure interface for nonisocentric cyberknife

- and isocentric intensity-modulated body radiotherapy for prostate cancer. *Int J Radiat Oncol Biol Phys* (2010) **78**:58–63. doi:10.1016/j.ijrobp.2009.07.1752
26. Oliai C, Lanciano R, Sprandio B, Yang J, Lamond J, Arrigo S, et al. Stereotactic body radiation therapy for the primary treatment of localized prostate cancer. *J Radiat Oncol* (2013) **2**:63–70. doi:10.1007/s13566-012-0067-2
27. Katz AJ, Santoro M, Diblasio F, Ashley R. Stereotactic body radiotherapy for localized prostate cancer: disease control and quality of life at 6 years. *Radiat Oncol* (2013) **8**:118. doi:10.1186/1748-717X-8-118
28. Bhattachari O, Chen LN, Woo J, Park J, Kim JS, Moures R, et al. Patient-reported outcomes following stereotactic body radiation therapy for clinically localized prostate cancer. *Radiat Oncol* (2014) **9**:52. doi:10.1186/1748-717X-9-52
29. King CR, Brooks JD, Gill H, Presti JC Jr. Long-term outcomes from a prospective trial of stereotactic body radiotherapy for low risk prostate cancer. *Int J Radiat Oncol Biol Phys* (2012) **82**:877–82. doi:10.1016/j.ijrobp.2010.11.054
30. McBride SM, Wong DS, Dombrowski JJ, Harkins B, Tapella P, Hanscom HN, et al. Hypofractionated stereotactic body radiotherapy in low-risk prostate adenocarcinoma: preliminary results of a multi-institutional phase I feasibility trial. *Cancer* (2012) **118**:3681–90. doi:10.1002/cncr.26699
31. Bolzicco G, Favretto MS, Satariano N, Scremin E, Tambone C, Tasca A. A single center study of 100 consecutive patients with localized prostate cancer treated with stereotactic body radiotherapy. *BMC Urol* (2013) **13**:49. doi:10.1186/1471-2490-13-49
32. Ju AW, Wang H, Oermann EK, Sherer BA, Uhm H, Chen VJ, et al. Hypofractionated stereotactic body radiation therapy as monotherapy for intermediate-risk prostate cancer. *Radiother Oncol* (2013) **8**:30. doi:10.1186/1748-717X-8-30
33. Lee YH, Son SH, Yoon SC, Yu M, Choi BQ, Kim YS, et al. Stereotactic body radiotherapy for prostate cancer: a preliminary report. *Asia Pac J Clin Oncol* (2014) **10**:e46–53. doi:10.1111/j.1743-7563.2012.01589.x
34. Kang JK, Cho CK, Choi CW, Yoo S, Kim MS, Yang K, et al. Image-guided stereotactic body radiation therapy for localized prostate cancer. *Tumori* (2011) **97**:43–8. doi:10.1700/611.7137
35. Yoshioka Y, Konishi K, Sumida I, Takahashi Y, Isohashi F, Ogata H, et al. Monotherapeutic high-dose rate brachytherapy for prostate cancer: five-year results of an extreme fractionation regimen with 54 Gy in nine fractions. *Int J Radiat Oncol Biol Phys* (2011) **80**:469–75. doi:10.1016/j.ijrobp.2010.02.013
36. Zamboglou N, Tselis N, Baltas D, Buhleir T, Martin T, Milickovis N, et al. High dose rate interstitial brachytherapy as monotherapy for clinically localized prostate cancer: treatment evolution and mature results. *Int J Radiat Oncol Biol Phys* (2013) **85**:672–8. doi:10.1016/j.ijrobp.2012.07.004
37. Yoshida K, Yamazaki H, Takenada T, Kotsuma T, Yoshida M, Masui K, et al. High dose rate interstitial brachytherapy in combination with androgen deprivation therapy for prostate cancer. *Strahlenther Oncol* (2014) **190**:1015–20. doi:10.1007/s00066-014-0675-4
38. Strom TJ, Hutchinson SZ, Shrinath K, Cruz AA, Figura NB, Nethers K, et al. External beam radiation therapy and a low dose rate brachytherapy boost without or with androgen deprivation therapy for prostate cancer. *Int Braz J Urol* (2014) **40**:474–83. doi:10.1590/S1677-5538.IBJU.2014.04.05
39. Ohashi T, Yorozu A, Saito S, Momma T, Nishiyama T, Yamashita S, et al. Combined brachytherapy and external beam radiotherapy without androgen deprivation therapy for high risk prostate cancer. *Radiat Oncol* (2014) **9**:13. doi:10.1186/1748-717X-9-13
40. Stone NN, Stock RG. 15-year cause specific and all cause specific survival following brachytherapy for prostate cancer. Negative impact of long-term hormonal therapy. *J Urol* (2014) **192**:754–9. doi:10.1016/j.juro.2014.03.094
41. Wahlgren T, Nilsson S, Ryberg M, Lennernas B, Brandberg Y. Combined curative radiotherapy including HDR brachytherapy and androgen deprivation in localized prostate cancer: a prospective assessment of acute and late treatment toxicity. *Acta Oncol* (2005) **44**:633–43. doi:10.1080/02841860510029716
42. Valero J, Cambeiro M, Galan C, Teijeira M, Romero P, Zudaire J, et al. Phase II trial of radiation dose escalation with conformal external beam radiotherapy and high dose rate brachytherapy combined with long-term androgen suppression in unfavorable prostate cancer: feasibility report. *Int J Radiat Oncol Biol Phys* (2010) **76**:386–92. doi:10.1016/j.ijrobp.2009.01.059
43. Ares C, Popowski Y, Pampallona S, Nouet P, Dipasquale P, Bieri S, et al. Hypofractionated boost with high dose rate brachytherapy and open magnetic resonance imaging-guided implants for locally aggressive prostate cancer: a sequentially dose escalation pilot study. *Int J Radiat Oncol Biol Phys* (2009) **75**:656–63. doi:10.1016/j.ijrobp.2008.11.023
44. Martinez AA, Gonzalez J, Ye H, Ghilezan M, Shetty S, Kernen K, et al. Dose escalation improves cancer-related events at 10 years for intermediate and high risk prostate cancer patients treated with hypofractionated high dose rate boost and external beam radiotherapy. *Int J Radiat Oncol Biol Phys* (2011) **79**:363–70. doi:10.1016/j.ijrobp.2009.10.035
45. Dearnaley DP, Jovic G, Syndikus A, Khoo V, Cowan RA, Graham JD, et al. Escalated dose versus control dose conformal radiotherapy for prostate cancer: long-term results from the MRC RT01 randomized controlled trial. *Lancet Oncol* (2014) **15**:464–73. doi:10.1016/S1470-2045(14)70040-3
46. Vargas CE, Demanes J, Boike TP, Barnaba MC, Skoolisriyaporn P, Schour L, et al. Matched pair analysis of prostate cancer patients with a high risk of positive pelvic lymph nodes treated with and without pelvic RT and high dose radiation using high dose rate brachytherapy. *Am J Clin Oncol* (2006) **29**:451–7. doi:10.1097/01.coc.0000221304.74360.8c
47. Pommier P, Chabaud S, Lagrange JL, Richaud P, Lesauvage F, Le Prise E, et al. Is there a role for pelvic irradiation in localized prostate adenocarcinoma. *J Clin Oncol* (2007) **25**:5366–73. doi:10.1200/JCO.2006.10.5171
48. Asbell SO, Krall JM, Pipelich MV, Baerwald H, Sause WT, Hanks GE, et al. Elective pelvic irradiation in stage A2, B carcinoma of the prostate: analysis of RTOG 77-06. *Int J Radiat Oncol Biol Phys* (1988) **15**:1307–16. doi:10.1016/0360-3016(88)90225-8
49. Hoskin P, Rojas A, Ostler P, Hughes R, Alonzi R, Lowe G, et al. High dose rate brachytherapy with two or three fractions as monotherapy in the treatment of locally advanced prostate cancer. *Radiother Oncol* (2014) **112**:63–7. doi:10.1016/j.radonc.2014.06.007
50. Malone S, Crook JM, Kendal WS, Szanto J. Respiratory-induced prostate motion: quantification and characterization. *Int J Radiat Oncol Biol Phys* (2000) **48**:105–9. doi:10.1016/S0360-3016(00)00603-9
51. Rudat V, Schraube P, Oetzel D, Zierhut D, Flentje M, Wannenmacher M. Combined error of patient positioning variability and prostate motion uncertainty in 3D conformal radiotherapy of localized prostate cancer. *Int J Radiat Oncol Biol Phys* (1996) **35**:1027–34. doi:10.1016/0360-3016(96)00204-0
52. Althof VG, Hoekstra CJ, te Loo HJ. Variation in prostate position relative to adjacent bony anatomy. *Int J Radiat Oncol Biol Phys* (1996) **34**:709–15. doi:10.1016/0360-3016(95)02162-0
53. Nederveen AJ, van der Heide UA, Dehnah H, van Morselaar RJ, Hofman P, Lagendijk JJ. Measurements and clinical consequences of prostate motion during a radiotherapy fraction. *Int J Radiat Oncol Biol Phys* (2002) **53**:206–14. doi:10.1016/S0360-3016(01)02823-1
54. Antolak JA, Rosen LL, Childress CH, Zagard GK, Pollack A. Prostate target volume variations during a course of radiotherapy. *Int J Radiat Oncol Biol Phys* (1998) **42**:661–72. doi:10.1016/S0360-3016(98)00248-X
55. Hanley J, Lumley MA, Mageras GS, Sun J, Zelefsky MJ, Leibel SA, et al. Measurement of patient positioning errors in three-dimensional conformal radiotherapy of prostate. *Int J Radiat Oncol Biol Phys* (1997) **37**:435–44. doi:10.1016/S0360-3016(96)00526-3
56. Smeenk RJ, Louwe RJW, Langen KJ, Shah AP, Kupelian AP, van Lin E, et al. An endorectal balloon reduces intrafraction prostate motion during radiotherapy. *Int J Radiat Oncol Biol Phys* (2012) **83**:661–9. doi:10.1016/j.ijrobp.2011.07.028
57. Mayyas E, Kim J, Kumar S, Liu C, Wen N, Movsas B, et al. A novel approach for evaluation of prostate deformation and associated dosimetric implications in IGRT of the prostate. *Med Phys* (2014) **41**:091709. doi:10.1111/1.4893196
58. Skarsgard D, Cadman P, El-Gayed A, Pearcey R, Tai P, Pervaz N, et al. Planning target volume margins for prostate radiotherapy using daily electronic portal imaging and implanted fiducial markers. *Radiat Oncol* (2010) **5**:52. doi:10.1186/1748-717X-5-52
59. Tanyi JA, He T, Summers PA, Mburu JA, Kato CM, Rhodes SM, et al. Assessment of planning target volume margins for intensity-modulated radiotherapy of the prostate gland: role of daily inter- and intra-fraction motion. *Int J Radiat Oncol Biol Phys* (2010) **78**:1579–85. doi:10.1016/j.ijrobp.2010.02.001
60. Zelefsky MJ, Kollmeier M, Cox B, Fidaleo A, Sperling D, Pei X, et al. Improved clinical outcomes with high dose image-guided radiotherapy compared with non-IGRT for the treatment of clinically localized prostate cancer. *Int J Radiat Oncol Biol Phys* (2012) **84**:125–9. doi:10.1016/j.ijrobp.2011.11.047
61. Hong SK, Eastham JA, Fine SW. Localization of higher grade tumor foci in potential candidates for active surveillance who opt for radical prostatectomy. *Prostate Int* (2013) **1**:152–7. doi:10.12954/PI.13029

62. Styles C, Ferris N, Mitchell C, Murphy D, Frydenberg M, Mills J, et al. Multi-parametric 3T MRI in the evaluation of intraglandular prostate cancer: correlation with histopathology. *J Med Imaging Radiat Oncol* (2014) **58**(4):439–48. doi:10.1111/1754-9485.12189
63. Anwar M, Westphalen AC, Jung AJ, Noworolski SM, Simko JP, Kurhanewicz J, et al. Role of endorectal and MR imaging and MR spectroscopy imaging in defining treatable intraprostatic tumor foci in prostate cancer: quantitative analysis of imaging contour compared to whole-mount histopathology. *Radiother Oncol* (2014) **110**:303–8. doi:10.1016/j.radonc.2013.12.003
64. Mena E, Turkbey B, Mani H, Adler H, Valera VA, Bernado M, et al. ¹¹C-Acetate PET-CT in localized prostate cancer: a study with MRI and histopathologic correlation. *J Nucl Med* (2012) **53**:538–45. doi:10.2967/jnumed.111.096032
65. Onal C, Sonmez S, Erbay G, Guler OC, Arslan G. Simultaneous integrated boost to intraprostatic lesions using different energy levels of intensity-modulated radiotherapy and volumetric arc therapy. *Br J Radiol* (2014) **87**:20130617. doi:10.1259/bjr.20130617
66. Fonteyne V, Villeirs G, Speelers B, de Neve W, de Wagter C, Lumen N, et al. Intensity-modulated radiotherapy as primary therapy for prostate cancer: report on acute toxicity after dose escalation with simultaneous integrated boost to the prostate. *Int J Radiat Oncol Biol Phys* (2008) **72**:799–807. doi:10.1016/j.ijrobp.2008.01.040
67. Kim DW, Cho LC, Straka C, Christie A, Lotan Y, Pistenmaa D, et al. Predictors of rectal tolerance observed in a dose-escalated phase 1-2 trial of stereotactic body radiotherapy for prostate cancer. *Int J Radiat Oncol Biol Phys* (2014) **89**:509–17. doi:10.1016/j.ijrobp.2014.03.012

Conflict of Interest Statement: The authors declare that the research was conducted in the absence of any commercial or financial relationships that could be construed as a potential conflict of interest.

Received: 01 August 2014; accepted: 15 January 2015; published online: 02 February 2015.

*Citation: Nguyen NP, Davis R, Bose SR, Dutta S, Vinh-Hung V, Chi A, Godinez J, Desai A, Woods W, Altdorfer G, D'Andrea M, Karlsson U, Vo RA, Sroka T and the International Geriatric Radiotherapy Group (2015) Potential applications of image-guided radiotherapy for radiation dose escalation in patients with early stage high-risk prostate cancer. *Front. Oncol.* **5**:18. doi: 10.3389/fonc.2015.00018*

This article was submitted to Radiation Oncology, a section of the journal Frontiers in Oncology.

Copyright © 2015 Nguyen, Davis, Bose, Dutta, Vinh-Hung, Chi, Godinez, Desai, Woods, Altdorfer, D'Andrea, Karlsson, Vo, Sroka and the International Geriatric Radiotherapy Group. This is an open-access article distributed under the terms of the Creative Commons Attribution License (CC BY). The use, distribution or reproduction in other forums is permitted, provided the original author(s) or licensor are credited and that the original publication in this journal is cited, in accordance with accepted academic practice. No use, distribution or reproduction is permitted which does not comply with these terms.



Rationale for stereotactic body radiation therapy in treating patients with oligometastatic hormone-naïve prostate cancer

Onita Bhattacharji¹, Leonard N. Chen¹, Michael Tong¹, Siyuan Lei¹, Brian T. Collins¹, Pranay Krishnan², Christopher Kalhorn³, John H. Lynch⁴, Simeng Suy¹, Anatoly Dritschilo¹, Nancy A. Dawson⁵ and Sean P. Collins^{1*}

¹ Department of Radiation Medicine, Georgetown University Hospital, Washington, DC, USA

² Department of Radiology, Georgetown University Hospital, Washington, DC, USA

³ Department of Neurosurgery, Georgetown University Medical Center, Washington, DC, USA

⁴ Department of Urology, Georgetown University Hospital, Washington, DC, USA

⁵ Department of Oncology, Lombardi Comprehensive Cancer Center, Georgetown University Medical Center, Washington, DC, USA

Edited by:

Nam Phong Nguyen, International Geriatric Radiotherapy Group, USA

Reviewed by:

Jaroslaw T. Hepel, Brown University, USA

Johnny Kao, Good Samaritan Hospital Medical Center, USA

***Correspondence:**

Sean P. Collins, Department of Radiation Medicine, Georgetown University Medical Center, 3800 Reservoir Road, NW, Washington, DC 20007, USA

e-mail: spc9@georgetown.edu

Despite advances in treatment for metastatic prostate cancer, patients eventually progress to castrate-resistant disease and ultimately succumb to their cancer. Androgen deprivation therapy (ADT) is the standard treatment for metastatic prostate cancer and has been shown to improve median time to progression and median survival time. Research suggests that castrate-resistant clones may be present early in the disease process prior to the initiation of ADT. These clones are not susceptible to ADT and may even flourish when androgen-responsive clones are depleted. Stereotactic body radiation therapy (SBRT) is a safe and efficacious method of treating clinically localized prostate cancer and metastases. In patients with a limited number of metastatic sites, SBRT may have a role in eliminating castrate-resistant clones and possibly delaying progression to castrate-resistant disease.

Keywords: prostate cancer, SBRT, IGRT, cyberknife, oligometastases, hormone-naïve

STEREOTACTIC BODY RADIATION THERAPY

Radiation oncologists strive to maximize tumor control while minimizing normal tissue toxicity. Over the past several years, advances in image-guided radiation treatment (IGRT) have allowed the treatment of tumors with increased efficacy and reduced toxicity (1–4). For example, stereotactic body radiation therapy (SBRT) may improve tumor control and reduce treatment-related toxicity through improved targeting and management of tumor motion (5). Accurate tumor targeting means that radiation may be delivered with relatively narrow margins to account for uncertainty in target position. This allows for high-dose, extremely hypofractionated treatment courses (1–5 fractions) that may be more radiobiologically effective and are certainly more convenient for patients (6, 7). For example, the CyberKnife Radiosurgical System (Accuray) is capable of localizing the prostate and adjusting the radiation beam accordingly in real time throughout a treatment fraction (8). This feature allows for a reduction in the planning target volume (PTV) and therefore better limits the dose to adjacent rectum and bladder (Figure 1). Multi-institutional experience demonstrates that this technology

allows investigators to administer higher doses to the prostate with biochemical disease-free survival and toxicity rates similar to conventional treatments (9–14). It is hoped that SBRT will also positively impact patient outcomes in patients with limited metastatic disease.

OLIGOMETASTASES

Patients with controlled primaries and “oligometastatic” disease may experience long-term stability in the number of metastatic sites (15). Oligometastatic prostate cancer has been defined as five or fewer sites due to the more favorable outcomes seen in these patients (Figure 2) (16). Hellman and Weichselbaum first proposed the existence of oligometastatic disease as a clinically significant state separate from polymetastatic disease and suggested a more causal relationship between the size or grade of a tumor and its propensity for metastatic spread (17). Corbin et al. expanded on this concept suggesting the development of a specific oligometastatic phenotype over the natural course of a cancer’s evolution that is less aggressive than other metastatic phenotypes (18). This theory has been corroborated by microRNA analysis of clinically limited metastatic disease that accurately characterizes which patients will remain oligometastatic and which patients will proceed to polymetastatic disease (19). For patients with limited metastatic sites, SBRT to the oligometastases may offer long-term disease control and impact survival (20). Data are emerging that patients with limited asymptomatic metastases may experience improved disease-free survival and quality of life after SBRT (21). We hypothesize

Abbreviations: ADT, androgen deprivation therapy; CRPC, castrate-resistant prostate cancer; DVH, dose-volume histogram; GTV, gross target volume; IGRT, image-guided radiation treatment; LHRH, luteinizing hormone-releasing hormone; PAP, prostatic acid phosphatase; PSA, prostate-specific antigen; PTV, planning target volume; SBRT, stereotactic body radiation therapy; TURP, transurethral resection of the prostate.

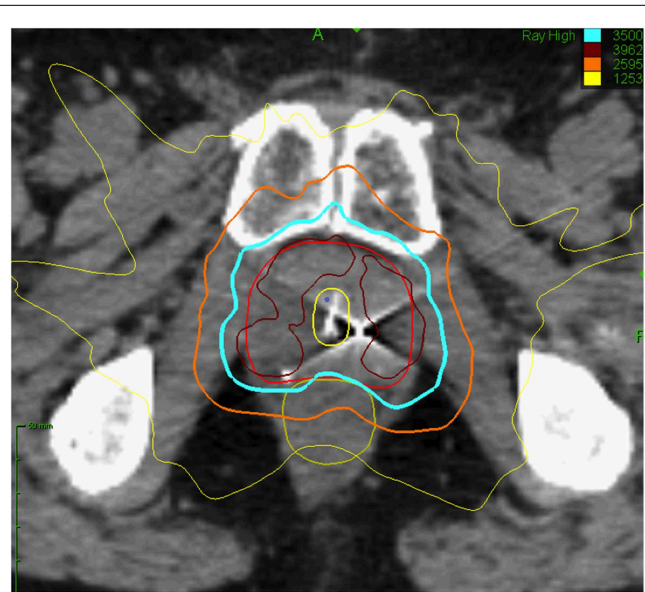


FIGURE 1 | Prostate SBRT: treatment planning axial computed tomography images demonstrating the prostate (red line), prostatic urethra (yellow), and rectum (green line). Isodose lines shown as follows: 115% of the prescription dose, maroon line; 100% of the prescription dose, light blue line; 75% of the prescription dose, orange line; and 35% of the prescription dose, green line.

that in oligometastatic prostate cancer patients, androgen deprivation therapy (ADT) would eliminate micrometastatic disease while SBRT would eradicate large tumor deposits that may be more likely to develop castrate-resistant clones.

ANDROGEN DEPRIVATION THERAPY FOR METASTATIC PROSTATE CANCER

The current treatment for newly diagnosed metastatic prostate cancer is hormone ablation via luteinizing hormone-releasing hormone (LHRH) analog until disease progression (22). The response rate for primary hormonal therapy for men with metastatic prostate cancer exceeds 80% and the median duration of response is approximately 18–24 months (22). Patients with high volume metastatic disease have a poorer prognosis with a median time to prostate-specific antigen (PSA) progression of about only 10 months and median time to clinical progression (e.g., worsening bone metastases) of about 14 months (23). In contrast, patients with low volume metastatic disease have a 22-month median time to PSA progression with androgen ablation alone and median time to clinical progression of more than 3 years (23). The median overall survival for men commencing androgen ablation with clinically evident metastatic disease is about 30 months (22). Survival varies depending on the extent of disease and location of the bone metastases (16, 23–27). All patients will ultimately progress despite the initial success of this approach. Castrate-resistant prostate cancer (CRPC) remains an incurable disease resulting in considerable morbidity. Alternative hormonal agents or chemotherapy may

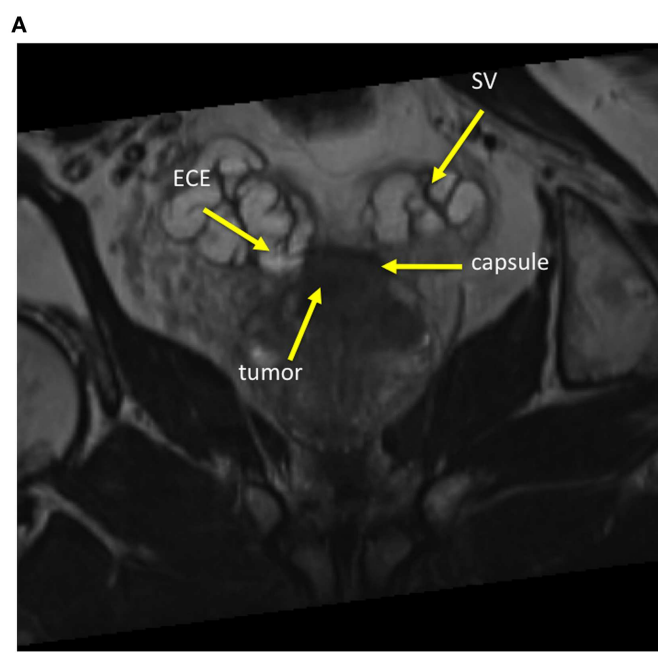


FIGURE 2 | Sixty-year-old gentleman with oligometastatic prostate cancer. He presented with back pain and his PSA was 35 ng/ml. DRE was abnormal and imaging revealed: **(A)** Coronal T2-weighted multiplanar

reconstruction MRI image demonstrating extracapsular extension into the seminal vesicles. **(B)** Bone scan demonstrating a solitary L5 vertebral body metastasis.

be employed at the time of castrate resistance and provide small overall survival benefits (28).

CHEMOTHERAPEUTIC AGENTS FOR CASTRATE-RESISTANT PROSTATE CANCER

Early investigation of chemotherapeutic agents for metastatic CRPC showed that mitoxantrone combined with prednisone improved pain and quality of life when compared to prednisone alone (29, 30). Unfortunately, mitoxantrone did not prolong survival in randomized trials (31, 32). Docetaxel was the first chemotherapeutic agent able to demonstrate increased survival in metastatic CRPC in addition to decreased pain and improved quality of life (33). Median survival increased by 2.9 months in the cohort who received docetaxel compared to mitoxantrone.

The breakthrough with docetaxel has led to subsequent advances in systemic therapy for metastatic prostate cancer. Multiple hormonal and non-hormonal agents have emerged in recent phase III clinical trials that demonstrate increased overall survival time (outlined in **Tables 1** and **2**) (34–39). Hormonal agents target adrenal testosterone production that is shielded from conventional ADT. Abiraterone inhibits androgen production by blocking enzymes crucial to testosterone synthesis (34). Enzalutamide does not lower intratumoral testosterone but is a potent androgen receptor antagonist that acts by blocking androgen activity within cancer cells (36). Novel non-hormonal agents have also been efficacious in the setting of CRPC. Sipuleucel-T is a therapeutic cancer vaccine that acts as an immunostimulant specifically targeting the prostatic acid phosphatase (PAP) antigen found on prostate cancer cells (37). Radium-223 is a radiopharmaceutical agent that targets bony tissue and destroys metastatic prostate cancer cells through alpha particle emission (38). Additional phase III trials with newer agents are underway. To date, no single agent has demonstrated a PSA response rate greater than 54% or an overall survival benefit greater than 5 months, and further innovation through new agents or combination regimens is necessary to optimize survival.

RATIONALE FOR TREATMENT OF THE PROSTATE IN THE PRESENCE OF OLIGOMETASTATIC DISEASE

We believe an effective radiotherapeutic approach in the prostate may improve long-term outcomes with limited toxicity in patients with oligometastatic disease. The addition of prostate radiotherapy to ADT has been shown to significantly improve progression-free survival and overall survival with acceptable morbidity in patients with locally advanced prostate cancer (40, 41). While a slight increase in overall bother from urinary and bowel symptoms may occur from combined therapy, the difference is minimal and does not meet the threshold for clinical significance (42). The SPCG-7/SFUO-3 trial for patients with locally advanced prostate cancer achieved a 12% reduction in 10-year prostate cancer specific mortality when radiotherapy was combined with endocrine treatment (41). The trial observed a 10-year overall survival benefit of 8.9% consistent with a 7-year overall survival benefit of 8% with the addition of radiation therapy in the NCIC CTG PR.3/MRC UK PR07 trial (40, 41).

The mechanism of such benefit is currently unclear. Castrate-resistant clones may be present in the prostate prior to the initiation of ADT and they could be enriched through clonal selection after testosterone decline (**Figure 3**) (43). Animal models support the use of early local treatment to eliminate androgen-independent clones (44, 45). Radiotherapy, which eradicates androgen-sensitive and androgen insensitive clones with similar efficacy, may be effective at eradicating androgen-independent clones. This has the potential to delay the time to castrate resistance and hence prolong disease control.

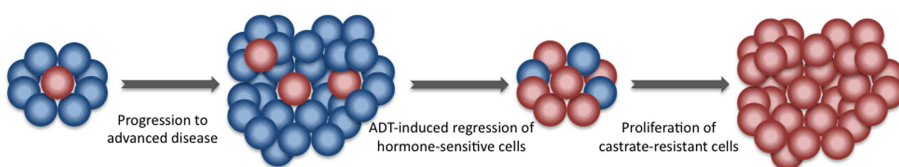
Studies in which routine post-radiotherapy prostate biopsies have been performed following primary ADT reveal a high rate of persistence of local disease (46). In the SPCG-7 trial, the post-radiation therapy biopsy positivity rate was an unacceptable 66% (46). Local control is important in this malignancy, as problems resulting from uncontrolled local disease are significant including urinary obstruction (47). Palliative transurethral resection of the prostate (TURP) and/or radiation therapy may be less effective than primary treatment when the disease burden is lower (48, 49).

Table 1 | Prostate-specific antigen response rate of new chemotherapeutic agents for metastatic CRPC.

Trial	Treatment group	Drug class	Mechanism of action	Control group	Treatment group response rate (%)	Control group response rate (%)	P-value
TAX 327	Docetaxel + prednisone	Taxoid	Microtubule disassembly inhibitor	Mitoxantrone + prednisone	45	32	<0.001
TROPIC	Cabazitaxel + prednisone	Taxoid	Microtubule disassembly inhibitor	Mitoxantrone + prednisone	39.2	17.8	=0.0002
COU-AA301	Abiraterone + prednisone	Hormonal agent	Cytochrome P450 17A1 inhibitor	Placebo + prednisone	29	6	<0.001
AFFIRM	Enzalutamide	Hormonal agent	Androgen receptor antagonist	Placebo	54	2	<0.001
IMPACT	Sipuleucel-T	Cancer vaccine	PA2024 activated peripheral-blood mononuclear cells	Placebo	2.6	1.3	Not significant
ALSYMPCA	Radium-223	Radio pharmaceutical	Bone-targeted alpha radiation	Placebo	16	6	<0.001

Table 2 | Overall survival benefit of new chemotherapeutic agents for metastatic CRPC.

Trial	Patients	Treatment group	Control group	Median improvement in overall survival (months)	P-value
TAX 327	1006	Docetaxel + prednisone	Mitoxantrone + prednisone	2.9	=0.004
TROPIC	755	Cabazitaxel + prednisone	Mitoxantrone + prednisone	2.4	<0.0001
COU-AA-301	1195	Abiraterone + prednisone	Placebo + prednisone	3.9	<0.001
AFFIRM	1199	Enzalutamide	Placebo	4.8	<0.0001
IMPACT	512	Sipuleucel-T	Placebo	4.1	=0.03
ALSYMPCA	922	Radium-223	Placebo	3.6	<0.001

**FIGURE 3 | Development of castrate-resistant prostate cancer.** Newly diagnosed prostate cancer is composed of a group of heterogeneous cells. The majority is hormone-sensitive. A minority are castration-resistant.

Following the initiation of ADT, castration-resistant cells have a survival advantage and give rise to a more aggressive castration-resistant prostate cancer.

It is also evident that local failures can lead to a second wave of distant metastases (50). Achieving improved local control within the prostate therefore carries promise of reducing the sequelae attributable to uncontrolled local disease as well as the prevention of new metastases.

Prostate cancer growth is dependent on androgen activation of androgen receptors. ADT decreases testicular androgens. Although testes are the major source of testosterone in normal men, the intratumoral synthesis of testosterone from weak adrenal androgens appears to be a substantial source of intraprostatic androgen following ADT (51). Intraprostatic androgen synthesis may protect primary prostate cancer cells from ADT and provide a sanctuary for prostate cancer cells to progress to castrate resistance. We propose that SBRT may eliminate this sanctuary delaying the emergence of castrate resistance.

RATIONALE FOR TREATMENT OF BONE OLIGOMETASTASES

Prostate cancer has a tropism for bone, making it the most common, and frequently the only, site of metastatic disease (52–54). Greater than 80% of men with metastatic prostate cancer have radiographic evidence of bone involvement. Skeletal complications are a major cause of morbidity in men with prostate cancer. Early in the natural history of the disease, bone metastases are generally asymptomatic, but ultimately at least 40% of patients will be affected by bone pain, 20% will experience a pathologic fracture, and 5% will develop a spinal cord compression. Collectively, skeletal metastases can lead to decreased performance status and devastating neurologic injury. Bone-targeted therapy, such as zoledronic acid and denosumab, decrease but do not eliminate the morbidity associated with bone lesions (55–57). Radiation therapy is typically reserved for symptomatic disease, when the burden of disease is greater and morbidity such as fracture may not be

avoidable. Delaying radiation therapy to this point might limit its efficacy in reducing bone morbidity.

Recent reports have suggested that SBRT is safe and effective in treating bone lesions involving long bones and the spinal column (58, 59). Earlier studies administered hypofractionated regimens more similar to conventional radiotherapy delivery with doses of 50 Gy in 10 fractions (21). Several questions remain given the lack of long-term data compared to more conventional radiation therapy. No optimal SBRT regimen has been established due to the variation in target volume and proximity to normal structures (60). However, SBRT has been administered up to 48 Gy in 3 fractions to multiple metastatic sites simultaneously, and results have shown promising long-term disease control with minimal grade 3+ toxicity (61). The potential benefits of combining radiation with systemic agents has also been demonstrated (62, 63).

Patients treated with SBRT at oligometastatic sites have demonstrated excellent outcomes. Among a cohort of patients with oligometastatic disease and detectable PSA, 100% achieved local control with SBRT to the metastatic lesions, and over half the patients achieved an undetectable or declining PSA by a median follow up of 4.8 months (64). In another study of men with oligometastases following prostate treatment, salvage SBRT deferred initiation of ADT with a 2-year local control rate of 100% and a clinical progression-free survival of 42% (65). Neither study observed grade 3+ toxicity. Larger studies with more homogeneous patient populations are required to define the potential benefits of SBRT in the setting of prostate cancer. In addition, further research is needed to determine the potential impact of SBRT on systemic disease when combined with immunostimulating agents such as sipuleucel-T (66).

Limited data exist on how radiation dose and fractionation affect the risk of fracture following radiation therapy. Pathologic

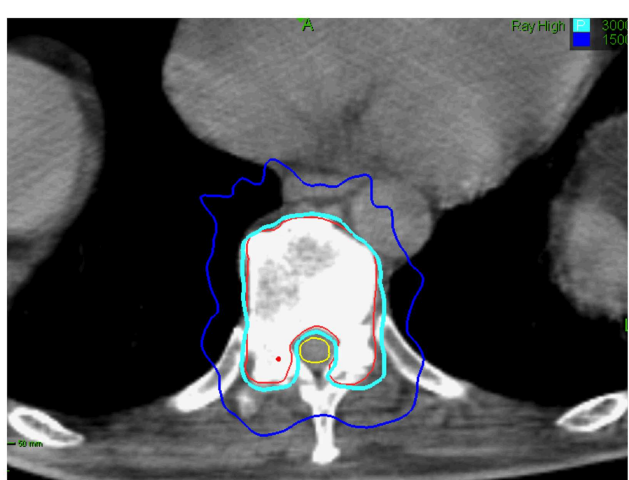


FIGURE 4 | Seventy-five-year-old gentleman with oligometastatic prostate cancer and a T11 vertebral body metastasis. The decision was to proceed with ADT and SBRT. ADT was initiated. The vertebral body was treated with 30 Gy in 5 fractions. Treatment planning axial computed tomography images demonstrating the GTV (red) and spinal cord (yellow). Isodose lines shown as follows: 100% of the prescription dose (light blue line) and 50% of the prescription dose (dark blue line). The maximum point to the spinal cord and esophagus were 30 and 35 Gy, respectively (69).

vertebral body fractures have been described in patients treated with SBRT. They are more common when the lesion is lytic and $\geq 20\%$ of the vertebral body is involved (67). Vertebral body fracture progression may occur in 40% of vertebrae treated with single-dose SBRT (67). Treating patients early in the disease course to decrease the extent of bone/vertebral body involvement at the time of SBRT treatment and fractionation may reduce the likelihood of normal bone injury (Figure 4) (68).

TREATMENT TOXICITY AND QUALITY OF LIFE

We hypothesize that SBRT will decrease tumor burden in the prostate and bone and hence improve long-term well-being. However, if SBRT to the prostate and oligometastases caused a significant rate of high-grade late toxicity and/or adversely affected patients' long-term quality of life this approach would not be worth pursuing further. Prostate SBRT may cause urinary and rectal injury while bone SBRT may promote fractures. The severity and duration of these toxicities varies among patients and has never been prospectively assessed in this patient population. Patients receiving primary ADT have a quality of life that is indistinguishable from a matched normal male population and a quality of life significantly better than that of men with castrate-resistant disease (70). Our experience suggests that prostate SBRT will not adversely affect this (71).

CONCLUSION

Castrate-resistant prostate cancer remains a complex and incurable disease. ADT is successful in delaying the progression to castrate-resistant disease and improving overall survival. Unfortunately, castrate-resistant clones may be present early in the disease process even prior to initiation of ADT, creating the need for

alternative treatments. Several chemotherapeutic agents have been developed to treat metastatic prostate cancer, but the benefits of these drugs have been small to date. Radiation therapy is effective for treating bone metastases but is typically reserved for late-stage, symptomatic disease. SBRT has been demonstrated as a safe and efficacious modality for bone lesions. Implementation of SBRT early in the disease process may decrease the morbidity associated with bone lesions and reduce overall tumor burden, in turn delaying progression of disease and improving both the quality and length of life.

AUTHOR CONTRIBUTIONS

Onita Bhattasali and Leonard N. Chen are lead authors who participated in manuscript drafting, table/figure creation, and manuscript revision. Michael Tong aided in table/figure creation. Siyuan Lei is the dosimetrist who contributed dosimetric data and figures. Pranay Krishnan aided in figure creation. Anatoly Dritschilo, Christopher Kalhorn, Simeng Suy, Brian T. Collins, John H. Lynch, and Nancy A. Dawson are senior authors who aided in drafting the manuscript and manuscript revision. Sean P. Collins is the corresponding author who initially developed the concept, and drafted and revised the manuscript. All authors read and approved the final manuscript.

ACKNOWLEDGMENTS

This work was supported by NIH Grant P30CA051008.

REFERENCES

1. Crook JM, Raymond Y, Salhani D, Yang H, Esche B. Prostate motion during standard radiotherapy as assessed by fiducial markers. *Radiother Oncol* (1995) **37**(1):35–42. doi:10.1016/0167-8140(95)01613-L
2. Dawson LA, Mah K, Franssen E, Morton G. Target position variability throughout prostate radiotherapy. *Int J Radiat Oncol Biol Phys* (1998) **42**(5):1155–61. doi:10.1016/S0360-3016(98)00265-X
3. Litzenberg DW, Balter JM, Hadley SW, Sandler HM, Willoughby TR, Kupelian PA, et al. Influence of intrafraction motion on margins for prostate radiotherapy. *Int J Radiat Oncol Biol Phys* (2006) **65**(2):548–53. doi:10.1016/j.ijrobp.2005.12.033
4. Kupelian PA, Langen KM, Willoughby TR, Zeidan OA, Meeks SL. Image-guided radiotherapy for localized prostate cancer: treating a moving target. *Semin Radiat Oncol* (2008) **18**(1):58–66. doi:10.1016/j.semradonc.2007.09.008
5. Timmerman RD, Kavanagh BD, Cho LC, Papiez L, Xing L. Stereotactic body radiation therapy in multiple organ sites. *J Clin Oncol* (2007) **25**(8):947–52. doi:10.1200/JCO.2006.09.7469
6. Miles EF, Robert Lee W. Hypofractionation for prostate cancer: a critical review. *Semin Radiat Oncol* (2008) **18**(1):41–47. doi:10.1016/j.semradonc.2007.09.006
7. Fowler JF. The radiobiology of prostate cancer including new aspects of fractionated radiotherapy. *Acta Oncol* (2005) **44**(3):265–76. doi:10.1080/02841860410002824
8. Xie Y, Djajaputra D, King CR, Hossain S, Ma L, Xing L. Intrafractional motion of the prostate during hypofractionated radiotherapy. *Int J Radiat Oncol Biol Phys* (2008) **72**(1):236–46. doi:10.1016/j.ijrobp.2008.04.051
9. King CR, Brooks JD, Gill H, Presti JC Jr. Long-term outcomes from a prospective trial of stereotactic body radiotherapy for low-risk prostate cancer. *Int J Radiat Oncol Biol Phys* (2012) **82**(2):877–82. doi:10.1016/j.ijrobp.2010.11.054
10. King CR, Collins SP, Fuller D, Wang PC, Kupelian PA, Steinberg M, et al. Health related quality of life after stereotactic body radiotherapy for localized prostate cancer: results from a multi-institutional consortium of prospective trials. *Int J Radiat Oncol Biol Phys* (2013) **87**(5):939–45. doi:10.1016/j.ijrobp.2013.08.019
11. King CR, Freeman DE, Kaplan ID, Fuller D, Bolzicco G, Collins SP, et al. Stereotactic body radiotherapy for localized prostate cancer: pooled analysis from a multi-institutional consortium of prospective phase II trials. *Radiother Oncol* (2013). doi:10.1016/j.radonc.2013.08.030

12. Freeman DE, Friedland J, Masterson-McGary M, Spellberg D. Stereotactic body radiotherapy: an emerging treatment approach for localized prostate cancer. *Int J Radiat Oncol Biol Phys* (2009) **75**(3):S307–8. doi:10.1016/j.ijrobp.2009.07.706
13. McBride SM, Wong DS, Dombrowski JJ, Harkins B, Tapella P, Hanscom HN, et al. Hypofractionated stereotactic body radiotherapy in low risk prostate adenocarcinoma. *Cancer* (2012) **118**(15):3681–90. doi:10.1002/cncr.26699
14. Katz AJ, Santoro M, Diblasio F, Ashley R. Stereotactic body radiotherapy for localized prostate cancer: disease control and quality of life at 6 years. *Radiat Oncol* (2013) **8**(1):118. doi:10.1186/1748-717X-8-118
15. Weichselbaum RR, Hellman S. Oligometastases revisited. *Nat Rev Clin Oncol* (2011) **8**(6):378–82. doi:10.1038/nrclinonc.2011.44
16. Singh D, Yi WS, Brasacchio RA, Muhs AG, Smudzin T, Williams JP, et al. Is there a favorable subset of patients with prostate cancer who develop oligometastases? *Int J Radiat Oncol Biol Phys* (2004) **58**(1):3–10. doi:10.1016/S0360-3016(03)01442-1
17. Hellman S, Weichselbaum RR. Oligometastases. *J Clin Oncol* (1995) **13**(1):8–10.
18. Corbin KS, Hellman S, Weichselbaum RR. Extracranial oligometastases: a subset of metastases curable with stereotactic radiotherapy. *J Clin Oncol* (2013) **31**(11):1384–90. doi:10.1200/JCO.2012.45.9651
19. Lussier YA, Xing HR, Salama JK, Khodarev NN, Huang Y, Zhang Q, et al. MicroRNA expression characterizes oligometastasis(es). *PLoS One* (2011) **6**(12):e28650. doi:10.1371/journal.pone.0028650
20. Alongi F, Arcangeli S, Filippi AR, Ricardi U, Scorsetti M. Review and uses of stereotactic body radiation therapy for oligometastases. *Oncologist* (2012) **17**(8):1100–7. doi:10.1634/theoncologist.2012-0092
21. Milano MT, Katz AW, Zhang H, Okunieff P. Oligometastases treated with stereotactic body radiotherapy: long-term follow-up of prospective study. *Int J Radiat Oncol Biol Phys* (2012) **83**(3):878–86. doi:10.1016/j.ijrobp.2011.08.036
22. Prostate Cancer Trialists' Collaborative G. Maximum androgen blockade in advanced prostate cancer: an overview of the randomised trials. *Lancet* (2000) **355**(9214):1491–8. doi:10.1016/S0140-6736(00)02163-2
23. Eisenberger MA, Blumenstein BA, Crawford ED, Miller G, McLeod DG, Loehrer PJ, et al. Bilateral orchectomy with or without flutamide for metastatic prostate cancer. *N Engl J Med* (1998) **339**(15):1036–42. doi:10.1056/NEJM199810083391504
24. Glass TR, Tangen CM, Crawford ED, Thompson I. Metastatic carcinoma of the prostate: identifying prognostic groups using recursive partitioning. *J Urol* (2003) **169**(1):164–9. doi:10.1016/S0022-5347(05)64059-1
25. Rana A, Chisholm GD, Khan M, Sekharjit SS, Merrick MV, Elton RA. Patterns of bone metastasis and their prognostic significance in patients with carcinoma of the prostate. *Br J Urol* (1993) **72**(6):933–6. doi:10.1111/j.1464-410X.1993.tb16301.x
26. Soloway MS, Hardeman SW, Hickey D, Todd B, Soloway S, Raymond J, et al. Stratification of patients with metastatic prostate cancer based on extent of disease on initial bone scan. *Cancer* (1988) **61**(1):195–202. doi:10.1002/1097-0142(19880101)61:1<195::AID-CNCR2820610133>3.0.CO;2-Y
27. Yamashita K, Denno K, Ueda T, Komatsubara Y, Kotake T, Usami M, et al. Prognostic significance of bone metastases in patients with metastatic prostate cancer. *Cancer* (1993) **71**(4):1297–302. doi:10.1002/1097-0142(19930215)71:4<1297::AID-CNCR2820710421>3.0.CO;2-S
28. Higano CS, Crawford ED. New and emerging agents for the treatment of castration-resistant prostate cancer. *Urol Oncol* (2011) **29**(Suppl 6):1–8. doi:10.1016/j.urolonc.2011.08.013
29. Tannock IF, Osoba D, Stockler MR, Ernst DS, Neville AJ, Moore MJ, et al. Chemotherapy with mitoxantrone plus prednisone or prednisone alone for symptomatic hormone-resistant prostate cancer: a Canadian randomized trial with palliative end points. *J Clin Oncol* (1996) **14**(6):1756–64.
30. Osoba D, Tannock IF, Ernst DS, Neville AJ. Health-related quality of life in men with metastatic prostate cancer treated with prednisone alone or mitoxantrone and prednisone. *J Clin Oncol* (1999) **17**(6):1654.
31. Kantoff PW, Halabi S, Conaway M, Picus J, Kirshner J, Hars V, et al. Hydrocortisone with or without mitoxantrone in men with hormone-refractory prostate cancer: results of the cancer and leukemia group B 9182 study. *J Clin Oncol* (1999) **17**(8):2506.
32. Berry W, Dakhil S, Modiano M, Gregurich M, Asmar L. Phase III study of mitoxantrone plus low dose prednisone versus low dose prednisone alone in patients with asymptomatic hormone refractory prostate cancer. *J Urol* (2002) **168**(6):2439–43. doi:10.1016/S0022-5347(05)64163-8
33. Berthold DR, Pond GR, Soban F, de Wit R, Eisenberger M, Tannock IF. Docetaxel plus prednisone or mitoxantrone plus prednisone for advanced prostate cancer: updated survival in the TAX 327 study. *J Clin Oncol* (2008) **26**(2):242–5. doi:10.1200/JCO.2007.12.4008
34. De Bono JS, Logothetis CJ, Molina A, Fizazi K, North S, Chu L, et al. Abiraterone and increased survival in metastatic prostate cancer. *N Engl J Med* (2011) **364**(21):1995–2005. doi:10.1056/NEJMoa1014618
35. de Bono JS, Oudard S, Ozguroglu M, Hansen S, Machiels J-P, Kocak I, et al. Prednisone plus cabazitaxel or mitoxantrone for metastatic castration-resistant prostate cancer progressing after docetaxel treatment: a randomised open-label trial. *Lancet* (2010) **376**(9747):1147–54. doi:10.1016/S0140-6736(10)61389-X
36. Scher HI, Fizazi K, Saad F, Taplin M-E, Sternberg CN, Miller K, et al. Increased survival with enzalutamide in prostate cancer after chemotherapy. *N Engl J Med* (2012) **367**(13):1187–97. doi:10.1056/NEJMoa1207506
37. Kantoff PW, Higano CS, Shore ND, Berger ER, Small EJ, Penson DF, et al. Sipuleucel-T immunotherapy for castration-resistant prostate cancer. *N Engl J Med* (2010) **363**(5):411–22. doi:10.1056/NEJMoa1001294
38. Parker C, Nilsson S, Heinrich D, Helle SI, O'Sullivan JM, Fosså SD, et al. Alpha emitter radium-223 and survival in metastatic prostate cancer. *N Engl J Med* (2013) **369**(3):213–23. doi:10.1056/NEJMoa1213755
39. Tannock IF, de Wit R, Berry WR, Horti J, Pluzanska A, Chi KN, et al. Docetaxel plus prednisone or mitoxantrone plus prednisone for advanced prostate cancer. *N Engl J Med* (2004) **351**(15):1502–12. doi:10.1056/NEJMoa040720
40. Warde P, Mason M, Ding K, Kirkbride P, Brundage M, Cowan R, et al. Combined androgen deprivation therapy and radiation therapy for locally advanced prostate cancer: a randomised, phase 3 trial. *Lancet* (2012) **378**(9809):2104–11. doi:10.1016/S0140-6736(11)61095-7
41. Widmark A, Klepp O, Solberg A, Damber J-E, Angelsen A, Fransson P, et al. Endocrine treatment, with or without radiotherapy, in locally advanced prostate cancer (SPCG-7/SFUO-3): an open randomised phase III trial. *Lancet* (2009) **373**(9660):301–8. doi:10.1016/S0140-6736(08)61815-2
42. Fransson P, Lund J-Å, Damber J-E, Klepp O, Wiklund F, Fosså S, et al. Quality of life in patients with locally advanced prostate cancer given endocrine treatment with or without radiotherapy: 4-year follow-up of SPCG-7/SFUO-3, an open-label, randomised, phase III trial. *Lancet Oncol* (2009) **10**(4):370–80. doi:10.1016/S1470-2045(09)70027-0
43. Ahmed M, Li LC. Adaptation and clonal selection models of castration-resistant prostate cancer: current perspective. *Int J Urol* (2012) **20**(4):362–71. doi:10.1111/iju.12005
44. Craft N, Chhor C, Tran C, Belldegrun A, DeKernion J, Witte ON, et al. Evidence for clonal outgrowth of androgen-independent prostate cancer cells from androgen-dependent tumors through a two-step process. *Cancer Res* (1999) **59**(19):5030–6.
45. Gingrich JR, Barrios RJ, Kattan MW, Nahm HS, Finegold MJ, Greenberg NM. Androgen-independent prostate cancer progression in the TRAMP model. *Cancer Res* (1997) **57**(21):4687–91.
46. Solberg A, Haugen OA, Viset T, Bergh A, Tasdemir I, Ahlgren G, et al. Residual prostate cancer in patients treated with endocrine therapy with or without radical radiotherapy: a side study of the SPCG-7 randomized trial. *Int J Radiat Oncol Biol Phys* (2011) **80**(1):55–61. doi:10.1016/j.ijrobp.2010.01.072
47. Khafagy R, Shackley D, Samuel J, O'Flynn K, Betts C, Clarke N. Complications arising in the final year of life in men dying from advanced prostate cancer. *J Palliat Med* (2007) **10**(3):705–11. doi:10.1089/jpm.2006.0185
48. Crain DS, Amling CL, Kane CJ. Palliative transurethral prostate resection for bladder outlet obstruction in patients with locally advanced prostate cancer. *J Urol* (2004) **171**(2):668–71. doi:10.1097/01.ju.0000104845.24632.92
49. Din OS, Thanvi N, Ferguson CJ, Kirkbride P. Palliative prostate radiotherapy for symptomatic advanced prostate cancer. *Radiat Oncol* (2009) **93**(2):192–6. doi:10.1016/j.radonc.2009.04.017
50. Fuks Z, Leibel SA, Wallner KE, Begg CB, Fair WR, Anderson LL, et al. The effect of local control on metastatic dissemination in carcinoma of the prostate: long-term results in patients treated with 125I implantation. *Int J Radiat Oncol Biol Phys* (1991) **21**(3):537–47. doi:10.1016/0360-3016(91)90668-T
51. Cai C, Balk SP. Intratumoral androgen biosynthesis in prostate cancer pathogenesis and response to therapy. *Endocr Relat Cancer* (2011) **18**(5):R175–82. doi:10.1530/ERC-10-0339

52. Coleman RE. Metastatic bone disease: clinical features, pathophysiology and treatment strategies. *Cancer Treat Rev* (2001) **27**(3):165–76. doi:10.1053/ctr.2000.0210
53. Saylor PJ, Lee RJ, Smith MR. Emerging therapies to prevent skeletal morbidity in men with prostate cancer. *J Clin Oncol* (2011) **29**(27):3705–14. doi:10.1200/JCO.2010.34.4994
54. Saad F, Olsson C, Schulman CC. Skeletal morbidity in men with prostate cancer: quality-of-life considerations throughout the continuum of care. *Eur Urol* (2004) **46**(6):731–40. doi:10.1016/j.euro.2004.08.016
55. Saad F, Gleason DM, Murray R, Tchekmedyian S, Venner P, Lacombe L, et al. A randomized, placebo-controlled trial of zoledronic acid in patients with hormone-refractory metastatic prostate carcinoma. *J Natl Cancer Inst* (2002) **94**(19):1458–68. doi:10.1093/jnci/94.19.1458
56. Fizazi K, Carducci M, Smith M, Damião R, Brown J, Karsh L, et al. Denosumab versus zoledronic acid for treatment of bone metastases in men with castration-resistant prostate cancer: a randomised, double-blind study. *Lancet* (2011) **377**(9768):813–22. doi:10.1016/S0140-6736(10)62344-6
57. Saad F, Gleason DM, Murray R, Tchekmedyian S, Venner P, Lacombe L, et al. Long-term efficacy of zoledronic acid for the prevention of skeletal complications in patients with metastatic hormone-refractory prostate cancer. *J Natl Cancer Inst* (2004) **96**(11):879–82. doi:10.1093/jnci/djh295
58. Jhaveri P, Teh BS, Bloch C, Amato R, Butler EB, Paulino A. Stereotactic body radiotherapy in the management of painful bone metastases. *Oncology* (2008) **22**(7):782.
59. Wang XS, Rhines LD, Shiu AS, Yang JN, Selek U, Gning I, et al. Stereotactic body radiation therapy for management of spinal metastases in patients without spinal cord compression: a phase 1–2 trial. *Lancet Oncol* (2012) **13**(4):395–402. doi:10.1016/S1470-2045(11)70384-9
60. Salama JK, Kirkpatrick JP, Yin F-F. Stereotactic body radiotherapy treatment of extracranial metastases. *Nat Rev Clin Oncol* (2012) **9**:654–65. doi:10.1038/nrclinonc.2012.166
61. Salama JK, Hasselle MD, Chmura SJ, Malik R, Mehta N, Yenice KM, et al. Stereotactic body radiotherapy for multisite extracranial oligometastases. *Cancer* (2012) **118**(11):2962–70. doi:10.1002/cncr.26611
62. Kao J, Packer S, Vu HL, Schwartz ME, Sung MW, Stock RG, et al. Phase 1 study of concurrent sunitinib and image-guided radiotherapy followed by maintenance sunitinib for patients with oligometastases. *Cancer* (2009) **115**(15):3571–80. doi:10.1002/cncr.24412
63. Kao J, Chen C-T, Tong CC, Packer SH, Schwartz M, Chen S-H, et al. Concurrent sunitinib and stereotactic body radiotherapy for patients with oligometastases. *Target Oncol* (2013). doi:10.1007/s11523-013-0280-y
64. Ahmed KA, Barney BM, Davis BJ, Park SS, Kwon ED, Olivier KR. Stereotactic body radiation therapy in the treatment of oligometastatic prostate cancer. *Front Oncol* (2012) **2**:215. doi:10.3389/fonc.2012.00215
65. Berkovic P, De Meerleer G, Delrue L, Lambert B, Fonteyne V, Lumen N, et al. Salvage stereotactic body radiotherapy for patients with limited prostate cancer metastases: deferring androgen deprivation therapy. *Clin Genitourin Cancer* (2012) **11**(1):27–32. doi:10.1016/j.clgc.2012.08.003
66. Gulley JL, Arlen PM, Bastian A, Morin S, Marte J, Beetham P, et al. Combining a recombinant cancer vaccine with standard definitive radiotherapy in patients with localized prostate cancer. *Clin Cancer Res* (2005) **11**(9):3353–62. doi:10.1158/1078-0432.CCR-04-2062
67. Rose PS, Laufer I, Boland PJ, Hanover A, Bilsky MH, Yamada J, et al. Risk of fracture after single fraction image-guided intensity-modulated radiation therapy to spinal metastases. *J Clin Oncol* (2009) **27**(30):5075–9. doi:10.1200/JCO.2008.19.3508
68. Sahgal A, Atenafu EG, Chao S, Al-Omair A, Boehling N, Balagamwala EH, et al. Vertebral compression fracture after spine stereotactic body radiotherapy: a multi-institutional analysis with a focus on radiation dose and the spinal instability neoplastic score. *J Clin Oncol* (2013) **31**(27):3426–31. doi:10.1200/JCO.2013.50.1411
69. Benedict SH, Yenice KM, Followill D, Galvin JM, Hinson W, Kavanagh B, et al. Stereotactic body radiation therapy: the report of AAPM Task Group 101. *Med Phys* (2010) **37**:4078. doi:10.1118/1.3438081
70. Albertsen PC, Aaronson NK, Muller MJ, Keller SD, Ware JE Jr. Health-related quality of life among patients with metastatic prostate cancer. *Urology* (1997) **49**(2):207–17. doi:10.1016/S0090-4295(96)00485-2
71. Chen LN, Suy S, Uhm S, Oermann EK, Ju AW, Chen V, et al. Stereotactic body radiation therapy (SBRT) for clinically localized prostate cancer: the Georgetown University experience. *Radiat Oncol* (2013) **8**(1):58. doi:10.1186/1748-717X-8-58

Conflict of Interest Statement: Sean P. Collins and Brian T. Collins serve as clinical consultants to Accuray Inc. The other authors declare that they have no competing interests.

Received: 07 October 2013; accepted: 18 November 2013; published online: 03 December 2013.

Citation: Bhattasali O, Chen LN, Tong M, Lei S, Collins BT, Krishnan P, Kalhorn C, Lynch JH, Suy S, Dritschilo A, Dawson NA and Collins SP (2013) Rationale for stereotactic body radiation therapy in treating patients with oligometastatic hormone-naïve prostate cancer. *Front. Oncol.* **3**:293. doi: 10.3389/fonc.2013.00293

This article was submitted to Radiation Oncology, a section of the journal *Frontiers in Oncology*.

Copyright © 2013 Bhattasali, Chen, Tong, Lei, Collins, Krishnan, Kalhorn, Lynch, Suy, Dritschilo, Dawson and Collins. This is an open-access article distributed under the terms of the Creative Commons Attribution License (CC BY). The use, distribution or reproduction in other forums is permitted, provided the original author(s) or licensor are credited and that the original publication in this journal is cited, in accordance with accepted academic practice. No use, distribution or reproduction is permitted which does not comply with these terms.



Image-guided radiotherapy and -brachytherapy for cervical cancer

Suresh Dutta¹, Nam Phong Nguyen^{2*}, Jacqueline Vock³, Christine Kerr⁴, Juan Godinez⁵, Satya Bose², Siyoung Jang⁶, Alexander Chi⁷, Fabio Almeida⁸, William Woods⁹, Anand Desai¹⁰, Rick David¹¹, Ulf Lennart Karlsson¹², Gabor Altdorfer¹³ and The International Geriatric Radiotherapy Group[†]

¹ Medicine and Radiation Oncology PA, San Antonio, TX, USA

² Department of Radiation Oncology, Howard University, Washington, DC, USA

³ Department of Radiation Oncology, Lindenhoftspital, Bern, Switzerland

⁴ Department of Radiation Oncology, Centre Val d'Aurelle, Montpellier, France

⁵ Florida Radiation Oncology Group, Department of Radiation Oncology, Jacksonville, FL, USA

⁶ Department of Radiation Oncology, University of Arizona, Tucson, AZ, USA

⁷ Department of Radiation Oncology, University of West Virginia, Morgantown, WV, USA

⁸ Southwest PET/CT Institute, Tucson, AZ, USA

⁹ Department of Radiation Oncology, Richard A. Henson Cancer Institute, Salisbury, MD, USA

¹⁰ Department of Radiation Oncology, Akron City Hospital, Akron, OH, USA

¹¹ Department of Radiation Oncology, Michael D. Watchtel Cancer Center, Oshkosh, WI, USA

¹² Department of Radiation Oncology, Marshfield Clinic, Marshfield, WI, USA

¹³ Department of Radiation Oncology, Camden Clark Cancer Center, Parkersburg, WV, USA

Edited by:

Soren M. Bentzen, University of Maryland School of Medicine, USA

Reviewed by:

Daniel Grant Petererit, Rapid City Regional Hospital, USA

Timothy James Kinsella, Brown University, USA

*Correspondence:

Nam Phong Nguyen, Howard University, 2041 Georgia Avenue NW, Washington, DC 20060, USA
e-mail: namphong.nguyen@yahoo.com

[†]All of the authors are affiliated with the International Geriatric Radiotherapy Group.

Conventional radiotherapy for cervical cancer relies on clinical examination, 3-dimensional conformal radiotherapy (3D-CRT), and 2-dimensional intracavitary brachytherapy. Excellent local control and survival have been obtained for small early stage cervical cancer with definitive radiotherapy. For bulky and locally advanced disease, the addition of chemotherapy has improved the prognosis but toxicity remains significant. New imaging technology such as positron-emission tomography and magnetic resonance imaging has improved tumor delineation for radiotherapy planning. Image-guided radiotherapy (IGRT) may decrease treatment toxicity of whole pelvic radiation because of its potential for bone marrow, bowel, and bladder sparing. Tumor shrinkage during whole pelvic IGRT may optimize image-guided brachytherapy (IGBT), allowing for better local control and reduced toxicity for patients with cervical cancer. IGRT and IGBT should be integrated in future prospective studies for cervical cancer.

Keywords: cervical cancer, IGRT, IGBT, normal tissue sparing

TREATMENT OF CERVICAL CANCER

Radiotherapy is an excellent modality for the treatment of cervical cancer because of the tolerance of the cervix to high-radiation dose. Traditionally, staging and treatment of cervical cancer are based on clinical examination. The conventional radiotherapy technique is 3-dimensional conformal radiotherapy (3D-CRT) of the pelvis followed by 2-dimensional (2D) intracavitary brachytherapy. Tumor shrinkage during whole pelvic radiation allows for a better geometric implant leading to excellent local control and survival in patients with early stage disease. However, for patients with bulky disease or with locally advanced stages, loco-regional recurrences remain significant leading to a poor survival. The combination of chemotherapy and radiation has improved the prognosis of these patients but toxicity of the combined modality remains significant (1, 2). Grade 3–4 hematologic toxicity, radiation enteritis, and cystitis are often the limiting factors of the conventional radiotherapy technique and may compromise treatment efficacy because of treatment breaks, which allow tumor regrowth. Thus, a radiotherapy technique that spares the normal pelvic organs from excessive toxicity may reduce the acute side-effects and late complications of radiotherapy and potentially

improve local control by an improved geometry of the brachytherapy implant. Image-guided radiotherapy (IGRT) based on modern imaging technology such as [¹⁸F]fluorodeoxyglucose positron-emission tomography (FDG-PET) scan and magnetic resonance imaging (MRI) may improve the therapeutic ratio and potentially decrease treatment toxicity.

THE ROLE OF PET SCAN IN RADIOTHERAPY PLANNING FOR CERVICAL CANCER

Lymph node metastasis is one of the poor prognostic factors for cervical cancer. Compared to computed tomography (CT) scan and MRI, FDG-PET is more sensitive for detecting pelvic and para-aortic lymph node metastasis (3, 4). Among 560 patients with cervical cancer stage IA–IVB who underwent FDG-PET for staging at diagnosis, 47% had lymph node metastasis (5). Among the patients with PET-positive lymph nodes, all had pelvic, 35% para-aortic, and 12% supraclavicular lymph node metastasis. Thus, PET, by virtue of its lymph node detection, can upstage the clinical stage, modify treatment decision making, and allow the radiation oncologist to extend the radiotherapy volume for inclusion of the metastatic lymph nodes. The para-aortic lymph nodes can

be treated with intensity-modulated radiotherapy (IMRT) achieving excellent regional control and acceptable morbidity (6). The feasibility of PET scan for para-aortic lymph nodes detection and radiotherapy planning was tested in a randomized trial. One hundred twenty-nine cervical cancer patients stage I–IVA with positive pelvic and negative para-aortic lymph nodes on staging MRI were randomized to have FDG-PET ($n = 66$) or no additional PET for staging ($n = 63$). Among patients who had para-aortic lymph nodes metastasis on PET scan, the radiotherapy fields were extended to include these metastatic lymph nodes. Seven patients had extra-pelvic metastases on PET scan: six of them para-aortic and one omental metastases. Even though there was no difference in survival between these two groups of patients, the ones who were randomized to PET scan had decreased para-aortic recurrences (7). As with all diagnostic modality, false negative results occur with PET staging. In a study of 237 patients with cervical cancer and negative para-aortic involvement on PET scan, 29 patients (12%) had occult para-aortic metastases on laparoscopic lymphadenectomy (8). Radiotherapy fields were extended to include these lymph nodes. However, among the 29 patients who had occult metastases, poor survival was observed in 16 patients who had para-aortic lymph nodes more than 5 mm in size raising the question about the benefit of lymphadenectomy in patients who had negative para-aortic lymph nodes on PET scan given the cost and the morbidity of the surgical procedure. FDG-PET can also be integrated in the IGRT treatment planning to escalate radiation dose to the positive lymph nodes with the simultaneous integrated boost (SIB) technique, potentially improving regional control (9). Even though patients with pelvic and/or/para-aortic lymph nodes metastases often developed distant metastases, regional control with increased radiation dose to the metastatic lymph nodes may improve patient quality of life (10). Thus, despite its limitations, FDG-PET should be included in all IGRT planning for cervical cancer to assess the risk of lymph node and distant metastasis.

THE ROLE OF MRI FOR RADIOTHERAPY PLANNING OF CERVICAL CANCER

Traditionally, staging and radiotherapy planning of cervical cancers are obtained through clinical information. However, clinical examination alone is often inaccurate to assess the local extension of the tumor especially its size, parametrium involvement, and pelvic side wall invasion. Even though MRI is less sensitive than FDG-PET for the detection of lymph node metastasis, its accuracy in the diagnosis of soft tissue tumor invasion and for the monitoring of tumor regression during radiotherapy makes this diagnostic imaging study indispensable for radiotherapy planning (11). Compared to CT scan, the T2-weighted images on MRI provide better resolution to outline the primary tumor and adjacent soft tissue invasion (parametrium, bladder, and rectum) due to its high soft tissue contrast (12). Following whole pelvic radiation, MRI is more accurate for the delineation of the residual gross tumor compared to both CT scan and clinical examination under anesthesia (13). The superiority of MRI in detecting residual disease following external beam irradiation for adaptive brachytherapy planning was also corroborated in another study (14). Serial MRI during whole pelvic radiotherapy may also predict the probability of local recurrence and poor survival.

In a study of 80 cervical cancer patients stage IB2–IVA undergoing concurrent chemoradiation, the tumor volume was measured with MRI before (V1), at 2–2.5 weeks (V2), at 4–5 weeks (V3), and following treatment (V4). Large tumor size and poor tumor regression during chemoradiation were predictors of poor prognosis. Patients with a tumor volume >40 cc before treatment (V1) and a tumor ratio V3/V1 of 20% or more at the fourth or fifth week of whole pelvic radiation had a local recurrence rate of 63% and a disease-free survival of 39% at 5 years (15). A correlation between tumor regression during pelvic radiotherapy and survival was also observed in another study of cervical cancer (16). Even though these data are preliminary and need to be corroborated by further prospective trials, cervical cancer patients with large tumor and poor tumor regression during pelvic radiotherapy may be candidates for radiation dose escalation with brachytherapy. MRI-based brachytherapy planning allows for higher tumor dose and sparing of radiosensitive organs such as the rectum and bladder compared to conventional 2-D planning (17). The potential of MRI-guided planning optimization in intracavitary radiotherapy to increase tumor dose without excessive irradiation of the normal pelvic organs was also corroborated in another study (18). Increasing tumor dose to large tumors with MRI-based image-guided brachytherapy (IGBT) may improve local control and needs to be investigated in future prospective studies (14). As most radiation oncologists lack training in diagnostic radiology, perhaps the most challenging aspect of MRI-based target volume delineation is the uncertainty in outlining the target volume (19). As a result, radiation dose to the target and normal organs at risk (OAR) for complications may differ depending on individual delineation of the target volume (20). Inclusion of an experienced diagnostic radiologist specialized in gynecologic malignancies in the treatment team may improve this issue. Recently, functional MRI, such as diffusion-weighted imaging (DWI), has been investigated as a non-invasive biomarker for tumors. As the tumor shrinks with treatment, water mobility increases. Thus, the apparent diffusion coefficient (ADC) may increase and may serve as an indicator of tumor response. Preliminary studies using DWI–MRI as an early biomarker to assess tumor response following concurrent chemoradiotherapy have been promising, raising the need for future prospective studies (21).

POTENTIAL ROLE OF IGRT IN CERVICAL CANCER

Intensity-modulated radiotherapy has been introduced to reduce treatment toxicity of whole pelvic irradiation compared to 3D-CRT. The steep dose fall-off of IMRT decreases significantly radiation dose to the normal pelvic organs. Grade 3–4 hematologic toxicity was significantly reduced in patients with cervical cancer undergoing weekly cisplatin and IMRT (22). Gastro-intestinal toxicity was also decreased with IMRT even though a large volume of the bowels was irradiated in patients with cervical cancer and para-aortic lymph node metastasis (23). Excellent loco-regional control was also observed with acceptable toxicity in patients receiving postoperative IMRT and chemotherapy for high-recurrence risk features (lymph node metastases, positive margins, and parametrial invasion) (24). Thus, IGRT by combining the steep dose gradient of IMRT and daily imaging may further decrease the toxicity of whole pelvic irradiation in patients with cervical cancer.

because the planning target volume (PTV) may be safely reduced without any compromise on target coverage. Preliminary data suggest a dosimetric advantage of IGRT over IMRT for normal organ sparing in patients with cervical cancer. The dosimetric plans of 20 patients with cervical cancer stage IB–IVA undergoing IGRT and chemotherapy were retrospectively compared with IMRT. Even though both techniques provided optimal target coverage, IGRT significantly decreased radiation dose to the bowels compared to IMRT (25). The superior bowel sparing of IGRT over IMRT was also corroborated in another study of locally advanced cervical cancer (26). The bladder dose was also significantly reduced when volumetric arc therapy (VMAT) was compared to fixed beam IMRT (27). As VMAT is currently integrated into image-guidance radiotherapy for treatment delivery, VMAT-based IGRT may further improve normal organ sparing. The dosimetric advantages of IGRT were translated into low treatment morbidity in preliminary clinical studies of cervical cancer with this new technique of radiation. Among 15 patients undergoing chemoradiation for stage IB–IVA with PET-based IGRT, only 1 patient developed long-term chronic gastro-intestinal toxicity even though 4 patients received para-aortic lymph node irradiation (28). Another study corroborated the safety and efficacy of IGRT for locally advanced cervical cancer (29). As cervical cancer patients with a large tumor size at diagnosis are at high risk of local recurrence following radiotherapy, IGRT may deliver a higher dose to the gross tumor and areas at high risk for recurrence with the SIB technique without increasing radiation dose to the adjacent normal organs. The feasibility of IGRT to increase radiation dose to regions of resected metastatic lymph nodes was reported in 20 patients with stage IBpN1–IIIB cervical cancer undergoing primary chemoradiation after pelvic and para-aortic lymphadenectomy. The gross tumor, regional lymph nodes, and parametrium were treated to 50.4 Gy in 1.8 Gy/fraction whereas the regions of metastatic lymph nodes were treated to 59.36 in 2.12 Gy/fraction. Grade 3 diarrhea and neutropenia occurred in 5 and 25% of the patients, respectively, during whole pelvic IGRT. All patients underwent high dose rate (HDR)-based IGBT following pelvic IGRT (30). Thus, radiation dose escalation may be safe when IGRT is integrated with IGBT. An update of the study with 40 patients did not report any increase of grade 3–4 toxicity. In addition, complete pathologic response was confirmed by curettage 3 months following chemoradiation in 38/40 patients (31). As tumor regression carries a good prognosis, this investigative study is promising but needs to be confirmed by future prospective studies. The feasibility of IGRT for gross tumor dose escalation was also reported in another study of six patients with stage IB–IIB cervical cancer. The GTV and grossly enlarged lymph nodes and the parametrium, upper third of the vagina and the pelvic lymph nodes were treated to 59.8 Gy in 2.1 Gy/fraction and 50.4 Gy in 1.8 Gy fraction, respectively. Significant regression of the GTV was observed without increased radiation dose to the normal OAR for complications (32). In patients who are not suitable for intracavitary implants following pelvic irradiation because of poor geometry or co-morbidity, IGRT may deliver a high-boost dose to the gross residual tumor without significant treatment toxicity and improve local control (33). Another study corroborated the feasibility of IGRT boost for cervical cancer patients unable to undergo intracavitary implant (34). Even though these

studies are preliminary, they suggest that IGRT by virtue of its steep dose gradient may produce a radiation dose distribution similar to the one performed with brachytherapy and allow a boost dose that can spare the OAR (35).

POTENTIAL ROLE OF IGBT IN CERVICAL CANCER

Conventional intracavitary brachytherapy for cervical cancer relies on point dose and 2-D treatment planning based on conventional radiography without conforming to the tumor shape and size. Point A is often the reference point for radiotherapy dose delivery and the lack of dose-volume histogram (DVH) of the target volume and normal OAR make estimation of complications risks following radiotherapy difficult. The definition of point A also varies depending on the institution making radiation dose comparison between different radiation centers problematic. The lack of tumor visualization may lead to under-dosing of the tumor and over-dosing of the adjacent normal organs and may result in tumor recurrences and late complications. The introduction of advanced imaging into treatment planning allows for clear visualization of the tumor and the normal OAR, which may translate into better local control and survival and potentially less complications. MRI-based brachytherapy remains the gold standard for IGBT because of its high-soft tissue resolution allowing accurate delineation of the gross tumor and possible tumor invasion of adjacent normal organs. Standardization of target and OAR delineation and radiation dose delivery according to international organizations such as the guidelines of the Groupe Européen de Curietherapie/European Society for Therapeutic Radiology and Oncology (GEC-ESTRO) may allow for compilation of DVH data between various institutions and ultimately establish a relationship between dose delivery, local control, and complications risks (36). As an illustration, the following targets were defined by GEC-ESTRO: GTV, high-risk clinical target volume (HR-CTV), and intermediate-risk clinical target volume (IR-CTV). Minimal dose delivered to 90% (D90) and 100% (D100) of the volume of interest should also be reported. By following GEC-ESTRO guidelines, many centers have achieved a satisfactory dose to the HR-CTV by using different planning methods (37). Adaptive planning in case of tumor regression between sequential brachytherapy sessions may further decrease the risk of complications because of a decreases radiation dose to the normal organs adjacent to the tumor (38). Thus, IGBT relies on solid scientific concepts allowing optimization of brachytherapy planning based on the tumor extent and the individual patient anatomy. Preliminary results suggest that compared to historic controls, IGBT may indeed improve local control and decrease late complications. Among 141 cervical cancer patients stage IB–IVA who had MRI-based IGRT according to GEC-ESTRO guidelines, local control was achieved in 134 patients (95%) at a median follow-up of 51 months (14). Local recurrences occurred in 35% of patients with a large tumor at diagnosis (>5 cm) and at the time of the implant (>5 cm). Regression of the tumor was a good prognostic factor as patients with large tumor at diagnosis and significant regression (<5 cm) during pelvic radiotherapy had a recurrence rate of 10.9%. There was a correlation between local control and the tumor dose for patients with large tumors. Local recurrence rate was 4 and 20% for HR-CTV D90 more than 87 and <87 Gy, respectively. An

update of the study demonstrated a relationship between the dose to the rectum and late toxicities. Normal OAR DVH illustrates the dose to 2 cc (D2cc), 1 cc (D1cc), and 0.1 cc (D0.1cc) of the bladder and rectum from both external beam and brachytherapy. Grade 2–4 rectal side effects occurred in 5, 10, and 20% of patients for rectal D2cc of 67, 78, and 90 Gy, respectively (39). There was no significant correlation between bladder dose and late toxicities. This study suggests that IGRT may be complementary to IGBT because of the higher dose to GTV and lower dose to the rectum that can be achieved with IGRT compared to 3D-CRT. In another multi-centric study of 235 patients stage IIB–IIIB treated with pelvic chemoradiation followed by either 2D- (118) or 3D- (117) intracavitary brachytherapy, the local control rate was 73.9 and 78.5%, and grade 3–4 toxicity occurred in 22.7 and 2.6% of patients using 2D- and 3-D implant, respectively (40). Other studies also corroborated the high rate of local control achieved with IGBT with acceptable morbidity (41, 42). As an illustration, when MRI-based IGBT was retrospectively compared to CT-based external beam therapy and 2D-based brachytherapy, overall survival was significantly improved while severe late complications were reduced with IGBT (43). Thus, IGBT for cervical cancer can be performed in multiple institutions following standard guidelines with less complications compared to conventional 2-D and 3-D implants. The efficacy of IGBT for the treatment of cervical cancer has led some institutions to abandon hysterectomy in favor of definitive radiotherapy with IGBT in patients who traditionally required preoperative irradiation because of the tumor size (44). However, more prospective studies should be performed in the future to establish a clear relationship between tumor dose and local control, OAR DVH and late toxicity to establish IGBT as the standard of care for intracavitary implants.

The limitations of IGBT include the utilization of resources, which may be labor intensive and increases the financial burden of institutions with limited revenue. The use of an MRI for each individual brachytherapy fraction adds significantly to the treatment cost and may prevent IGBT implementation in many centers. A compromise would be to use MRI for the first fraction and CT-based plans for subsequent fractions. The feasibility of this approach was tested in a dosimetry study. Following the first MRI-based IGBT, the target structures delineated on MRI were loaded into the CT dataset while the OAR was contoured on the CT images (45). For small tumors, both MRI-based and hybrid-based plans were similar in terms of target coverage and OAR-constraints. Such innovative approach is intriguing and merits further investigation. Another limitation for the implementation of IGRT and IGBT in patients with cervical cancer is the shift of the normal organs during radiotherapy secondary to tumor regression and/or the filling of the bladder and rectum, which may result into higher dose to the OAR. Adaptive therapy is currently being investigated and may further improve the sparing of normal organs in the future (46).

CONCLUSION

Image-guided radiotherapy and IGBT are promising radiotherapy techniques that can improve local control and decrease complication rates in patients with cervical carcinoma. The

two image-based irradiation modalities are complementary and should be integrated in future prospective trials to improve patient quality of life and survival.

REFERENCES

- Rosa DD, Medeiros LR, Edelweiss MI, Pohlmann PR, Stein AT. Adjuvant platinum-based chemotherapy for early stage cervical cancer. *Cochrane Database Syst Rev* (2012) **13**:6. doi:10.1002/14651858.CD005342.pub3
- Duenas-Gonzalez A, Orlando M, Zhou Y, Quinlivan M, Barraclough H. Efficacy in high burden locally advanced cervical cancer with concurrent gemcitabine and cisplatin chemoradiotherapy plus adjuvant gemcitabine and cisplatin: prognostic and predictive factors and the impact of disease stage on outcomes from a prospective randomized phase III trial. *Gynecol Oncol* (2012) **126**:334–40. doi:10.1016/j.ygyno.2012.06.011
- Havrilesky LJ, Kulasingam SL, Matchar DB, Myers ER. FDG-PET for management of cervical and ovarian cancer. *Gynecol Oncol* (2005) **97**:183–91. doi:10.1016/j.ygyno.2004.12.007
- Akkas BE, Demirel BB, Vural GE. Clinical impact of ¹⁸F-FDG PET/CT in the pretreatment evaluation of patients with locally advanced cervical carcinoma. *Nucl Med Commun* (2012) **33**:1081–8. doi:10.1097/MNM.0b013e3283570fd3
- Kidd EA, Siegel BA, Dehdashti F, Rader JS, Mutch DG, Powell MA, et al. Lymph node staging by positron emission tomography in cervical cancer. *J Clin Oncol* (2010) **28**:2108–13. doi:10.1200/JCO.2009.25.4151
- Beriwal S, Gan GN, Heron DE, Selvaraj RN, Kim H, Lalonde R, et al. Early clinical outcome with concurrent chemotherapy and extended field, intensity-modulated radiotherapy for cervical cancer. *Int J Radiat Oncol Biol Phys* (2007) **68**:166–71. doi:10.1016/j.ijrobp.2006.12.023
- Tsai CS, Lai CH, Chang TC, Yen TC, Ng KK, Hsueh S, et al. A prospective randomized trial to study the impact of pretreatment FDG-PET for cervical cancer patients with MRI-detected positive pelvic but negative para-aortic lymphadenopathy. *Int J Radiat Oncol Biol Phys* (2010) **76**:477–84. doi:10.1016/j.ijrobp.2009.02.020
- Gouy S, Morice P, Narducci F, Uzan C, Martinez A, Rey A, et al. Prospective multicenter study evaluating the survival of patients with locally advanced cervical cancer undergoing laparoscopic para-aortic lymphadenectomy before chemoradiotherapy in the era of positron emission tomography imaging. *J Clin Oncol* (2013) **31**:3026–33. doi:10.1200/JCO.2012.47.3520
- Lazzari R, Cecconi A, Jereczek-Fossa BA, Travaini LL, Dell'Acqua V, Cattani F, et al. The role of [(18)F]FDG-PET/CT in staging and treatment planning for volumetric modulated RapidArc radiotherapy in cervical cancer: experience of the European Institute of Oncology, Milan, Italy. *Eancermedicalsce* (2014) **8**:405. doi:10.3332/ecancer.2014.409
- Grigsby PW, Singh AK, Siegel BA, Dehdashti F, Rader J, Zoberi I. Lymph node control in cervical cancer. *Int J Radiat Oncol Biol Phys* (2004) **59**:706–12. doi:10.1016/j.ijrobp.2003.12.038
- Kerkhof EM, Raaymakers BW, van der Heide UA, van de Bunt L, Jurgenliemk-Schulz IM, Lagendijk JJ. On line MRI guidance for healthy tissue sparing in patients with cervical cancer. *Radiother Oncol* (2008) **88**:241–9. doi:10.1016/j.radonc.2008.04.009
- Bipat S, Glas AS, van der Velden J, Zwinderman AH, Bossuyt PM, Stoker J. Computed tomography and magnetic resonance imaging in staging of uterine cervical carcinoma. *Gynecol Oncol* (2003) **91**:59–66. doi:10.1016/S0090-8258(03)00409-8
- Krishnatry R, Patel FD, Singh P, Sharma SC, Oinam AS, Shukla AK. CT or MRI for image-based brachytherapy in cervical cancer. *Jpn J Clin Oncol* (2012) **42**:309–13. doi:10.1093/jjco/hys010
- Dimopoulos JC, Lang S, Kirisits C, Fidarova EF, Berger D, Georg P, et al. Dose-volume histogram parameters and local tumor control in magnetic resonance image-guided cervical cancer brachytherapy. *Int J Radiat Oncol Biol Phys* (2009) **75**:56–63. doi:10.1016/j.ijrobp.2008.10.033
- Wang JZ, Mayr NA, Zhang D, Li K, Grecula JC, Montebelo JE, et al. Sequential magnetic resonance imaging of cervical cancer. *Cancer* (2010) **116**:5093–101. doi:10.1002/cncr.25260
- Nam H, Park W, Huh SJ, Bae DS, Kim BG, Lee JH, et al. The prognostic significance of tumor volume regression during radiotherapy and concurrent chemoradiotherapy for cervical cancer using MRI. *Gynecol Oncol* (2007) **107**:320–5. doi:10.1016/j.ygyno.2007.06.022

17. Dolezel M, Odrazka K, Vanasek J, Kohlova T, Kroulik T, Kudelka K, et al. MRI-based pre-planning in patients with cervical cancer treated with three-dimensional brachytherapy. *Br J Radiol* (2011) **84**:850–6. doi:10.1259/bjrad75446993
18. Jürgenliemk-Schulz IM, Tersteeg RJHA, Roesink JM, Bijmolt S, Nomden CN, Moerland MA, et al. MRI-guided treatment planning optimisation in intracavitary or combined intracavitary/interstitial PDR brachytherapy using tandem ovoid applicators in locally advanced cervical cancer. *Radiother Oncol* (2009) **93**:322–30. doi:10.1016/j.radonc.2009.08.014
19. Petric P, Hudej R, Rogelj P, Blas M, Tanderup K, Fidarova E, et al. Uncertainties of target volume delineation in MRI guided adaptive brachytherapy of cervix cancer: a multi-institutional study. *Radiother Oncol* (2013) **107**:6–12. doi:10.1016/j.radonc.2013.01.014
20. Hellebust TP, Tanderup K, Lervag C, Fidarova E, Berger D, Malinen E, et al. Dosimetric impact of interobserver variability in MRI-based delineation for cervical cancer brachytherapy. *Radiother Oncol* (2012) **107**:13–9. doi:10.1016/j.radonc.2012.12.017
21. Park JJ, Kim CK, Park SY, Simonetti AW, Kim E, Park BK, et al. Assessment of early response to concurrent chemoradiotherapy in cervical cancer: value of diffusion-weighted and dynamic contrast-enhanced MR imaging. *Magn Reson Imaging* (2014) **32**:993–1000. doi:10.1016/j.mri.2014.05.009
22. Klopp AH, Moughan J, Portelance L, Miller BE, Salehpour MR, Hildebrandt E, et al. Hematologic toxicity in RTOG 0418: a phase II study of postoperative IMRT for gynecologic cancer. *Int J Radiat Oncol Biol Phys* (2013) **86**:83–90. doi:10.1016/j.ijrobp.2013.01.017
23. Poorvu PD, Sadow CA, Townamchai K, Damato AL, Viswanathan AN. Duodenal and other gastrointestinal toxicity in cervical and endometrial cancer treated with extended-field intensity modulated radiotherapy to paraaortic lymph nodes. *Int J Radiat Oncol Biol Phys* (2012) **85**:1262–8. doi:10.1016/j.ijrobp.2012.10.004
24. Folkert MR, Shih KK, Abu-Rustum NR, Jewell E, Kollmeier MA, Makker V, et al. Post operative pelvic intensity-modulated radiotherapy and concurrent chemotherapy in intermediate and high risk cervical cancer. *Int J Radiat Oncol Biol Phys* (2013) **128**:288–93. doi:10.1016/j.ygyno.2012.11.012
25. Marnitz S, Lukarski D, Kohler C, Włodarczyk W, Ebert A, Budach V, et al. Helical tomotherapy versus conventional intensity-modulated radiation therapy for primary chemoradiation in cervical cancer patients: an individual comparison. *Int J Radiat Oncol Biol Phys* (2011) **81**:424–30. doi:10.1016/j.ijrobp.2010.06.005
26. Renard-Oldrini S, Brunaud C, Huger S, Marchesi V, Tournier-Rangeard L, Bouzid D, et al. Dosimetric comparison between the intensity modulated radiotherapy with fixed field and RapidArc of cervix cancer. *Cancer Radiother* (2012) **16**:209–14. doi:10.1016/j.canrad.2012.02.002
27. Cozzi L, Dinshaw KA, Shrivastava SK, Mahantshetty U, Engineer R, Deshpande DD, et al. A treatment planning study comparing volumetric arc modulation with RapidArc and fixed field IMRT for cervix uteri radiotherapy. *Radiat Oncol* (2008) **89**:180–91. doi:10.1016/j.radonc.2008.06.013
28. Chang AJ, Richardson S, Grigsby PW, Schwarz JK. Split-field helical tomotherapy with or without chemotherapy for definitive treatment of cervical cancer. *Int J Radiat Oncol Biol Phys* (2012) **82**:263–9. doi:10.1016/j.ijrobp.2010.09.049
29. Hsieh CH, Wei MC, Lee HY, Hsiao SM, Chen CA, Wang LY, et al. Whole pelvic helical tomotherapy for locally advanced cervical cancer: technical implementation of IMRT with helical tomotherapy. *Radiat Oncol* (2009) **4**:62. doi:10.1186/1748-717X-4-62
30. Marnitz S, Stromberger C, Kawgan-Kagan M, Włodarczyk W, Jahn U, Schneider A, et al. Helical tomotherapy in cervical cancer patients. *Strahlenther Onkol* (2010) **186**:572–9. doi:10.1007/s00066-010-2121-6
31. Marnitz S, Kohler C, Burova E, Włodarczyk W, Jahn U, Grun A, et al. Helical tomotherapy with simultaneous integrated boost after laparoscopic staging in patients with early cervical cancer: analysis of feasibility and toxicity. *Int J Radiat Oncol Biol Phys* (2012) **82**:e137–43. doi:10.1016/j.ijrobp.2010.10.066
32. Le Tinier F, Reynaert N, Casterlain B, Lartigau E, Lacornerie T, Nickers P. Is adaptive radiation therapy for uterine cervical carcinoma mandatory. *Cancer Radiother* (2012) **16**:681–7. doi:10.1016/j.canrad.2012.06.007
33. Hsieh CH, Tien HJ, Hsiao SM, Wei MC, Wu WY, Sun HD, et al. Stereotactic body radiation therapy via helical tomotherapy to replace brachytherapy for brachytherapy-unsuitable cervical cancer-a preliminary result. *Onco Targets Ther* (2013) **6**:59–66. doi:10.2147/OTT.S40370
34. Haas JA, Witten MR, Clancey O, Episcopia K, Accordino D, Chalas E. Cyberknife boost for patients with cervical cancer unable to undergo brachytherapy. *Front Oncol* (2012) **2**:25. doi:10.3389/fonc.2012.00025
35. Sethi RA, Jozsef G, Grew D, Marciscano A, Pennell R, Babcock M, et al. Is there a role for an external beam boost in cervical cancer radiotherapy. *Front Oncol* (2013) **3**:3. doi:10.3389/fonc.2013.00003
36. Haie-Meder C, Potter R, van Limbergen E, Briot E, de Brabandere M, Dimopoulos J, et al. Recommendations from gynaecological (GYN) GEC-ESTRO working group (I): concepts and terms in 3D image based 3D treatment planning in cervix cancer brachytherapy with emphasis on MRI assessment of GTV and CTV. *Radiat Oncol* (2005) **74**:235–45. doi:10.1016/j.radonc.2004.12.015
37. Jürgenliemk-Schulz IM, Lang S, Tanderup K, de Leeuw A, Kirisits C, Lindergaard J, et al. Variation of treatment planning parameters (D90 HR-CTV, D2cc for OAR) for cervical cancer tandem ring brachytherapy in a multicenter setting: comparison of standard planning and 3D image guided optimization based on a joint protocol for dose-volume constraints. *Radiat Oncol* (2010) **94**:339–45. doi:10.1016/j.radonc.2009.10.011
38. Chi A, Gao M, Sinacore J, Nguyen NP, Vali F, Albuquerque K. Single versus customized treatment planning for image-guided high-dose-rate brachytherapy for cervical cancer: dosimetric comparison and predicting factor for organs at risk overdose with single approach. *Int J Radiat Oncol Biol Phys* (2009) **75**:309–14. doi:10.1016/j.ijrobp.2009.03.041
39. Georg P, Potter R, Georg D, Lang S, Dimopoulos JCA, Sturdza AE, et al. Dose-effect relationship for late side effects of the rectum and urinary bladder in magnetic resonance image-guided adaptive cervical cancer brachytherapy. *Int J Radiat Oncol Biol Phys* (2012) **82**:653–7. doi:10.1016/j.ijrobp.2010.12.029
40. Charra-Brunaud C, Harter V, Delannes M, Haie-Meder C, Quetin P, Kerr C, et al. Impact of 3D image-based pulsed PDR brachytherapy on outcome of patients treated for cervical carcinoma in France. *Radiat Oncol* (2012) **103**:305–13. doi:10.1016/j.radonc.2012.04.007
41. Nomden CN, de Leeuw AAC, Roesink JM, Tersteeg RJHA, Moerland MA, Witteveen PO, et al. Clinical outcome and dosimetric parameters of chemo-radiation including MRI guided adaptive brachytherapy with tandem-ovoid applicators for cervical cancer patients: a single institution experience. *Radiat Oncol* (2013) **107**:69–74. doi:10.1016/j.radonc.2013.04.006
42. Potter R, Georg P, Dimopoulos JCA, Grimm M, Berger D, Nesvacil N, et al. Clinical outcome of protocol based image (MRI) guided adaptive brachytherapy combined with 3D conformal radiotherapy with or without chemotherapy in patients with locally advanced cervical cancer. *Radiat Oncol* (2011) **100**:116–23. doi:10.1016/j.radonc.2011.07.012
43. Lindegaard JC, Fokdal LU, Nilesen SK, Juul-Christensen J, Tanderup K. MRI-guided adaptive radiotherapy in locally advanced cervical cancer from a Nordic perspective. *Acta Oncol* (2013) **52**:1510–9. doi:10.3109/0284186X.2013.818253
44. Mazerón R, Gilmore J, Dumas I, Champoudry J, Goulard J, Vanneste B, et al. Adaptive 3D image-guided brachytherapy: a strong argument in the debate on systematic radical hysterectomy for locally advanced cervical cancer. *Oncologist* (2013) **18**:415–22. doi:10.1634/theoncologist.2012-0367
45. Nesvacil N, Potter R, Sturdza A, Hegazy N, Federico M, Kirisits C. Adaptive image guided brachytherapy for cervical cancer: a combined MRI-/CT-planning technique with MRI only at first fraction. *Radiat Oncol* (2013) **107**:75–81. doi:10.1016/j.radonc.2012.09.005
46. Heijkkoop ST, Langetak TR, Quint S, Bondar L, Mens JW, Heijmen BJ, et al. Clinical implementation of an online adaptive plan of the day protocol for nonrigid motion management in locally advanced cervical cancer IMRT. *Int J Radiat Oncol Biol Phys* (2014) **90**(3):673–9. doi:10.1016/j.ijrobp.2014.06.046

Conflict of Interest Statement: The authors declare that the research was conducted in the absence of any commercial or financial relationships that could be construed as a potential conflict of interest.

Received: 31 July 2014; **paper pending published:** 26 August 2014; **accepted:** 02 March 2015; **published online:** 17 March 2015.

Citation: Dutta S, Nguyen NP, Vock J, Kerr C, Godinez J, Bose S, Jang S, Chi A, Almeida F, Woods W, Desai A, David R, Karlsson UL, Aldorfer G and The International Geriatric Radiotherapy Group (2015) Image-guided radiotherapy and -brachytherapy for cervical cancer. *Front. Oncol.* **5**:64. doi:10.3389/fonc.2015.00064

This article was submitted to Radiation Oncology, a section of the journal *Frontiers in Oncology*.

Copyright © 2015 Dutta, Nguyen, Vock, Kerr, Godinez, Bose, Jang, Chi, Almeida, Woods, Desai, David, Karlsson, Altdorfer and The International Geriatric Radiotherapy Group. This is an open-access article distributed under the terms of the Creative Commons Attribution License (CC BY). The use, distribution or reproduction in other

forums is permitted, provided the original author(s) or licensor are credited and that the original publication in this journal is cited, in accordance with accepted academic practice. No use, distribution or reproduction is permitted which does not comply with these terms.



Image-guided radiotherapy for cardiac sparing in patients with left-sided breast cancer

Claire Lemanski¹, Juliette Thariat², Federico L. Ampil³, Satya Bose⁴, Jacqueline Vock⁵, Rick Davis⁶, Alexander Chi⁷, Suresh Dutta⁸, William Woods⁹, Anand Desai¹⁰, Juan Godinez¹¹, Ulf Karlsson¹², Melissa Mills¹³, Nam Phong Nguyen^{4*}, Vincent Vinh-Hung¹⁴ and The International Geriatric Radiotherapy Group

¹ Department of Radiation Oncology, Centre Val d'Aurelle, Montpellier, France

² Department of Radiation Oncology, University of Nice, Nice, France

³ Department of Radiation Oncology, Louisiana State University, Shreveport, LA, USA

⁴ Department of Radiation Oncology, Howard University, Washington, DC, USA

⁵ Department of Radiation Oncology, Lindenhofspital, Bern, Switzerland

⁶ Michael D. Watchtel Cancer Center, Oshkosh, WI, USA

⁷ Department of Radiation Oncology, University of West Virginia, Morgantown, WV, USA

⁸ Department of Radiation Oncology, Medicine and Radiation Oncology PA, San Antonio, TX, USA

⁹ Department of Radiation Oncology, Richard A. Henson Institute, Salisbury, MD, USA

¹⁰ Department of Radiation Oncology, Akron City Hospital, Akron, OH, USA

¹¹ Florida Radiation Oncology Group, Department of Radiation Oncology, Jacksonville, FL, USA

¹² Department of Radiation Oncology, Marshfield Clinic, Marshfield, WI, USA

¹³ Department of Radiation Oncology, University of Arizona, Tucson, AZ, USA

¹⁴ Department of Radiation Oncology, University of Martinique Hospital, Martinique, France

Edited by:

John Varlotta, University of Massachusetts Medical Center, USA

Reviewed by:

John E. Mignano, Tufts Medical Center, USA

Heloisa De Andrade Carvalho, Hospital das Clínicas da Faculdade de Medicina da Universidade de São Paulo, Brazil

***Correspondence:**

Nam Phong Nguyen, Howard University, 2041 Georgia Avenue NW, Washington, DC 20060, USA

e-mail: namphong.nguyen@yahoo.com

Patients with left-sided breast cancer are at risk of cardiac toxicity because of cardiac irradiation during radiotherapy with the conventional 3-dimensional conformal radiotherapy technique. In addition, many patients may receive chemotherapy prior to radiation, which may damage the myocardium and may increase the potential for late cardiac complications. New radiotherapy techniques such as intensity-modulated radiotherapy (IMRT) may decrease the risk of cardiac toxicity because of the steep dose gradient limiting the volume of the heart irradiated to a high dose. Image-guided radiotherapy (IGRT) is a new technique of IMRT delivery with daily imaging, which may further reduce excessive cardiac irradiation. Preliminary results of IGRT for cardiac sparing in patients with left-sided breast cancer are promising and need to be investigated in future prospective clinical studies.

Keywords: breast cancer, left breast, cardiac toxicity, IGRT

CARDIAC TOXICITY FOLLOWING LEFT BREAST CANCER IRRADIATION

Patients with left-sided breast cancer are at risk of long-term cardiac complications following irradiation. In a study of 2168 breast cancer patients who had post-operative breast irradiation, the risk of major coronary events was significantly higher among the patients who had radiation to the left breast. The rates of major coronary events were proportional to the mean heart dose and continued into the third decade after surgery (1). All study patients were treated with the conventional 3-dimensional conformal radiotherapy technique (3D-CRT), which has been reported to increase radiation dose to the heart despite physician attempts to shield the heart from the radiation (2). Indeed, a higher risk of cardiac mortality was observed among patients with left-sided breast cancer compared to the ones with right breast cancer following post-operative irradiation (3). Even though recent studies suggest that the mortality of left breast irradiation was not different than the right breast after 1993, long-term cardiac damage frequently occurs after two decades, prompting some caution that

these adverse events may arise in the next decade as the patients become older (4). Significant reduction in myocardial function was observed in patients with left breast cancer following radiation dose as low as 3 Gy 2 months after treatment (5). Set up variation with two tangent fields has been demonstrated to expose the myocardium to a higher dose of radiation leading to myocardial hypoperfusion (6). Radiation-induced myocardial damage is often clinically silent even when there was significant reduction of the left ventricular ejection fraction (7). The damage to the heart may be worse in patients with pre-existing cardiovascular conditions such as high blood pressure or left ventricle dysfunction (8). In addition, in patients who required adjuvant chemotherapy in addition to radiation following breast cancer surgery, cardiac toxicity may be compounded from the radiosensitization effect of chemotherapy.

Cardiac toxicity following chemotherapy and radiotherapy for breast cancer occurs late and increases on long-term follow-up with serial echocardiography (9). As radiation damage to the myocardium is primarily due to the inflammation and scarring of

the heart microvascular structure, which leads to hypoperfusion and ventricular dysfunction, minimizing irradiation of the normal heart without compromise of target coverage should be the primary objective in patients with left-sided breast cancer (10, 11). To achieve this goal, new radiotherapy techniques such as intensity-modulated radiotherapy (IMRT) and image-guided radiotherapy (IGRT) have been introduced to limit cardiac toxicity.

INTENSITY-MODULATED RADIOTHERAPY FOR CARDIAC PROTECTION IN PATIENTS WITH LEFT-SIDED BREAST CANCER

The ability to modulate radiation beams during radiation treatment has been investigated extensively to spare normal organs from excessive radiation. Breast cancer IMRT is usually delivered using dynamic multileaf collimation (MLC) or as a limited number of static MLC segments delivered sequentially in the step-and-shoot fashion. The beam modulation allows for a homogeneous dose distribution within the breast avoiding areas of high dose leading to less side effects and possibly better cosmesis in randomized studies (12, 13). Compared to 3D-CRT, IMRT may significantly reduce radiation dose to the myocardium in patients with left-sided breast cancer when the internal mammary nodes were included in the radiation fields because of the steep dose fall off away from the target volume. The average heart volume receiving more than 30 Gy were 2.6 and 16.4% for IMRT and 3D-CRT, respectively (14). The superiority of IMRT over 3D-CRT for left-sided breast cancer was particularly beneficial in patients with a significant heart volume (more than 1 cm) included in the radiation fields. The mean percentage of the heart volume receiving more than 60% of the prescription dose was 2.2 and 4.4% for IMRT and 3D-CRT, respectively (15). The benefit of IMRT to decrease cardiac irradiation while improving target coverage and dose homogeneity was also corroborated in other dosimetric studies (16). As randomized studies demonstrated a significant reduction of side effects during radiotherapy for breast cancer with IMRT compared to 3D-CRT, it is quite possible that long-term cardiac complications may also be reduced in the future with IMRT given its cardiac sparing properties. However, long-term follow-up is needed to confirm this hypothesis.

POTENTIAL ADVANTAGES OF IGRT FOR CARDIAC SPARING IN PATIENTS WITH LEFT-SIDED BREAST CANCER

Image-guided radiotherapy is a tool that can be used in different radiotherapy treatments, including IMRT that gives the possibility of reduction of set up margins, with a better sparing of normal tissue, while promoting dose-escalation to the tumor. Thus, the visualization of the surgical tumor bed as outlined by the fiducial markers or the lumpectomy cavity and the organs at risk (OAR) during radiotherapy may allow the delivery of a higher radiation dose to the areas at risk for recurrence while reducing irradiation of the normal organs such as the heart and lungs. As an illustration, compared to IMRT, IGRT may substantially reduce radiation dose to a small organ such as the cochlea without sacrificing target coverage in patients with head and neck cancer (17). Preliminary results of IGRT for normal organs sparing in patients with breast cancer are encouraging. As the lumpectomy cavity decreases in size during breast irradiation, re-planning for

the tumor boost toward the end of whole breast irradiation may decrease the volume of the normal breast irradiated to a higher dose and potentially improve cosmetic results (18). This issue is particularly important in patients who develop a large seroma as a complication of surgery. Visualization of the lumpectomy cavity with daily imaging allows the delivery of a higher radiation dose to the tumor bed while treating the whole breast to a lower dose with the simultaneous integrated boost (SIB) technique. In patients with left-sided breast cancers, the volume of the heart irradiated to a high radiation dose may be significantly reduced. The volume of the heart radiated to 30 Gy (V30) and the mean heart dose were 0.03 and 1.14% and 1.35 and 2.22 Gy for IGRT and 3D-CRT, respectively (19). The cardiac sparing effect of IGRT over 3D-CRT was also corroborated in another study (20). Treatment time may also be shortened with the SIB technique as radiation may be delivered over 28 fractions instead of the conventional 38 fractions (21). Another potential advantage of IGRT over IMRT is its ability to monitor the patient breathing pattern during radiotherapy with pre-treatment imaging such as cone-beam CT (CBCT). In patients who are able to maintain a deep breath hold in inspiration, the volume of myocardium irradiated may be significantly reduced during radiation because the heart shifts away from the chest wall (22). The feasibility of IGRT for cardiac sparing in patients with left-sided breast cancer was investigated in a prospective study. Nineteen left-sided breast cancer patients were treated with the deep inspiration breath hold (DIBH) technique during IGRT. Compared to the free-breathing (FB) technique, DIBH significantly reduced radiation dose to the heart. The percentage of the left ventricle radiated was 28 and 71% for DIBH and FB, respectively (23). For selected patients with pathological stage T1 infiltrating ductal carcinoma completely resected without nodal involvement who could lay prone during radiotherapy, the tumor cavity and margins can also be treated with IGRT to 30 Gy in five fractions without compromise of loco-regional control (24). As the prone position allows reduction of radiation dose to the heart compared to the supine position (25), IGRT may potentially spare the heart from excessive radiation while shortening the treatment course in patients with left-sided breast cancer (26). The feasibility of IGRT to spare the heart in the prone position with an accelerated partial breast radiotherapy regimen was also corroborated in another study (27). For breast cancer patients with a special chest anatomy such as pectus excavatum or funnel chest where a large heart volume is frequently included in the radiation fields, IGRT may also be beneficial in avoiding excessive cardiac irradiation (28). Thus, daily imaging with IGRT allows delivery of IMRT through various treatment positions and breathing cycles, which may improve cardiac sparing without compromise of the target volume in patients with left-sided breast cancer.

CLINICAL STUDIES OF IGRT FOR BREAST CANCER TREATMENT

Preliminary studies of IGRT for breast cancer treatment have been promising. In a phase II study, 50 patients with stage I–III infiltrating ductal carcinoma of the breast were treated with IGRT in the supine position with hypofractionation. The whole breast and lumpectomy cavity were treated to 40.5 and 48 Gy in 15 fractions with the SIB technique. Daily CBCT was performed to verify the

patient set up before each treatment. The constraint for the cardiac dose was D40 less than 3%. In patients with left breast lesions, the dose to the heart was kept to a maximum dose of 27 Gy. Despite a shorter treatment course, only one patient developed a grade 3 skin reaction. There were no complications or loco-regional recurrences after a median follow-up of 12 months (29). The benefit of hypofractionated IGRT for breast cancer was also corroborated in another randomized study (30). In all, 123 stage I and II breast cancer patients were randomized to IGRT (59) and 3D-CRT (64). The patients were treated to 42–51 Gy over 3 weeks and 50–66 Gy over 5–7 weeks with IGRT and 3D-CRT, respectively. Quality of life (QOL) was assessed with questionnaires at 3 months, and 1, 2, and 3 years after treatment. At 3 months post-radiotherapy, patients who had IGRT developed less fatigue and had improved physical and emotional functioning compared to those undergoing 3D-CRT. After a median follow-up of 26 months, the IGRT group still had a better QOL score even though the difference was no longer statistically significant. Thus, despite a shorter treatment course, IGRT may provide a better QOL for breast cancer patients possibly because of improved normal organ sparing. In another randomized study of 59 stage I and II breast cancer patients treated with IGRT (37) and 3D-CRT (32) treated with a similar fractionation, cardiac toxicity was similar for both groups (31). Despite the small number of patients and the short follow-up, these preliminary studies raised intriguing questions about the potential benefit of IGRT to decrease treatment toxicity and to improve QOL in breast cancer patients. It remains to be seen whether the potential of IGRT to reduce cardiac irradiation for left-sided breast cancer may translate into long-term reduction of cardiac complications.

IDENTIFICATION OF PATIENTS WHO MAY BENEFIT FROM IGRT FOR LEFT-SIDED BREAST CANCER

Patients with human epidermal growth factor receptor-2 (Her-2) positive breast cancer had improved survival when trastuzumab was added to their chemotherapy regimen. Even though trastuzumab is well tolerated in most patients, a small proportion may develop congestive heart failure and left ventricular dysfunction as complication. As the half-life of trastuzumab is 4 weeks, it will take 16–20 weeks to be cleared from the body and as a result may still be present at clinically significant levels at the time of radiotherapy. Preliminary results suggest that trastuzumab may potentiate the cardiotoxicity of radiation. Even a mean heart dose of 10 Gy may increase the risk of low grade cardiac toxicity when trastuzumab was administered with radiation in patients with left breast cancer (32). In another study of 95 breast cancer patients who had radiotherapy and concurrent trastuzumab, 58 patients experienced left ventricular ejection dysfunction (33). Grade 2 decrease in left ventricular ejection fraction was also observed in 10% of the patients receiving trastuzumab and breast radiotherapy (34). As radiotherapy should not be delayed in Her-2 positive breast cancer patients receiving trastuzumab and the long-term effect of the combined treatment remains unknown, these patients may benefit from IGRT if the tumor is located in the left breast. As the risk cardiac toxicity increases over time following treatment with anthracycline-based chemotherapy and radiotherapy for breast cancer, these patients may also benefit from IGRT to minimize radiation dose to the myocardium (9). However, as most

chemotherapy agents have cardiac effects, left-sided breast cancer patients who had a history of chemotherapy and radiotherapy should be monitored closely to determine any deterioration of their cardiac function over time (35). Elderly breast cancer patients (70 years or older) are more likely to have pre-existing cardiovascular morbidities and less likely to receive radiotherapy following surgery compared to younger patients because of the fear of treatment toxicity (36). The elderly breast cancer patients are more likely to benefit from a short course of hypofractionated IGRT to reduce treatment time and to decrease the toxic effect of cardiac irradiation. Such study should be conducted in the future to assess the beneficial effect of IGRT for local control and survival in elderly breast cancer patients.

CONCLUSION

Image-guided radiotherapy is a promising new technique of radiation that may significantly decrease cardiac irradiation in patients with left-sided breast cancers and potentially decrease long-term cardiac complications. Future prospective studies should be performed to verify this hypothesis.

REFERENCES

1. Darby SC, Ewert M, McGale P, Bennett AM, Blom-Goldman U, Bronnum D, et al. Risk of ischemic heart disease in women after radiotherapy for breast cancer. *N Engl J Med* (2013) **368**:987–98. doi:10.1056/NEJMoa1209825
2. Goody RB, O'Hare J, Mc Kenna K, Dearey L, Robinson J, Bell P, et al. Unintended cardiac irradiation during left-sided breast cancer radiotherapy. *Br J Radiol* (2013) **86**:20120434. doi:10.1259/bjr.20120434
3. Roychoudhuri R, Robinson D, Putcha V, Cuzick J, Darby S, Moller H. Increased cardiovascular mortality more than fifteen years after radiotherapy of breast cancer: a population-based study. *BMC Cancer* (2007) **7**:9. doi:10.1186/1471-2407-7-9
4. Henson KE, Mc Gale P, Taylor C, Darby SC. Radiation-related mortality from heart disease and lung cancer more than 20 years after radiotherapy for breast cancer. *Br J Cancer* (2013) **108**:179–82. doi:10.1038/bjc.2012.575
5. Erven K, Jurgut R, Weltens C, Giusca S, Ector J, Wildiers H, et al. Acute radiation effects on cardiac function detected by strain rate imaging in breast cancer patients. *Int J Radiat Oncol Biol Phys* (2011) **79**:1444–51. doi:10.1016/j.ijrobp.2010.01.004
6. Evans ES, Prosnitz RG, Yu X, Zhou SM, Hollis DR, Wong TZ, et al. Impact of patient-specific factors, irradiated left ventricular volume, and treatment set up errors on the development of myocardial perfusion defects after radiation therapy for left-sided breast cancer. *Int J Radiat Oncol Biol Phys* (2006) **66**:1125–34. doi:10.1016/j.ijrobp.2006.06.025
7. Livi L, Meattini I, Scotti V, Saieva C, Simontacchi G, Marrazzo L, et al. Concurrent adjuvant chemo-radiation therapy with anthracycline-based regimens in breast cancer: a single centre experience. *Radiol Med* (2011) **116**:1050–8. doi:10.1007/s11547-011-0652-2
8. Schmitz KH, Prosnitz RG, Schwartz AL, Carver JR. Prospective surveillance and management of cardiac toxicity and health in breast cancer survivors. *Cancer* (2012) **118**:2270–6. doi:10.1002/cncr.27462
9. Bustova I. Risk of cardiotoxicity of combination treatment radiotherapy and chemotherapy of locally advanced breast cancer stage III. *Klin Onkol* (2009) **22**:17–21.
10. Stewart FA, Hoving S, Russell NS. Vascular damage as an underlying mechanism of cardiac and cerebral toxicity in irradiated cancer patients. *Radiat Res* (2010) **174**:865–9. doi:10.1667/RR1862.1
11. Prosnitz RG, Hubbs JL, Evans ES, Zhou SM, Yu X, Blazing MA, et al. Prospective assessment of radiotherapy-associated cardiac toxicity in breast cancer patients: analysis of data 3 to 6 years after treatment. *Cancer* (2007) **110**:1840–50. doi:10.1002/cncr.22965
12. Donovan E, Bleakley N, Denholm E, Evans P, Gothard L, Hanson J, et al. Randomized trials of standard 2D radiotherapy versus intensity-modulated radiotherapy (IMRT) in patients prescribed breast radiotherapy. *Radiat Oncol* (2007) **82**:254–64. doi:10.1016/j.radonc.2006.12.008

13. Pignol JP, Olivotto I, Rakovitch E, Gardner S, Sixel K, Beckham W, et al. A multicenter randomized trial of breast intensity-modulated radiation therapy to reduce acute radiation dermatitis. *J Clin Oncol* (2008) **26**:2085–92. doi:10.1200/JCO.2007.15.2488
14. Popescu CC, Olivotto IA, Beckham WA, Ansbacher W, Zavgorodni S, Shaffer R, et al. Volumetric modulated arc therapy improves dosimetry and reduce treatment time compared to conventional intensity-modulated radiotherapy for locoregional therapy of left-sided breast cancer and internal mammary lymph nodes. *Int J Radiat Oncol Biol Phys* (2010) **76**:287–95. doi:10.1016/j.ijrobp.2009.05.038
15. Landau D, Adams EJ, Webb S, Ross G. Cardiac avoidance in breast radiotherapy: a comparison of simple shielding techniques with intensity-modulated radiotherapy. *Radiother Oncol* (2001) **60**:247–55. doi:10.1016/S0167-8140(01)00374-7
16. Rongsrivam K, Rojporpradit P, Lertbutsanukul C, Sanghangthum T, Oonsiri S. Dosimetric study of inverse-planned intensity-modulated, forward-planned intensity modulated and conventional tangential techniques in breast conserving radiotherapy. *J Med Assoc Thai* (2008) **91**:1571–82.
17. Nguyen NP, Smith-Raymond L, Vinh-Hung V, Sloan D, Davis R, Vos P, et al. Feasibility of tomotherapy to spare the cochlea from excessive radiation in head and neck cancer. *Oral Oncol* (2011) **47**:414–9. doi:10.1016/j.oraloncology.2011.03.011
18. Truong MT, Hirsch AE, Kovalchuk N, Qureshi MM, Damato A, Schuller B, et al. Cone beam computed tomography image-guided radiotherapy to evaluate lumpectomy cavity variation before and during breast radiotherapy. *J Appl Clin Med Phys* (2013) **14**:4243. doi:10.1120/jacmp.v14i2.4243
19. Hijal T, Fournier-Bidoz N, Castro-Pena P, Kirova YM, Zefkili F, Bollet MA, et al. Simultaneous integrated boost in breast conservative treatment of cancer: a dosimetric comparison of helical tomotherapy and three-dimensional conformal radiotherapy. *Radiother Oncol* (2010) **94**:300–6. doi:10.1016/j.radonc.2009.12.043
20. Caudrelier J, Morgan SC, Montgomery L, Lacelle M, Nyiri B, MacPherson M. Helical tomotherapy for locoregional radiation including the internal mammary chain in left-sided breast cancer: dosimetric evaluation. *Radiother Oncol* (2008) **90**:99–105. doi:10.1016/j.radonc.2008.09.028
21. Hurkmans CW, Dijkmans I, Reijnen M, van der Leer J, van Vliet-Vroegindeweij C, van der Sangen M. Adaptive radiation therapy for breast IMRT-simultaneously integrated boost: three-year clinical experience. *Radiother Oncol* (2012) **103**:183–7. doi:10.1016/j.radonc.2011.12.014
22. Betgen A, Alderliesten T, Sonke JJ, van Vliet-Vroegindeweij C, Bartelink H, Remeijer P. Assessment of set-up variability during deep inspiration breath hold radiotherapy for breast cancer patients by 3D-surface imaging. *Radiother Oncol* (2013) **106**:225–30. doi:10.1016/j.radonc.2012.12.016
23. Borst GR, Sonke JJ, den Hollander S, Betgen A, Remeijer P, van Giersbergen A, et al. Clinical results of image-guided deep inspiration breath hold breast irradiation. *Int J Radiat Oncol Biol Phys* (2010) **78**:1345–51. doi:10.1016/j.ijrobp.2009.10.006
24. Jozsef G, DeWyngaert JK, Becker SJ, Lymberis S, Formenti SC. Prospective study of cone-beam computed tomography image-guided radiotherapy for prone accelerated partial breast irradiation. *Int J Radiat Oncol Biol Phys* (2011) **81**:568–74. doi:10.1016/j.ijrobp.2010.11.029
25. Kainz K, White J, Chen GP, Hermand J, England M, Li XA. Simultaneous irradiation of the breast and regional lymph nodes in prone position using helical tomotherapy. *Br J Radiol* (2012) **85**:e899–905. doi:10.1259/bjr/18685881
26. Lymberis SC, deWyngaert JK, Parhar P, Chhabra AM, Fenton-Kerimian M, Chang J, et al. Prospective assessment of optimal individual position (prone versus supine) for breast radiotherapy: volumetric and dosimetric correlation in 100 patients. *Int J Radiat Oncol Biol Phys* (2012) **84**:902–9. doi:10.1016/j.ijrobp.2012.01.040
27. Leonard CE, Tallhammer M, Johnson T, Hunter K, Howell K, Kercher J, et al. Clinical experience with image-guided radiotherapy in an accelerated partial breast intensity-modulated radiotherapy protocol. *Int J Radiat Oncol Biol Phys* (2010) **76**:528–34. doi:10.1016/j.ijrobp.2009.02.001
28. Uhl M, Sterzing F, Habl G, Schubert K, Holger F, Debus J, et al. Breast cancer and funnel chest. Comparing helical tomotherapy and three-dimensional conformal radiotherapy with regards to the shape of the pectus excavatum. *Strahlenther Onkol* (2012) **188**:127–35. doi:10.1007/s00066-011-0022-y
29. Scorsetti M, Alonqui F, Fogliani A, Pentimalli S, Navarra P, Lobefalo F, et al. Phase I-II study of hypofractionated simultaneous integrated boost using volumetric modulated arc therapy for adjuvant radiotherapy in breast cancer patients: a report of feasibility and early toxic results in the first 50 treatments. *Radiat Oncol* (2012) **7**:145. doi:10.1186/1748-717X-7-145
30. Versmessen H, Vinh-Hung V, van Parijs H, Miedema G, Voordekkers M, Adriaenssens N, et al. Health related quality of life in survivors of stage I-II breast cancer: randomized trial of post-operative conventional radiotherapy and hypofractionated tomotherapy. *BMC Cancer* (2012) **12**:495. doi:10.1186/1471-2407-12-495
31. Van Parijs H, Miedema G, Vinh-Hung V, Verbanck S, Adriaenssens N, Kerkhove D, et al. Short course radiotherapy with simultaneous integrated boost for stage I-II breast cancer, early toxicities of a randomized trial. *Radiat Oncol* (2012) **7**:80. doi:10.1186/1748-717X-7-80
32. Cao L, Hu WG, Kirova YM, Yang ZZ, Cai G, Xu XL, et al. Potential impact of cardiac dose-volume on acute cardiac toxicity following concurrent trastuzumab and radiotherapy. *Cancer Radiother* (2014) **15**:119–24. doi:10.1016/j.cancrad.2014.01.001
33. Meattini I, Cecchini S, Muntoni C, Scotti V, De Luca Cardillo C, Mangoni M, et al. Cutaneous and cardiac toxicity of concurrent trastuzumab and adjuvant breast radiotherapy. *Med Oncol* (2014) **31**:891. doi:10.1007/s12032-014-0891-x
34. Balkacemi Y, Chauvet MP, Giard S, Villette S, Lacornerie T, Bonodean F, et al. Concurrent trastuzumab with adjuvant radiotherapy in Her2 positive breast cancer, acute toxicity analysis from the French multicentric study. *Ann Oncol* (2008) **19**:1110–6. doi:10.1093/annonc/mdn029
35. Galderisi M, Marra F, Esposito R, Lomoriello VS, Pardo M, de Divitiis O. Cardiac therapy and cardiotoxicity: the need for serial Doppler echocardiography. *Cardiovasc Ultrasound* (2007) **5**:4. doi:10.1186/1476-7120-5-4
36. Panjari M, Robinson PJ, Davis SR, Schwarz M, Bell JR. A comparison of the characteristics, treatment, and outcome after 5 years, of Australian women age 70+ with those aged <70 years at the time of diagnosis of breast cancer. *J Geriatr Oncol* (2014) **5**:141–7. doi:10.1016/j.jgo.2013.12.003

Conflict of Interest Statement: The authors declare that the research was conducted in the absence of any commercial or financial relationships that could be construed as a potential conflict of interest.

Received: 31 July 2014; accepted: 05 September 2014; published online: 23 September 2014.

Citation: Lemanski C, Thariat J, Ampil FL, Bose S, Vock J, Davis R, Chi A, Dutta S, Woods W, Desai A, Godinez J, Karlsson U, Mills M, Nguyen NP, Vinh-Hung V and The International Geriatric Radiotherapy Group (2014) Image-guided radiotherapy for cardiac sparing in patients with left-sided breast cancer. Front. Oncol. 4:257. doi: 10.3389/fonc.2014.00257

This article was submitted to Radiation Oncology, a section of the journal Frontiers in Oncology.

Copyright © 2014 Lemanski, Thariat, Ampil, Bose, Vock, Davis, Chi, Dutta, Woods, Desai, Godinez, Karlsson, Mills, Nguyen, Vinh-Hung and The International Geriatric Radiotherapy Group. This is an open-access article distributed under the terms of the Creative Commons Attribution License (CC BY). The use, distribution or reproduction in other forums is permitted, provided the original author(s) or licensor are credited and that the original publication in this journal is cited, in accordance with accepted academic practice. No use, distribution or reproduction is permitted which does not comply with these terms.



Image-guided radiotherapy for locally advanced head and neck cancer

Nam P. Nguyen^{1*}, Sarah Kratz², Claire Lemanski³, Jacqueline Vock⁴, Vincent Vinh-Hung⁵, Olena Gorobets⁶, Alexander Chi⁷, Fabio Almeida⁸, Michael Betz⁹, Rihan Khan¹⁰, Juan Godinez¹¹, Ulf Karlsson¹² and Fred Ampil¹³

¹ Department of Radiation Oncology, University of Arizona, Tucson, AZ, USA

² Division of Hematology/Oncology, University of Arizona, Tucson, AZ, USA

³ Department of Radiation Oncology, Centre Val d'Aurelle, Montpellier, France

⁴ Department of Radiation Oncology, Lindenhoftspital, Bern, Switzerland

⁵ Department of Radiation Oncology, University Hospitals of Geneva, Geneva, Switzerland

⁶ Department of Oral Maxillofacial Surgery, The Ministry and Education of Ukraine, Kiev, Ukraine

⁷ Department of Radiation Oncology, University of West Virginia, Morgantown, WV, USA

⁸ Southwest PET Institute, Tucson, AZ, USA

⁹ Department of Radiation Oncology, Hirslanden Radiation Oncology Institute, Lausanne, Switzerland

¹⁰ Department of Radiology, University of Arizona, Tucson, AZ, USA

¹¹ Florida Radiation Oncology Group, Palatka, FL, USA

¹² Department of Radiation Oncology, Marshfield Clinic, Marshfield, WI, USA

¹³ Department of Radiation Oncology, Louisiana State University, Shreveport, LA, USA

Edited by:

Kwan-Hwa Chi, Shin-Kong Wu Ho-Su Memorial Hospital, Taiwan

Reviewed by:

Seong Ki Mun, Virginia Tech, USA

Kai-Lin Yang, Shin-Kong Wu Ho-Su Memorial Hospital, Taiwan

*Correspondence:

Nam P. Nguyen, Department of Radiation Oncology, University of Arizona, 1501 N. Campbell Ave, Tucson, AZ 85724-5081, USA

e-mail: nampngh.nguyen@yahoo.com

Treatment of locally advanced head and neck cancer remains a challenge because of the head and neck complex anatomy and the tumor invasion to the adjacent organs and/or metastases to the cervical nodes. Postoperative irradiation or concurrent chemoradiation may lead to damage of radiosensitive structures such as the salivary glands, mandible, cochlea, larynx, and pharyngeal muscles. Xerostomia, osteoradionecrosis, deafness, hoarseness of the voice, dysphagia, and aspiration remain serious complications of head and neck irradiation and impair patient quality of life. Intensity-modulated and image-guided radiotherapy by virtue of steep dose gradient and daily imaging may allow for decreased radiation of the organs at risk for complication while preserving loco-regional control.

Keywords: head and neck cancer, image-guided radiotherapy, preservation of radiosensitive organs

TREATMENT OF LOCALLY ADVANCED HEAD AND NECK CANCER

Treatment of locally advanced head and neck cancer remains a challenge because of the high rate of loco-regional failures and the potential for serious complications following treatment. The tumor frequently invades adjacent organs and/or regional neck nodes. Standard of care has been either postoperative irradiation or concurrent chemoradiation (1). Regardless of the modality chosen, serious complications may occur because of the presence of radiosensitive organs such as the salivary glands, cochlea, mandible, larynx, and pharyngeal muscles in the radiation field. Xerostomia, deafness, osteoradionecrosis, dysphagia, weight loss, chronic hoarse voice, and aspiration are potential long-term complications of radiation treatment with conventional radiotherapy techniques. Intensity-modulated radiotherapy (IMRT) has been introduced to decrease the toxicity of irradiation because of the steep dose gradient allowing for sparing of radiosensitive organs. Randomized studies have demonstrated significant sparing of the parotid glands following IMRT of head and neck cancer and decreased severity of the xerostomia with improvement of patient quality of life (QOL) (2, 3). However, a significant amount of normal tissues is still irradiated because the inclusion of the tumor and areas at high risk for invasion with a large rim of normal

tissue called planning target volume or PTV, to avoid marginal miss. Recently, image-guided radiotherapy (IGRT) by combining the steep dose gradient of IMRT and daily imaging may potentially improve further the toxicity of head and neck irradiation because of the possibility of safe PTV reduction given the reduced inter-fraction movement through daily imaging.

Significant reduction of spinal cord dose may be achieved with IGRT compared to IMRT by a reduced PTV margin (4). However, the flip side of IGRT is also the risk of under-dosing the tumor if the target area is not adequately outlined. Thus, pre-treatment imaging to meticulously delineate the tumor and areas at risk of invasion is a critical component for the success of IGRT.

IMAGING STUDIES CRITICAL FOR IGRT PLANNING

Positron-emission tomography (PET) scan or PET-computed tomography (PET-CT) allows accurate delineation of the tumor and cervical lymph nodes that can be incorporated into the planning CT. PET-CT is superior to CT for tumor imaging because of its ability to detect the tumor metabolic activity in addition to its anatomic location. In a study of 102 unresectable head and neck cancer, PET-CT significantly changed the staging and management of these patients compared to CT alone (5). Twelve patients had modifications of the radiotherapy planning following review

of their PET-CT. In another study of 20 patients with oropharyngeal cancers, the incorporation of PET-CT into radiotherapy planning prevented marginal miss in two patients (6). The ability of PET-CT for better tumor delineation compared to CT for radiotherapy planning was also corroborated in other studies (7, 8). Thus, PET-CT should be included in the planning for head and neck IGRT.

Although PET-CT is the diagnostic imaging of choice for head and neck cancer IGRT, magnetic resonance imaging (MRI) also plays a critical role when there is suspicion of nerves infiltration, base of skull or parapharyngeal space invasion by the tumor given its better soft tissue discrimination compared to CT. For patients with nasopharyngeal cancer, MRI is complementary to PET-CT because of the tumor location with high risks for intracranial invasion through the skull base foramen and parapharyngeal extension (9, 10). In addition head and neck MRI may also have a prognostic value for survival after head and neck irradiation of nasopharyngeal cancer (11).

IMAGE-GUIDED RADIOTHERAPY POTENTIAL FOR PAROTID GLAND PRESERVATION

Xerostomia remains one of the most common complications of head and neck cancer Irradiation and may severely affect the QOL of patients. Xerostomia results from apoptosis of the acinar glands secondary to radiation and its severity is proportional to the radiation dose to the parotid glands (12).

Compared to the three-dimensional conformal radiotherapy technique (3D-CRT), IMRT may significantly reduce radiation dose to the parotid glands because of the steep dose gradient. Mean dose to the parotids is usually kept around 26 Gy to allow recovery of the saliva following head and neck irradiation. However, if only one parotid gland can be spared from radiation, current recommendation is to keep mean parotid dose at 20 Gy or lower (13). A recent study suggested that preservation of the contralateral parotid gland may lead to improvement of patient QOL following head and neck cancer irradiation. Among 31 patients with head neck cancer treated with IMRT, there was significant preservation of salivary flow and better QOL as measured by QOL questionnaires if the contralateral parotid gland can be preserved because of less sticky saliva (14). Preliminary experience suggests that IGRT may preserve salivary function and QOL without compromising target coverage. In a study of 76 patients treated with IGRT for head and neck cancer, excellent loco-regional control was obtained as the gross tumor was treated to 70.5 Gy in 2.2–2.3 Gy/fraction while most of the patients were able to preserve a good QOL because of parotid preservation (15). In another study of parotid preservation, IGRT can significantly decrease the mean contralateral parotid gland dose to 14 Gy without compromising target coverage, suggesting that IGRT may further improve patient QOL compared to IMRT (16).

POTENTIAL OF IGRT FOR HEARING PRESERVATION

Hearing loss commonly occurred following concurrent head and neck chemoradiation. A significant proportion of head and neck patients had baseline hearing deficit prior to radiation related to their age. Cisplatin can cause hearing loss which is dose-dependent and may exacerbate the elderly patients hearing deficits. When

cisplatin is combined with radiotherapy, the hearing loss may worsen because of the radiosensitization effects of cisplatin on the normal cochlea cells. The threshold for hearing deficit ranges from 10 to 13 Gy when radiotherapy is combined with chemotherapy and affects mainly the high frequency range (>4,000 Hz) (17). However, severe deafness may occur when cochlea radiation dose exceeds 47 Gy because the low frequencies range (<3,000 Hz) is then also affected (18). Deafness is a handicap and may lead to social isolation and poor QOL. In addition, it may affect the patient gainful employment because of the difficulty to communicate at work. Thus, lowering cochlea dose below the threshold for hearing deficit may preserve the patients' hearing and conserve their QOL. Compared to 3D-CRT, IMRT may decrease radiotherapy dose to the cochlea and provide better hearing preservation (19). Mean cochlea dose reported in the literature for patients with head and neck cancer undergoing IMRT ranged from 16 to 55 Gy. Preliminary data for IGRT of head and neck cancer for cochlea sparing is encouraging. In a study of 52 patients who had IGRT for locally advanced head and neck cancer, mean cochlea dose was reduced to 6–6.5 Gy which is below the threshold for radiotherapy damage without compromising target volume coverage (20). Thus, hearing preservation with IGRT is feasible and needs to be investigated in future prospective studies of head and neck cancer.

POTENTIAL OF IGRT FOR MANDIBULAR SPARING

Osteoradionecrosis remains one of the most feared complications of head and neck cancer irradiation because of its effect on patient QOL. In severe cases of osteoradionecrosis unresponsive to conservative management, resection of the damaged bone may result in severe alteration of speech, chewing, and swallowing. The risk of radionecrosis is related to the volume of normal bone radiated to high radiation dose. Damage of the microvasculature irrigating the mandible may lead to decreased blood flow, poor wound healing, and ultimately necrosis. Mandibular radionecrosis usually occurs when the mandible dose exceeds 66 Gy (21). The prevalence of osteoradionecrosis ranges from 5 to 7% in head and neck cancer patients treated with the conventional fractionation (1.8–2 Gy/fraction) and 3D-CRT. The risk of radionecrosis may be reduced with IMRT because of the sharp dose gradient allowing for reduction of the volume of normal bone radiated to a high dose. The reported prevalence of osteoradionecrosis ranges from 1 to 5% depending on the anatomic site of the cancer as cancers of the oral cavity usually require treating a large of volume of the mandible to a high radiation dose (22, 23). The IGRT technique may further decrease radiation dose to the mandible and thus the risk of radionecrosis. In a study of 83 head and neck cancer patients of various anatomic sites treated with IMRT (17) and IGRT (66), only one patient developed radionecrosis (24). Thus, IGRT may be a promising technique for mandibular preservation in future clinical trials.

POTENTIAL OF IGRT TO PREVENT LARYNGEAL EDEMA IN NON-LARYNGEAL AND NON-HYPOPHARYNGEAL HEAD AND NECK CANCER

Laryngeal edema and resulting dysphonia commonly occur following head and neck cancer radiation when the laryngeal dose exceeds 43.5 Gy (25). The dysphonia severity is proportional to the

radiation dose and related on the abnormal cord vibrations caused by the edema which may be persistent up to 72 months after radiation (26). Chronic hoarseness of the voice may impair patient QOL or affect their professional activity if the patient depends on the quality of his voice to make a living. Laryngeal edema is unavoidable when the tumor is located in the larynx or hypopharynx because of the high radiation dose required for cure (70 Gy). When the tumor is located in other anatomic sites, shielding of the larynx with a midline block would significantly decrease radiation dose to the larynx and prevent the risk of laryngeal edema. However, in the presence of cervical lymph nodes, a laryngeal shield may under-dose the cervical lymph nodes leading to an increased risk of regional recurrence. Whole field head and neck IMRT is usually recommended in the presence of neck node metastases to avoid geographic miss. Compared to whole field head and neck IMRT, IGRT can significantly reduce radiation dose to the larynx in patients with non-laryngeal and non-hypopharyngeal head and neck cancers (27). Preliminary results suggest that IGRT may also reduce the risk of laryngeal edema and effectively preserve patient voice following head and neck radiation (28).

POTENTIAL OF IGRT TO REDUCE ASPIRATION RISK FOLLOWING RADIATION FOR NON-LARYNGEAL AND NON-HYPOPHARYNGEAL HEAD AND NECK CANCER

Aspiration is a life-threatening complication of a head and cancer irradiation because of the risk of pneumonia and sepsis. Aspiration commonly occurs following head and neck cancer irradiation because of damage to the pharyngeal constrictor muscles. Aspiration risk is proportional to radiation dose to the pharyngeal muscles. Even though there are still controversies about which pharyngeal muscles are critical for the development of aspiration, 32% of the patients developed aspiration when the dose to the inferior pharyngeal muscles exceeds 52 Gy (29). Thus, patients with laryngeal and hypopharyngeal cancer are at highest risk of aspiration following head and neck cancer irradiation. However, a high rate of aspiration is still observed following radiation of non-laryngeal and non-hypopharyngeal head and neck cancers.

REFERENCES

1. Soo KC, Tan EH, Wee J, Lim D, Tai BC, Khoo ML, et al. Surgery and adjuvant radiotherapy vs concurrent chemoradiotherapy in stage III/IV non-metastatic squamous cell head and neck cancer. *Br J Cancer* (2005) **93**:279–86. doi:10.1038/sj.bjc.6602696
2. Gupta T, Agarwall J, Jain S, Phurailatpam R, Kannan S, Ghosh-Laskar S, et al. Three-dimensional conformal radiotherapy (3D-CRT) versus intensity modulated radiotherapy (IMRT) in squamous cell carcinoma of the head and neck: a randomized controlled trial. *Radiother Oncol* (2012) **104**:343–8. doi:10.1016/j.radonc.2012.07.001
3. Nutting CM, Morden JP, Harrington KJ, Urbano TG, Bhide SA, Clark C, et al. Parotid-sparing intensity modulated versus conventional radiotherapy in head and neck cancer (PASSPORT): a phase 3 multicentre randomized controlled trial. *Lancet Oncol* (2011) **12**:127–36. doi:10.1016/S1470-2045(10)70290-4
4. Schwarz M, Giske K, Stoll A, Nill S, Huber PE, Debus J, et al. IGRT versus non-IGRT for postoperative head and neck IMRT patients: dosimetric consequences arising from a PTV reduction. *Radiat Oncol* (2012) **7**:133. doi:10.1186/1748-717X-7-133
5. Abramlyuk A, Appold S, Zophel K, Baumann M, Abolmaali N. Modification of staging and treatment of head and neck cancer by FDG-PET/CT prior to radiotherapy. *Strahlenther Onkol* (2013) **189**:197–201. doi:10.1007/s00066-012-0283-0
6. Chatterjee S, Frew J, Mott J, McCallum H, Stevenson P, Maxwell R, et al. Variation in radiotherapy target volume definition, dose to organs at risk and clinical target volumes using anatomic (computed tomography) versus combined anatomic and molecular imaging (positron emission tomography/computed tomography): intensity-modulated radiotherapy delivered using a tomotherapy Hi-Art machine: final results of the VortigERN study. *Clin Oncol* (2012) **24**:e173–9.
7. Delouya G, Igibashian L, Houle A, Belair M, Boucher L, Cohade C, et al. ¹⁸F-FDG-PET imaging in radiotherapy volume delineation in treatment of head and neck cancer. *Radiother Oncol* (2011) **101**:362–8. doi:10.1016/j.radonc.2011.07.025
8. Garg MK, Glantzman J, Kalnicki S. The evolving role of positron emission tomography-computed tomography in organ-preserving treatment of head and neck cancer. *Semin Nucl Med* (2012) **42**:320–7. doi:10.1053/j.semnuclmed.2012.04.005
9. Liao XB, Mao YP, Liu LZ, Tang LL, Sun Y, Wang Y, et al. How does magnetic resonance imaging influence staging according to AJCC staging system for nasopharyngeal carcinoma compared with computed tomography. *Int J Radiat Biol Phys* (2008) **72**:1368–77. doi:10.1016/j.ijrobp.2008.03.017

Aspiration rates ranged from 16 to 54% following non-laryngeal and non-hypopharyngeal cancer irradiation with 3D-CRT and whole field IMRT (30, 31). Whole field IGRT reduces significantly the risk of aspiration for these patients. Only 2 out of 48 patients developed minimal aspiration which resolved with swallowing therapy following IGRT for non-laryngeal and non-hypopharyngeal head and neck cancer (32). Thus, IGRT is a promising technique to reduce the risk of aspiration and to improve patient QOL in head and neck cancer patients.

EFFECTIVENESS OF IGRT FOR LOCO-REGIONAL CONTROL IN PATIENTS WITH HEAD AND NECK CANCERS

Preliminary clinical experiences of IGRT for head and neck cancers have been very encouraging. Excellent loco-regional control and survival have been achieved for various anatomic head and neck cancer sites. In a study of 19 patients with locally advanced oral cavity cancer who received postoperative irradiation with IGRT, the 2-year survival and loco-regional control were 94 and 92%, respectively (33). In another study of 28 patients who underwent concurrent chemotherapy and IGRT for locally advanced nasopharyngeal cancer, the 3-year survival and loco-regional control were respectively 83.5 and 88.4% respectively (34). Similar high rates of loco-regional control were also observed for oropharyngeal and laryngeal cancers (35, 36). Because of the small number of patients and the short follow-up, these studies should be interpreted with caution but they may be helpful for the design of future prospective studies of head and neck cancer IGRT.

CONCLUSION

Image-guided radiotherapy for head and neck cancer is a promising technique of radiation because of the potential for normal organ sparing without compromise of target coverage. Preliminary clinical results suggest that the dosimetric advantages of IGRT may be translated into excellent loco-regional control for patients with head and neck cancer. Further prospective studies with a large number of patients should be performed to verify this hypothesis.

10. Nemzek WR, Hecht S, Gandon-Edwards R, Donald P. Perineural spread of head and neck tumors: how accurate is MR imaging? *AJNR Am J Neuroradiol* (1998) **19**:701–6.
11. Tang LL, Li WF, Chen L, Sun Y, Chen Y, Liu LZ, et al. Prognostic values and staging categories of anatomic masticator space involvement in nasopharyngeal carcinoma: a study of 924 cases with MRI imaging. *Radiology* (2010) **257**:151–7. doi:10.1148/radiol.10100033
12. Roesink JM, Moerland MA, Batterman JJ, Hordijk G, Terhaard CHJ. Quantitative dose-volume response analysis of changes in parotid gland function after radiotherapy in the head and neck region. *Int J Radiat Oncol Biol Phys* (2001) **4**:938–46. doi:10.1016/S0360-3016(01)01717-5
13. Deasy JO, Moisenko V, Marks L, Chao KSC, Nam J, Eisbruch A. Radiotherapy dose-volume effects on salivary gland function. *Int J Radiat Oncol Biol Phys* (2010) **76**:S58–63. doi:10.1016/j.ijrobp.2009.06.090
14. Chen WC, Lai CH, Lee TF, Hung CH, Liu KC, Tsai MF, et al. Scintigraphic assessment of salivary function after intensity-modulated radiotherapy for head and neck cancer: correlation with parotid dose and quality of life. *Oral Oncol* (2013) **49**:42–8. doi:10.1016/j.oraloncology.2012.07.004
15. Voordeckers M, Farrag A, Everaert H, Tournel K, Storme G, Verellen D, et al. Parotid sparing with helical tomotherapy in head and neck cancer. *Int J Radiat Oncol Biol Phys* (2012) **84**: 443–448. doi:10.1016/j.ijrobp.2011.11.070
16. Nguyen NP, Vos P, Vinh-Hung V, Ceizyk M, Smith-Raymond L, Stevie M, et al. Feasibility of image-guided radiotherapy based on helical tomotherapy to reduce contralateral parotid dose in head and neck cancer. *BMC Cancer* (2012) **12**:175. doi:10.1186/1471-2407-12-175
17. Hitchcock YJ, Tward JD, Szabo A, Bentz BG, Shrieve DC. Relative contributions of radiation and cisplatin-based chemotherapy to sensori-neural hearing loss in head and neck cancer patients. *Int J Radiat Oncol Biol Phys* (2009) **73**:779–88. doi:10.1016/j.ijrobp.2008.05.040
18. Chan SH, Ng WT, Kam KL, Lee MC, Choi CW, Yau TK, et al. Sensorineural hearing loss after treatment of nasopharyngeal carcinoma: a longitudinal analysis. *Int J Radiat Oncol Biol Phys* (2009) **73**:1335–42. doi:10.1016/j.ijrobp.2008.07.034
19. Petsuksiri J, Sermsree A, Thephamongkhol K, Keskool P, Thongvai K, Chansilpa Y, et al. Sensorineural hearing loss after concurrent chemoradiotherapy for head and neck cancer. *Radiat Oncol* (2011) **6**:19. doi:10.1186/1748-717X-6-19
20. Nguyen NP, Smith-Raymond L, Vinh-Hung V, Sloan D, Davis R, Vos P, et al. Feasibility of tomotherapy to spare the cochlea from excessive radiation in head and neck cancer. *Oral Oncol* (2011) **47**:414–9. doi:10.1016/j.oraloncology.2011.03.011
21. Glanzmann C, Grätz KW. Radionecrosis of the mandible: a retrospective analysis of the incidence and risk factors. *Radiother Oncol* (1995) **36**:94–100. doi:10.1016/0167-8140(95)01583-3
22. Gomez DR, Zhung JE, Gomez J, Chan K, Wu AJ, Wolden SL, et al. Intensity-modulated radiotherapy in postoperative treatment of oral cavity cancer. *Laryngoscope* (2009) **73**:1096–103. doi:10.1016/j.ijrobp.2008.05.024
23. Huang K, Xia P, Chuang C, Weinberg D, Glastonbury CM, Eisele DW, et al. Intensity-modulated chemoradiation for treatment of stage III and IV oropharyngeal carcinoma: the University of California-San Francisco experience. *Cancer* (2008) **113**:497–507. doi:10.1002/cncr.23578
24. Nguyen NP, Vock C, Chi A, Ewell L, Vos P, Mills M, et al. Effectiveness of intensity-modulated and image-guided radiotherapy to spare the mandible from excessive radiation. *Oral Oncol* (2012) **48**:653–7. doi:10.1016/j.oraloncology.2012.01.016
25. Sanguineti G, Adapala P, Endres EJ, Brack C, Fiorino C, Sormani P, et al. Dosimetric predictor of laryngeal edema. *Int J Radiat Oncol Biol Phys* (2007) **68**: 741–9. doi:10.1016/j.ijrobp.2007.01.010
26. Hamdan A, Geara F, Rameh C, Husseini HT, Eid T, Fuleihan N. Vocal changes following radiotherapy to the head and neck for non-laryngeal tumors. *Eur Arch Otorhinolaryngol* (2009) **266**:1435–9. doi:10.1007/s00405-009-0950-7
27. Nguyen NP, Ceizyk M, Vos P, Vinh-Hung V, Davis R, Desai A, et al. Effectiveness of image-guided radiotherapy for laryngeal sparing in head and neck cancer. *Oral Oncol* (2010) **46**:283–6. doi:10.1016/j.oraloncology.2010.01.010
28. Nguyen NP, Abraham D, Desai A, Betz M, Davis R, Sroka T, et al. Impact of image-guided radiotherapy to reduce laryngeal edema following treatment for non-laryngeal and non-hypopharyngeal head and neck cancer. *Oral Oncol* (2011) **47**:900–4. doi:10.1016/j.oraloncology.2011.06.004
29. Caglar HB, Tishler RB, Othus M, Burke E, Li Y, Goguen L, et al. Dose to larynx predicts for swallowing complications after intensity-modulated radiotherapy. *Int J Radiat Oncol Biol Phys* (2008) **72**:1110–8.
30. Feng FY, Kim HM, Lyden TH, Haxer MJ, Worden FP, Feng FM, et al. Intensity-modulated chemoradiotherapy aiming to reduce dysphagia in patients with oropharyngeal cancers. *J Clin Oncol* (2010) **28**:2732–8. doi:10.1200/JCO.2009.24.6199
31. Nguyen NP, Frank C, Moltz CC, Vos P, Smith HJ, Nguyen PD, et al. Analysis of factors influencing aspiration rates following chemoradiation for head and neck cancer. *Br J Radiol* (2009) **82**:675–80. doi:10.1259/bjr/72852974
32. Nguyen NP, Smith-Raymond L, Vinh-Hung V, Vos P, Davis R, Desai A, et al. Feasibility of Tomotherapy based image-guided radiotherapy to reduce aspiration risk in patients with non-laryngeal and non-hypopharyngeal head and neck cancer. *PLoS One* (2013) **8**:e62690.
33. Hsieh C, Kuo Y, Liao L, Hu K, Lin S, Lin Y, et al. Image-guided intensity-modulated radiotherapy with helical tomotherapy for post-operative high risk oral cavity cancer. *BMC Cancer* (2011) **11**:37. doi:10.1186/1471-2407-11-37
34. Shuang PW, Shen BJ, Wu LJ, Liao LJ, Hsiao CH, Lin YC, et al. Concurrent image-guided guided intensity modulated radiotherapy and chemotherapy following neoadjuvant chemotherapy for locally advanced nasopharyngeal carcinoma. *Radiat Oncol* (2011) **6**:95. doi:10.1186/1748-717X-6-95
35. Nguyen NP, Ceizyk M, Vos P, Betz M, Chi A, Almeida F, et al. Feasibility of tomotherapy-based image-guided radiotherapy for locally advanced oropharyngeal cancers. *PLoS ONE* (2013) **8**:e60268. doi:10.1371/journal.pone.0060268
36. Nguyen NP, Chi A, Betz M, Almeida F, Vos P, Davis R, et al. Feasibility of intensity-modulated and image-guided radiotherapy for functional organ preservation in locally advanced laryngeal cancer. *PLoS ONE* (2012) **7**: e42729. doi:10.1371/journal.pone.0042729

Conflict of Interest Statement: The authors declare that the research was conducted in the absence of any commercial or financial relationships that could be construed as a potential conflict of interest.

Received: 24 May 2013; accepted: 17 June 2013; published online: 08 July 2013.

Citation: Nguyen NP, Kratz S, Lemanski C, Vock J, Vinh-Hung V, Gorobets O, Chi A, Almeida F, Betz M, Khan R, Godinez J, Karlsson U and Ampil F (2013) Image-guided radiotherapy for locally advanced head and neck cancer. *Front. Oncol.* **3**:172. doi: 10.3389/fonc.2013.00172

This article was submitted to Frontiers in Radiation Oncology, a specialty of *Frontiers in Oncology*.

Copyright © 2013 Nguyen, Kratz, Lemanski, Vock, Vinh-Hung, Gorobets, Chi, Almeida, Betz, Khan, Godinez, Karlsson and Ampil. This is an open-access article distributed under the terms of the Creative Commons Attribution License, which permits use, distribution and reproduction in other forums, provided the original authors and source are credited and subject to any copyright notices concerning any third-party graphics etc.

Advantages of publishing in Frontiers



OPEN ACCESS

Articles are free to read,
for greatest visibility



COLLABORATIVE PEER-REVIEW

Designed to be rigorous
– yet also collaborative,
fair and constructive



FAST PUBLICATION

Average 85 days from
submission to publication
(across all journals)



COPYRIGHT TO AUTHORS

No limit to article
distribution and re-use



TRANSPARENT

Editors and reviewers
acknowledged by name
on published articles



SUPPORT

By our Swiss-based
editorial team



IMPACT METRICS

Advanced metrics
track your article's impact



GLOBAL SPREAD

5'100'000+ monthly
article views
and downloads



LOOP RESEARCH NETWORK

Our network
increases readership
for your article

Frontiers

EPFL Innovation Park, Building I • 1015 Lausanne • Switzerland
Tel +41 21 510 17 00 • Fax +41 21 510 17 01 • info@frontiersin.org
www.frontiersin.org

Find us on

